UNIVERSITÀ DELLA CALABRIA

UNIVERSITA' DELLA CALABRIA

Dipartimento di Farmacia e Scienze della Salute e della Nutrizione

Dottorato di Ricerca in

Biochimica Cellulare ed Attività dei Farmaci in Oncologia

CICLO XXVIII

Expression and Function of Phosphodiesterase Type 5 in Human Breast Cancer Cell Lines and Tissues: Implications for Targeted Therapy.

Settore Scientifico Disciplinare MED/05

Coordinatore:

Ch.mo Prof. Diego Sisci

Tutors:

Prof. Diego Sisci

Dott.ssa Ines Barone

Dottorando:

Dott.ssa Antonella Campana

Table of Contents

Introduction

Carcinoma of the breast is the most common cancer among women in industrialized countries, and results in substantial morbidity and mortality. In 2012, an estimated 1,67 million new cases of invasive breast cancer were diagnosed among women and approximately 522,000 patients were expected to die from breast cancer world-wide (Ferlay J. et al., 2015). The leading cause of breast cancer death is mainly due to its higher incidence, poor early diagnosis, inefficient therapeutic approach and aggressive metastasis (Tazhibi et al., 2014). Once diagnosed, breast cancer is usually treated with a combination of surgery, radiotherapy, endocrine therapy or chemotherapy. The choice of the treatments depends on the stage of the disease and hormone receptor status. Notably, significantly better outcomes and performance of therapeutic agents have been reported for smaller tumors detected at an earlier stage. Unfortunately, concurrent metastasis has been observed in 20-30% of the breast cancer patients even at stage 0. It is estimated that up to 30% of node-negative breast cancer patients and an even larger fraction of patients with node-positive disease will develop metastatic disease despite receiving standard treatment (Kennecke H. et al., 2010). In addition, some cancer patients either do not respond to initial therapy or experience relapse after an initial response and ultimately die from progressive metastatic disease (Holohan C. et al., 2013). Indeed, distant metastases rather than the primary tumor are the most life-threatening event in breast cancer patients.

Studies of cancer molecular and cellular biology have shown that various genetic and epigenetic changes, acting together, may lead to the activation of signaling pathways, which ultimately result in increased cell proliferation and carcinogenesis. Thus, the identification of single or multiple genes that tumor cells essentially require for the genesis and maintenance of their malignant phenotype is critical. This approach contrasts with the conventional cytotoxic chemotherapeutics that have been used in major cancer therapy in past decades and are usually accompanied by severe side effects and acquired drug resistance. In the search for tumor targeted therapy, a promising approach is the modulation of the intracellular cyclic guanosine monophosphate (cGMP) signaling by the activity of specific phosphodiesterases (PDEs). Indeed, dysregulation of cGMP homeostasis was observed in various (patho)physiological conditions,

including cancers, and recently it has been reported that the expression of PDE type 5 is increased in several cancers compared to normal or surrounding non-neoplastic tissues (Piazza G.A. et al., 2000; Piazza G.A. et al., 2001; Pusztai L. et al, 2003; Whitehead C.M. et al., 2003). Concomitantly, a significant number of studies have indicated that PDE5 inhibitors can inhibit cancer progression and enhance cancer cell sensitivity to standard chemotherapeutic drugs (Savai R. et al., 2010; Kloner R.A. et al., 2011).

cGMP signaling in (patho)physiological processes.

For more than four decades, the cyclic nucleotides cGMP e cAMP have been recognized as important intracellular signal transduction molecules, acting as ubiquitous second messengers between an extracellular signal, such as a cytokine or hormone, and the elicited intracellular response (Fajardo A.M. et al., 2014). Although the specific function of a given signal differs according to the cell type, its environment, the activation stimulus and the cyclic nucleotide involved, an extracellular signal will generally activate a selective cyclase enzyme, which catalyzes the formation of the cyclic nucleotide from its nucleotide triphosphate precursor. In particular, cGMP is generated by cytoplasmic soluble guanylate cyclases (sGCs), which are activated by nitric oxide (NO), and by receptor guanylate cyclases (rGCs), which are activated by natriuretic peptides [atrial natriuretic peptide(ANP) or B- and C-type natriuretic peptides (BNP and CNP)]. cGMP can lead to activation of cGMP-dependent protein kinase G (PKG), cyclic nucleotide–gated (CNG) ion channels or certain cGMP-binding phosphodiesterases (PDEs), resulting in protein phosphorylation, ion fluxes, or cyclic nucleotide hydrolysis to affect gene expression or other aspects of cellular activity (Lugnier C., 2006; Rehmann H. et al., 2007; Levy I. et al., 2011). Modulation of CNG channel activity is an important step for mediating cGMP effects on phosphotransduction, natriuresis and intestinal fluid and electrolyte secretion (Lincoln T.M. et al., 1993). A central mediator of cGMP signaling is PKG, which phosphorylates downstream substrates (Francis S.H. et al., 1999). PKG is a serine/threonine protein kinase which is highly versatile and plays a diverse role in regulating multiple cellular processes (i.e., vasodilation, cell differentiation, cell proliferation and apoptosis). Two major forms of PKG have been identified in mammalian cells: PKG I and PKG II. In addition, there are two splice variants of PKG I,

which are designated as Iα and Iβ (Ruth P., 1999). Both PKG Iα and PKG Iβ are cytosolic enzymes that differ only in their amino-terminal sequence. Both isoforms are widely distributed, but vary in their tissue expression. PKGIα is found mainly in the lung, heart, platelets and cerebellum, while PKGIβ and PKGIα are highly expressed in the smooth muscles of the uterus, intestine and trachea (Das A. et al., 2008). PKGII is a membrane-bound enzyme and is more restricted in its expression to the brain, intestine and kidney (Ruth P., 1999; Browning D.D., 2008). The downstream substrates regulated by PKG include those involved in calcium homeostasis, platelet activation and adhesion, smooth muscle contraction, cardiac function, and gene expression (Francis S.H. et al., 2010). In addition, altered cyclic nucleotide signaling has been observed in a number of pathophysiological conditions, such as cancer (Fajardo A.M. et al., 2014) cGMP signaling, through activation of downstream effectors and/or crosstalk with cAMP pathways, appears to play an important role in promoting apoptosis and inhibiting proliferation of certain cancer epithelial cells, acting as a tumor suppressor pathway (Pitari G.M. et al., 2001; Lugnier C. et al., 2006; Fallahian F. et al., 2011). For instance, one of the downstream signaling events mediated by PKG is the regulation of β-catenin protein levels. Studies indicate that upon cGMP increase, PKG is activated and directly phosphorylates β-catenin leading to increased proteasomal degradation and inhibition of growth-related target genes in cancer cells (Liu L. et al., 2001; Kwon I.K. et al., 2008; Tinsley H.N. et al., 2011). In addition, cGMP activates c-Jun NH2-terminal kinase (JNK), inhibits extracellular-signal regulated kinases 1/2 (ERK1/2) and down-regulates cyclin D1 expression (Li H. et al., 2002; Rice P.L. et al., 2004). cGMP signaling has also been shown to be implicated in extracellular remodeling, a crucial step in tumor invasion and metastasis (Lubbe W.J. et al., 2006). Alternatively, cGMP signaling has only a minimal role on cell differentiation, growth and survival of hematopoietic malignancies (Lerner A. et al., 2006), suggesting that cGMP role in tumorigenesis may be related to tissue context.

Both the amplitude and duration of cGMP signaling is dependent on the expression and activity of cyclic nucleotide PDE enzymes, which catalyze the hydrolytic breakdown of cGMP into the biologically inactive 5′ derivative.

Phosphodiesterases.

PDEs represent a large family of ubiquitously expressed hydrolases that are categorized into different families based on structural similarity such as sequence homology, protein domains, and enzymatic properties, including substrate specificity, kinetic properties, and sensitivity to specific inhibitors and modulators. PDEs superfamily contains 11 PDE gene families (PDE1 to PDE11, Figure 1), comprising 21 genes that generate approximately 100 (or more) proteins via alternative splicing of mRNA or multiple promoters and transcription start sites (Azevedo M.F. et al., 2014).

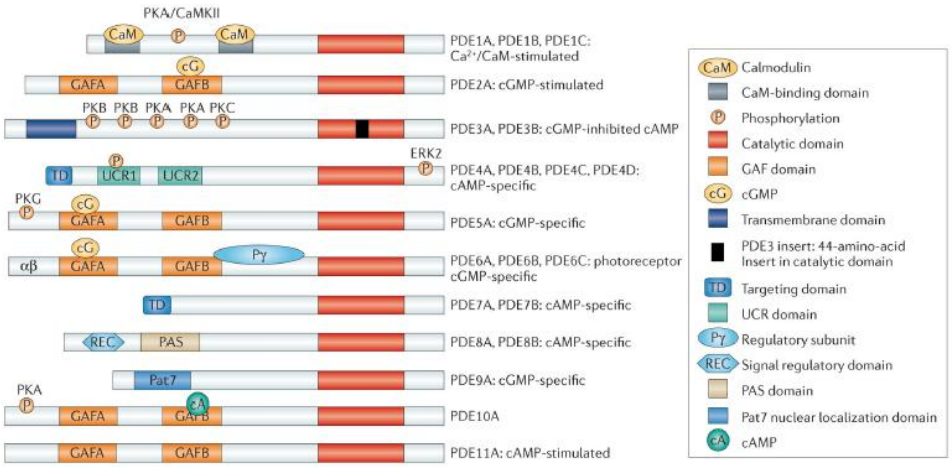

Adopted from Maurice DH et al., Nat Rev Drug Discov. 2014.

Figure 1: Structure and domain organization of the 11 mammalian PDE families. UCR, upstream conserved region.

The 11 PDE families can be grouped into three classes based on their substrate affinity. PDE4, PDE7, and PDE8 specifically hydrolyze cAMP; PDE5, PDE6, and PDE9 hydrolyze cGMP, while PDE1, PDE2, PDE3, PDE10, and PDE11 possess dual specificity, acting on both cAMP and cGMP with varying affinities, depending on the isoform (Azevedo M.F. et al., 2014). PDEs exhibit a common structural organization, with divergent amino-terminal regulatory regions and a conserved carboxy-terminal catalytic core (Figure 2).

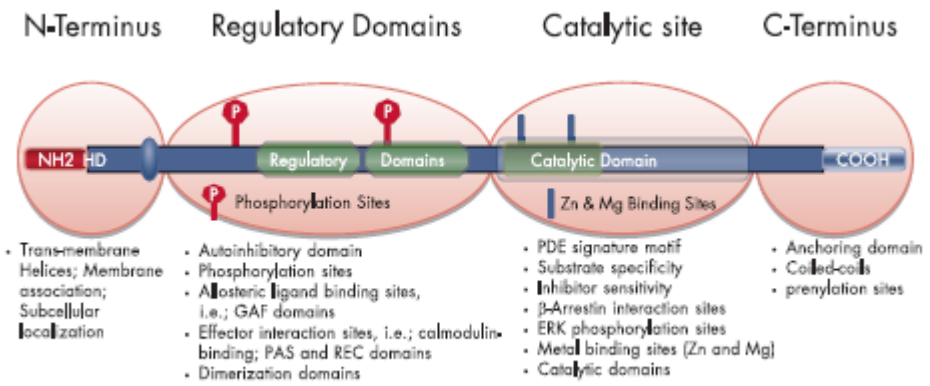

Adopted from Azevedo MF et al., Endocr Rev. 2014.

Figure 2: General structure of PDE enzyme molecules. HD, hydrophobic domains.

The catalytic domains of PDEs share a similar topography, composed of ~350 amino acids folded into 16 helices. In addition to conserved elements that are responsible for binding to cyclic nucleotides and inhibitors, the catalytic core contains variable determinants that regulate PDE family specific substrate and inhibitor affinities and selectivities (Manallack D.T. et al., 2005; Bender A.T. et al., 2006; Keravis T. et al., 2012). The N-terminal regulatory regions of PDEs contain structural determinants that target individual PDEs to different sub-cellular locations and signalosomes (Houslay M.D. et al., 2007; Kritzer M.D. et al., 2012; Lee L.C.Y. et al., 2013) and also allow individual PDEs to specifically respond to different post-translational modifications, regulatory molecules and signals. These structural elements include dimerization domains, autoinhibitory modules, binding sites for ligands and allosteric effectors, phosphorylation sites and other covalent modification sites. Approximately half of PDE gene families (PDE2, PDE5, PDE6, PDE10, and PDE11) have a protein domain termed GAF. The known functions of GAF domains are cGMP binding-mediated allosteric regulation and dimerization of GAF-PDEs. Among PDEs, PDE5A has 2 GAF domains (GAF A and GAF B) in the N-terminal half. The modulation of PDE activity is unique to cGMP signaling and has multiple roles within the cells, such as functioning as negative feedback for cGMP signaling by activating the cGMP-specific PDE5 or as crosstalk between cyclic nucleotide pathways by influencing the activity of non-selective PDE isoenzymes (e.g. PDE2 or PDE3) (Omori K. et al., 2007). Other PDEs

(PDE1, PDE3, PDE4, and PDE7–9) have no GAF domain. PDE1 contains a Ca^{2+}/calmodulin (CaM)-binding site, PDE3 has a transmembrane domain, PDE4 has upstream conserved regions (UCRs), and PDE8 has a response regulator receiver (REC) domain. PDE7 and PDE9 have no specific protein domain in addition to the PDE catalytic domain (Omori K. et al., 2007).

As expected from their complex genomic organization, multiple PDE isoforms are expressed in almost every cell (Bender A.T. et al., 2006; Francis S.H. et al., 2011). Some cells are relatively enriched in specific PDEs (eg, photoreceptor PDE6, which is virtually exclusively expresses in retina rods and cones and in the pineal gland). Recent studies have shown that many PDEs, that are tightly connected to different cellular functions, are also involved in various pathological conditions (Keravis T. et al., 2010). For instance, PDE4B abnormalities have been linked to schizophrenia (Millar J.K. et al., 2005), whereas defects in PDE6 subunits cause hereditary eye diseases (Gal A. et al., 1994; Huang S.H. et al., 1995). Recently, genetic alterations in PDE genes were described to be associated with tumor development. Polymorphisms in the genes encoding PDE8A and PDE11A have been associated with a predisposition to developing certain adrenocortical tumors (Horvath A. et al., 2008), testicular (Horvath A. et al., 2009) and prostatic cancers (Faucz F.R. et al., 2011). More importantly, PDE5 overexpression has been reported in several types of cancers (Anant J.S. et al., 1992; Baillie G.S. et al., 2000; Ke H. et al., 2007).

PDE5 structure, regulation, distribution and function.

PDE5 specifically hydrolyzes cGMP (Hamet P. et al., 1978; Coquil J.F. et al., 1980; Francis S.H. et al.,1980) and is encoded by a single PDE5A gene (chromosome 4q27), which gives rise to three N-terminal variants (PDE5A1, PDE5A2, and PDE5A3) in humans. PDE5 transcripts are relatively highly expressed in certain human tissues, especially in smooth muscle, including the vascular tissues of the penis, and also in platelets (Hamet P. et al., 1978; Loughney K. et al., 1998; Yanaka N. et al., 1998; Kotera J. et al., 1999; Lin C.S. et al., 2000). PDE5A1 and PDE5A2 are widely expressed, whereas specific expression of PDE5A3 in smooth and/or cardiac muscle has been suggested (Lin C.S. et al., 2000). The activity of the PDE5 enzyme is tightly controlled by cGMP signaling itself. PDE5A contains two GAF domains: GAF-A and

GAF-B (Figure 3). GAF-A is responsible for allosteric binding of cGMP, which promotes PDE5 phosphorylation, increasing both catalytic activity and cGMP-binding affinity (Turko I.V. et al., 1998; Zoraghi R. et al., 2005). Moreover, a PKA-dependent phosphorylation site in the N-terminal region regulates the activation of PDE5A enzyme (Corbin J.D. et al., 2000).

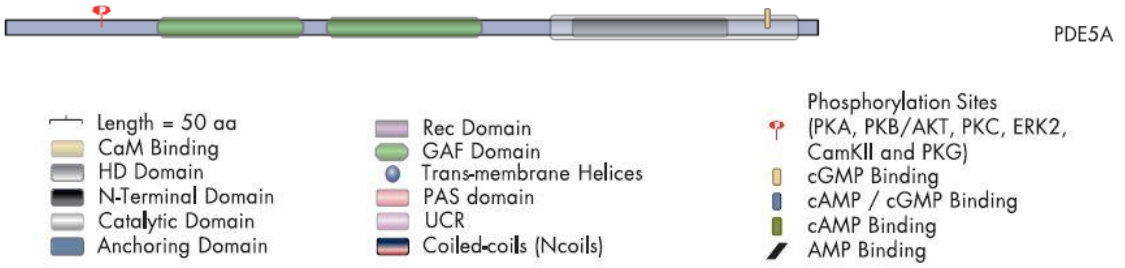

Adapted from Azevedo MF et al., Endocr Rev. 2014.

Figure 3. Schematic representation of PDE5.

The principal function of PDE5A is the regulation of vascular smooth muscle contraction through modulation of cGMP and calcium levels, especially in the lung and penis (Bender A.T. et al., 2006). Indeed, cGMP regulates intracellular free calcium concentrations by several mechanisms, including inhibition of inositol 1,4,5-trisphosphate (IP3)-mediated calcium release from intracellular stores, calcium removal and sequestration through specific pump mechanisms, and inhibition of the influx of extracellular calcium through voltage-gated calcium channels (Lincoln T.M. et al., 2006; Tsai E.J. et al., 2009). In addition, cGMP-PKG signaling within the vascular endothelium stimulates cell proliferation and increases permeability (Hood J. et al., 1998; Smolenski A. et al., 2000; Kook H. et al., 2003); while in cardiac myocardium, it negatively modulates hypertrophy and contractility (Takimoto E. et al., 2005; Nagendran J. et al., 2007). PDE5 has been also implicated in regulating platelet aggregation (Dunkern T.R. et al., 2005) and is also thought to be important in enhancing learning and memory (Prickaerts J. et al., 2004). Recently, a role for PDE5 has been suggested in tumorogenesis, due to its capability to act as a negative regulator of cGMP tumor suppressor signaling (Savai R. et al., 2010). Indeed, increased PDE5 expression

occurs in various human carcinomas, including urinary bladder cancers (Piazza G.A. et al., 2001), metastatic breast cancers (Pusztai L. et al., 2003) and non-small cell lung cancers (Whitehead C.M. et al., 2003). Increased PDE5 expression has been also associated with the development of human oropharyngeal squamous cell carcinoma (Spoto G. et al., 2003). An increase in the expression of PDE5 has been confirmed in various cell lines originating from breast cancer (MCF-7, HTB-26, MDA-MB-468), prostate cancer (LNCAP, PC3), colonic adenocarcinomas (HT29, HCT-116, SW480, T84), bladder cancer (HTB-76, HT1376) and some chronic lymphocytic leukemia cells (CLL) (Zhu B. et al., 2007).

PDE5 inhibitors

Overview.

PDE family-specific inhibitors allow insight into the functional role of PDEs and may be useful for predicting the potential therapeutic effects of targeting specific PDEs. Methilxantine was the first inhibitor to be described in the literature in 1962 (Butcher R.W. et al., 1962). This agent and other nonselective PDE inhibitors, including papaverine, have been used therapeutically for over 70 years to treat a range of diseases. However, it was only in the last 10 years that potent PDE-selective drugs began to make an impact on disease treatments. New studies have yielded crucial information on the active sites of PDE (Wang H. et al., 2007; Ke H. et al., 2007) and have allowed rational drug design, resulting in improved inhibitor potency and selectivity. All known PDE inhibitors contain one or more rings that mimic the purine ring in the cyclic nucleotide substrates of PDEs and directly compete with cyclic nucleotides for the access to the catalytic site. Selective PDE inhibitors are currently being investigated for the treatment of a wide range of disease. PDE2 inhibitors may be of therapeutic interest in sepsis and acute respiratory distress syndrome (Seybold J. et al., 2005). Milrinone is the most studied and the most extensively used PDE3 inhibitor and is currently used in the acute treatment of heart failure to diminish long-term risks (Cruickshank J.M., 1993). Another highly PDE3 selective inhibitor, cilostazol, is used therapeutically in the USA and Japan for treating intermittent heart failure and claudication (Reilly M.P. et al., 2001; Kambayashi J. et al., 2003; Dobesh P.P. et al., 2009) PDE4 inhibitors have been developed to treat asthma (van Schalkwyk E. et al., 2005), chronic obstructive

pulmonary disease (Calverley P.M. et al., 2007), allergic rhinitis (Schmidt B.M. et al., 2001), psoriasis (Gottlieb A.B. et al., 2008) and depression (Zeller E. et al., 1984). In clinical practice, PDE5 inhibitors are used to treat erectile dysfunction (ED) and pulmonary artery hypertension (PAH), due to their ability to induce vasodilation and a consequent increase in blood flow by hampering cGMP breakdown. Indeed, PDE5 inhibitors induce relaxation of smooth muscle in the corpus cavernosum of the penis through cGMP-mediated augmentation of NO, and thereby stimulate penile erection (Corbin J.D., 2004). Similarly, in the lung, PDE5 inhibition opposes smooth muscle vasoconstriction, decreases proliferation and increases apoptosis of pulmonary artery smooth muscle cells (Archer S.L. et al., 2009). In addition, PDE5 inhibition can directly protect the heart against ischemia/reperfusion injury (Kukreja R.C. et al., 2004; Kumar P. et al., 2009). In particular, PDE5 inhibitors, sildenafil (Viagra and Revatio, Pfizer), and tadalafil (Cialis, Eli Lilly; Adcirca, United Therapeutics) are currently used for the treatment of ED and PAH; whereas vardenafil (Levitra; Bayer) and Avanafil (Stendra; Vivus) are used only for ED. However, because of their safety and high tolerability profiles (Nehra A., 2009; Palit V. et al., 2010), a wide range of research is investigating the potential use of PDE5 inhibitors in other pathophysiological conditions, for which therapeutic choices are restricted and in which they may act through mechanisms other than the known vasodilatory effects. These comprise different urological disorders beyond ED (i.e. benign prostatic hyperplasia and lower urinary tract symptoms), cutaneous ulcerations, tissue and organ protection, transplant and reconstructive surgery, female sexual dysfunction, neurological conditions, diabetes, and importantly cancer (Savai R. et al., 2010; Kloner R.A. et al., 2011). Today, close to 500 clinical trials with these drugs have been completed or are ongoing (htpp://www.clinicaltrials.gov), showing mainly their potential cardiovascular benefits.

PDE5 inhibitors in cancer: "in vitro" and clinical studies.

The increased expression of PDE5 in various human malignancies and the lack of such expression in normal cells, coupled with the safety and high tolerability of PDE5 inhibitors in different deseases, have led to an increased interest in investigating their possible roles in the management of cancer. Thus, PDE5 inhibitors have shown: 1)

direct anticancer effects on tumor cell lines; 2) the ability to sensitize cancer cells to chemotherapeutic agents and 3) cancer chemopreventive actions (Figure 4).

PDE5 inhibitors as promising anticancer agents.

Accumulating evidences indicate that PDE5 inhibitors could have anticancer activities, through a regulation of cGMP levels and thereby of its regulated downstream pathways, in multiple carcinomas and cancer cell lines. Both vardenafil and sildenafil exert a pro-apoptotic activity against cancer cells. Indeed, Sarfati et al. demonstrated that treatment with sildenafil and vardenafil resulted in suppression of tumor cell growth along with induction of caspase-dependent apoptosis in B-cell chronic lymphatic leukemia. Instead, normal B lymphocytes isolated from control donors were completely resistant to the PDE5 inhibitor-induced apoptosis (Sarfati M. et al., 2003). Sildenafil has also shown promising anticancer activity against Waldenstrom's Macroglobulinemia, an incurable B-cell malignancy (Treon S.P. et al., 2004). Another study by Zhu et al. confirmed the importance of PDE5 as a therapeutic target for treatment of cancer through a genetic approach (Zhu B. et al., 2005). They reported that transfection of human colonic carcinoma (HT29) cells with PDE5 anti-sense constructs results in suppression of PDE5 gene expression, sustained increase in intracellular cGMP concentrations, growth inhibition and apoptosis. Exisulind (sulindac sulfone), a derivative of the oral anti-inflammatory drug sulindac, and its higher affinity analogues selectively exerted pro-apoptotic and antiproliferative effects in various human prostate, colon, and breast cancer cells with minimal effects on normal epithelial cells. This is a consequence of PDE5 inhibition, since they did not affect prostaglandin levels, or cyclooxygenase inducing actions (Thompson, et al., 2000; Piazza, et al., 2001; Whitehead, et al., 2003; Zhu B. et al., 2005; Tinsley, et al., 2009; Tinsley et al., 2010; Tinsley, et al., 2011; Whitt et al., 2012). Its antiproliferative effects on cell growth were associated with inhibition of β-catenin-mediated transcriptional activity and consequent suppression of the synthesis of target genes, such as cyclin D1 and survivin (Tinsley H.N. et al., 2010; Tinsley H.N. et al., 2011). This drug has also been shown to directly inhibit growth of human prostate cancers (Goluboff E.T. et al., 1999) and lung tumors (Whitehead C.M. et al., 2003) in murine models by enhancing apoptosis. Similarly, stable downregulation of PDE5 in the aggressive human breast cancer cell line MDA-MB-231T resulted in

reduced *in vitro* motility as well as fewer lung metastasis in an experimental metastasis assay *in vivo* (Marino N. et al., 2014). Furthermore, vardenafil has been shown to synergize with the major constituent of green tea (epigallocatechin-3-O-gallate) to induce cancer cell death (Kumazoe M. et al., 2013).

Recently, it has been reported that PDE5 inhibitors may block tumor progression through the modulation of host immune response. Indeed, PDE5 is expressed in different immune cells, such as macrophage, dendritic and T cells (Essayan D.M., 2001). Importantly, PDE5 expression was also detected in tumor-derived myeloid-derived suppressor cells (MDSC), known to play a critical role in suppressing immune function through several mechanisms (i.e. secretion of cytokines, release of reactive oxygen species, upregulation of NO synthase and arginase) (Wesolowski R. et al., 2013). Treatment of mice with PDE5 inhibitors leads to delay of tumor outgrowth and progression by decreasing MDSC numbers and increasing intratumoral $CD8^+$ T infiltration, activation and tumoricidal activity (Serafini P. et al., 2006). The inhibition of MDSCs by PDE5 inhibitors has also been reported in patients with multiple myeloma and head and neck cancers (Serafini P. et al., 2006; Noonan K.A. et al., 2014). These data strongly propose the potential of PDE5 inhibitors to alter the tumor microenvironment by maximally enhancing antitumor immunity.

PDE5 inhibitors as sensitizers of cancer cells to chemotherapeutic agents.

One of the major obstacles in the successful treatment of cancer is the phenomenon of multidrug resistance (MDR). The mainly cause of MDR, both *in vitro* and *in vivo*, is overexpression of the adenosine-triphosphate-binding cassette (ABC) transporters, such as ABC sub-family B member 1 ABCB1 (P-glycoprotein/MDR1), the most important mediator of MDR, multidrug resistance proteins (ABCCs/MRPs) and breast cancer resistant protein (ABCG2/BCRP) (Szakács G. et al., 2006). When such transporters are overexpressed in cancer cells, they actively pump out of cells a variety of structurally and mechanistically unrelated chemotherapeutic drugs, thereby lowering their intracellular accumulation along with their chemotherapeutic effect. This mechanism was shown to be responsible for chemotherapeutic drug resistance to various anticancer agents, including anthracyclines, vinca alkaloids, epipodophyllotoxins and taxanes. Interestingly, Jedlitschky et al. discovered a link between cGMP elimination and ABC

transporters (Jedlitschky G. et al., 2000). They showed that the multidrug resistance protein isoform MRP5 (ABCC5) mediates cellular export of cGMP and that sildenafil enhances intracellular cGMP concentrations by a dual action involving inhibition of its degradation by PDE5 and its export by ABCC5. In this regard, Shi et al. recently reported that sildenafil significantly decreased the efflux activity of the ABC transporters ABCB1 and ABCG2, but had no significant effects on ABCC1 (Shi Z. et al., 2011). They also reported that vardenafil significantly sensitized ABCB1 over-expressing cells to the ABCB1 substrates vinblastine and paclitaxel. Furthermore, Chen et al. recently showed that sildenafil and vardenafil enhanced the sensitivity of multidrug resistance protein 7 (MRP7; ATP-binding cassette C10)-transfected HEK293 cells to paclitaxel, docetaxel and vinblastine, and reversed MRP7-mediated MDR through inhibition of the drug efflux function of MRP7 (Chen J.J. et al., 2012). In addition, Black et al. reported that sildenafil and vardenafil increased the transport of doxorubicin across blood-brain tumor barrier in 9L gliosarcoma (Black K.L. et al., 2008). Vardenafil also potentiated the efficacy of doxorubicin in the 9L gliosarcoma-bearing rats. These effects appeared to be mediated by a selective increase in tumor cGMP levels and increased vesicular transport through tumor capillaries, although the involvement of ABC transporters in such effects was not reported in this study. Vardenafil treatment also led to a 2-fold increase in tumor permeability to the monoclonal antibody Herceptin in HER2-positive intracranial lung and breast tumors (Hu J. et al., 2010). These data suggest that PDE5 inhibitors by modulating BTB permeability may enhance delivery and therapeutic efficacy of drugs in hard-to-treat primary brain tumors and metastasis. Moreover, it has been recently reported that co-treatment with sildenafil enhanced the antitumor efficacy of doxorubicin in both prostate cancer cells, *in vitro*, and in mice bearing prostate tumor xenografts, while simultaneously ameliorating doxorubicin-induced cardiac dysfunction (Das A. et al., 2010). The increased apoptosis by sildenafil and DOX was associated with enhanced expression of proapoptotic proteins caspase-3, caspase-9, Bad and Bax and suppression of the anti-apoptotic protein Bcl-xL. Furthermore, in a clinical study, sildenafil (50 mg) has aided radiotherapy for the treatment of Kaposi's sarcoma of the penis, resulting in complete resolution of such lesions (Ekmekci T.R. et al., 2005). Another PDE5 inhibitor, exisulind, has been utilized in several pre-clinical, as well as clinical studies to augment

the chemotherapeutic efficacy of well-known anticancer agents. Exisulind in combination with docetaxel has been shown to prolong survival, inhibit tumor growth and metastases and increase apoptosis in athymic nude rats with orthotopic lung tumors (Chan D.C. et al., 2002). These results have been corroborated by Whitehead et al. who have shown that exisulind-induced apoptosis significantly enhanced docetaxel anticancer effects in non-small cell lung cancer orthotopic lung tumor (Whitehead C.M. et al., 2003). However, Lin et al. have reported that sildenafil, at a supraclinical dose (50mg/kg), did not improve the brain penetration of docetaxel and topotecan, although it increased the plasma concentrations of the two drugs (Lin F. et al., 2013). They have also shown that sildenafil did not improve the efficacy of doxorubicin against subcutaneous CT26 colon tumors in mice. Therefore, results on the augmentation of the efficacy of antineoplastic drugs induced by PDE5 inhibitors still need to be corroborated.

PDE5 inhibitors as cancer chemopreventive agents.

The high expression of PDE5 in cancerous cells, coupled with the high safety profile of PDE5 inhibitors, has encouraged researchers to investigate cancer chemopreventive activity of such drugs. One of the earliest studies in this regard was that reported by Thompson and colleagues (Thompson H.J et al., 1997). They showed that sulindac sulfone (exisulind) dose-dependently inhibited 1-methyl-1-nitrosourea (MNU)-induced mammary carcinogenesis in rats, and at concentrations that were well tolerated by the animals. In addition, Piazza et al. reported that sulindac sulfone dose-dependently suppressed azoxymethane-induced colon carcinogenesis in rats without reducing prostaglandin levels (Piazza G.A. et al., 1997). Moreover, exisulind has been shown to inhibit N-butyl-N-(4-hydroxybutyl) nitrosamine-induced rat urinary bladder tumorigenesis, at least in part by cGMP-mediated apoptosis induction (Piazza G.A. et al., 1997). Exisulind inhibited UVB-induced skin tumor development in a murine model (Singh T. et al., 2012) by blocking proliferation, inducing apoptosis and reducing epithelial-mesenchymal transition (EMT) markers in tumor keratinocytes. In clinical studies, exisulind has shown modest chemopreventive activity in patients with familial adenomatous polyposis (FAP), as suggested by regression of small polyps and stimulation of mucus differentiation and apoptosis in glandular epithelium (Stoner G.D.

et al., 1999; van Stolk R. et al., 2000). In addition, exisulind has been shown to significantly prevent the increase in prostate specific antigen (PSA) and prolonged PSA doubling time in men with increasing PSA after radical prostatectomy compared with placebo (Goluboff E.T. et al., 2001). Remarkably, PDE5 inhibitors reduced proliferation and myofibroblast transdifferentiation of prostate fibroblasts, suggesting a potential value of PDE5 inhibitors in preventing and treating benign prostatic hyperplasia (Zenzmaier C. et al., 2010).

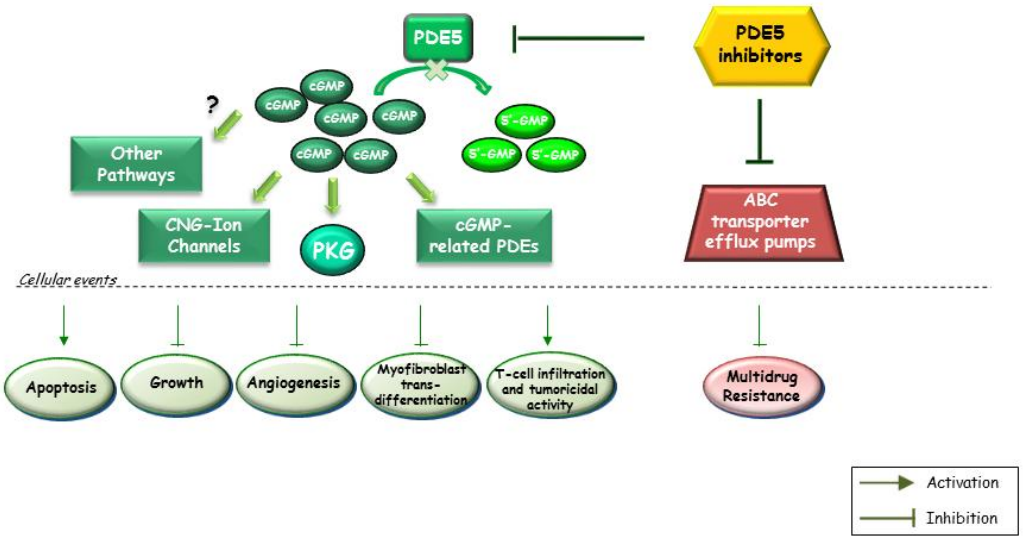

Adopted from Barone I et al., Curr Pathobiol Rep. 2015.

Figure 4: Schematic illustration of the anticancer activities of PDE5 inhibitors. PDE5 inhibitors may inhibit cancer progression by increasing cGMP levels via PDE5 activity inhibition and activating downstream signaling pathways, mainly PKG-mediated ones, which induce apoptosis, suppression of growth, of angiogenesis and of myofibroblast transdifferentiation and proliferation as well as increase intratumoral T-cell infiltration and tumoricidal activity; and blocking the substrate efflux activity of ABC multidrug-resistant transporters. PDE phosphodiesterase, cGMP cyclic guanosine monophosphate, PKG cGMP-dependent protein kinase, ABC-transporter ATP-binding cassette transporter, CNG (=cyclic nucleotide-gated) ion channels. Proposed mechanisms for the anticancer role of PDE5 inhibitors

Aim of the study

Aim of the study

In the last ten years, overexpression of PDE5 has been described in multiple carcinomas, including breast cancers (Piazza G.A. et al., 2001; Pusztai L. et al., 2003; Whitehead C.M. et al., 2003; Karami-Tehrani F. et al., 2012). Several "in vitro" observations have shown anti-proliferative and pro-apoptotic effects of PDE5 inhibitors in breast cancer cell lines (Savai R. et al., 2010). However, despite these studies, neither the expression of PDE5 in breast cancer cell lines and tissues nor the underlying regulatory molecular mechanisms by which PDE5 expression may contribute to breast cancer progression have been deeply studied. Being PDE5 a well-characterized druggable target, in this study we propose to examine PDE5's impact on breast cancer phenotype "in vitro", as well as to assess its clinical relevance in breast cancer patients.

Materials and Methods

Materials and methods

Reagents, antibodies and plasmids.

The following reagents and antibodies were used: Sildenafil and Y-27632 from Sigma; PDE5A, p-c-Myc$^{Thr58/Ser62}$, c-Myc, p-IκB-α$^{Ser32/36}$, IκB-α, NF-Kb p65, Lamin b and GAPDH antibodies from Santa Cruz Biotechnology; RhoA-C, Cdc42 and Rac1-3 antibodies from Life Technologies. Cofilin activation and myosin light chain 2 antibody sampler kits were obtained from Cell Signaling. pEGFP-C1 vector and the fusion protein expression vector pEGFP-PDE5A were kindly provided by Dr F. Barbagallo (Sapienza University, Rome, Italy). Scrambled and 4 unique 29mer PDE5A shRNA constructs in pGFP-CshLenti vector were obtained from Origene.

Cell culture.

MCF-7, T47D, ZR-75, SKBR3 and BT-20 breast cancer cell lines were acquired from American Type Culture Collection. MDA-MB-468 and MDA-MB-435 breast cancer cell lines were acquired from Interlab Cell Line Collection. MCF-7 cells were cultured in DMEM:F12 medium containing 5% Newborn Calf Serum (NCS, Life Technologies); MDA-MB-435 and MDA-MB-468 cells in DMEM supplemented with 10% Fetal Bovine Serum (FBS, Life Technologies); ZR-75 cells in DMEM:F12 medium with 5% FBS; T47D cells in RPMI medium with 10% FBS and 0,2 U/ml insulin; BT-20 in Minimum Essential Medium (MEM; Life Technologies) with 10% FBS. All cell lines were maintained in 1% L-glutamine and 1 mg/ml penicillin-streptomycin at 37 °C with 5% CO2 air. All cell lines were used within six-months after frozen aliquot resuscitations and regularly tested for Mycoplasma-negativity (MycoAlert, Lonza). To generate PDE5A-overexpressing MCF-7 cells, cells were transfected with pEGFP-PDE5A vector (5μg/10cm dishes) using Fugene 6 reagent, following manufacturer's protocol (Promega). Stable clones were selected with G418 antibiotic (1mg/ml, Life Technologies), and positive clones were identified using fluorescence microscopy and immunoblot analysis.

Transient transfection.

For overexpression studies, T47D cells were transfected with pEGFP-C1 or pEGFP-PDE5A vectors (3μg/6cm dishes) using Fugene 6 reagent. For gene silencing, MDA-MB-468 cells were transfected with scrambled or PDE5A shRNA constructs (3μg/6cm dishes) using Fugene 6 reagent. After 48h, cells were harvested and used in the different experimental procedures.

RT-PCR assays.

Total RNA was extracted from cells using TRIzol reagent and the evaluation of PDE5 and 36B4 gene expression was performed by the reverse transcription-PCR method using a RETROscript kit. Primers used for the amplification included: forward 5'-ACTTGCATTGCTGATTGCTG-3' and reverse 5'-TTGAATAGGCCAGGGTTTTG-3' (PDE5A); forward 5'-CAAATCCCATATCCTCGTCC-3' and reverse 5'-CTCAACATCTCCCCCTTCTC-3' (36B4, housekeeping gene).

Immunoblot analysis.

Cell extracts were resolved by SDS-PAGE (sodium dodecyl sulfate polyacrylamide gel electrophoresis), as previously described (Gu G. et al., 2012). Immunoblots show a single representative of at least two or three separate experiments.

Fluorescence microscopy.

Cells were fixed with 4% paraformaldehyde and permeabilized with PBS + 0.2% Triton X-100. 4',6-Diamidino-2-phenylindole (DAPI, Sigma) staining was used for nuclei detection. Fluorescence was photographed with OLYMPUS-BX51 microscope, 100X magnification.

MTT cell proliferation assays.

Three days after seeding, cell proliferation was assessed using 3-[4,5-Dimethylthiazol-2-yl]-2,5-diphenyltetrazolium bromide reagent/MTT (Sigma) and expressed as fold change relative to empty vector-transfected cells. Data represent three-independent experiments, performed in triplicate.

Wound-healing assays.

Cell monolayers were scraped and subjected to the various experimental conditions. Wound closure was monitored over 24h, cells were fixed and stained with Comassie Brillant Blue. Pictures represent one of three independent experiments (10X magnification, phase contrast microscopy).

Transmigration assays.

Cells under the various experimental conditions were placed in upper compartments of Boyden chambers (8μm-membranes, Corning). Bottom well contained regular growth media. After 24h, migrated cells were fixed and stained with DAPI. Migration was quantified by viewing five separate fields/membrane (OLYMPUS-BX51 microscope, 10X magnification) and expressed as mean numbers of migrated cells. Data represent three independent experiments, assayed in triplicate.

Invasion assays.

Matrigel-based invasion assay was performed in chambers (8μm-membranes) coated with Matrigel (BD Bioscences, 0.4μg/ml), as described (Barone I. et al., 2012). Cells under the various experimental conditions were seeded into top transwell-chambers, regular growth medium was used in lower chambers. After 24h, invaded cells were quantified as reported for transmigration assays. Data represent three independent experiments, assayed in triplicate.

RNA library preparation and sequencing.

Total RNA was extracted from vector- and PDE5-stable MCF-7 clones, as previously described (Gu G. et al., 2012). RNA concentration was determined with NanoDrop-1000 spectrophotometer and quality assessed with Agilent-2100-Bioanalyzer and Agilent-RNA-6000 nanocartridges (Agilent Technologies). High quality RNA from three-independent purifications for each experimental point was used for library preparation. Indexed libraries were prepared from 1μg/ea. of purified RNA with TruSeq-RNASample- Prep-Kit (Illumina) following suppliers. Libraries quality controls were performed using Agilent-2100-Bioanalyzer and Agilent DNA-1000 cartridges and concentrations were determined with Qubit-2.0 Fluorometer (Life Technologies).

Libraries were sequenced (paired-end, 2×100 cycles) at a concentration of 8pmol/L per lane on HiSeq2500 platform (Illumina) as described (Dago D.N. et al., 2015). RNA sequencing data have been deposited in the EBI ArrayExpress database (http://www.ebi.ac.uk/arrayexpress) with Accession Number E-MTAB-3801.

Rho GTPase activation assays.

Rho GTPases activation was determined by active Rho and Cdc42 pull-down and detection kits, following manufacturers (Life Technologies). Briefly, cells were washed with Tris-buffered-saline (25 mM TrisHCl pH 7.5, 150 mM NaCl) and lysed in Lysis/Binding/Wash Buffer with protease inhibitors (10 mg/mL leupeptin, 10 mg/mL aprotinin, and 1 mM sodium orthovanadate). For Rho and Cdc42/Rac GTPase activation, 1 mg of cellular proteins were incubated with 400 μg GST/Rhotekin/Rho-Binding-Domain or 20 μg of GST/PAK1/p21-Binding-Domain (4°C, 90 min), respectively. Pulled-down activated proteins were detected by immunoblotting.

Phalloidin staining.

Polymerized actin stress fibers were stained with Alexa Fluor 568-conjugated phalloidin, following manufacturers (Life Technologies). Cell nuclei were counterstained with DAPI. OLYMPUS-BX51 microscope (100X magnification) was used for imaging.

Patients and tissue specimens.

A total of 35 primary breast carcinomas and three nonneoplastic breast tissues were analyzed in this study. These carcinomas were obtained from patients who had undergone initial surgery and signed informed consent between 2012-2014 at Annunziata Hospital (Cosenza, Italy). The patients' age at diagnosis varied from 33 to 85 years (mean, 60.6 years; median, 57 years). Characteristics of the patient cohort are reported in Table 1. Fresh tissues were formalin-fixed/paraffin-embedded after surgical removal. Sections were stained with H&E to select samples consisting of at least 50% tumor cells and to establish the histologic type and grade (Table 1). The clinical investigation conformed the Declaration of Helsinki of 1975 and was approved by ethics and institutional human subjects committees at Annunziata Hospital.

Table 1. Characteristic of breast cancer cohort. Thirty-five patient-derived breast cancer samples were used in this study. Abbreviation: **POS** positive, **NEG** negative, **ER** Estrogen Receptor, **PR** Progesterone Receptor, **HER2,** epidermal growth factor receptor 2.

SAMPLE	AGE	Histology	GRADE	ER	PR	HER2
1	85	Invasive Ductal	2	POS	POS	NEG
2	88	Invasive Ductal	2	POS	POS	NEG
3	74	Invasive Ductal	2	POS	POS	NEG
4	82	**Invasive** Ductal	2	POS	POS	NEG
5	49	Invasive Ductal	2	POS	POS	NEG
6	67	In situ Ductal	2	POS	POS	NEG
7	75	Invasive Ductal	2	POS	POS	NEG
8	46	Invasive Ductal	2	POS	POS	NEG
9	57	Invasive Ductal	2	POS	POS	NEG
10	54	Invasive Ductal	2	POS	POS	NEG
11	76	Invasive Ductal	2	POS	POS	NEG
12	67	Invasive Ductal	2	POS	POS	NEG
13	64	Invasive Ductal	2	POS	POS	NEG
14	74	Invasive Ductal	2	POS	POS	NEG
15	68	Invasive Ductal	2	POS	POS	NEG
16	55	Invasive Ductal	3	POS	POS	NEG
17	52	Invasive Ductal	3	POS	POS	NEG
18	33	Invasive Ductal	3	POS	POS	NEG
19	51	Invasive Ductal	3	POS	POS	NEG
20	57	Invasive Ductal	3	POS	POS	NEG
21	56	Invasive Ductal	3	NEG	NEG	POS
22	52	Invasive Ductal	3	NEG	NEG	POS
23	45	Invasive Ductal	3	NEG	NEG	POS
24	56	Invasive Ductal	3	NEG	NEG	POS
25	50	Invasive Ductal	2	NEG	NEG	POS
26	57	In situ Ductal	2	NEG	NEG	POS
27	72	Invasive Ductal	2	NEG	NEG	POS
28	75	Invasive Ductal	3	NEG	NEG	NEG
29	83	Invasive Ductal	3	NEG	NEG	NEG
30	45	Invasive Ductal	3	NEG	NEG	NEG
31	61	Invasive Ductal	3	NEG	NEG	NEG
32	75	In situ Ductal	3	NEG	NEG	NEG
33	64	Mucinous	3	NEG	NEG	NEG
34	53	Invasive Ductal	3	NEG	NEG	NEG
35	60	In situ Ductal	3	NEG	NEG	NEG

Classification of molecular subtypes.

In breast cancer, utilization of immunohistochemistry as a surrogate for molecular classification by gene expression profiling has been used in large population-based studies and has been shown to provide an acceptable level of accuracy for determining molecular phenotypes (Carey L.A. et al., 2006; Yang X.R. et al., 2007; Collins L.C. et al., 2012). Using histologic tumor-grade obtained by central pathology review and biomarkers (estrogen and progesterone receptors (ER/PR) and HER2 status) extracted from pathology reports, cases were classified as one of four molecular subtypes. Cases that were ER-positive and/or PR-positive, HER2-negative and either histologic grade 1 or 2 were classified as Luminal A; cases that were ERpositive and/or PR-positive and HER2-positive, or ER-positive and/or PR-positive, HER2-negative and histologic grade 3 as Luminal B; ER/PR-negative, HER2-positive cases were classified as HER2-type and ER/PR/HER2-negative cases as triple negative. HER2 was considered positive if immunohistochemical stains were 3+ and/or if HER2 FISH showed gene amplification.

Immunohistochemical analysis.

PDE5A protein was detected using anti-PDE5A antibody diluted 1:100 in real-antibody-diluent (DAKO). Deparaffinization, rehydration, and antigen unmasking were obtained by incubation in tris-phosphate buffer (Envision-Flex-target-retrieval-solution) in a Pre-Treatment Module for Tissue Specimens (PTLINK), following suppliers (DAKO). The staining was performed in a Dako Autostainer-Link48-immunostainer, using a linked streptavidin-biotin technique (Envision Flex kit High pH, DAKO). Sections were counterstained in hematoxylin and coverslipped using DPX mounting medium (Sigma). PDE5 expression/localization were evaluated microscopically by two pathologist independently in a blind fashion. Pictures of representative fields were taken at 20X magnification using ViewFinder™ Software, through Olympus camera-system dp50. Negative controls showed no staining.

Database setup for retrospective study.

The entire database contains 1988 patients (average overall survival: 8.07 years, ER-positive patients: 76%, lymphnode-positive patients: 47.3%). Illumina gene-chips published by the Metabric-consortia were downloaded from the EGA repository (Curtis

C. et al., 2012). The raw gene-chip data were imported into R and summarized using beadarray package (Dunning M.J. et al., 2007). Quantile normalization was performed using preprocess Core package (Bolstad B.M. et al., 2003).

Statistical analysis.

Data were analyzed for statistical significance using two-tailed student's Test, GraphPad-Prism4. Standard deviations/S.D. are shown. For RNA sequencing bioinformatics analysis, sequencing reads (50-60 million reads/sample on average) were trimmed, quality filtered and aligned, including junction-spanning reads back, to the human genome hg19 (Homo sapiens Ensembl GRCh37) using Tophat v.2.0.10 (Kim D. et al., 2013). HTSeq (Anders S. et al., 2015) was used to compute read counts across each gene, which in turn were used as input to R package DESeq2 (Love M.I. et al., 2014). DESeq2 was used to normalize the read counts for library size and dispersion followed by tests for differential gene expression. The significant differentially expressed genes were determined using false discovery rate (FDR) cutoff $\leqslant$ 0.05 and at least 1.5 fold change between conditions. Functional analyses were performed with the Ingenuity Pathway Analysis suit (Ingenuity Systems). For immunohistochemistry, the correlations between PDE5 and grading/ER/PR/HER2 status were examined with Mann-Whitney-U test, between PDE5 and breast cancer subtypes by Kruskal-Wallis test (GraphPad-Prism4). Kaplan-Meier survival plot, hazard ratio with 95% confidence intervals and logrank P value were calculated and plotted in R as described (Mihaly Z. et al., 2013). In addition, Cox proportional hazard regression was computed to compare the association between gene expression, clinical variables including ER/HER2/lymphnode status and survival in multivariate analysis using WinSTAT 2014 for Microsoft Excel (Robert K. Fitch Software). Statistical significance was set at $p<0.05$.

Results

Results

PDE5 expression varies among different breast cancer cell subtypes.

On the basis of gene expression signatures in breast cancer patients, researchers have currently identified at least four major molecular and clinically distinct subtypes of neoplasm: luminal A (ER-positive) and B (ER-positive/HER2-enriched), HER2-positive and basal-like (Perou C.M. et al., 2000; Sørlie T. et al., 2001). Thus, we first aimed to evaluate mRNA and protein expression levels of PDE5 in breast cancer cell lines of different molecular subtypes (n=7) (Neve R.M. et al., 2006; Holliday D.L. et al., 2011) by RT-PCR and immunoblot analyses. As shown in Fig. 1A and B, PDE5 expression was detected at very low levels in luminal A-type breast cancer cells (MCF-7 and T47D cells). Luminal B-like cells (ZR-75cells) exhibited a modest induction in PDE5 expression in respect with luminal A-like cells. Notably, higher PDE5 levels were observed in HER2-overexpressing (SKBR3 cells) and basal-like (BT-20, MDA-MB-468 and MDA-MB-435 cells) breast cancer cells. These results may suggest that high PDE5 expression may be associated with more aggressive breast cancer phenotypes.

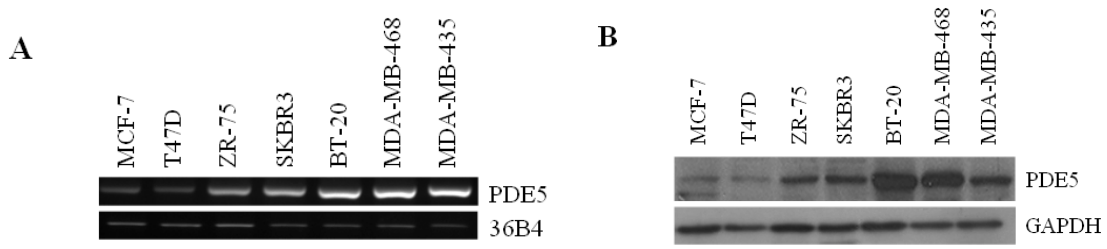

Figure 1. Expression levels of PDE5 in breast cancer cell lines of different molecular subtypes. A, RT-PCR analysis for PDE5 and 36B4 (internal standard) mRNA levels in Luminal A-type (MCF-7/T47D), Luminal B-like (ZR-75), HER2-overexpressing (SKBR3) and basal-like (BT-20/MDA-MB-468/MDA-MB-435) breast cancer cells. **B**, Immunoblotting for PDE5 expression in indicated cells. GAPDH, control for equal loading and transfer.

PDE5 overexpression affects motility and invasion of MCF-7 breast cancer cells.

In order to explore PDE5's role in breast cancer growth and progression, a breast tumor cell line that expresses the lowest levels of this enzyme, MCF-7, was chosen to generate breast cancer *in vitro* models exhibiting forced PDE5 overexpression. For direct visualization of PDE5 cellular location, the corresponding cDNA was cloned in frame with enhanced-green-fluorescent-protein (EGFP) in the mammalian expression vector pEGFP-C1 and stable clones were screened using fluorescence microscopy (Fig. 2A). Parental MCF-7 breast cancer cells are shown along with one clone stable expressing EGFP (MCF-7 e.v.) and three clones expressing cytoplasmic EGFP-PDE5 (PDE5 1/2/3). This was further evaluated by immunoblotting detection, showing the presence of an exogenous PDE5 band (EGFP-tagged, ~125 kDa) in protein extracts from PDE5-overexpressing stable clones (Fig. 2B). We used these experimental models to first investigate whether PDE5 overexpression may cause any changes in cellular phenotypes, including proliferation, migration, and invasion. Anchorage-dependent growth assays revealed a slight, but significant increase in cell proliferation in all three PDE5 clones compared to vector-expressing cells (Fig. 2C). We then evaluated the ability of PDE5 overexpression to influence cell migration in wound-healing scratch assays and found that PDE5-expressing cells moved the farthest in either direction to close the gap compared with vector-expressing cells (Fig. 2D). Given the evident enhancement of motility in PDE5-overexpressing cells, the capacity of cells to migrate across uncoated membrane in transmigration assays or invade an artificial basement membrane Matrigel in invasion assays was also tested. Although vector-expressing cells exhibited little motile and no invasive behavior *in vitro*, our data clearly showed that PDE5 overexpression significantly increased both motility and invasion of MCF-7 cells (Fig. 2E and F respectively).

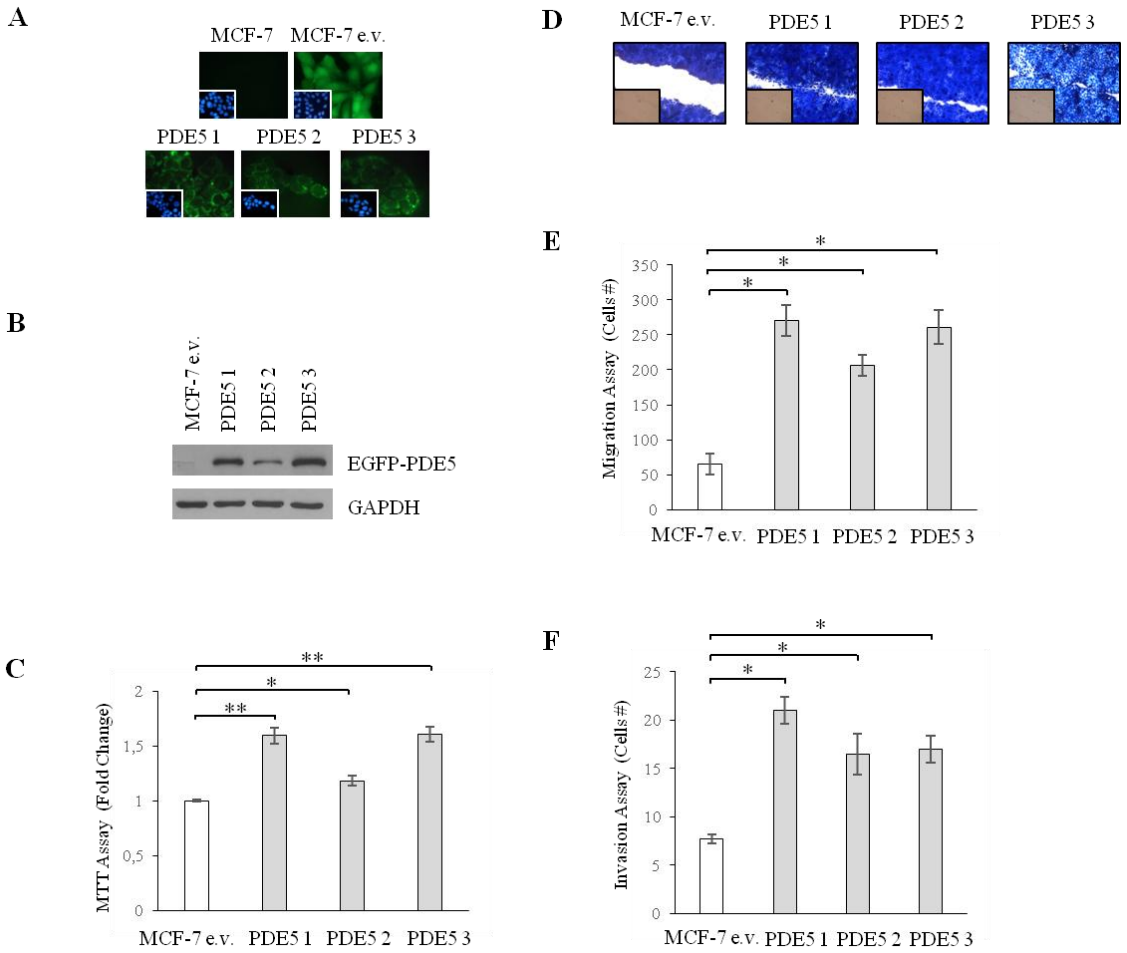

Figure 2. Impact of PDE5 overexpression on MCF-7 breast cancer cell proliferation, motility and invasion. A, Fluorescence-microscopic analysis to visualize EGFP-fluorescence in MCF-7 cells stably transfected with pEGFP-C1 (e.v.) or fusion protein expression pEGFP-PDE5A vectors (PDE5 1/2/3). MCF-7 cells, negative control. Insets: DAPI, nuclear staining. **B**, Immunoblotting showing EGFP-PDE5 expression in e.v. and PDE5 1/2/3 MCF-7 cells. GAPDH, control for equal loading and transfer. MTT growth (**C**), wound-healing (**D**, insets: time 0), transmigration (**E**) and invasion (**F**) assays in cells under basal nonstimulated conditions. *p<0.05, **p<0.005.

To evaluate the effects of PDE5 inhibition on breast tumor cell migratory and invasive properties, cells were treated with the specific PDE5 inhibitor sildenafil (Fig. 3 A-C). We found that sildenafil treatment was able to completely restore in PDE5 1, 2 and 3 clones the less motile and weak invasive behavior similar to that of control MCF-7 e.v. cells. Interestingly, although at less extent, sildenafil caused a significant decrease in motility and invasion of vector-expressing cells (Fig. 3 A-C). This may suggest that

PDE5 activity is required for controlling migration and invasion processes also of malignant breast epithelial cells expressing low levels of the enzyme.

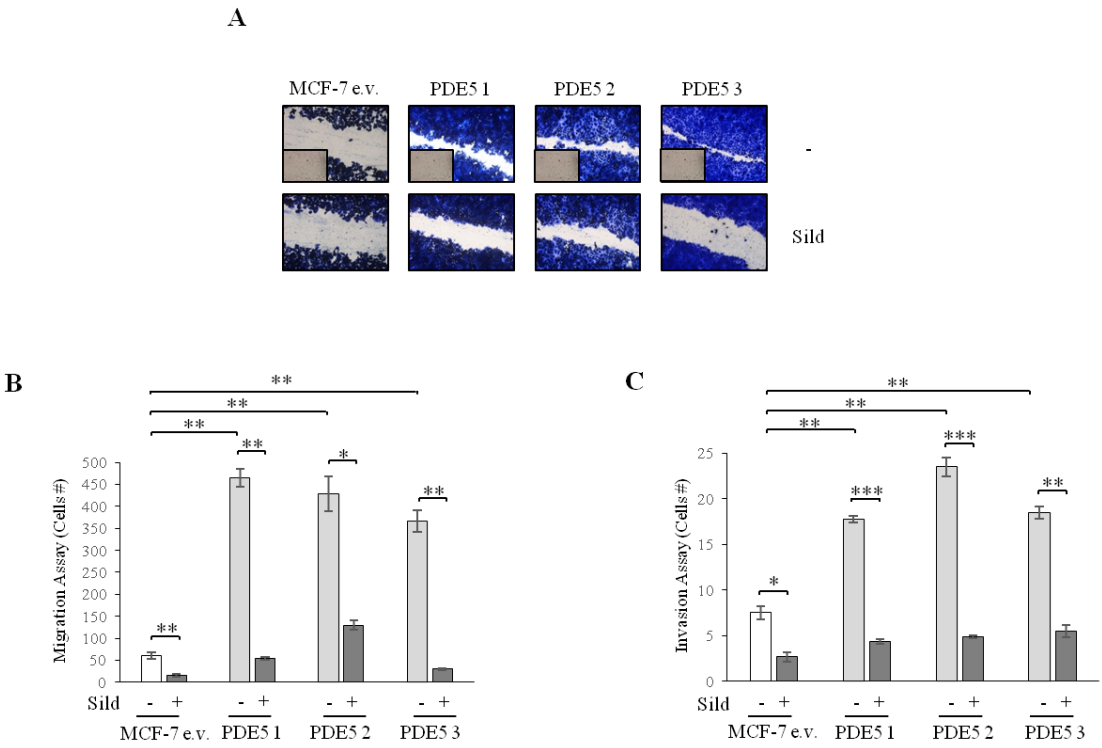

Figure 3. Effects of sildenafil on motility and invasion of PDE5-overexpressing MCF-7 breast cancer cells. Wound-healing (**A**, *insets*: time 0), transmigration (**B**) and invasion (**C**) assays in cells treated with vehicle (-) or sildenafil (Sild, 10μM). *****p<0.05, **p<0.005, ***p<0.0005.

Role of PDE5 in motility and invasion of T47D and MDA-MB-468 breast cancer cells.

To extend the results obtained, we transfected vector and PDE5-expression plasmids in T47D luminal A-like breast cancer cells (Fig. 4A). As previously shown for MCF-7 cells, we found a significant increase in both migratory and invasive cell potential when PDE5 was overexpressed and treatment with the selective PDE5 inhibitor sildenafil completely abrogated these effects (Fig. 4B and C). Again, PDE5 inhibition was associated with a significant reduction of motility and invasion also in vector-expressing cells (Fig. 4B and C). In addition, as a third confirmatory model we silenced PDE5 expression in MDA-MB-468 breast cancer cells, that express high levels of PDE5

compared to MCF-7 and T47D cells (Fig. 4D). Motility and invasion were significantly reduced in PDE5sh-transfected cells compared to control shRNA-transfected cells (Fig. 4E and F). Thus, PDE5 may be an important determinant of breast tumor cell motility and invasion.

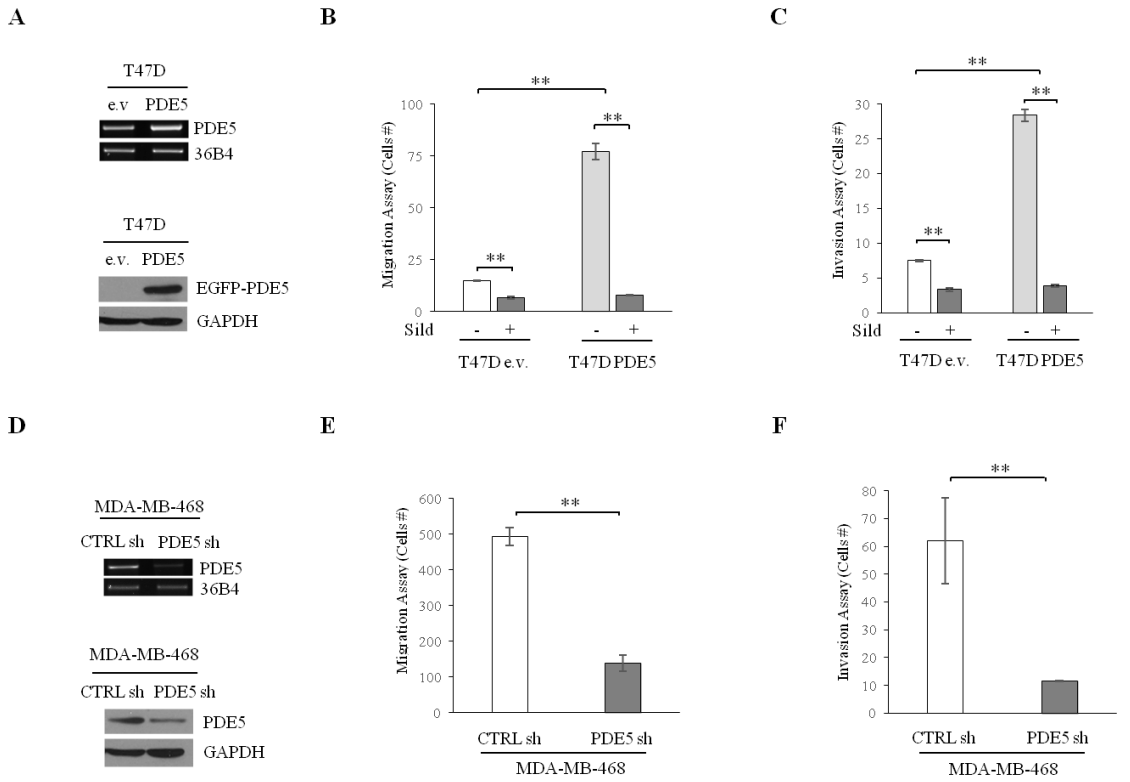

Figure 4. Influence of PDE5 on T47D and MDA-MB-468 breast cancer cell motility and invasion. A, RT-PCR (*upper panel*) and immunoblot (*lower panel*) analyses for PDE5 expression in vector (e.v.) and PDE5-expressing T47D cells. 36B4, internal standard. GAPDH, control for equal loading and transfer. Transmigration (**B**) and invasion (**C**) assays in cells treated with vehicle (-) or sildenafil (Sild, 10µM). **D**, RT-PCR (*upper panel*) and immunoblot (*lower panel*) analyses for PDE5 expression in MDA-MB-468 cells transfected with control scrambled-shRNA (CTRLsh) and PDE5 shRNA (PDE5sh) constructs. 36B4, internal standard. GAPDH, control for equal loading and transfer. Transmigration (**E**) and invasion (**F**) assays in CTRLsh and PDE5sh transfected MDA-MB-468 cells. **p<0.005.

PDE5-overexpressing cells exhibit increased Rho GTPase activation.

To gain insights into the biological properties of the highly migratory and invasive PDE5-expressing breast cancer cells, quantitative transcriptome profiling of vector- and PDE5-overexpressing MCF-7 cells was carried out by RNA-sequencing analysis. Comparison of the whole transcriptome of the two cell models revealed 4425 differentially expressed genes (FDR<0.05), of which 611 were up-regulated and 468 were down-regulated in response to PDE5 overexpression (fold change≥1.5). These genes were next subjected to Ingenuity Pathway Analysis (IPA) to rank enriched biological processes (Fig. 5A), and to calculate the activation z-score of molecular and cellular functions and pathways (Fig. 5B and C). In line with our previous experiments, cellular movement was the most significantly overrepresented biological process in PDE5-expressing cells. In addition, many differentially expressed genes were involved in cell death and survival, cell-to-cell signaling and interaction, cell growth and proliferation, cellular development, thus concurring to identify the five top enriched functional categories in PDE5 clones (Fig. 5A). Interestingly, analyzing the functions involving differentially expressed genes, migration of cells and cell movement resulted to be highly activated by PDE5 overexpression (Fig. 5B). Then, considering the most affected pathways by PDE5 overexpression, we found marked changes in the activity of Rho GTPase family, with RhoA, Cdc42 and Rac signalings showing activation z-score of 1.9, 1.342, and 0.302, respectively (Fig. 5C).

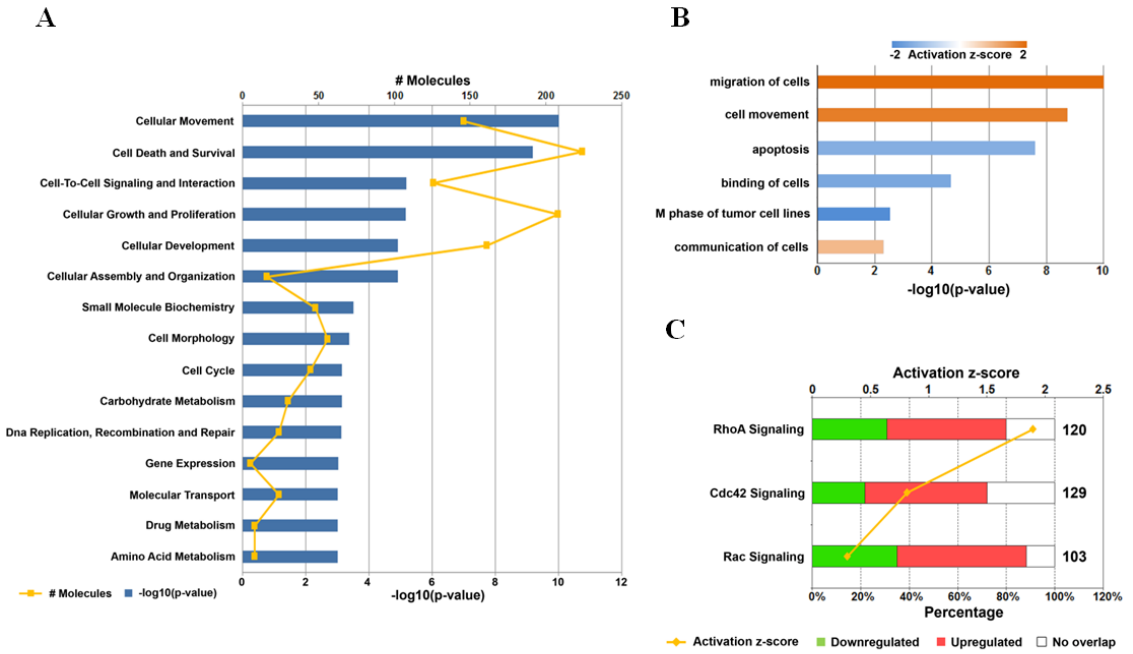

Figure 5. Biological processes, functions and pathways identified from RNA sequencing data in PDE5-overexpressing MCF-7 cells. Ingenuity Pathway Analysis (IPA) used to identify biological processes significantly associated with differentially expressed genes (**A**) and to calculate activation z-score of biological functions (**B**) and pathways (**C**).

The predicted activation of these canonical pathways was confirmed using molecule activity predictor analysis of IPA (Fig. 6). An enriched Rho GTPases signaling profile is consistent with the enhanced migration and invasion capabilities of PDE5-expressing cells, as these proteins are known to govern cell cytoskeleton organization, migration, and metastasis dissemination (Schmitz A.A. et al., 2000).

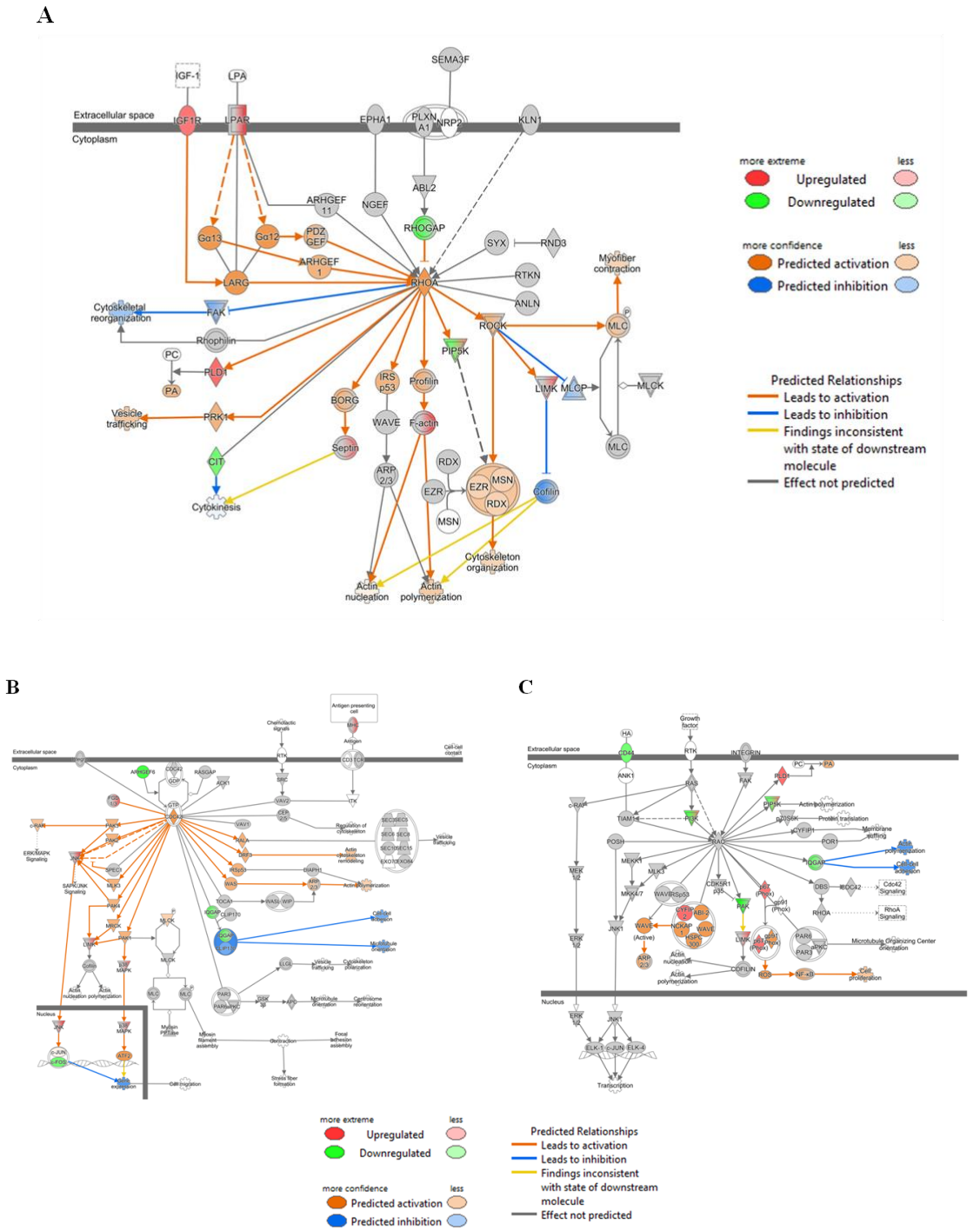

Figure 6. Molecule activity predictor analysis of Ingenuity Pathway Analysis. Predicted activation of RhoA signaling (**A**), Cdc42 signaling (**B**) and Rac signaling (**D**) pathways by molecule activity predictor analysis of IPA in PDE5-overexpressing versus vector-transfected MCF-7 cells.

To validate the gene expression profile identified by RNA sequencing, we compared expression and activation of Rho family of GTPases in vector and PDE5 clones. Increased protein levels of Rho A-C, Cdc42 and Rac 1-3 (Fig. 7A, *input panel*) along with increased levels of activated forms (Fig. 7A, *GTP-bound panel*) were detected in PDE5-overexpressing cells. In the GTP-bound form, these proteins are able to interact with effector molecules (i.e. mainly the Rho kinase ROCK and the p21-activated kinase PAK1) to induce phosphorylation of LIM Kinase (LIMK), which is able to inhibit (by phosphorylation) Cofillin, leading to stabilization of filamentous actin structures (Bishop A.L. et al., 2000). ROCK has also been shown to phosphorylate the regulatory Myosin Light Chain (MLC), which enhances its binding to F-actin (Riento K. et al., 2003). Consistent with increased Rho GTPase activation, the levels of phosphorylated LIMK, Cofillin and MLC are greatly increased in PDE5 clones compared to e.v. cells (Fig. 7B and C). Among other downstream targets of Rho signaling, c-Myc and NF-κB are important for cell motility and invasion (Bishop A.L. et al., 2000; Helbig G. et al., 2003; Liu S. et al., 2009). In PDE5-overespressing cells, we detected elevated levels of the activated form of c-Myc (phospho c-Myc) (Fig. 7D), whereas we did not observe NF-κB activation, as evidenced by no changes in phosphorylation of the inhibitor of NF-κB (IκB protein) as well as in NF-κB nuclear translocation (Fig. 7E and F). To further investigate the role of Rho GTPases activation on cytoskeletal organization in our model systems, we evaluated the formation of stress fibers, since they provide the contractile force required for motility (Fig. 7G). In vector-expressing cells actin filament remained diffusely distributed in the cytoplasm, while overexpression of PDE5 resulted in visible stress fiber formation.

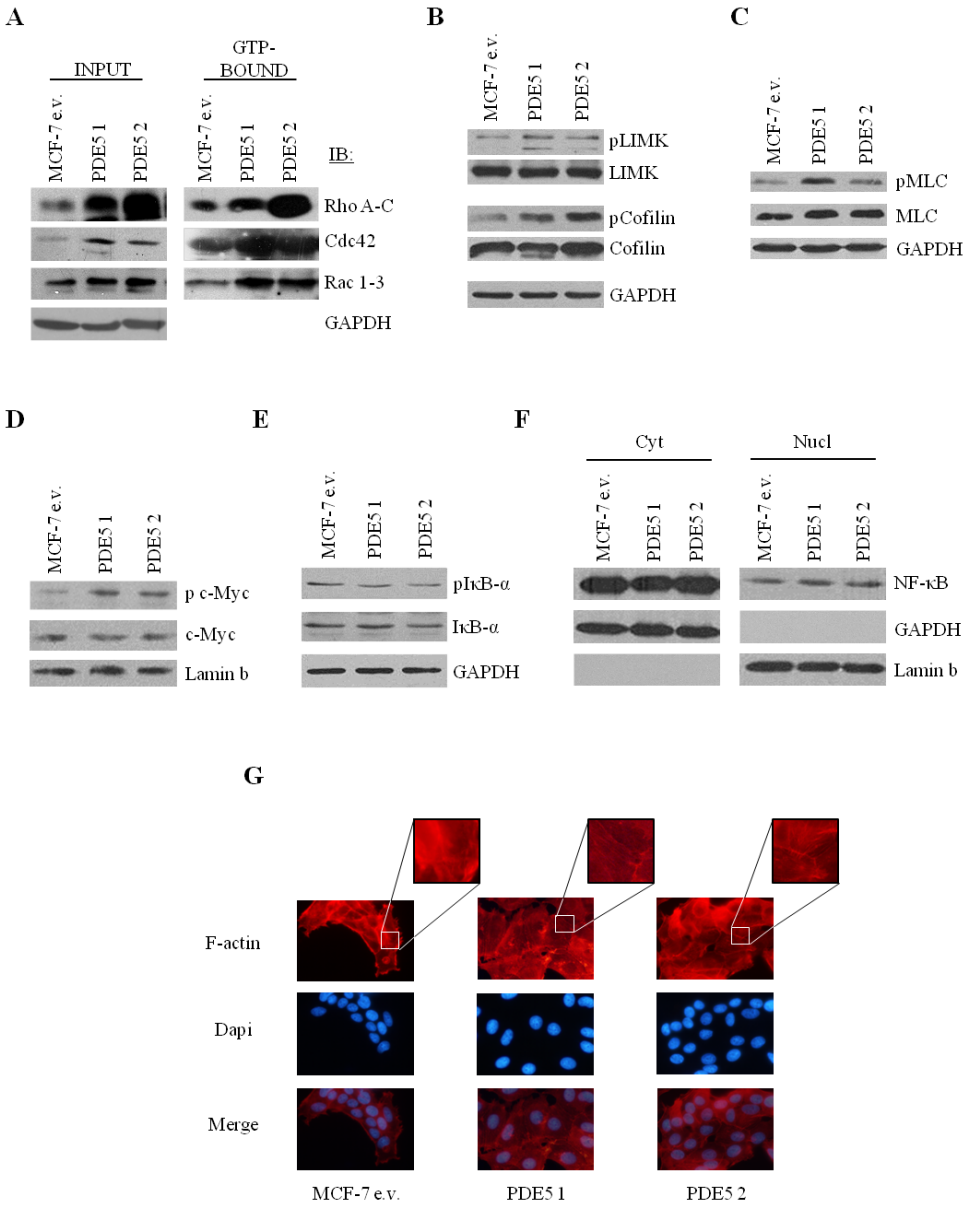

Figure 7. Rho GTPase activation in PDE5-overexpressing MCF-7 cells. A, *Input panel*, immunoblotting for Rho A-C, Cdc42 and Rac 1-3 expression. *GTP-bound panel*, activation assays of Rho A-C, Cdc42 and Rac 1-3. Immunoblotting showing phosphorylated LIM Kinase (pLIMK1^{Thr508}/pLIMK2^{Thr505}), Cofilin (p-Cofilin^{Ser3}) (**B**), Myosin Light Chain (pMLC$^{Thr18/Ser19}$) (**C**) and total proteins from whole-cell lysates. GAPDH, control for equal loading and transfer. **D**, Immunoblotting analysis showing phosphorylated (p) c-Myc$^{Thr58/Ser62}$ and total c-Myc proteins from nuclear extracts from vector (e.v.) and PDE5-expressing MCF-7 cells. Lamin b was used as a control for equal loading and transfer. **E**, Immunoblotting analysis showing phosphorylated nuclear factor of kappa light polypeptide gene enhancer in B-cells inhibitor (pIκB-α$^{Ser32/36}$) and total IkB-α proteins from whole-cell lysates from vector- and PDE5-expressing MCF-7 cells. GAPDH was used as a control for equal loading and transfer. **F**, Activation of NF-κB induced by its translocation to the nucleus was evaluated by immunoblot analysis of cytosolic (Cyt) and nuclear (Nucl) extracts from e.v. and PDE5-expressing cells. GAPDH and Lamin b were used as loading controls for cytosolic and nuclear extracts, respectively. Blots show a single representative of three independent experiments. **G**, Phalloidin staining of F-actin (stress fibers, red). DAPI, nuclear staining. Insets: Stress fibers with higher resolution.

According to all these results, treatment with the selective ROCK inhibitor Y-27632 was able to significantly reduce both migration and invasion of PDE5 clones (Fig. 8A and B). Collectively, our data strongly suggest that the molecular and cellular functions identified with IPA are biologically relevant and PDE5 may regulate motility and invasion through activation of the Rho family of GTPases.

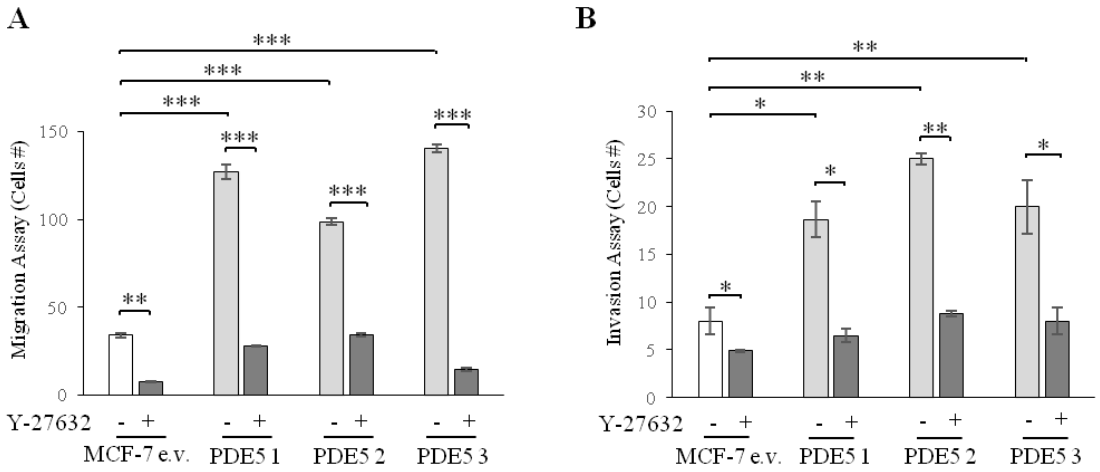

Figure 8. Effects of ROCK inhibitor on PDE5 MCF-7 clones. Transmigration **(A)** and invasion **(B)** assays in cells treated with vehicle (-) or the ROCK inhibitor Y-27632 (10 μM). *p<0.05, **p<0.005, ***p<0.0005.

PDE5 expression in human breast cancers.

To evaluate the clinical significance of PDE5 in human breast tumors, we analyzed its expression levels in patient-derived tissues (n=35) by immunohistochemistry analysis. We found that ~85% of cases showed cytoplasmic staining for PDE5 in cancer cells. Interestingly, ER/PR-positive tumors exhibited weak (n=5) or intermediate (n=15) PDE5 staining, while the strongest staining intensity was observed among HER2-positive or triple negative (TN) samples (n=15). In contrast, in non-neoplastic (NN) breast tissues (n=3), a weak to missing PDE5 expression was detected in the cytoplasm. Representative images of PDE5 staining patterns are shown in Figure 9A. Accordingly, PDE5 expression had a significant inverse correlation with ER and PR status (Fig. 9B and C) and a significant positive correlation with HER2 status (Fig. 9D). Of note, as the staining intensity of PDE5 increases, grading of cancer cells also tended to increase (p =

0.001), indicating that the higher expression of PDE5 might be related with a higher malignancy phenotype. We then correlated PDE5 expression with the different subtypes of breast carcinoma and found that its cytoplasmic expression was significantly different among the four molecular subtypes (Fig. 9E). In particular, in HER-2 and triple-negative subtypes, PDE5 expression was the highest, followed by the luminal B-type and the luminal A-type, that showed the lowest percentage of cells with PDE5 expression. Since HER2- and TN-types are correlated with a generally more aggressive tumor phenotype and poorer prognosis (Yang X.R. et al., 2007), these results suggest that PDE5 overexpression may be correlated with poor prognosis.

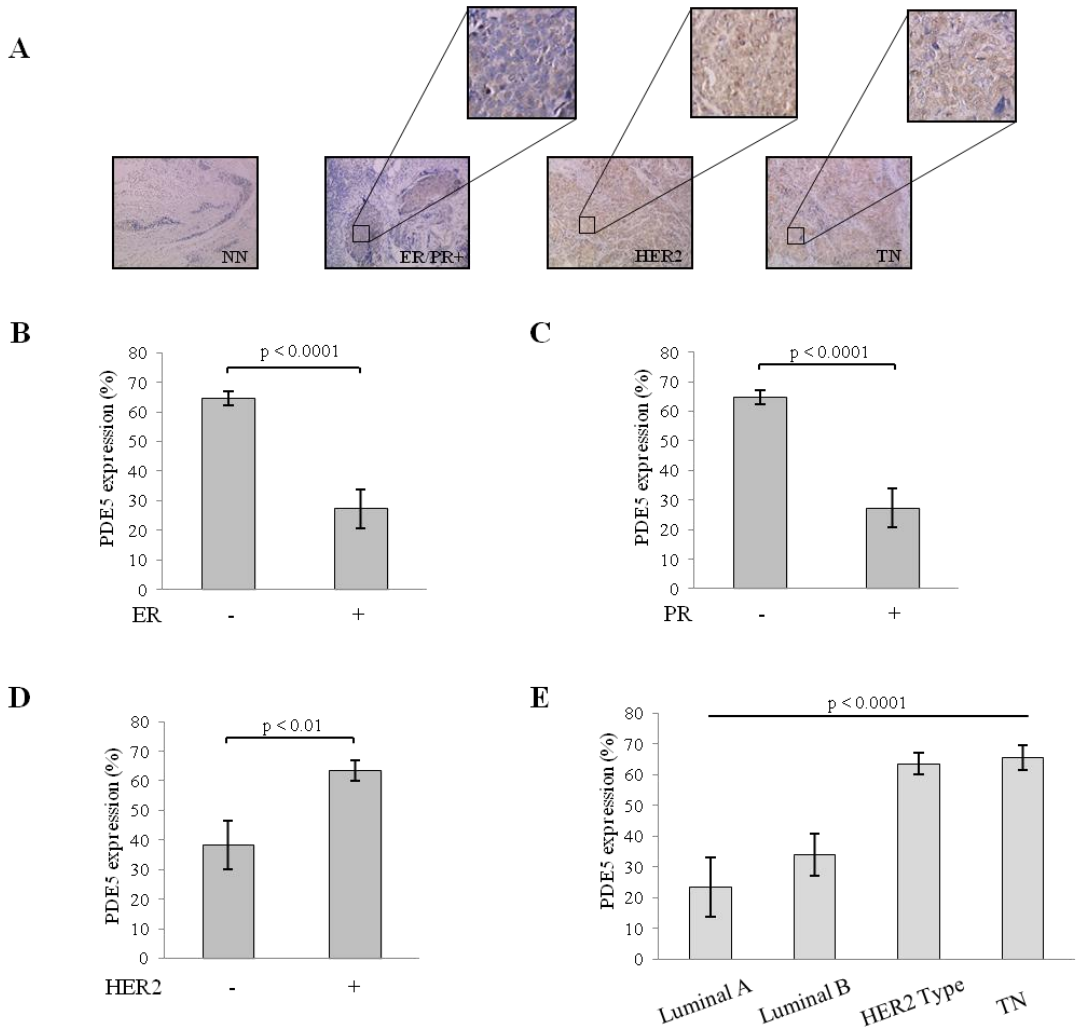

Figure 9. PDE5 expression in different subtypes of breast carcinomas. A, Immunohistochemical detection of PDE5 expression in non-neoplastic breast tissues (NN), ER/PR-positive (+), HER2-overexpressing (HER2) and triple–negative (TN) breast cancer tissues. Representative fields were photographed at 20X magnification (Insets: details of PDE5 subcellular localization). PDE5 immunohistochemical expression was correlated to ER **(B)**, PR **(C)**, HER2 **(D)** status or molecular subtypes **(E)** of breast cancer patients.

High levels of PDE5 are associated with shorter survival in breast cancer patients.

To strengthen the results obtained in human breast tumor tissues, we conducted retrospective analyses of the correlation between PDE5 expression and survival in patients with breast cancer. In the univariate analysis, the Kaplan-Meier overall survival (OS) curve obtained from a cohort of 1988 patients indicated that increased expression levels of PDE5 are associated with a statistically significant shorter OS when compared to those tumors expressing low levels of PDE5 (p=0.014, HR=1.2, Fig. 10A). Interestingly, significant difference could also be observed between OS for ER-positive patients having high or low PDE5 levels (p=7.4E-04, HR=1.4, Fig. 10B), suggesting a role for PDE5 in predicting disease progression in ER-positive tumors that according to immunohistochemistry may have lower levels of the enzyme compared to ER-negative ones. In addition, PDE5 retained its significance when performing a multivariate analysis including PDE5 expression, ER, HER2 and lymphnode status in the entire database (PDE5: p=6.6E-03, HR=1.24, ER status: p=6.6E-05, HR=0.69, HER2 status: p=1E-05, HR=1.6, lymph node status: p=1.1E-06, HR=2.24). Therefore, high levels of PDE5 expression may independently predict poor outcome among breast cancer patients.

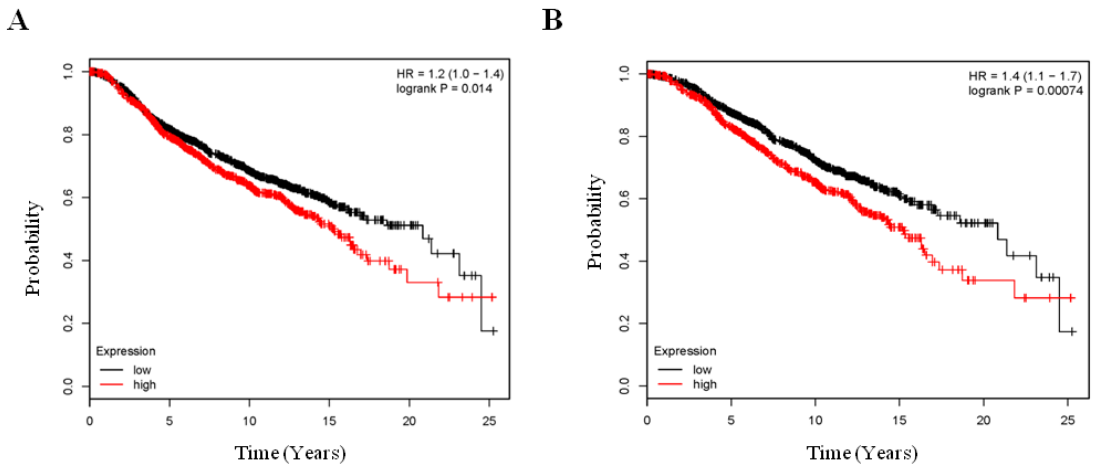

Figure 10. Role of PDE5 in breast cancer patients. Kaplan-Meier survival analysis relating PDE5 levels and overall survival in all patients **(A)** or in patients with ER-positive breast cancers **(B)**.

Discussion

Discussion

Despite vast improvement in the overall survival rate of breast cancer patients, advanced metastatic disease remains a life-threatening stage of cancer. One of the major challenges in mammary cancer research is to identify key proteins that are directly involved in pathways promoting tumorigenesis and tissue invasion. These proteins can then be explored as early markers for invasive tumors as well as potential targets for the development of therapeutic strategies aimed at controlling and curing malignant disease. In this report, we show that phosphodiesterase type 5 (PDE5) is differentially expressed in human breast cancer subtypes, with a significant positive correlation with tumor grading. Importantly, high PDE5 levels predict a worse prognosis for patients at 8-year median follow-up. In experimental breast cancer models, PDE5 overexpression increased motile and invasive properties of cells through activation of the Rho family of GTPases, highlighting the potential benefit of therapeutic targeting PDE5.

Breast cancer is a complex and highly heterogeneous disease due to its diverse morphological features, variable clinical outcomes and disparate therapeutic responses. By using hierarchical clustering analysis of gene expression profiling, Perou et al. were able to identify molecularly-defined and clinically-distinct classes of breast cancer (Luminal, HER2-enriched, basal-like and normal-like) (Perou C.M. et al., 2000; Sørlie T. et al., 2001). Due to the prognostic and predictive values of this molecular classification in clinical setting, attempts have been made to identify surrogate markers that would allow subtype identification using the more familiar immunohistochemical approach. Accordingly, the combined evaluation of histopathological grade and immunohistochemical parameters (ER/PR/HER2) would approximate the molecular classification of Luminal A, Luminal B, HER2-enriched and triple-negative breast cancers (Carey L.A. et al., 2006; Yang X.R. et al., 2007; Collins L.C. et al., 2012). Despite the lack of complete overlapping, the panelists of the last St. Gallen Consensus have endorsed the use of the immunohistochemical assays to identify breast cancer subtypes and allow the physicians to tailor properly the systemic interventions (Goldhirsch A. et al., 2011). Here, we found a significant increase in PDE5 expression in breast tumors when compared to non-neoplastic breast tissues. Although ~85% of the tumor entities examined showed cytoplasmic staining for PDE5, our results clearly

indicate that PDE5 is differentially expressed between each molecular breast cancer subset. In particular, the lowest expression of this enzyme is detected in the more favorable Luminal A subtypes of breast tumors, whereas its overexpression is closely related to breast cancers of high histological grade including triple-negative and HER2-positive molecular subtypes. Accordingly, PDE5 levels have a negative correlation with hormone receptor status, and a positive one with HER2 status and tumor grading. The clinical significance of PDE5 overexpression is strongly supported by its significant association with a shorter overall survival time in retrospective studies. This association is also significant in patients with ER-positive diseases, advocating the utility of PDE5 as a predictor of breast cancer prognosis in ER-positive tumors that immunohistochemically may have lower PDE5 levels compared to ER-negative ones. In line with findings on patients, PDE5 expression also varies among different breast cancer cell line models. Taken together, our results suggest that the differential expression of PDE5 may contribute to breast cancer heterogeneity and, being PDE5 a known druggable target, it could help to integrate subsets of aggressive breast cancer into clinically meaningful subtypes.

At the present time, the selective PDE5 inhibitors sildenafil (Viagra and Revatio-Pfizer) and tadalafil (Cialis-Eli Lilly; Adcirca-United Therapeutics) have Food and Drug Administration approval for the treatment of erectile dysfunction (ED) as well as pulmonary artery hypertension; whereas vardenafil (Levitra and Vivanza-Bayer) and avanafil (Stendra-Vivus) are approved only for ED. However, due to their favorable toxicity profile (Nehra A., 2009), these agents are being investigated in a wide range of other potential medical and surgical applications, including neurological and cardiovascular disorders, transplant and reconstructive surgery, and several clinical trials are currently in progress (Kloner R.A. et al., 2011) (htpp://www.clinicaltrials.gov). In the last ten years, various PDE5 inhibitors have been also reported to inhibit growth and induce apoptosis in many cancer cell lines, without affecting normal epithelial cells (Piazza G.A. et al., 2001; Sarfati M. et al., 2003; Whitehead C.M. et al., 2003; Tinsley H.N. et al., 2009; Savai R. et al., 2010; Li N. et al., 2013). Recently, two reports have suggested a role for PDE5 inhibition in influencing cancer cell motility (Marino N. et al., 2014; Sponziello M. et al., 2015). Indeed, tadalafil and sildenafil reduced the capacity of thyroid cancer cells to migrate at lower doses than those used to block proliferation

(Sponziello M. et al., 2015). Similarly, down-regulation of PDE5 in the aggressive human breast cancer cell line MDA-MB-231T resulted in no difference in cell proliferation and reduced motility *in vitro* and *in vivo* (Marino N. et al., 2014). Here, we show that genetic and pharmacological inhibition of PDE5 significantly decreases migration and invasion of different human breast cancer cell lines. In contrast, overexpression of PDE5 strongly increases motility and invasion of MCF-7 cells and sildenafil treatment completely restores in PDE5 stable clones the less motile and weak invasive behavior similar to that of control cells. Interestingly, although at less extent, a reduction of migration and invasion was observed after treatment with sildenafil also in vector cells, expressing lower levels of the enzyme, further highlighting a role for PDE5 in controlling migration and invasion processes of malignant breast epithelial cells. Increased formation of actin stress fibers and enhanced contractility are common features of motile cells in 2D culture conditions (Ridley A.J. et al., 2003). Indeed, immunofluorescent staining of polymerized actin (F-actin) reveals an induced formation of stress fibers in cells bearing PDE5 overexpression. Accordingly, ingenuity pathway analysis on PDE5 modulated genes by RNA-sequencing highlights cellular movement as the most significantly represented biological process. Moreover, most of the genes differentially regulated by PDE5 overexpression are significantly involved in migration of cells. Taken together, these results indicate that PDE5 may be important for sustaining malignant motile and invasive behavior of breast cancers. The acquisition of a remodeled cytoskeleton and a motile phenotype are important steps in tissue invasion and metastasis establishment, and the Rho family of GTP-binding proteins have been reported to mediate these processes. Although at least 20 Rho family proteins have been identified in humans, the most widely characterized molecules for their effects on cell migration are Rho A-C, which regulate stress fibers and focal adhesion formation, and Rac 1-3 and Cdc42, which control membrane ruffling, and filopodium formation (Schmitz A.A. et al., 2000). In the GTP-bound form, these proteins are able to interact with effector molecules to regulate actin cytoskeleton assembly and organization through phosphorylation of specific substrates, such as Cofilin or Myosin Light Chain, as well as to modulate a variety of other biochemical signalings involved in cell transformation and metastasis, including the c-Myc pathway (Bishop A.L. et al., 2000; Riento K. et al., 2003; Liu S. et al., 2009). In breast tumors, Rho expression and/or

activity are frequently increased (Vega F.M. et al., 2008). On the other hand, a complex signaling interplay between cGMP and Rho GTPase pathways has been described. For instance, cGMP-PKG cascade inhibits RhoA in various cell types (Sawada N. et al., 2001; Sauzeau V. et al., 2003). Similarly, vardenafil prevents RhoA membrane translocation/activation, and decreases activity of its downstream effector ROCK in human bladder smooth muscle cells, inhibiting endothelin-1-induced migration (Morelli A. et al., 2009). On the molecular level, increased levels of total and activated Rho A-C, Cdc42 and Rac 1-3 are detected in PDE5-overexpressing cells compared with vector cells. Phosphorylation levels of Rho GTPase downstream targets, including LIM Kinase, Cofillin, Myosin Light Chain and c-Myc, are also greatly increased in PDE5 clones compared to vector cells. Moreover, transcriptome analysis identifies an enriched Rho GTPase signaling profile in PDE5-overexpressing cells. Consistent with these findings, a selective ROCK inhibitor significantly reduces both migration and invasion of PDE5 clones.

In conclusion, results of this study highlight a novel role for PDE5 in controlling malignant breast epithelial cell behavior and provide the first indications for the clinical relevance of this enzyme in human breast cancers. Since PDE5 overexpression greatly enhances the invasive potential of breast cancer cells and reduces survival in patients, it is tempting to speculate that this enzyme may represent a novel prognostic biomarker candidate. In addition, having already addressed the delivery, stability and toxicity issues of PDE5 inhibitors in other diseases, our findings may offer promising insights into future cancer treatments by providing the rationale to implement safer and more efficacious drugs in the adjuvant therapy for improving clinical care and reducing mortality from breast cancer. This may assume particular significance in triple-negative breast cancers in which PDE5 may be an attractive target. Based on these observations, it is evident that the impact of PDE5 in the prediction of the risk, and the treatment of breast cancer patients deserves further attention.

Translational Relevance

Translational Relevance

Although early detection and conventional therapies have changed the natural history of breast cancer, many patients die from progressive advanced disease. Dissection of the mechanisms underlying breast cancer progression may identify early markers for invasive tumors as well as specific targeted therapeutics, providing further improvement in the clinical outcomes of patients. This study recognizes a novel function for phosphodiesterase (PDE) type 5 in controlling malignant breast epithelial cell behavior, and provides important clinical implications that can impact the prediction of the risk, and the treatment of breast cancer patients. First, since enhanced PDE5 expression promotes the invasive potential of breast cancer cells and predicts a worse survival in patients, this enzyme may represent a valuable molecular candidate with prognostic significance. In addition, being PDE5 a known druggable target, our findings may be promising for antitumor therapy with reduced adverse effects. Certainly, future studies could clarify the role of PDE5 in breast cancer.

References

Anant JS, OngOC, XieHY, Clarke S, O'Brien PJ, Fung BK. In vivo differential prenylation of retinal cyclicGMPphosphodiesterase catalytic subunits. J Biol Chem. 1992; 267: 687–690.

Anders S, Pyl PT, Huber W. HTSeq--a Python framework to work with high-throughput sequencing data. Bioinformatics 2015; 31: 166-9.

Archer SL, Michelakis ED. Phosphodiesterase type 5 inhibitors for pulmonary arterial hypertension. N Engl J Med. 2009; 361: 1864-1871.

Azevedo MF, Faucz FR, Bimpaki E, Horvath A, Levy I, de Alexandre RB, Ahmad F, Manganiello V, Stratakis CA. Clinical and molecular genetics of the phosphodiesterases (PDEs). Endocr Rev. 2014; 35(2): 195-233.

Baillie GS, MacKenzie SJ, McPhee I, Houslay MD. Subfamily selective actions in the ability of Erk2 MAP kinase to phosphorylate and regulate the activity of PDE4 cyclic AMP-specific phosphodiesterases. Br J Pharmacol. 2000; 131: 811–819.

Barone I, Catalano S, Gelsomino L, Marsico S, Giordano C, Panza S, Bonofiglio D, Bossi G, Covington KR, Fuqua SA, Andò S. Leptin mediates tumor-stromal interactions that promote the invasive growth of breast cancer cells. Cancer Res 2012; 72: 1416-27.

Barone I, Giordano C, Bonofiglio D, Catalano S, Andò S. Phosphodiesterase Type 5 as a Candidate Therapeutic Target in Cancers. Curr Pathobiol Rep. 2015; 3: 193–201

Bender AT, Beavo JA. Cyclic nucleotide phosphodiesterases: molecular regulation to clinical use. Pharmacol Rev. 2006; 58: 488-520.

Bishop AL,Hall A. Rho GTPases and their effector proteins. Biochem J. 2000; 348 Pt 2: 241-55.

Black KL, Yin D, Ong JM, Hu J, Konda BM, Wang X, Ko MK, Bayan JA, Sacapano MR, Espinoza A, Irvin DK, Shu Y. PDE5 inhibitors enhance tumor permeability and efficacy of chemotherapy in a rat brain tumor model. Brain Res. 2008; 1230: 290-302.

Bolstad BM, Irizarry RA, Astrand M, Speed TP. A comparison of normalization methods for high density oligonucleotide array data based on variance and bias. Bioinformatics 2003; 19: 185-93.

Browning DD. Protein kinase G as a therapeutic target for the treatment of metastatic colorectal cancer. Expert Opin. Ther. Targets 2008; 12: 367–376.

Butcher RW, Sutherland EW. Adenosine 3',5'-phosphate in biological materials. I. Purification and properties of cyclic 3',5'-nucleotide phosphodiesterase and use of this enzyme to characterize adenosine 3',5'-phosphate in human urine. J Biol Chem. 1962; 237: 1244-50.

Calverley PM, Sanchez-Toril F, McIvor A, Teichmann P, Bredenbroeker D, Fabbri LM. Effect of 1-year treatment with roflumilast in severe chronic obstructive pulmonary disease. Am J Respir Crit Care Med. 2007; 176(2): 154-61.

Carey LA, Perou CM, Livasy CA, Dressler LG, Cowan D, Conway K, Karaca G, Troester MA, Tse CK, Edmiston S, Deming SL, Geradts J, Cheang MC, Nielsen TO, Moorman PG, Earp HS, Millikan RC. Race, breast cancer subtypes, and survival in the Carolina Breast Cancer Study. JAMA 2006; 295: 2492-502.

Chan DC, Earle KA, Zhao TL, Helfrich B, Zeng C, Baron A, Whitehead CM, Piazza G, Pamukcu R, Thompson WJ, Alila H, Nelson P, Bunn PA Jr. Exisulind in combination with docetaxel inhibits growth and metastasis of human lung cancer and prolongs survival in athymic nude rats with orthotopic lung tumors. Clin Cancer Res. 2002; 8: 904-912.

Chen JJ, Sun YL, Tiwari AK, Xiao ZJ, Sodani K, Yang DH, Vispute SG, Jiang WQ, Chen SD, Chen ZS. PDE5 inhibitors, sildenafil and vardenafil, reverse multidrug resistance by inhibiting the efflux function of multidrug resistance protein 7 (ATP binding Cassette C10) transporter. Cancer Sci. 2012; 103: 1531-1537.

Collins LC, Marotti JD, Gelber S, Cole K, Ruddy K, Kereakoglow S, Brachtel EF, Schapira L, Come SE, Winer EP, Partridge AH. Pathologic features and molecular phenotype by patient age in a large cohort of young women with breast cancer. Breast Cancer Res Treat 2012; 131: 1061-6.

Coquil JF, Franks DJ, Wells JN, Dupuis M, Hamet P. Characteristics of a new binding protein distinct from the kinase for guanosine 3’:5’-monophosphate in rat platelets. Biochim Biophys Acta. 1980; 631: 148–165.

Corbin JD, Turko IV, Beasley A, Francis SH. Phosphorylation of phosphodiesterase-5 by cyclic nucleotide-dependent protein kinase alters its catalytic and allosteric cGMP-binding activities. Eur J Biochem. 2000; 267(9): 2760-7.

Corbin JD. Mechanisms of action of PDE5 inhibition in erectile dysfunction. Int J Impot Res. 2004; 16: S4-S7.

Cruickshank JM. Phosphodiesterase III inhibitors: long-term risks and short-term benefits. Cardiovasc Drugs Ther. 1993; 7(4): 655-60.

Curtis C, Shah SP, Chin SF, Turashvili G, Rueda OM, Dunning MJ, Speed D, Lynch AG, Samarajiwa S, Yuan Y, Gräf S, Ha G, Haffari G, Bashashati A, Russell R, McKinney S; METABRIC Group, Langerød A, Green A, Provenzano E, Wishart G, Pinder S, Watson P, Markowetz F, Murphy L, Ellis I, Purushotham A, Børresen-Dale

AL, Brenton JD, Tavaré S, Caldas C, Aparicio S. The genomic and transcriptomic architecture of 2,000 breast tumours reveals novel subgroups. Nature 2012; 486: 346-52.

Dago DN, Scafoglio C, Rinaldi A, Memoli D, Giurato G, Nassa G, Ravo M, Rizzo F, Tarallo R, Weisz A. Estrogen receptor beta impacts hormone-induced alternative mRNA splicing in breast cancer cells. BMC Genomics 2015; 16: 367.

Das A, Durrant D, Mitchell C, Mayton E, Hoke NN, Salloum FN, Park MA, Qureshi I, Lee R, Dent P, Kukreja RC. Sildenafil increases chemotherapeutic efficacy of doxorubicin in prostate cancer and ameliorates cardiac dysfunction. Proc Natl Acad Sci USA. 2010; 107: 18202-18207.

Das A, Xi L, Kukreja RC. Protein kinase G-dependent cardioprotective mechanism of phosphodiesterase-5 inhibition involves phosphorylation of ERK and GSK3beta. J. Biol. Chem. 2008; 283: 29572–29585.

Dobesh PP, Stacy ZA, Persson EL. Pharmacologic therapy for intermittent claudication. Pharmacotherapy. 2009; 29(5): 526-53.

Dunkern TR, Hatzelmann A. The effect of sildenafil on human platelet secretory function is controlled by a complex interplay between phosphodiesterases 2, 3 and 5. Cell Signal. 2005; 17: 331-339.

Dunning MJ, Smith ML, Ritchie ME, Tavaré S. beadarray: R classes and methods for Illumina bead-based data. Bioinformatics 2007; 23: 2183-4.

Ekmekci TR, Kendirci M, Kizilkaya O, Koslu A. Sildenafil citrate-aided radiotherapy for the treatment of Kaposi's sarcoma of the penis. J Eur Acad Dermatol Venereol. 2005; 19: 603-604.

Essayan DM. Cyclic nucleotide phosphodiesterases. J Allergy Clin Immunol. 2001; 108: 671-680.

Fajardo AM, Piazza GA, Tinsley HN3. The role of cyclic nucleotide signaling pathways in cancer: targets for prevention and treatment. Cancers (Basel). 2014; 6(1): 436-58.

Fallahian F, Karami-Tehrani F, Salami S, Aghaei M. Cyclic GMP induced apoptosis via protein kinase G in oestrogen receptor-positive and -negative breast cancer cell lines. FEBS J. 2011; 278(18): 3360-9.

Faucz FR, Horvath A, Rothenbuhler A, et al. Phosphodiesterase 11A (PDE11A) genetic variants may increase susceptibility to prostatic cancer. J Clin Endocrinol Metab. 2011; 96: E135–E140.

Ferlay J, Soerjomataram I, Dikshit R, Eser S, Mathers C, Rebelo M, Parkin DM, Forman D, Bray F. Cancer incidence and mortality worldwide: sources, methods and major patterns in GLOBOCAN 2012. Int J Cancer 2015; 136: E359-86.

Francis SH, Blount MA, Corbin JD. Mammalian cyclic nucleotide phosphodiesterases: molecular mechanisms and physiological functions. Physiol Rev. 2011; 91: 651–690.

Francis SH, Busch JL, Corbin JD,Sibley D cGMP-dependent protein kinases and cGMP phosphodiesterases in nitric oxide and cGMP action. Pharmacol Rev 2010; 62: 525-63.

Francis SH, Corbin JD. Cyclic nucleotide-dependent protein kinases: Intracellular receptors for cAMP and cGMP action. Crit. Rev. Clin. Lab. Sci. 1999; 36: 275–328.

Francis SH, Lincoln TM, Corbin JD. Characterization of a novel cGMP binding protein from rat lung. J Biol Chem. 1980; 255: 620–626.

Gal A, Orth U, Baehr W, Schwinger E, Rosenberg T. Heterozygous missense mutation in the rod cGMP phosphodiesterase β-subunit gene in autosomal dominant stationary night blindness. Nat Genet. 1994; 7: 64–68.

Goldhirsch A, Wood WC, Coates AS, Gelber RD, Thürlimann B, Senn HJ; Panel members. Strategies for subtypes--dealing with the diversity of breast cancer: highlights of the St. Gallen International Expert Consensus on the Primary Therapy of Early Breast Cancer 2011. Ann Oncol. 2011; 22: 1736-47.

Goluboff ET, Prager D, Rukstalis D, Giantonio B, Madorsky M, Barken I, Weinstein IB, Partin AW, Olsson CA; UCLA Oncology Research Network. Safety and efficacy of exisulind for treatment of recurrent prostate cancer after radical prostatectomy. J Urol. 2001; 166: 882-886.

Goluboff ET, Shabsigh A, Saidi JA, Weinstein IB, Mitra N, Heitjan D, Piazza GA, Pamukcu R, Buttyan R, Olsson CA. Exisulind (sulindac sulfone) suppresses growth of human prostate cancer in a nude mouse xenograft model by increasing apoptosis. Urology.1999; 53: 440-445.

Gottlieb AB, Strober B, Krueger JG, Rohane P, Zeldis JB, Hu CC, Kipnis C. An open-label, single-arm pilot study in patients with severe plaque-type psoriasis treated with an oral anti-inflammatory agent, apremilast. Curr Med Res Opin. 2008; 24(5): 1529-38.

Gu G, Barone I, Gelsomino L, Giordano C, Bonofiglio D, Statti G, Menichini F, Catalano S, Andò S. Oldenlandia diffusa extracts exert antiproliferative and apoptotic effects on human breast cancer cells through ERalpha/Sp1-mediated p53 activation. J Cell Physiol 2012; 227: 3363-72.

Hamet P, Coquil JF. Cyclic GMP binding and cyclic GMP phosphodiesterase in rat platelets. J Cyclic Nucleotide Res. 1978; 4: 281–290.

Helbig G, Christopherson KW, Bhat-Nakshatri P, Kumar S, Kishimoto H, Miller KD, Broxmeyer HE, Nakshatri H. NF-kappaB promotes breast cancer cell migration and metastasis by inducing the expression of the chemokine receptor CXCR4. J Biol Chem. 2003; 278: 21631-8.

Holliday DL,Speirs V. Choosing the right cell line for breast cancer research. Breast Cancer Res 2011; 13: 215.

Holohan C, Van Schaeybroeck S, Longley DB, Johnston PG. Cancer drug resistance: an evolving paradigm. Nat Rev Cancer. 2013; 13(10): 714-26.

Hood J, Granger HJ. Protein kinase G mediates vascular endothelial growth factor-induced Raf-1 activation and proliferation in human endothelial cells. J Biol Chem. 1998; 273: 23504-23508.

Horvath A, Korde L, Greene MH, Libe R, Osorio P, Faucz FR, Raffin-Sanson ML, Tsang KM, Drori-Herishanu L, Patronas Y, Remmers EF, Nikita ME, Moran J, Greene J, Nesterova M, Merino M, Bertherat J, Stratakis CA. Functional phosphodiesterase 11A mutations may modify the risk of familial and bilateral testicular germ cell tumors. Cancer Res. 2009; 69: 5301–5306.

Horvath A, Mericq V, Stratakis CA. Mutation in PDE8B, a cyclic AMP-specific phosphodiesterase in adrenal hyperplasia. N Engl J Med. 2008; 358: 750–752.

Houslay MD, Baillie GS, Maurice DH. cAMP-Specific phosphodiesterase-4 enzymes in the cardiovascular system: a molecular toolbox for generating compartmentalized cAMP signaling. Circ Res. 2007; 100: 950–966.

Hu J, Ljubimova JY, Inoue S, Konda B, Patil R, Ding H, Espinoza A, Wawrowsky KA, Patil C, Ljubimov AV, Black KL. Phosphodiesterase type 5 inhibitors increase Herceptin transport and treatment efficacy in mouse metastatic brain tumor models. PLoS One. 2010; 5: e10108.

Huang SH, Pittler SJ, Huang X, Oliveira L, Berson EL, Dryja TP. Autosomal recessive retinitis pigmentosa caused by mutations in the α subunit of rod cGMP phosphodiesterase. Nat Genet. 1995; 11: 468–471.

Jedlitschky G, Burchell B, Keppler D. The multidrug resistance protein 5 functions as an ATP-dependent export pump for cyclic nucleotides. J Biol Chem. 2000; 275: 30069-30074.

Kambayashi J, Liu Y, Sun B, Shakur Y, Yoshitake M, Czerwiec F. Cilostazol as a unique antithrombotic agent. Curr Pharm Des. 2003; 9(28): 2289-302.

Karami-Tehrani F, Moeinifard M, Aghaei M, Atri M. Evaluation of PDE5 and PDE9 expression in benign and malignant breast tumors. Arch Med Res. 2012; 43: 470-5.

Ke H, Wang H. Crystal structures of phosphodiesterases and implications on substrate specificity and inhibitor selectivity. Curr Top Med Chem. 2007; 7(4): 391-403.

Kennecke H, Yerushalmi R, Woods R, Cheang MC, Voduc D, Speers CH, Nielsen TO, Gelmon K. Metastatic Behavior of Breast Cancer Subtypes. J Clin Oncol 2010; 28: 3271-3277.

Keravis T, Lugnier C. Cyclic nucleotide phosphodiesterase (PDE) isozymes as targets of the intracellular signalling network: benefits of PDE inhibitors in various diseases and perspectives for future therapeutic developments. Br J Pharmacol. 2012; 165: 1288–1305.

Keravis T, Lugnier C. Cyclic nucleotide phosphodiesterases (PDE) and peptide motifs. Curr Pharm Des. 2010; 16: 1114–1125.

Kim D, Pertea G, Trapnell C, Pimentel H, Kelley R, Salzberg SL. TopHat2: accurate alignment of transcriptomes in the presence of insertions, deletions and gene fusions. Genome Biol 2013; 14: R36.

Kloner RA, Comstock G, Levine LA, Tiger S, Stecher VJ. Investigational noncardiovascular uses of phosphodiesterase-5 inhibitors. Expert Opin Pharmacother. 2011; 12(15): 2297-313.

Kook H, Itoh H, Choi BS, Sawada N, Doi K, Hwang TJ, Kim KK, Arai H, Baik YH, Nakao K. Physiological concentration of atrial natriuretic peptide induces endothelial regeneration in vitro. Am J Physiol Heart Circ Physiol. 2003; 284: H1388-H1397.

Kotera J, Fujishige K, Imai Y, et al. Genomic origin and transcriptional regulation of two variants of cGMP-binding cGMP-specific phosphodiesterases. Eur J Biochem. 1999; 262: 866–873.

Kritzer MD, Li J, Dodge-Kafka K, Kapiloff MS. AKAPs: the architectural underpinnings of local cAMP signaling. J Mol Cell Cardiol. 2012; 52: 351–358.

Kukreja RC, Ockaili R, Salloum F, Yin C, Hawkins J, Das A, Xi L. Cardioprotection with phosphodiesterase-5 inhibition—a novel preconditioning strategy. J Mol Cell Cardiol. 2004; 36: 165-173.

Kumar P, Francis GS, Tang WH. Phosphodiesterase 5 inhibition in heart failure: mechanisms and clinical implications. Nat Rev Cardiol. 2009; 6: 349-355.

Kumazoe M, Sugihara K, Tsukamoto S, Huang Y, Tsurudome Y, Suzuki T, Suemasu Y, Ueda N, Yamashita S, Kim Y, Yamada K, Tachibana H. 67-kDa laminin receptor increases cGMP to induce cancer-selective apoptosis. J Clin Invest. 2013; 123: 787-799.

Kwon IK, Schoenlein PV, Delk J, Liu K, Thangaraju M, Dulin NO, Ganapathy V, Berger FG, Browning DD. Expression of cyclic guanosine monophosphate-dependent protein kinase in metastatic colon carcinoma cells blocks tumor angiogenesis. Cancer. 2008; 112(7): 1462-70.

Lee LCY, Maurice DH, Baillie GS. Targeting protein-protein interactions within the cyclic AMP signaling system as a therapeutic strategy for cardiovascular disease. Future Med Chem. 2013; 5: 451–464.

Lerner A, Epstein PM. Cyclic nucleotide phosphodiesterases as targets for treatment of haematological malignancies. Biochem J. 2006; 393(Pt 1): 21-41.

Levy I, Horvath A, Azevedo M, de Alexandre RB, Stratakis CA. Phosphodiesterase function and endocrine cells: links to human disease and roles in tumor development and treatment. Curr Opin Pharmacol. 2011; 11(6): 689-97.

Li H, Liu L, David ML, Whitehead CM, Chen M, Fetter JR, Sperl GJ, Pamukcu R, Thompson WJ. Pro-apoptotic actions of exisulind and CP461 in SW480 colon tumor cells involve beta-catenin and cyclin D1 down-regulation. Biochem Pharmacol. 2002; 64(9): 1325-36.

Li N, Xi Y, Tinsley HN, Gurpinar E, Gary BD, Zhu B, Li Y, Chen X, Keeton AB, Abadi AH, Moyer MP, Grizzle WE, Chang WC, Clapper ML, Piazza GA. Sulindac selectively inhibits colon tumor cell growth by activating the cGMP/PKG pathway to suppress Wnt/beta-catenin signaling. Mol Cancer Ther. 2013; 12: 1848-59.

Lin CS, Lau A, Tu R, Lue TF. Expression of three isoforms of cGMP-binding cGMP-specific phosphodiesterase (PDE5) in human penile cavernosum. Biochem Biophys Res Commun. 2000; 268: 628–635.

Lin F, Hoogendijk L, Buil L, Beijnen JH, van Tellingen O. Sildenafil is not a useful modulator of ABCB1 and ABCG2 mediated drug resistance in vivo. Eur J Cancer. 2013; 49: 2059-2064.

Lincoln TM, Cornwell T.L. Intracellular cyclic GMP receptor proteins. FASEB J. 1993; 7: 328–338.

Lincoln TM, Wu X, Sellak H, Dey N, Choi CS. Regulation of vascular smooth muscle cell phenotype by cyclic GMP and cyclic GMP-dependent protein kinase. Front Biosci. 2006; 11: 356-67.

Liu L, Li H, Underwood T, Lloyd M, David M, Sperl G, Pamukcu R, Thompson WJ. Cyclic GMP-dependent protein kinase activation and induction by exisulind and CP461 in colon tumor cells. J Pharmacol Exp Ther. 2001; 299(2): 583-92.

Liu S, Goldstein RH, Scepansky EM,Rosenblatt M. Inhibition of rho-associated kinase signaling prevents breast cancer metastasis to human bone. Cancer Res. 2009; 69: 8742-51.

Loughney K, Hill TR, Florio VA, et al. Isolation and characterization of cDNAs encoding PDE5A, a human cGMPbinding, cGMP-specific 3',5'-cyclic nucleotide phosphodiesterase. Gene. 1998; 216: 139–147.

Love MI, Huber W,Anders S. Moderated estimation of fold change and dispersion for RNA-seq data with DESeq2. Genome Biol 2014; 15: 550.

Lubbe WJ, Zhou ZY, Fu W, Zuzga D, Schulz S, Fridman R, Muschel RJ, Waldman SA, Pitari GM. Tumor epithelial cell matrix metalloproteinase 9 is a target for antimetastatic therapy in colorectal cancer. Clin Cancer Res. 2006; 12(6): 1876-82.

Lugnier C. Cyclic nucleotide phosphodiesterase (PDE) superfamily: a new target for the development of specific therapeutic agents. Pharmacol Therapeut. 2006; 109: 366-398.

Manallack DT, Hughes RA, Thompson PE. The next generation of phosphodiesterase inhibitors: structural clues to ligand and substrate selectivity of phosphodiesterases. J Med Chem. 2005; 48: 3449–3462.

Marino N, Collins JW, Shen C, Caplen NJ, Merchant AS, Gökmen-Polar Y, Goswami CP, Hoshino T, Qian Y, Sledge GW Jr, Steeg PS. Identification and validation of genes with expression patterns inverse to multiple metastasis suppressor genes in breast cancer cell lines. Clin Exp Metastasis. 2014; 31: 771-786.

Maurice DH, Ke H, Ahmad F, Wang Y, Chung J, Manganiello VC. Advances in targeting cyclic nucleotide phosphodiesterases. Nat Rev Drug Discov. 2014; 13(4): 290-314.

Mihály Z, Kormos M, Lánczky A, Dank M, Budczies J, Szász MA, Győrffy B. . A meta-analysis of gene expression-based biomarkers predicting outcome after tamoxifen treatment in breast cancer. Breast Cancer Res Treat 2013; 140: 219-32.

Millar JK, Pickard BS, Mackie S, James R, Christie S, Buchanan SR, Malloy MP, Chubb JE, Huston E, Baillie GS, Thomson PA, Hill EV, Brandon NJ, Rain JC, Camargo LM, Whiting PJ, Houslay MD, Blackwood DH, Muir WJ, Porteous DJ. DISC1 and PDE4Bare interacting genetic factors in schizophrenia that regulate cAMP signaling. Science. 2005; 310: 1187–1191.

Morelli A, Filippi S, Sandner P, Fibbi B, Chavalmane AK, Silvestrini E, Sarchielli E, Vignozzi L, Gacci M, Carini M, Vannelli GB, Maggi M. Vardenafil modulates bladder contractility through cGMP-mediated inhibition of RhoA/Rho kinase signaling pathway in spontaneously hypertensive rats. J Sex Med. 2009; 6: 1594-608.

Nagendran J, Archer SL, Soliman D, Gurtu V, Moudgil R, Haromy A, St Aubin C, Webster L, Rebeyka IM, Ross DB, Light PE, Dyck JR, Michelakis ED. Phosphodiesteras type 5 (PDE5) is highly expressed in the hypertrophied human right ventricle and acute inhibition of PDE5 improves contractility. Circulation. 2007; 116: 238-248.

Nehra A. Erectile dysfunction and cardiovascular disease: efficacy and safety of phosphodiesterase type 5 inhibitors in men with both conditions. Mayo Clin Proc. 2009; 84: 139-148.

Neve RM, Chin K, Fridlyand J, Yeh J, Baehner FL, Fevr T, Clark L, Bayani N, Coppe JP, Tong F, Speed T, Spellman PT, DeVries S, Lapuk A, Wang NJ, Kuo WL, Stilwell JL, Pinkel D, Albertson DG, Waldman FM, McCormick F, Dickson RB, Johnson MD, Lippman M, Ethier S, Gazdar A, Gray JW. A collection of breast cancer cell lines for the study of functionally distinct cancer subtypes. Cancer Cell 2006; 10: 515-27.

Noonan KA, Ghosh N, Rudraraju L, Bui M, Borrello I. Targeting immune suppression with PDE5 inhibition in end-stage multiple myeloma. Cancer Immunol Res. 2014; 2: 725-731.

Omori K, Kotera J. Overview of PDEs and their regulation. Circ Res. 2007; 100: 309-327.

Palit V, Eardley I. An update on new oral PDE5 inhibitors for the treatment of erectile dysfunction. Nat Rev Urol. 2010; 7: 603-609.

Perou CM, Sørlie T, Eisen MB, van de Rijn M, Jeffrey SS, Rees CA, Pollack JR, Ross DT, Johnsen H, Akslen LA, Fluge O, Pergamenschikov A, Williams C, Zhu SX, Lønning PE, Børresen-Dale AL, Brown PO, Botstein D. Molecular portraits of human breast tumours. Nature 2000; 406: 747-52.

Piazza GA, Alberts DS, Hixson LJ, Paranka NS, Li H, Finn T, Bogert C, Guillen JM, Brendel K, Gross PH, Sperl G, Ritchie J, Burt RW, Ellsworth L, Ahnen DJ, Pamukcu R. Sulindac sulfone inhibits azoxymethane-induced colon carcinogenesis in rats without reducing prostaglandin levels. Cancer Res. 1997; 57: 2909-2915.

Piazza GA, Thompson WJ, Pamukcu R, Alila HW, Whitehead CM, Liu L, Fetter JR, Gresh WE Jr, Klein-Szanto AJ, Farnell DR, Eto I, Grubbs CJ. Exisulind, a novel proapoptotic drug, inhibits rat urinary bladder tumorigenesis. Cancer Res. 2001; 61(10): 3961-8.

Piazza GA, Xu S, Klein-Szanto A, Ahnen DJ, Li H, Liu L, David M, Pamukcu M, Thompson WJ. Overexpression of cGMP phosphodiesterase in colonic neoplasias compared to normal mucosa. Gastroenterology 2000; 118: A282.

Pitari GM, Di Guglielmo MD, Park J, Schulz S, Waldman SA. Guanylyl cyclase C agonists regulate progression through the cell cycle of human colon carcinoma cells. Proc Natl Acad Sci U S A. 2001; 98(14): 7846-51.

Prickaerts J, Sik A, van Staveren WC, Koopmans G, Steinbusch HW, van der Staay FJ, de Vente J, Blokland A. Phosphodiesterase type 5 inhibition improves early memory consolidation of object information. Neurochem Int. 2004; 45: 915-928.

Pusztai L, Zhen JH, Arun B, Rivera E, Whitehead C, Thompson WJ, Nealy KM, Gibbs A, Symmans WF, Esteva FJ, Booser D, Murray JL, Valero V, Smith TL, Hortobagyi GN. Phase I and II study of exisulind in combination with capecitabine in patients with metastatic breast cancer. J Clin Oncol. 2003; 21(18): 3454-61.

Rehmann H, Wittinghofer A, Bos JL. Capturing cyclic nucleotides in action: snapshots from crystallographic studies. Nat Rev Mol Cell Biol. 2007; 8: 63-73.

Reilly MP, Mohler ER 3rd. Cilostazol: treatment of intermittent claudication. Ann Pharmacother. 2001; 35(1): 48-56.

Rice PL, Beard KS, Driggers LJ, Ahnen DJ. Inhibition of extracellular-signal regulated kinases 1/2 is required for apoptosis of human colon cancer cells in vitro by sulindac metabolites. Cancer Res. 2004; 64(22): 8148-51.

Ridley AJ, Schwartz MA, Burridge K, Firtel RA, Ginsberg MH, Borisy G, Parsons JT, Horwitz AR. Cell migration: integrating signals from front to back. Science 2003; 302: 1704-9.

Riento K, Ridley AJ. Rocks: multifunctional kinases in cell behaviour. Nat Rev Mol Cell Biol. 2003; 4: 446-56.

Ruth P. Cyclic GMP-dependent protein kinases: understanding in vivo functions by gene targeting. Pharmacol Ther, 1999; 82: 355–372.

Sarfati M, Mateo V, Baudet S, Rubio M, Fernandez C, Davi F, Binet JL, Delic J, Merle-Beral H. Sildenafil and vardenafil, types 5 and 6 phosphodiesterase inhibitors, induce caspase-dependent apoptosis of B-chronic lymphocytic leukemia cells. Blood. 2003; 101: 265-269.

Sauzeau V, Rolli-Derkinderen M, Marionneau C, Loirand G, Pacaud P. RhoA expression is controlled by nitric oxide through cGMP-dependent protein kinase activation. J Biol Chem. 2003; 278: 9472-80.

Savai R, Pullamsetti SS, Banat GA, Weissmann N, Ghofrani HA, Grimminger F, Schermuly RT. Targeting cancer with phosphodiesterase inhibitors. Expert Opin Investig Drugs. 2010; 19(1): 117-31.

Sawada N, Itoh H, Yamashita J, Doi K, Inoue M, Masatsugu K, Fukunaga Y, Sakaguchi S, Sone M, Yamahara K, Yurugi T, Nakao K. cGMP-dependent protein kinase

phosphorylates and inactivates RhoA. Biochem Biophys Res Commun. 2001; 280: 798-805.

Schmidt BM, Kusma M, Feuring M, Timmer WE, Neuhäuser M, Bethke T, Stuck BA, Hörmann K, Wehling M. The phosphodiesterase 4 inhibitor roflumilast is effective in the treatment of allergic rhinitis. J Allergy Clin Immunol. 2001; 108(4): 530-6.

Schmitz AA, Govek EE, Bottner B,Van Aelst L. Rho GTPases: signaling, migration, and invasion. Exp Cell Res. 2000; 261: 1-12.

Serafini P, Meckel K, Kelso M, Noonan K, Califano J, Koch W, Dolcetti L, Bronte V, Borrello I. Phosphodiesterase-5 inhibition augments endogenous antitumor immunity by reducing myeloid-derived suppressor cell function. J Exp Med. 2006; 203: 2691-2702.

Seybold J, Thomas D, Witzenrath M, Boral S, Hocke AC, Bürger A, Hatzelmann A, Tenor H, Schudt C, Krüll M, Schütte H, Hippenstiel S, Suttorp N. Tumor necrosis factor-alpha-dependent expression of phosphodiesterase 2: role in endothelial hyperpermeability. Blood. 2005; 105(9): 3569-76.

Shi Z, Tiwari AK, Patel AS, Fu LW, Chen ZS. Roles of sildenafil in enhancing drug sensitivity in cancer. Cancer Res. 2011; 71: 3735-3738.

Singh T, Chaudhary SC, Kapur P, Weng Z, Elmets CA, Kopelovich L, Athar M. Nitric oxide donor exisulind is an effective inhibitor of murine photocarcinogenesis. Photochem Photobiol. 2012; 88: 1141-1148.

Smolenski A, Poller W, Walter U, Lohmann SM. Regulation of human endothelial cell focal adhesion sites and migration by cGMP-dependent protein kinase I. J Biol Chem. 2000; 275: 25723-25732.

Sørlie T, Perou CM, Tibshirani R, Aas T, Geisler S, Johnsen H, Hastie T, Eisen MB, van de Rijn M, Jeffrey SS, Thorsen T, Quist H, Matese JC, Brown PO, Botstein D, Lønning PE, Børresen-Dale AL. Gene expression patterns of breast carcinomas distinguish tumor subclasses with clinical implications. Proc Natl Acad Sci U S A 2001; 98: 10869-74.

Sponziello M, Verrienti A1, Rosignolo F1, De Rose RF2, Pecce V1, Maggisano V2, Durante C1, Bulotta S2, Damante G3, Giacomelli L4, Di Gioia CR5, Filetti S1, Russo D6, Celano M2. PDE5 expression in human thyroid tumors and effects of PDE5 inhibitors on growth and migration of cancer cells. Endocrine. 2015; 50(2): 434-41.

Spoto G, Fioroni M, Rubini C, Contento A, Di Nicola M, Forcella S, Piattelli A. Cyclic guanosine monophosphate phosphodiesterase activity in human gingival carcinoma. J Oral Pathol Med. 2003; 32: 189-194.

Stoner GD, Budd GT, Ganapathi R, DeYoung B, Kresty LA, Nitert M, Fryer B, Church JM, Provencher K, Pamukcu R, Piazza G, Hawk E, Kelloff G, Elson P, van Stolk RU.

Sulindac sulfone induced regression of rectal polyps in patients with familial adenomatous polyposis. Adv Exp Med Biol. 1999; 470: 45-53.

Szakács G, Paterson JK, Ludwig JA, Booth-Genthe C, Gottesman MM. Targeting multidrug resistance in cancer. Nat Rev Drug Discov. 2006; 5: 219-234.

Takimoto E, Champion HC, Li M, Belardi D, Ren S, Rodriguez ER, Bedja D, Gabrielson KL, Wang Y, Kass DA. Chronic inhibition of cyclic GMP phosphodiesterase 5A prevents and reverses cardiac hypertrophy. Nat Med. 2005; 11: 214-222.

Tazhibi M, Feizi A. Awareness Levels about Breast Cancer Risk Factors, Early Warning Signs, and Screening and Therapeutic Approaches among Iranian Adult Women: A large Population Based Study Using Latent Class Analysis. BioMed Res Int 2014; 2014: 306352.

Thompson HJ, Jiang C, Lu J, Mehta RG, Piazza GA, Paranka NS, Pamukcu R, Ahnen DJ. Sulfone metabolite of sulindac inhibits mammary carcinogenesis. Cancer Res. 1997; 57: 267-271.

Thompson WJ, Piazza GA, Li H, Liu L, Fetter J, Zhu B, Sperl G, Ahnen D, Pamukcu R. Exisulind induction of apoptosis involves guanosine 3',5'-cyclic monophosphate phosphodiesterase inhibition, protein kinase G activation, and attenuated beta-catenin. Cancer Res. 2000; 60: 3338-3342.

Tinsley HN, Gary BD, Keeton AB, Lu W, Li Y, Piazza GA. Inhibition of PDE5 by sulindac sulfide selectively induces apoptosis and attenuates oncogenic Wnt/β-catenin-mediated transcription in human breast tumor cells. Cancer Prev Res (Phila). 2011; 4(8): 1275-84

Tinsley HN, Gary BD, Keeton AB, Zhang W, Abadi AH, Reynolds RC, Piazza GA. Sulindac sulfide selectively inhibits growth and induces apoptosis of human breast tumor cells by phosphodiesterase 5 inhibition, elevation of cyclic GMP, and activation of protein kinase G. Mol Cancer Ther. 2009; 8(12): 3331-40.

Tinsley HN, Gary BD, Thaiparambil J, Li N, Lu W, Li Y, Maxuitenko YY, Keeton AB, Piazza GA. Colon tumor cell growth inhibitory activity of sulindac sulfide and other nonsteroidal anti-inflammatory drugs is associated with phosphodiesterase 5 inhibition. Cancer Prev Res (Phila). 2010; 3: 1303-1313.

Treon SP, Tournilhac O, Branagan AR, Hunter Z, Xu L, Hatjiharissi E, Santos DD. Clinical responses to sildenafil in Waldenstrom's macroglobulinemia. Clin Lymphoma. 2004; 5: 205-207.

Tsai EJ, Kass DA. Cyclic GMP signaling in cardiovascular pathophysiology and therapeutics. Pharmacol Ther. 2009; 122: 216-238.

Turko IV, Francis SH, Corbin JD. Binding of cGMP to both allosteric sites of cGMP-binding cGMP-specific phosphodiesterase (PDE5) is required for its phosphorylation. Biochem J. 1998; 329: 505–510.

van Schalkwyk E, Strydom K, Williams Z, Venter L, Leichtl S, Schmid-Wirlitsch C, Bredenbröker D, Bardin PG. Roflumilast, an oral, once-daily phosphodiesterase 4 inhibitor, attenuates allergen-induced asthmatic reactions. J Allergy Clin Immunol. 2005; 116(2): 292-8.

van Stolk R, Stoner G, Hayton WL, Chan K, DeYoung B, Kresty L, Kemmenoe BH, Elson P, Rybicki L, Church J, Provencher K, McLain D, Hawk E, Fryer B, Kelloff G, Ganapathi R, Budd GT. Phase I trial of exisulind (sulindac sulfone, FGN-1) as a chemopreventive agent in patients with familial adenomatous polyposis. Clin Cancer Res. 2000; 6: 78-89.

Vega FM, Ridley AJ. Rho GTPases in cancer cell biology. FEBS Lett. 2008; 582: 2093-101.

Wang H, Peng MS, Chen Y, Geng J, Robinson H, Houslay MD, Cai J, Ke H. Structures of the four subfamilies of phosphodiesterase-4 provide insight into the selectivity of their inhibitors. Biochem J. 2007; 408(2): 193-201.

Wesolowski R, Markowitz J, Carson WE 3rd. Myeloid derived suppressor cells-a new therapeutic target in the treatment of cancer. J Immunother Cancer. 2013; 1: 10.

Whitehead CM, Earle KA, Fetter J, Xu S, Hartman T, Chan DC, Zhao TL, Piazza G, Klein-Szanto AJ, Pamukcu R, Alila H, Bunn PA Jr, Thompson WJ. Exisulind-induced apoptosis in a non-small cell lung cancer orthotopic lung tumor model augments docetaxel treatment and contributes to increased survival. Mol Cancer Ther. 2003; 2(5): 479-88.

Whitt JD, Li N, Tinsley HN, Chen X, Zhang W, Li Y, Gary BD, Keeton AB, Xi Y, Abadi AH, Grizzle WE, Piazza GA. A novel sulindac derivative that potently suppresses colon tumor cell growth by inhibiting cGMP phosphodiesterase and beta-catenin transcriptional activity. Cancer Prev Res (Phila). 2012; 5: 822-833.

Yanaka N, Kotera J, Ohtsuka A, et al. Expression, structure and chromosomal localization of the human cGMPbinding cGMP-specific phosphodiesterase PDE5A gene. Eur J Biochem. 1998; 255: 391–399.

Yang XR, Sherman ME, Rimm DL, Lissowska J, Brinton LA, Peplonska B, Hewitt SM, Anderson WF, Szeszenia-Dabrowska N, Bardin-Mikolajczak A, Zatonski W, Cartun R, Mandich D, Rymkiewicz G, Ligaj M, Lukaszek S, Kordek R, García-Closas M. Differences in risk factors for breast cancer molecular subtypes in a population-based study. Cancer Epidemiol Biomarkers Prev 2007; 16: 439-43.

Zeller E, Stief HJ, Pflug B, Sastre-y-Hernández M. Results of a phase II study of the antidepressant effect of rolipram. Pharmacopsychiatry. 1984; 17(6): 188-90.

Zenzmaier C, Sampson N, Pernkopf D, Plas E, Untergasser G, Berger P. Attenuated proliferation and trans-differentiation of prostatic stromal cells indicate suitability of phosphodiesterase type 5 inhibitors for prevention and treatment of benign prostatic hyperplasia. Endocrinol. 2010; 151: 3975-3984.

Zhu B, Strada SJ. The novel functions of cGMP-specific phosphodiesterase 5 and its inhibitors in carcinoma cells and pulmonary/cardiovascular vessels. Curr Top Med Chem. 2007; 7: 437-454.

Zhu B, Vemavarapu L, Thompson WJ, Strada SJ. Suppression of cyclic GMP-specific phosphodiesterase 5 promotes apoptosis and inhibits growth in HT29 cells. J Cell Biochem. 2005; 94: 336-350.

Zoraghi R, Bessay EP, Corbin JD, Francis SH. Structural and functional features in human PDE5A1 regulatory domain that provide for allosteric cGMP binding, dimerization, and regulation. J Biol Chem. 2005; 280: 12051–12063.

AUTHOR OF 4 FULL PAPERS

1. Catalano S[*], **Campana A**[*], Giordano C, Győrffy B, Tarallo R, Rinaldi A, Bruno G, Ferraro A, Romeo F, Lanzino M, Naro F, Bonofiglio D, Andò S[#], Barone I[#]. Expression and Function of Phosphodiesterase Type 5 in Human Breast Cancer Cell Lines and Tissues: Implications for Targeted Therapy. *Clinical Cancer Research.* 2015. In revision. *Joint first authors. #Joint senior authors.

2. Giordano C, Chemi F, Panza S, Barone I, Bonofiglio D, Lanzino M, Cordella A, **Campana A**, Hashim A, Rizza P, Leggio A, Győrffy B, Simões BM, Clarke RB, Weisz A, Catalano S, Andò S. Leptin as a Mediator of Tumor-Stromal Interactions Promotes Breast Cancer Stem Cell Activity. *Oncotarget.* 2015 Oct 27. doi: 10.18632/oncotarget.6014.

3. Maris P, **Campana A**, Barone I, Giordano C, Morelli C, Malivindi R, Sisci D, Aquila S, Rago V, Bonofiglio D, Catalano S, Lanzino M, Andò S. Androgens inhibit aromatase espression trough DAX-1: insights into the molecular link between hormone balance and Leydig cancer development. *Endocrinology.* 2015 Jan 15. doi: 10.1210/en.2014-1654. ISSN: 0013-7227.

4. Catalano S, Leggio A, Barone I, De Marco R, Gelsomino L, **Campana A**, Malivindi R, Panza A, Giordano C, Liguori A, Bonofiglio D, Liguori A, Andò S. A novel leptin antagonist peptide inhibits breast cancer growth *in vitro* and *in vivo*. *Journal of Cellular and Molecular Medicine.* 2014 Nov 7. doi: 10.1111/jcmm.12517 ISSN: 0223-5234.

AUTHOR OF 10 ABSTRACTS AND PRESENTATIONS

1. Barone I, **Campana A**, Giordano C, Tarallo R, Rinaldi A, Bruno G, Győrffy B, Lanzino M, Bonofiglio D, Catalano S, Andò S. Phosphodiesterase type 5 promotes the invasive potential of breast cancer cells through Rho GTPase activation. San Antonio Breast Cancer Symposium, San Antonio, TX, December 8-12, 2015.

2. **Campana A**, Barone I, Giordano C, Lanzino M, Bonofiglio D, Győrffy B, Catalano S, Andò S. PDE5 as a potential marker for prognosis and targeted therapy of breast cancer. XI Meeting "Lilli Funaro" Foundation, Cosenza, Italy, March 6-7, 2015.

3. Barone I, **Campana A**, Giordano C, Lanzino M, Bonofiglio D, Győrffy B, Catalano S, Andò S. PDE5 as a novel biomarker and a potential therapeutic target for breast cancer. San Antonio Breast Cancer Symposium, San Antonio, TX, December 9-13, 2014.

4. Barone I, **Campana A**, Giordano C, Lanzino M, Bonofiglio D, Magnani L, Catalano S, Andò S. PDE5 as a novel potential therapeutic target in breast

cancer. 32° SIPMeT Meeting, Palermo, Italy, September 19-20, 2014. *Supplement to the American Journal Pathology, vol. 184.*

5. Morelli C, Maris P, Trombino GE, **Campana A**, Donà AA, Rizza P, Cesario MG, Lanzino M, Andò S, Sisci D. FOXO3A transcription factor restores the sensitivity to the antiestrogen treatment in MCF-7 tamoxifen resistant cells. 32° SIPMeT Meeting, Palermo, Italy, September 19-20, 2014. *Supplement to the American Journal Pathology, vol. 184.*

6. **Campana A**, Maris P, Barone I, Giordano C, Morelli C, Malivindi R, Sisci D, Aquila S, Bonofiglio D, Catalano S, Lanzino M, Andò S. Androgens inhibit aromatase expression through DAX-1: disclosing the molecular link between hormone balance and leydig cancer development. 32° SIPMeT Meeting, Palermo, Italy, September 19-20, 2014. *Supplement to the American Journal Pathology, vol. 184.*

7. De amicis F, Santoro M, Giordano C, Barone I, **Campana A**, Morelli C, Bonofiglio D, Lanzino M, Andò S. AR/ER coactivator squelcing contributes to the inhibition of estrogen-dependent cyclin D1 expression in breast cancer. 32° SIPMeT Meeting, Palermo, Italy, September 19-20, 2014. *Supplement to the American Journal Pathology, vol. 184.*

8. **Campana A,** Barone I, Gelsomino L, Leggio A, De Marco R, Giordano C, Bonofiglio D, Liguori A, Catalano S, Andò S. *In vitro* e *in vivo* efficacy of a novel leptin antagonist peptide in breast cancer models. X Meeting "Lilli Funaro" Foundation, Cosenza, Italy, March 21-22, 2014.

9. Barone I, **Campana A**, Gelsomino L, Chemi F, Panza S, Giordano C, Marsico S, Lanzino M, Bonofiglio D, Fuqua S, Catalano S, Andò S. Aromatase Inhibitor Resistance in Breast Cancer: a Potential Role for Inflammation. SIPMET/ASIP Young Scientist Meeting, Rome, Italy, October 23-24, 2013.

10. **Campana A**, Barone I, Gelsomino L, Giordano C, Lanzino M, Bonofiglio D, Catalano S, Andò S. Aromatase Inhibitor Resistance in Breast Cancer: a Potential Role for Cytokine Signaling Network. IX Meeting "Lilli Funaro" Foundation, Cosenza, Italy, March 01-02, 2013.

Expression and Function of Phosphodiesterase Type 5 in Human Breast Cancer Cell Lines and Tissues: Implications for Targeted Therapy.

Stefania Catalano[1*], Antonella Campana[1*], Cinzia Giordano[2], Balázs Győrffy[3], Roberta Tarallo[4], Antonio Rinaldi[4], Giuseppina Bruno[4], Aurora Ferraro[5], Francesco Romeo[5], Marilena Lanzino[1], Fabio Naro[6], Daniela Bonofiglio[1], Sebastiano Andò[1,2#], Ines Barone[1#].

Author Affiliations:
[1]Department of Pharmacy, Health and Nutritional Sciences, [2]Centro Sanitario, University of Calabria, Rende (CS), Italy; [3]MTA TTK Lendület Cancer Biomarker Research Group, Semmelweis University 2nd Dept. of Pediatrics, Budapest, Hungary; [4]Laboratory of Molecular Medicine and Genomics, Department of Medicine and Surgery, University of Salerno, Baronissi (SA), Italy; [5]Division of Anatomic Pathology, Annunziata Hospital, Cosenza (CS), Italy; [6]Department of Anatomical, Histological, Forensic, and Orthopedic Sciences, Sapienza University, Rome, Italy.

[*] Joint first authors
[#] Joint senior authors

Running Title: PDE5 enhances breast cancer cell invasive potential.

Key Words: breast cancer, PDE5, Rho GTPases, targeted therapy, biomarkers

Correspondence and requests should be addressed to:

Prof. Sebastiano Andò: Department of Pharmacy, Health and Nutritional Sciences, University of Calabria, Arcavacata di Rende (CS), 87036, ITALY, Tel: +39 0984 496201, Fax: +39 0984 496203, e-mail: sebastiano.ando@unical.it

Dr Ines Barone: Department of Pharmacy, Health and Nutritional Sciences, University of Calabria, Arcavacata di Rende (CS), 87036, ITALY Tel: +39 0984 496216, Fax: +39 0984 496203, e-mail: inesbarone@virgilio.it, ines.barone@unical.it

Disclosure of Potential Conflict of Interest: No potential conflicts of interest were disclosed.

Word Count: 4989

Number of Figures and Tables: 6 Figures, 2 Suppl. Figures, 2 Suppl. Tables.

First Submission to: Clinical Cancer Research, August 6, 2015

Second Submission to: Clinical Cancer Research, November 12, 2015

Translational Relevance

Although early detection and conventional therapies have changed the natural history of breast cancer, many patients die from progressive advanced disease. Dissection of the mechanisms underlying breast cancer progression may identify early markers for invasive tumors as well as specific targeted therapeutics, providing further improvement in the clinical outcomes of patients. This study recognizes a novel function for phosphodiesterase (PDE) type 5 in controlling malignant breast epithelial cell behavior, and provides important clinical implications that can impact the prediction of the risk, and the treatment of breast cancer patients. First, since enhanced PDE5 expression promotes the invasive potential of breast cancer cells and predicts a worse survival in patients, this enzyme may represent a valuable molecular candidate with prognostic significance. In addition, being PDE5 a known druggable target, our findings may be promising for antitumor therapy with reduced adverse effects. Certainly, future studies could clarify the role of PDE5 in breast cancer.

Abstract

Purpose: By catalyzing cGMP hydrolysis, phosphodiesterase (PDE) 5 is a critical regulator of its concentration and effects in different (patho)physiological processes, including cancers. Being PDE5 a known druggable target, we investigated the clinical significance of its expression in breast cancers and the underlying mechanisms by which it may contribute to tumor progression.

Experimental Design: PDE5 expression was evaluated in seven breast cancer cells by RT-PCR and immunoblotting. To examine PDE5's impact on cancer phenotype, MCF-7 cells, expressing lower levels of the enzyme, were engineered to stably overexpress PDE5. Proliferation was evaluated by MTT assays, motility and invasion by wound-healing/transmigration/invasion assays; transcriptome-profiling by RNA-sequencing; Rho GTPase signaling activation by GST-pulldown assays and immunoblotting. Clinical relevance was investigated by immunohistochemistry on tissues and retrospective studies from Metabric-cohort.

Results: PDE5 is differentially expressed in each molecular subtypes of both breast cancer cell lines and tissues, with higher levels representing a startling feature of HER2-positive and triple-negative breast cancers. A positive correlation was established between elevated PDE5 levels and cancers of high-histological grade. Higher PDE5 expression correlated with shorter patient survival in retrospective analyses. On molecular level, stable PDE5 overexpression in Luminal-A-like MCF-7 cells resulted in enhanced motility and invasion through Rho GTPase signaling activation. Treatment of PDE5-stable clones with selective ROCK or PDE5 inhibitors completely restored the less motile and weak invasive behavior of control-vector cells.

Conclusion: PDE5 expression enhances breast cancer cell invasive potential, highlighting this enzyme as a novel prognostic candidate and an attractive target for future therapy in breast cancers.

Introduction

In 2012, an estimated 1,67 million new cases of invasive breast cancer were diagnosed among women and approximately 522,000 patients were expected to die from breast cancer world-wide (1). Despite advances in surgery, radiation and therapy, metastatic disease represents the most important contributor to breast cancer-related mortality (2). Thus, novel marker and therapeutic target exploration is critical to the early detection, metastasis prevention, and effective treatment of human breast cancers.

Phosphodiesterases (PDEs) are metallo-hydrolases which catalyze the breakdown of cyclic adenosine monophosphate (cAMP) and cyclic guanosine monophosphate (cGMP) into their biologically inactive 5′-derivatives, thus modulating the amplitude and duration of their intracellular signalings. In most tissues, PDE5 is the predominant isoform responsible for cGMP hydrolysis and its activity is tightly controlled by cGMP itself (3). cGMP regulates a myriad of biological processes, including cell growth and adhesion, energy homeostasis, neuronal signaling, and muscle relaxation (4, 5). In addition, dysregulation of cGMP homeostasis was observed in various (patho)physiological conditions, including cancers. Indeed, cGMP signaling, through activation of downstream effectors (i.e., cGMP-dependent protein kinase G-PKG, cyclic-nucleotide-gated ion channels) and/or crosstalk with cAMP pathways, appears to play an important role in promoting apoptosis and inhibiting proliferation of certain epithelial cells (6, 7). Interestingly, PKG expression or cGMP levels are reduced in cancer cells and tissues compared to their normal counterparts (8, 9). In the last ten years, overexpression of PDE5 has been described in multiple human carcinomas, including bladder, lung and breast cancers (10-13). The increased expression of PDE5 in human malignancies coupled with the efficacy and high tolerability profiles of PDE5 inhibitors (i.e. sildenafil and vardenafil) in the treatment of erectile dysfunction and pulmonary hypertension have led to an increased interest in investigating PDE5-targeted drugs in cancer management (14, 15). Indeed, several *in vitro* observations have shown anti-proliferative and pro-apoptotic effects of

PDE5 inhibitors in cancer cell lines, as those of the breast (13, 14, 16, 17). Another PDE5 inhibitor, the nonsteroidal anti-inflammatory drug exisulinid inhibited growth and induced apoptosis in human tumor cells through cGMP elevation and PKG activation (12, 18, 19). PDE5 inhibitors also increased the efficacy of chemotherapy agents in cancer models (20). Recently, it has been reported that modulation of host immune response represents an additional mechanism by which PDE5 inhibitors may block tumor progression (21). However, despite these studies, neither the expression of PDE5 in breast cancer cell lines and tissues nor the underlying regulatory molecular mechanisms by which PDE5 expression may contribute to breast cancer progression have been deeply studied. Being PDE5 a well-characterized druggable target, in this study we propose to examine PDE5's impact on breast cancer phenotype *in vitro*, as well as to assess its clinical relevance in breast cancer patients.

Materials and Methods

Reagents, antibodies and plasmids

Sildenafil and Y-27632 were from Sigma; PDE5A/p-c-Myc$^{Thr58/Ser62}$/c-Myc/p-IκB-α$^{Ser32/36}$/IκB-α/NF-kBp65/Laminb/GAPDH antibodies from Santa Cruz Biotechnology; RhoA-C/Cdc42/Rac1-3 from Life Technologies; Cofilin activation and Myosin Light Chain 2 antibody sampler kits from Cell Signaling. pEGFP-C1 vector and the fusion protein expression vector pEGFP-PDE5A were kindly provided by Dr F. Barbagallo (Sapienza University, Rome-Italy). Scrambled and 4 unique 29mer PDE5A shRNA constructs in pGFP-C-shLenti vector were from Origene.

Cell culture

MCF-7/T47D/ZR-75/SKBR3/BT-20 and MDA-MB-468/MDA-MB-435 breast cancer cell lines were from American-Type-Culture-Collection and Interlab-Cell-Line-Collection, respectively. All cell lines, stored and authenticated following suppliers, were used within six-months after frozen-

aliquot resuscitations and regularly tested for Mycoplasma-negativity (MycoAlert, Lonza). To generate PDE5A-overexpressing MCF-7 cells, cells were transfected with pEGFP-PDE5A vector using Fugene6 reagent (Promega). Stable clones were selected with G418 antibiotic (1mg/ml, Life Technologies), and positive clones were identified using fluorescence microscopy and immunoblot analysis.

Transient transfection

For overexpression studies, T47D cells were transfected with pEGFP-C1 or pEGFP-PDE5A vectors and for gene silencing, MDA-MB-468 cells with scrambled or PDE5A shRNA constructs using Fugene6. After 48h, cells were harvested and used in different experimental procedures.

RT-PCR assays

PDE5 and 36B4 gene expression were evaluated by reverse transcription (RT)-PCR method as described (22). Primers: forward 5'-ACTTGCATTGCTGATTGCTG-3' and reverse 5'-TTGAATAGGCCAGGGTTTTG-3' (*PDE5A*); forward 5'-CAAATCCCATATCCTCGTCC-3' and reverse 5'-CTCAACATCTCCCCCTTCTC-3' (*36B4*).

Immunoblot analysis

Cell extracts were resolved by SDS-PAGE, as described (22). Immunoblots show a single representative of three-separate experiments.

Fluorescence microscopy

Cells were fixed with 4% paraformaldehyde and permeabilized with PBS+0.2% Triton X-100. 4',6-Diamidino-2-phenylindole (DAPI, Sigma) was used for nuclei detection. Fluorescence was photographed with OLYMPUS-BX51 microscope, 100X-magnification.

MTT cell proliferation assays

Three days after seeding, cell proliferation was assessed using 3-[4,5-Dimethylthiazol-2-yl]-2,5-diphenyltetrazolium bromide reagent/MTT (Sigma) and expressed as fold change relative to empty vector-transfected cells. Data represent three-independent experiments, performed in triplicate.

Wound-healing assays

Cell monolayers were scraped and subjected to various experimental conditions. Wound closure was monitored over 24h, cells were fixed and stained with Comassie-Brillant-Blue. Pictures represent one of three-independent experiments (10X-magnification, phase-contrast microscopy).

Transmigration assays

Cells under the various experimental conditions were placed in upper compartments of Boyden-chambers (8µm-membranes, Corning). Bottom well contained regular-growth media. After 24h, migrated cells were fixed and stained with DAPI. Migration was quantified by viewing five-separate fields/membrane (OLYMPUS-BX51 microscope, 10X-magnification) and expressed as mean numbers of migrated cells. Data represent three-independent experiments, assayed in triplicate.

Invasion assays

Matrigel-based invasion assay was performed in Boyden-chambers (8µm-membranes) coated with Matrigel (BD Bioscences, 0.4µg/ml), as described (23). After 24h, invaded cells were quantified as reported for transmigration assays.

RNA library preparation and sequencing

Total RNA was extracted from vector- and PDE5-expressing cells and libraries were prepared and sequenced as described in supplementary information.

Rho GTPase activation assays

Rho GTPases activation was determined by active Rho and Cdc42 pull-down and detection kits, following manufacturers (Life Technologies).

Phalloidin staining

Polymerized actin stress fibers were stained with Alexa Fluor 568-conjugated phalloidin, following manufacturers (Life Technologies). Cell nuclei were counterstained with DAPI. OLYMPUS-BX51 microscope (100X-magnification) was used for imaging.

Patients and tissue specimens

A total of 35 primary breast carcinomas and three non-neoplastic breast tissues were analyzed in this study. These carcinomas were obtained from patients who had undergone initial surgery and signed informed consent between 2012-2014 at Annunziata Hospital (Cosenza, Italy). The patients' age at diagnosis varied from 33 to 85 years (mean, 60.6 years; median, 57 years). Characteristics of the patient cohort are reported in Supplementary Table 1. Fresh tissues were formalin-fixed/paraffin-embedded after surgical removal. Sections were stained with H&E to select samples consisting of at least 50% tumor cells and to establish the histologic type and grade (Supplementary Table 1). The clinical investigation conformed the Declaration of Helsinki of 1975 and was approved by ethics and institutional human subjects committees at Annunziata Hospital.

Classification of molecular subtypes

In breast cancer, immunohistochemistry has been used as a surrogate for molecular classification by gene expression profiling in large population-based studies, showing an acceptable level of accuracy for determining molecular phenotypes (24-26). Breast subtype classification is described in supplementary information.

Immunohistochemical analysis

PDE5A expression in non-neoplastic and neoplastic breast tissues was detected as described in supplementary information.

Database setup for retrospective study

The entire database contains 1988 patients (average overall survival: 8.07 years, ER-positive patients: 76%, lymphnode-positive patients: 47.3%). Illumina gene-chips published by the Metabric-consortia were downloaded from the EGA repository (27). The raw gene-chip data were imported into R and summarized using beadarray package (28). Quantile normalization was performed using preprocessCore package (29).

Statistical analysis

Data were analyzed for statistical significance using two-tailed student's Test, GraphPad-Prism4. Standard deviations/S.D. are shown. For RNA sequencing bioinformatics analysis, sequencing reads (50-60 million reads/sample on average) were trimmed, quality filtered and aligned, including junction-spanning reads back, to the human genome hg19 (Homo sapiens Ensembl GRCh37) using Tophat v.2.0.10 (30). HTSeq (31) was used to compute read counts across each gene, which were then used as input to R package DESeq2 (32). DESeq2 was used to normalize read counts for library size and dispersion followed by tests for differential gene expression. Significant differentially expressed genes were determined using false discovery rate (FDR) cutoff ≤ 0.05 and at least 1.5-fold change between conditions. Functional analyses were performed with Ingenuity Pathway Analysis suit (Ingenuity Systems). For immunohistochemistry, the correlations between PDE5 and grading/ER/PR/HER2 status were examined with Mann-Whitney-U test, between PDE5 and breast cancer subtypes by Kruskal-Wallis test (GraphPad-Prism4). Kaplan-Meier survival plot, hazard ratio with 95% confidence intervals and logrank P value were calculated and plotted in R as

described (33). Cox proportional hazard regression was computed to compare the association between gene expression, clinical variables including ER/HER2/lymphnode status and survival in multivariate analysis using WinSTAT 2014 for Microsoft Excel (Robert Fitch Software). Statistical significance was set at $p<0.05$.

Results

PDE5 expression varies among different breast cancer cell subtypes.

On the basis of gene expression signatures in breast cancer patients, researchers have currently identified at least four major molecular and clinically distinct subtypes of neoplasm: Luminal A (ER-positive) and B (ER-positive/HER2-enriched), HER2-positive and basal-like (34, 35). Thus, we first aimed to evaluate mRNA and protein expression levels of PDE5 in breast cancer cell lines of different molecular subtypes (n=7) (36, 37) by RT-PCR and immunoblot analyses. As shown in Fig. 1A and B, PDE5 expression was detected at very low levels in luminal A-type (MCF-7/T47D) breast cancer cells. Luminal B-like (ZR-75) cells exhibited a modest induction in PDE5 expression in respect with Luminal A-like cells. Notably, higher PDE5 levels were observed in HER2-overexpressing (SKBR3) and basal-like (BT-20/MDA-MB-468/MDA-MB-435) breast cancer cells. These results may suggest that high PDE5 expression may be associated with more aggressive breast cancer phenotypes.

PDE5 overexpression affects motility and invasion of MCF-7 breast cancer cells.

In order to explore PDE5's role in breast cancer growth and progression, a breast tumor cell line that expresses the lowest levels of this enzyme, MCF-7, was chosen to generate breast cancer *in vitro* models exhibiting forced PDE5 overexpression. For direct visualization of PDE5 cellular location, the corresponding cDNA was cloned in frame with enhanced-green-fluorescent-protein (EGFP) in the mammalian expression vector pEGFP-C1 and stable clones were screened using

fluorescence microscopy (Fig. 1C). Parental MCF-7 breast cancer cells are shown along with one clone stably expressing EGFP (MCF-7 e.v.) and three clones expressing cytoplasmic EGFP-PDE5 (PDE5 1/2/3). This was further evaluated by immunoblotting detection, showing the presence of an exogenous PDE5 band (EGFP-tagged, ~125 kDa) in protein extracts from PDE5-overexpressing cells (Fig. 1D). We used these experimental models to first investigate whether PDE5 overexpression may cause any changes in cellular phenotypes, including proliferation, migration, and invasion. Anchorage-dependent growth assays revealed a slight, but significant increase in cell proliferation in all three PDE5 clones compared to vector-expressing cells (Fig. 1E). We then evaluated the ability of PDE5 overexpression to influence cell migration in wound-healing scratch assays and found that PDE5-expressing cells moved the farthest in either direction to close the gap compared with vector-expressing cells (Fig. 1F). Given the evident enhancement of motility in PDE5-overexpressing cells, the capacity of cells to migrate across uncoated membrane in transmigration assays or invade an artificial basement membrane Matrigel in invasion assays was tested. Although vector-expressing cells exhibited little motile and no invasive behavior *in vitro*, our data clearly showed that PDE5 overexpression significantly increased both motility and invasion of MCF-7 cells (Fig. 1G and H).

To evaluate the effects of PDE5 inhibition on breast tumor cell migratory and invasive properties, cells were treated with the specific PDE5 inhibitor sildenafil (Fig. 2A-C). We found that sildenafil treatment was able to completely restore in PDE5 1/2/3 clones the less motile and weak invasive behavior similar to that of control MCF-7 e.v. cells. Interestingly, although at less extent, sildenafil caused a significant decrease in motility and invasion of vector-expressing cells (by 73% and 65%, respectively). This may suggest that PDE5 activity is required for controlling migration and invasion processes also of malignant breast epithelial cells expressing low levels of the enzyme.

Role of PDE5 in motility and invasion of T47D and MDA-MD-468 breast cancer cells.

To extend the results obtained, we transfected vector and PDE5-expression plasmids in T47D luminal A-like breast cancer cells (Fig. 3A). As previously shown for MCF-7 cells, we found a significant increase in both migratory and invasive cell potential when PDE5 was overexpressed and treatment with the selective PDE5 inhibitor sildenafil completely abrogated these effects (Fig. 3B and C). Again, PDE5 inhibition was associated with a significant reduction of motility and invasion also in vector-expressing cells (Fig. 3B and C). In addition, as a third confirmatory model we silenced PDE5 expression in MDA-MB-468 breast cancer cells, that express high levels of PDE5 compared to MCF-7 and T47D cells (Fig. 3D). Motility and invasion were significantly reduced in PDE5sh-transfected cells compared to control shRNA-transfected cells (Fig. 3E and F). Thus, PDE5 may be an important determinant of breast tumor cell motility and invasion.

PDE5-overexpressing cells exhibit increased Rho GTPase activation.

To gain insights into the biological properties of the highly migratory and invasive PDE5-expressing breast cancer cells, quantitative transcriptome profiling of vector- and PDE5-overexpressing MCF-7 cells was carried out by RNA-sequencing analysis. Comparison of the whole transcriptome of the two cell models revealed 4425 differentially expressed genes (FDR<0.05), of which 611 were up-regulated and 468 were down-regulated in response to PDE5 overexpression (fold change≥1.5, Supplementary Table 2). These genes were next subjected to Ingenuity Pathway Analysis (IPA) to rank enriched biological processes (Fig. 4A), and to calculate the activation z-score of molecular and cellular functions and pathways (Fig. 4B and C). In line with our previous experiments, cellular movement was the most significantly overrepresented biological process in PDE5-expressing cells. In addition, many differentially-expressed genes were involved in cell death and survival, cell-to-cell signaling and interaction, cell growth and proliferation, cellular development, thus concurring to identify the five top enriched functional categories in PDE5 clones (Fig. 4A). Interestingly, analyzing the functions involving differentially-expressed genes, migration of cells and cell movement resulted to be highly activated by PDE5

overexpression (Fig. 4B). Then, considering the most affected pathways by PDE5 overexpression, we found marked changes in the activity of Rho GTPase family, with RhoA, Cdc42 and Rac signalings showing activation z-score of 1.9, 1.342, and 0.302, respectively (Fig. 4C). The predicted activation of these canonical pathways was confirmed using molecule activity predictor analysis of IPA (Fig. 4D and Supplementary Fig. 1). An enriched Rho GTPases signaling profile is consistent with the enhanced migration and invasion capabilities of PDE5-expressing cells, as these proteins are known to govern cell cytoskeleton organization, migration, and metastasis dissemination (38). To validate the gene expression profile identified by RNA sequencing, we compared expression and activation of Rho family of GTPases in vector and PDE5 clones. Increased protein levels of Rho A-C, Cdc42 and Rac 1-3 (Fig. 5A, *input panel*) along with increased levels of activated forms (Fig. 5A, *GTP-bound panel*) were detected in PDE5-overexpressing cells. In the GTP-bound form, these proteins are able to interact with effector molecules (i.e. mainly the Rho kinase ROCK and the p21-activated kinase PAK1) to induce phosphorylation of LIM Kinase (LIMK), which is able to inhibit (by phosphorylation) Cofilin, leading to stabilization of filamentous actin structures (39). ROCK has also been shown to phosphorylate the regulatory Myosin Light Chain (MLC), which enhances its binding to F-actin (40). Consistent with increased Rho GTPase activation, the levels of phosphorylated LIMK, Cofilin and MLC are greatly increased in PDE5 clones compared to e.v. cells (Fig. 5B and C). Among other downstream targets of Rho signaling, c-Myc and NF-κB are important for cell motility and invasion (39, 41, 42). In PDE5-overespressing cells, we detected elevated levels of the activated form of c-Myc (phospho c-Myc), whereas we did not observe NF-κB activation, as evidenced by no changes in phosphorylation of the inhibitor of NF-κB IκBα as well as in NF-κB nuclear translocation (Supplementary Fig. 2). To further investigate the role of Rho GTPases activation on cytoskeletal organization in our model systems, we evaluated the formation of stress fibers, since they provide the contractile force required for motility (Fig. 5D). In vector-expressing cells, actin filament remained diffusely distributed in the cytoplasm; while overexpression of PDE5 resulted in visible stress fibers. According to these results, treatment with

the selective ROCK inhibitor Y-27632 was able to significantly reduce both migration and invasion of PDE5 clones (Fig. 5E and F). Collectively, our data strongly suggest that the molecular and cellular functions identified with IPA are biologically relevant and PDE5 may regulate motility and invasion through activation of the Rho family of GTPases.

PDE5 expression in human breast cancers.

To evaluate the clinical significance of PDE5 in human breast tumors, we analyzed its expression levels in patient-derived tissues (n=35) by immunohistochemistry analysis. The characteristics of all patients are listed in Supplementary Table 1. We found that ~85% of cases showed cytoplasmic staining for PDE5 in cancer cells. Interestingly, ER/PR-positive tumors exhibited weak (n=5) or intermediate (n=15) PDE5 staining, while the strongest staining intensity was observed among HER2-positive or triple negative (TN) samples (n=15). In contrast, in non-neoplastic (NN) breast tissues (n=3), a weak to missing PDE5 expression was detected in the cytoplasm. Representative images of PDE5 staining patterns are shown in Figure 6A. Accordingly, PDE5 expression had a significant inverse correlation with ER and PR status (Fig. 6B and C) and a significant positive correlation with HER2 status (Fig. 6D). Of note, as the staining intensity of PDE5 increases, grading of cancer cells also tended to increase ($p = 0.001$), indicating that the higher expression of PDE5 might be related with a higher malignancy phenotype.

We then correlated PDE5 expression with the different subtypes of breast carcinoma and found that its cytoplasmic expression was significantly different among the four molecular subtypes (Fig. 6E). In particular, in HER2 and triple-negative subtypes, PDE5 expression was the highest, followed by the luminal B-type and the luminal A-type, that showed the lowest percentage of cells with PDE5 expression. Since HER2 and TN types are correlated with a generally more aggressive tumor phenotype and poorer prognosis (26), these results suggest that PDE5 overexpression may be correlated with poor prognosis.

High levels of PDE5 are associated with shorter survival in breast cancer patients.

To strengthen the results obtained in human breast tumor tissues, we conducted retrospective analyses of the correlation between PDE5 expression and survival in patients with breast cancer. In the univariate analysis, the Kaplan-Meier overall survival (OS) curve obtained from a cohort of 1988 patients indicated that increased expression levels of PDE5 are associated with a statistically significant shorter OS when compared to those tumors expressing low levels of PDE5 (p=0.014, HR=1.2, Fig. 6F). Interestingly, significant difference could also be observed between OS for ER-positive patients having high or low PDE5 levels (p=7.4E-04, HR=1.4, Fig. 6G), suggesting a role for PDE5 in predicting disease progression in ER-positive tumors that according to immunohistochemistry may have lower levels of the enzyme compared to ER-negative ones. In addition, PDE5 retained its significance when performing a multivariate analysis including PDE5 expression, ER, HER2 and lymphnode status in the entire database (PDE5: p=6.6E-03, HR=1.24, ER status: p=6.6E-05, HR=0.69, HER2 status: p=1E-05, HR=1.6, lymph node status: p=1.1E-06, HR=2.24). Therefore, high levels of PDE5 expression may independently predict poor outcome among breast cancer patients.

Discussion

Despite vast improvement in the overall survival rate of breast cancer patients, advanced metastatic disease remains a life-threatening stage of cancer. One of the major challenges in mammary cancer research is to identify key proteins that are directly involved in pathways promoting tumorigenesis and tissue invasion. These proteins can then be explored as early markers for invasive tumors as well as potential targets for the development of therapeutic strategies aimed at controlling and curing malignant disease. In this report, we show that phosphodiesterase type 5 (PDE5) is differentially expressed in human breast cancer subtypes, with a significant positive correlation with tumor grading. Importantly, high PDE5 levels predict a worse prognosis for

patients at 8-year median follow-up. In experimental breast cancer models, PDE5 overexpression increased motile and invasive properties of cells through activation of the Rho family of GTPases, highlighting the potential benefit of therapeutic targeting PDE5.

Breast cancer is a complex and highly heterogeneous disease due to its diverse morphological features, variable clinical outcomes and disparate therapeutic responses. By using hierarchical clustering analysis of gene expression profiling, Perou et al. were able to identify molecularly-defined and clinically-distinct classes of breast cancer (Luminal, HER2-enriched, basal-like and normal-like) (34, 35). Due to the prognostic and predictive values of this molecular classification in clinical setting, attempts have been made to identify surrogate markers that would allow subtype identification using the more familiar immunohistochemical approach. Accordingly, the combined evaluation of histopathological grade and immunohistochemical parameters (ER/PR/HER2) would approximate the molecular classification of Luminal A, Luminal B, HER2-enriched and triple-negative breast cancers (24-26). Despite the lack of complete overlapping, the panelists of the last St. Gallen Consensus have endorsed the use of the immunohistochemical assays to identify breast cancer subtypes and allow the physicians to tailor properly the systemic interventions (43). Here, we found a significant increase in PDE5 expression in breast tumors when compared to non-neoplastic breast tissues. Although ~85% of the tumor entities examined showed cytoplasmic staining for PDE5, our results clearly indicate that PDE5 is differentially expressed between each molecular breast cancer subset. In particular, the lowest expression of this enzyme is detected in the more favorable Luminal A subtypes of breast tumors, whereas its overexpression is closely related to breast cancers of high histological grade including triple-negative and HER2-positive molecular subtypes. Accordingly, PDE5 levels have a negative correlation with hormone receptor status, and a positive one with HER2 status and tumor grading. The clinical significance of PDE5 overexpression is strongly supported by its significant association with a shorter overall survival time in retrospective studies. This association is also significant in patients with ER-positive diseases, advocating the utility of PDE5 as a predictor of breast cancer prognosis in ER-positive tumors that

immunohistochemically may have lower PDE5 levels compared to ER-negative ones. In line with findings on patients, PDE5 expression also varies among different breast cancer cell line models. Taken together, our results suggest that the differential expression of PDE5 may contribute to breast cancer heterogeneity and, being PDE5 a known druggable target, it could help to integrate subsets of aggressive breast cancer into clinically meaningful subtypes.

At the present time, the selective PDE5 inhibitors sildenafil (Viagra and Revatio-Pfizer) and tadalafil (Cialis-Eli Lilly; Adcirca-United Therapeutics) have Food and Drug Administration approval for the treatment of erectile dysfunction (ED) as well as pulmonary artery hypertension; whereas vardenafil (Levitra and Vivanza-Bayer) and avanafil (Stendra-Vivus) are approved only for ED. However, due to their favorable toxicity profile (44), these agents are being investigated in a wide range of other potential medical and surgical applications, including neurological and cardiovascular disorders, transplant and reconstructive surgery, and several clinical trials are currently in progress (15) (htpp://www.clinicaltrials.gov). In the last ten years, various PDE5 inhibitors have been also reported to inhibit growth and induce apoptosis in many cancer cell lines, without affecting normal epithelial cells (12-14, 16, 18, 19). Recently, two reports have suggested a role for PDE5 inhibition in influencing cancer cell motility (17, 45). Indeed, tadalafil and sildenafil reduced the capacity of thyroid cancer cells to migrate at lower doses than those used to block proliferation (17). Similarly, down-regulation of PDE5 in the aggressive human breast cancer cell line MDA-MB-231T resulted in no difference in cell proliferation and reduced motility *in vitro* and *in vivo* (45). Here, we show that genetic and pharmacological inhibition of PDE5 significantly decreases migration and invasion of different human breast cancer cell lines. In contrast, overexpression of PDE5 strongly increases motility and invasion of MCF-7 cells and sildenafil treatment completely restores in PDE5 stable clones the less motile and weak invasive behavior similar to that of control cells. Interestingly, although at less extent, a reduction of migration and invasion was observed after treatment with sildenafil also in vector cells, expressing lower levels of the enzyme, further highlighting a role for PDE5 in controlling migration and invasion processes of

malignant breast epithelial cells. Increased formation of actin stress fibers and enhanced contractility are common features of motile cells in 2D culture conditions (46). Indeed, immunofluorescent staining of polymerized actin (F-actin) reveals an induced formation of stress fibers in cells bearing PDE5 overexpression. Accordingly, ingenuity pathway analysis on PDE5 modulated genes by RNA-sequencing highlights cellular movement as the most significantly represented biological process. Moreover, most of the genes differentially regulated by PDE5 overexpression are significantly involved in migration of cells. Taken together, these results indicate that PDE5 may be important for sustaining malignant motile and invasive behavior of breast cancers.

The acquisition of a remodeled cytoskeleton and a motile phenotype are important steps in tissue invasion and metastasis establishment, and the Rho family of GTP-binding proteins have been reported to mediate these processes . Although at least 20 Rho family proteins have been identified in humans, the most widely characterized molecules for their effects on cell migration are Rho A-C, which regulate stress fibers and focal adhesion formation, and Rac 1-3 and Cdc42, which control membrane ruffling, and filopodium formation (38). In the GTP-bound form, these proteins are able to interact with effector molecules to regulate actin cytoskeleton assembly and organization through phosphorylation of specific substrates, such as Cofilin or Myosin Light Chain, as well as to modulate a variety of other biochemical signalings involved in cell transformation and metastasis, including the c-Myc pathway (39-41). In breast tumors, Rho expression and/or activity are frequently increased (47). On the other hand, a complex signaling interplay between cGMP and Rho GTPase pathways has been described. For instance, cGMP-PKG cascade inhibits RhoA in various cell types (48, 49). Similarly, vardenafil prevents RhoA membrane translocation/activation, and decreases activity of its downstream effector ROCK in human bladder smooth muscle cells, inhibiting endothelin-1-induced migration (50). On the molecular level, increased levels of total and activated Rho A-C, Cdc42 and Rac 1-3 are detected in PDE5-overexpressing cells compared with vector cells. Phosphorylation levels of Rho GTPase downstream targets, including LIM Kinase,

Cofillin, Myosin Light Chain and c-Myc, are also greatly increased in PDE5 clones compared to vector cells. Moreover, transcriptome analysis identifies an enriched Rho GTPase signaling profile in PDE5-overexpressing cells. Consistent with these findings, a selective ROCK inhibitor significantly reduces both migration and invasion of PDE5 clones.

In conclusion, results of this study highlight a novel role for PDE5 in controlling malignant breast epithelial cell behavior and provide the first indications for the clinical relevance of this enzyme in human breast cancers. Since PDE5 overexpression greatly enhances the invasive potential of breast cancer cells and reduces survival in patients, it is tempting to speculate that this enzyme may represent a novel prognostic biomarker candidate. In addition, having already addressed the delivery, stability and toxicity issues of PDE5 inhibitors in other diseases, our findings may offer promising insights into future cancer treatments by providing the rationale to implement safer and more efficacious drugs in the adjuvant therapy for improving clinical care and reducing mortality from breast cancer. This may assume particular significance in triple-negative breast cancers in which PDE5 may be an attractive target. Based on these observations, it is evident that the impact of PDE5 in the prediction of the risk, and the treatment of breast cancer patients deserves further attention.

Acknowledgements:

This work was supported by PROGRAMMA "FUTURO IN RICERCA" Anno 2012 # RBFR12FI27 to IB, and #RBFR12W5V5_003 to RT.

References

1. Ferlay J, Soerjomataram I, Dikshit R, Eser S, Mathers C, Rebelo M, et al. Cancer incidence and mortality worldwide: sources, methods and major patterns in GLOBOCAN 2012. Int J Cancer 2015;136:E359-86.

2. Kraljevic Pavelic S, Sedic M, Bosnjak H, Spaventi S, Pavelic K. Metastasis: new perspectives on an old problem. Mol Cancer 2011;10:22.

3. Zoraghi R, Bessay EP, Corbin JD, Francis SH. Structural and functional features in human PDE5A1 regulatory domain that provide for allosteric cGMP binding, dimerization, and regulation. J Biol Chem 2005;280:12051-63.

4. Francis SH, Busch JL, Corbin JD, Sibley D. cGMP-dependent protein kinases and cGMP phosphodiesterases in nitric oxide and cGMP action. Pharmacol Rev 2010;62:525-63.

5. Rehmann H, Wittinghofer A, Bos JL. Capturing cyclic nucleotides in action: snapshots from crystallographic studies. Nat Rev Mol Cell Biol 2007;8:63-73.

6. Fajardo AM, Piazza GA, Tinsley HN. The role of cyclic nucleotide signaling pathways in cancer: targets for prevention and treatment. Cancers (Basel) 2014;6:436-58.

7. Fallahian F, Karami-Tehrani F, Salami S, Aghaei M. Cyclic GMP induced apoptosis via protein kinase G in oestrogen receptor-positive and -negative breast cancer cell lines. FEBS J 2011;278:3360-9.

8. Karami-Tehrani F, Fallahian F, Atri M. Expression of cGMP-dependent protein kinase, PKGIalpha, PKGIbeta, and PKGII in malignant and benign breast tumors. Tumour Biol 2012;33:1927-32.

9. Hou Y, Gupta N, Schoenlein P, Wong E, Martindale R, Ganapathy V, et al. An anti-tumor role for cGMP-dependent protein kinase. Cancer Lett 2006;240:60-8.

10. Karami-Tehrani F, Moeinifard M, Aghaei M, Atri M. Evaluation of PDE5 and PDE9 expression in benign and malignant breast tumors. Arch Med Res 2012;43:470-5.

11. Pusztai L, Zhen JH, Arun B, Rivera E, Whitehead C, Thompson WJ, et al. Phase I and II study of exisulind in combination with capecitabine in patients with metastatic breast cancer. J Clin Oncol 2003;21:3454-61.

12. Whitehead CM, Earle KA, Fetter J, Xu S, Hartman T, Chan DC, et al. Exisulind-induced apoptosis in a non-small cell lung cancer orthotopic lung tumor model augments docetaxel treatment and contributes to increased survival. Mol Cancer Ther 2003;2:479-88.

13. Piazza GA, Thompson WJ, Pamukcu R, Alila HW, Whitehead CM, Liu L, et al. Exisulind, a novel proapoptotic drug, inhibits rat urinary bladder tumorigenesis. Cancer Res 2001;61:3961-8.

14. Savai R, Pullamsetti SS, Banat GA, Weissmann N, Ghofrani HA, Grimminger F, et al. Targeting cancer with phosphodiesterase inhibitors. Expert Opin Investig Drugs 2010;19:117-31.

15. Kloner RA, Comstock G, Levine LA, Tiger S, Stecher VJ. Investigational noncardiovascular uses of phosphodiesterase-5 inhibitors. Expert Opin Pharmacother 2011;12:2297-313.

16. Sarfati M, Mateo V, Baudet S, Rubio M, Fernandez C, Davi F, et al. Sildenafil and vardenafil, types 5 and 6 phosphodiesterase inhibitors, induce caspase-dependent apoptosis of B-chronic lymphocytic leukemia cells. Blood 2003;101:265-9.

17. Sponziello M, Verrienti A, Rosignolo F, De Rose RF, Pecce V, Maggisano V, et al. PDE5 expression in human thyroid tumors and effects of PDE5 inhibitors on growth and migration of cancer cells. Endocrine 2015;

18. Tinsley HN, Gary BD, Keeton AB, Zhang W, Abadi AH, Reynolds RC, et al. Sulindac sulfide selectively inhibits growth and induces apoptosis of human breast tumor cells by phosphodiesterase 5 inhibition, elevation of cyclic GMP, and activation of protein kinase G. Mol Cancer Ther 2009;8:3331-40.

19. Li N, Xi Y, Tinsley HN, Gurpinar E, Gary BD, Zhu B, et al. Sulindac selectively inhibits colon tumor cell growth by activating the cGMP/PKG pathway to suppress Wnt/beta-catenin signaling. Mol Cancer Ther 2013;12:1848-59.

20. Shi Z, Tiwari AK, Patel AS, Fu LW, Chen ZS. Roles of sildenafil in enhancing drug sensitivity in cancer. Cancer Res 2011;71:3735-8.
21. Serafini P, Meckel K, Kelso M, Noonan K, Califano J, Koch W, et al. Phosphodiesterase-5 inhibition augments endogenous antitumor immunity by reducing myeloid-derived suppressor cell function. J Exp Med 2006;203:2691-702.
22. Gu G, Barone I, Gelsomino L, Giordano C, Bonofiglio D, Statti G, et al. Oldenlandia diffusa extracts exert antiproliferative and apoptotic effects on human breast cancer cells through ERalpha/Sp1-mediated p53 activation. J Cell Physiol 2012;227:3363-72.
23. Barone I, Catalano S, Gelsomino L, Marsico S, Giordano C, Panza S, et al. Leptin mediates tumor-stromal interactions that promote the invasive growth of breast cancer cells. Cancer Res 2012;72:1416-27.
24. Collins LC, Marotti JD, Gelber S, Cole K, Ruddy K, Kereakoglow S, et al. Pathologic features and molecular phenotype by patient age in a large cohort of young women with breast cancer. Breast Cancer Res Treat 2012;131:1061-6.
25. Carey LA, Perou CM, Livasy CA, Dressler LG, Cowan D, Conway K, et al. Race, breast cancer subtypes, and survival in the Carolina Breast Cancer Study. JAMA 2006;295:2492-502.
26. Yang XR, Sherman ME, Rimm DL, Lissowska J, Brinton LA, Peplonska B, et al. Differences in risk factors for breast cancer molecular subtypes in a population-based study. Cancer Epidemiol Biomarkers Prev 2007;16:439-43.
27. Curtis C, Shah SP, Chin SF, Turashvili G, Rueda OM, Dunning MJ, et al. The genomic and transcriptomic architecture of 2,000 breast tumours reveals novel subgroups. Nature 2012;486:346-52.
28. Dunning MJ, Smith ML, Ritchie ME, Tavare S. beadarray: R classes and methods for Illumina bead-based data. Bioinformatics 2007;23:2183-4.
29. Bolstad BM, Irizarry RA, Astrand M, Speed TP. A comparison of normalization methods for high density oligonucleotide array data based on variance and bias. Bioinformatics 2003;19:185-93.
30. Kim D, Pertea G, Trapnell C, Pimentel H, Kelley R, Salzberg SL. TopHat2: accurate alignment of transcriptomes in the presence of insertions, deletions and gene fusions. Genome Biol 2013;14:R36.
31. Anders S, Pyl PT, Huber W. HTSeq--a Python framework to work with high-throughput sequencing data. Bioinformatics 2015;31:166-9.
32. Love MI, Huber W, Anders S. Moderated estimation of fold change and dispersion for RNA-seq data with DESeq2. Genome Biol 2014;15:550.
33. Mihaly Z, Kormos M, Lanczky A, Dank M, Budczies J, Szasz MA, et al. A meta-analysis of gene expression-based biomarkers predicting outcome after tamoxifen treatment in breast cancer. Breast Cancer Res Treat 2013;140:219-32.
34. Perou CM, Sorlie T, Eisen MB, van de Rijn M, Jeffrey SS, Rees CA, et al. Molecular portraits of human breast tumours. Nature 2000;406:747-52.
35. Sorlie T, Perou CM, Tibshirani R, Aas T, Geisler S, Johnsen H, et al. Gene expression patterns of breast carcinomas distinguish tumor subclasses with clinical implications. Proc Natl Acad Sci U S A 2001;98:10869-74.
36. Holliday DL, Speirs V. Choosing the right cell line for breast cancer research. Breast Cancer Res 2011;13:215.
37. Neve RM, Chin K, Fridlyand J, Yeh J, Baehner FL, Fevr T, et al. A collection of breast cancer cell lines for the study of functionally distinct cancer subtypes. Cancer Cell 2006;10:515-27.
38. Schmitz AA, Govek EE, Bottner B, Van Aelst L. Rho GTPases: signaling, migration, and invasion. Exp Cell Res 2000;261:1-12.
39. Bishop AL, Hall A. Rho GTPases and their effector proteins. Biochem J 2000;348 Pt 2:241-55.
40. Riento K, Ridley AJ. Rocks: multifunctional kinases in cell behaviour. Nat Rev Mol Cell Biol 2003;4:446-56.

41. Liu S, Goldstein RH, Scepansky EM, Rosenblatt M. Inhibition of rho-associated kinase signaling prevents breast cancer metastasis to human bone. Cancer Res 2009;69:8742-51.
42. Helbig G, Christopherson KW, 2nd, Bhat-Nakshatri P, Kumar S, Kishimoto H, Miller KD, et al. NF-kappaB promotes breast cancer cell migration and metastasis by inducing the expression of the chemokine receptor CXCR4. J Biol Chem 2003;278:21631-8.
43. Goldhirsch A, Wood WC, Coates AS, Gelber RD, Thurlimann B, Senn HJ, et al. Strategies for subtypes--dealing with the diversity of breast cancer: highlights of the St. Gallen International Expert Consensus on the Primary Therapy of Early Breast Cancer 2011. Ann Oncol 2011;22:1736-47.
44. Nehra A. Erectile dysfunction and cardiovascular disease: efficacy and safety of phosphodiesterase type 5 inhibitors in men with both conditions. Mayo Clin Proc 2009;84:139-48.
45. Marino N, Collins JW, Shen C, Caplen NJ, Merchant AS, Gokmen-Polar Y, et al. Identification and validation of genes with expression patterns inverse to multiple metastasis suppressor genes in breast cancer cell lines. Clin Exp Metastasis 2014;31:771-86.
46. Ridley AJ, Schwartz MA, Burridge K, Firtel RA, Ginsberg MH, Borisy G, et al. Cell migration: integrating signals from front to back. Science 2003;302:1704-9.
47. Vega FM, Ridley AJ. Rho GTPases in cancer cell biology. FEBS Lett 2008;582:2093-101.
48. Sauzeau V, Rolli-Derkinderen M, Marionneau C, Loirand G, Pacaud P. RhoA expression is controlled by nitric oxide through cGMP-dependent protein kinase activation. J Biol Chem 2003;278:9472-80.
49. Sawada N, Itoh H, Yamashita J, Doi K, Inoue M, Masatsugu K, et al. cGMP-dependent protein kinase phosphorylates and inactivates RhoA. Biochem Biophys Res Commun 2001;280:798-805.
50. Morelli A, Filippi S, Sandner P, Fibbi B, Chavalmane AK, Silvestrini E, et al. Vardenafil modulates bladder contractility through cGMP-mediated inhibition of RhoA/Rho kinase signaling pathway in spontaneously hypertensive rats. J Sex Med 2009;6:1594-608.

Figures Legends

Figure 1. Impact of PDE5 overexpression on breast cancer cell proliferation, motility and invasion. **A**, RT-PCR analysis for PDE5 and 36B4 (internal standard) mRNA levels in Luminal A-type (MCF-7/T47D), Luminal B-like (ZR-75), HER2-overexpressing (SKBR3) and basal-like (BT-20/MDA-MB-468/MDA-MB-435) breast cancer cells. **B**, Immunoblotting for PDE5 expression in indicated cells. GAPDH, control for loading. **C**, Fluorescence-microscopic analysis to visualize EGFP-fluorescence in MCF-7 cells stably transfected with pEGFP-C1 (e.v.) or fusion protein expression pEGFP-PDE5A vectors (PDE5 1/2/3). MCF-7 cells, negative control. *Insets*: DAPI, nuclear staining. **D**, Immunoblotting showing EGFP-PDE5 expression in e.v. and PDE5 1/2/3 MCF-7 cells. GAPDH, control for loading. MTT growth (**E**), wound-healing (**F**, *insets*: time 0), transmigration (**G**) and invasion (**H**) assays in cells under basal nonstimulated conditions. *P<0.05, **P<0.005.

Figure 2. Effects of sildenafil on motility and invasion of PDE5-overexpressing MCF-7 breast cancer cells. Wound-healing (**A**, *insets*: time 0), transmigration (**B**) and invasion (**C**) assays in cells treated with vehicle (-) or sildenafil (Sild, 10μM). *P<0.05, **P<0.005, ***P<0.0005.

Figure 3. Influence of PDE5 on motility and invasion of T47D and MDA-MB-468 breast cancer cells. **A**, RT-PCR (*upper panel*) and immunoblot (*lower panel*) analyses for PDE5 expression in vector (e.v.) and PDE5-expressing T47D cells. 36B4, internal standard. GAPDH, control for loading. Transmigration (**B**) and invasion (**C**) assays in cells treated with vehicle (-) or sildenafil (Sild, 10μM). **D**, RT-PCR (*upper panel*) and immunoblot (*lower panel*) analyses for PDE5 expression in MDA-MB-468 cells transfected with control scrambled-shRNA (CTRLsh) and PDE5 shRNA (PDE5sh) constructs. 36B4, internal standard. GAPDH, control for loading.

Transmigration (**E**) and invasion (**F**) assays in CTRLsh and PDE5sh transfected MDA-MB-468 cells. **P<0.005.

Figure 4. Biological processes, functions and pathways identified from RNA sequencing data in PDE5-overexpressing MCF-7 cells. Ingenuity Pathway Analysis (IPA) used to identify biological processes significantly associated with differentially-expressed genes (**A**) and to calculate activation z-score of biological functions (**B**) and pathways (**C**). **D**, Predicted activation of RhoA signaling pathway by molecule activity predictor analysis of IPA in PDE5-overexpressing versus vector-transfected MCF-7 cells.

Figure 5. Rho GTPase activation in PDE5-overexpressing cells. **A**, *Input panel,* immunoblotting for Rho A-C, Cdc42 and Rac 1-3 expression. *GTP-bound panel,* activation assays of Rho A-C, Cdc42 and Rac 1-3. Immunoblotting showing phosphorylated LIM Kinase (pLIMK1^{Thr508}/pLIMK2^{Thr505}), Cofilin (p-Cofilin^{Ser3}) (**B**), Myosin Light Chain (pMLC$^{Thr18/Ser19}$) (**C**) and total proteins from whole-cell lysates. GAPDH, control for loading. **D**, Phalloidin staining of F-actin (stress fibers, red). DAPI, nuclear staining. *Insets*: Stress fibers with higher resolution. Transmigration (**E**) and invasion (**F**) assays in cells treated with vehicle (-) or ROCK inhibitor (Y-27632, 10μM). *P<0.05, **P<0.005, ***P<0.0005.

Figure 6. Role of PDE5 in breast cancer patients. **A**, Immunohistochemical detection of PDE5 expression in nonneoplastic breast tissues (NN), ER/PR-positive (+), HER2-overexpressing (HER2) and triple–negative (TN) breast cancer tissues. Representative fields were photographed at 20X-magnification (*insets*: details of PDE5 subcellular localization). PDE5 immunohistochemical expression was correlated to ER (**B**), PR (**C**), HER2 (**D**) status or molecular subtypes (**E**) of breast cancer patients. Kaplan-Meier survival analysis relating PDE5 levels and overall survival in all patients (**F**) or in patients with ER-positive breast cancers (**G**).

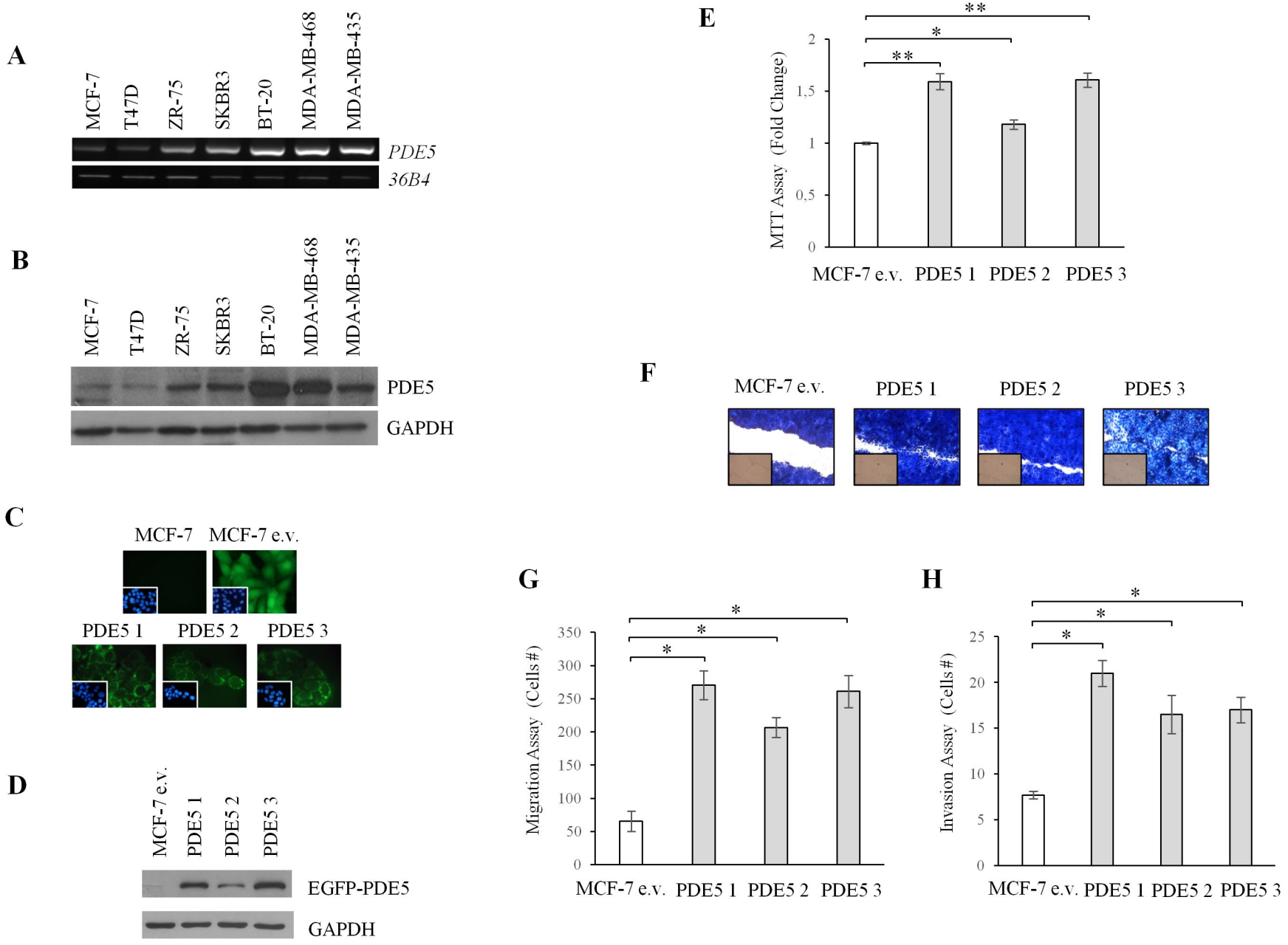
A
MCF-7
T47D
ZR-75
SKBR3
BT-20
MDA-MB-468
MDA-MB-435
PDE5
36B4
B
PDE5
GAPDH
C
MCF-7
MCF-7 e.v.
PDE5 1
PDE5 2
PDE5 3
D
MCF-7 e.v.
EGFP-PDE5
GAPDH
E
MTT Assay (Fold Change)
MCF-7 e.v.
PDE5 1
PDE5 2
PDE5 3
F
G
Migration Assay (Cells #)
H
Invasion Assay (Cells #)

Figure 1

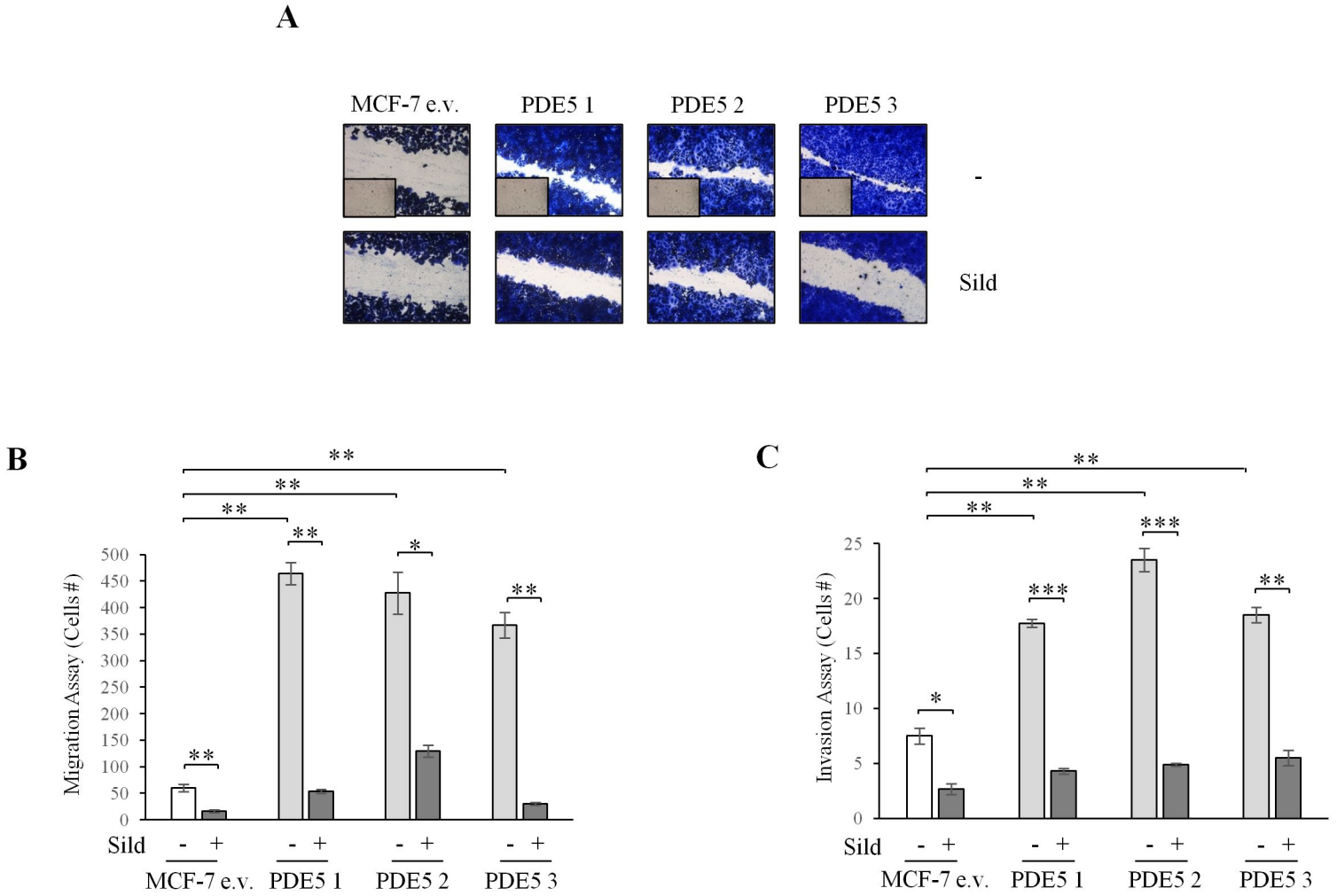
A
MCF-7 e.v.
PDE5 1
PDE5 2
PDE5 3
-
Sild
B
Migration Assay (Cells #)
500
450
400
350
300
250
200
150
100
50
0
**
*
Sild
- +
MCF-7 e.v.
PDE5 1
PDE5 2
PDE5 3
C
Invasion Assay (Cells #)
25
20
15
10
5
0
***

Figure 2

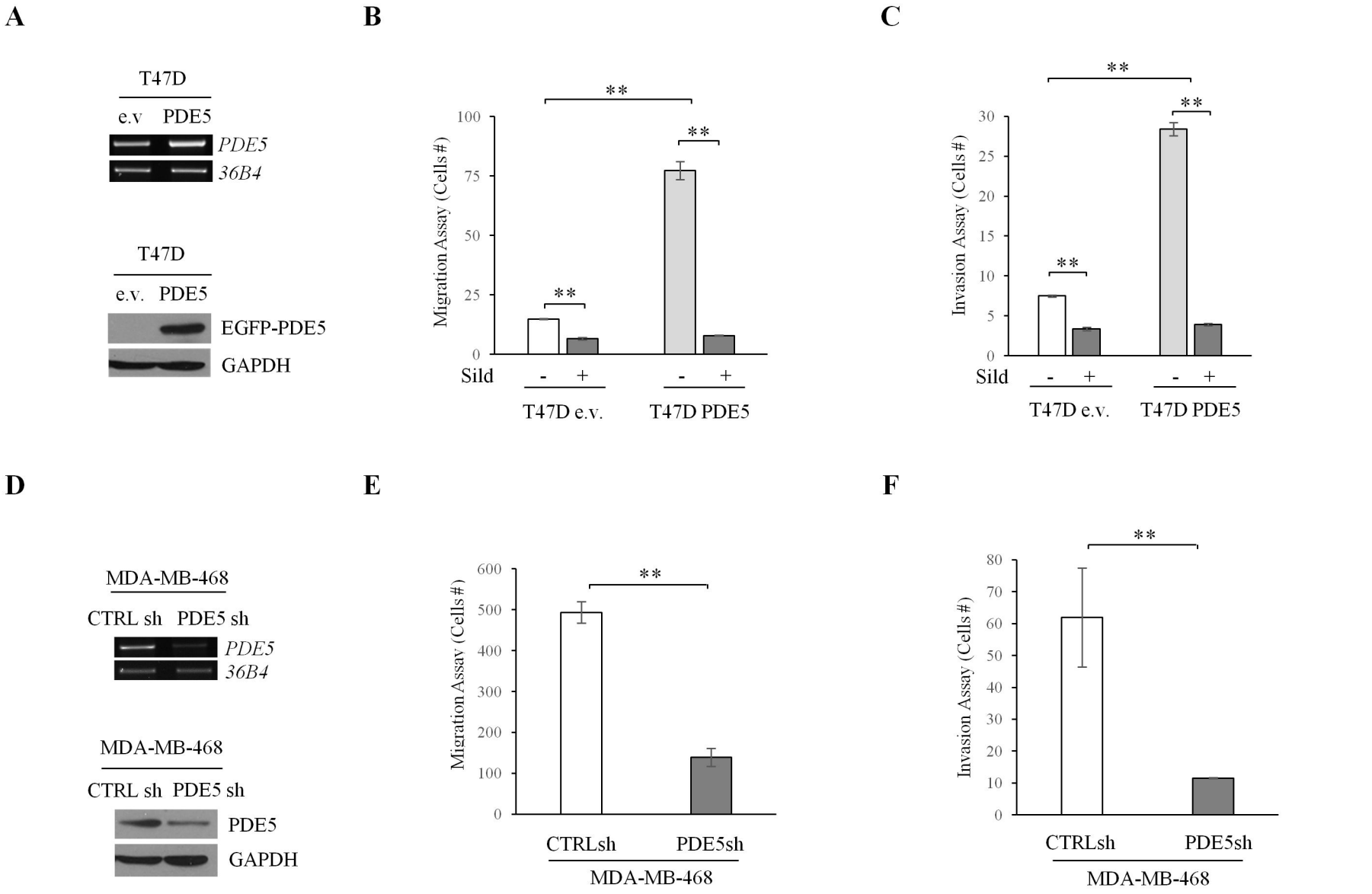
A
T47D
e.v PDE5
PDE5
36B4
T47D
e.v. PDE5
EGFP-PDE5
GAPDH
B
Migration Assay (Cells #)
100
75
50
25
0
**
**
Sild
- + - +
T47D e.v.
T47D PDE5
C
Invasion Assay (Cells #)
30
25
20
15
10
5
0
**
**
Sild
- + - +
T47D e.v.
T47D PDE5
D
MDA-MB-468
CTRL sh PDE5 sh
PDE5
36B4
MDA-MB-468
CTRL sh PDE5 sh
PDE5
GAPDH
E
Migration Assay (Cells #)
600
500
400
300
200
100
0
**
CTRLsh
PDE5sh
MDA-MB-468
F
Invasion Assay (Cells #)
80
70
60
50
40
30
20
10
0
**
CTRLsh
PDE5sh
MDA-MB-468

Figure 3

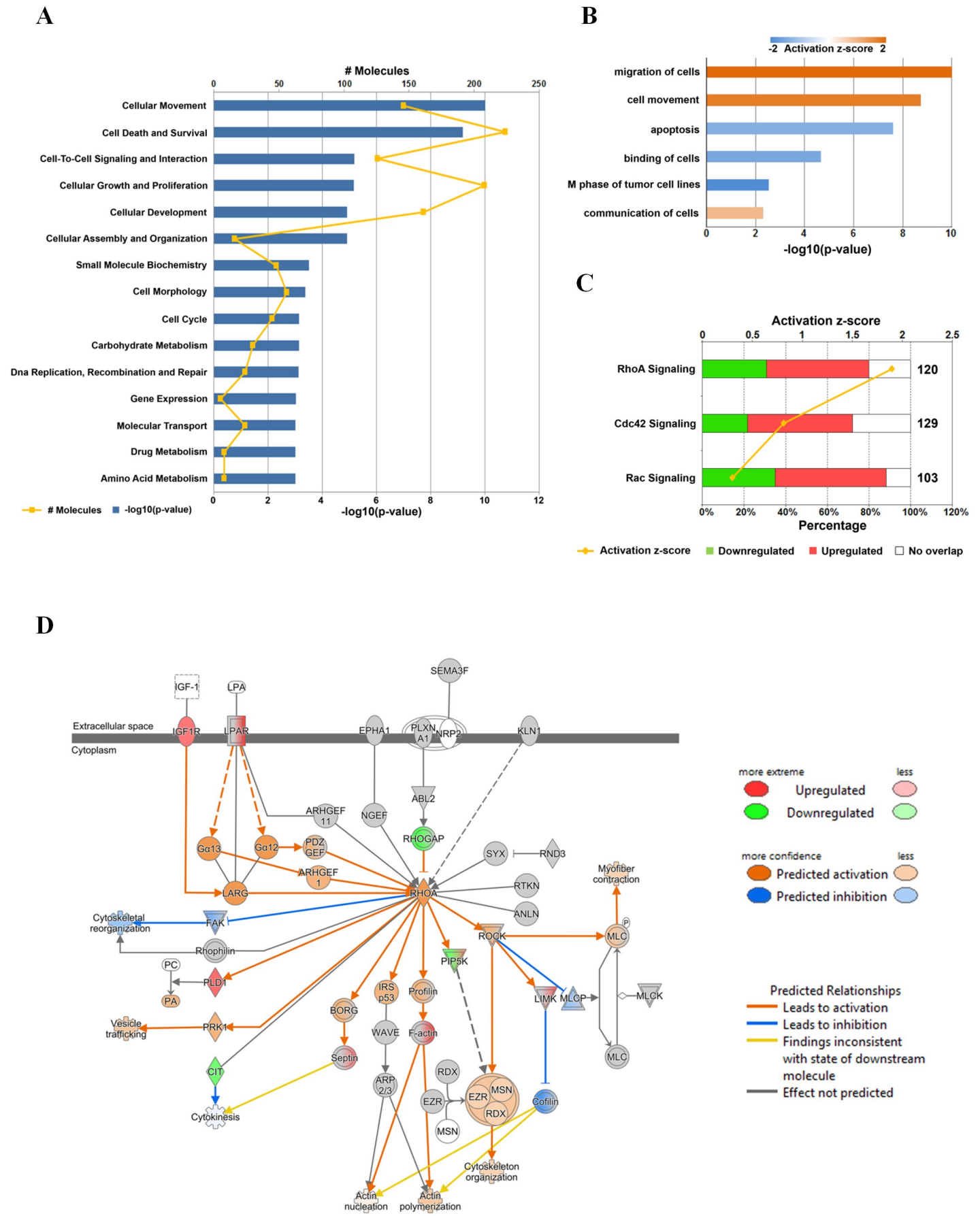
A
Molecules
Cellular Movement
Cell Death and Survival
Cell-To-Cell Signaling and Interaction
Cellular Growth and Proliferation
Cellular Development
Cellular Assembly and Organization
Small Molecule Biochemistry
Cell Morphology
Cell Cycle
Carbohydrate Metabolism
Dna Replication, Recombination and Repair
Gene Expression
Molecular Transport
Drug Metabolism
Amino Acid Metabolism
Molecules
-log10(p-value)
-log10(p-value)
B
-2 Activation z-score 2
migration of cells
cell movement
apoptosis
binding of cells
M phase of tumor cell lines
communication of cells
-log10(p-value)
C
Activation z-score
RhoA Signaling
Cdc42 Signaling
Rac Signaling
120
129
103
Percentage
Activation z-score
Downregulated
Upregulated
No overlap
D
Extracellular space
Cytoplasm
IGF-1
LPA
SEMA3F
IGF1R
LPAR
EPHA1
PLXNA1
NRP2
KLN1
ABL2
ARHGEF11
NGEF
RHOGAP
Gα13
Gα12
PDZGEF
ARHGEF1
SYX
RND3
LARG
RHOA
RTKN
ANLN
Myofiber contraction
Cytoskeletal reorganization
FAK
Rhophilin
PC
PA
PLD1
ROCK
PIP5K
MLC
P
IRS p53
Profilin
LIMK
MLCP
MLCK
BORG
WAVE
F-actin
PRK1
Vesicle trafficking
Septin
CIT
Cytokinesis
ARP 2/3
RDX
EZR
MSN
Cofilin
Cytoskeleton organization
Actin nucleation
Actin polymerization
more extreme
less
Upregulated
Downregulated
more confidence
less
Predicted activation
Predicted inhibition
Predicted Relationships
Leads to activation
Leads to inhibition
Findings inconsistent with state of downstream molecule
Effect not predicted

Figure 4

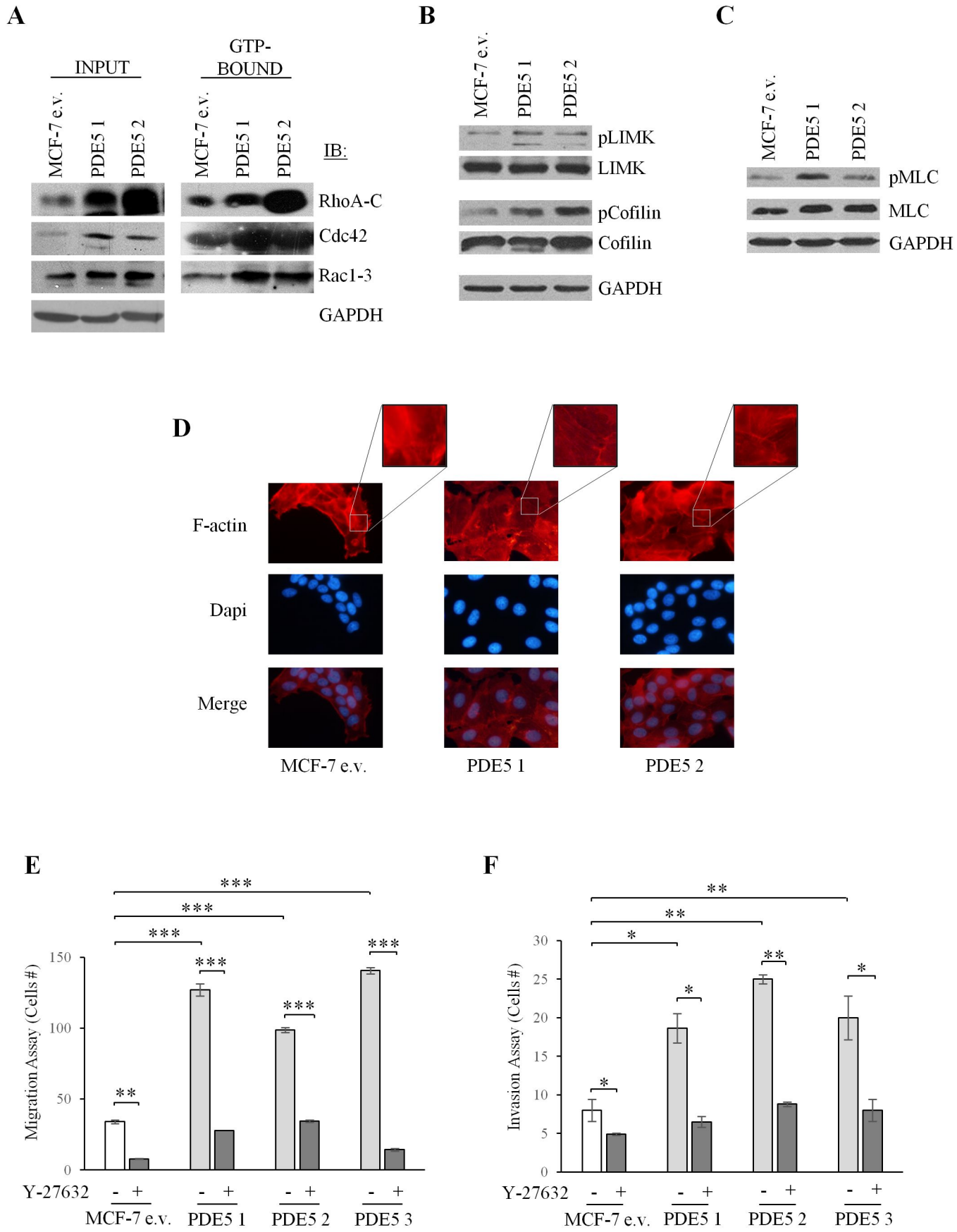
A
INPUT
GTP-BOUND
MCF-7 e.v.
PDE5 1
PDE5 2
IB:
RhoA-C
Cdc42
Rac1-3
GAPDH
B
pLIMK
LIMK
pCofilin
Cofilin
GAPDH
C
pMLC
MLC
GAPDH
D
F-actin
Dapi
Merge
MCF-7 e.v.
PDE5 1
PDE5 2
E
Migration Assay (Cells #)
150
100
50
0
Y-27632
MCF-7 e.v.
PDE5 1
PDE5 2
PDE5 3
F
Invasion Assay (Cells #)
30
25
20
15
10
5
0
Y-27632
MCF-7 e.v.
PDE5 1
PDE5 2
PDE5 3

Figure 5

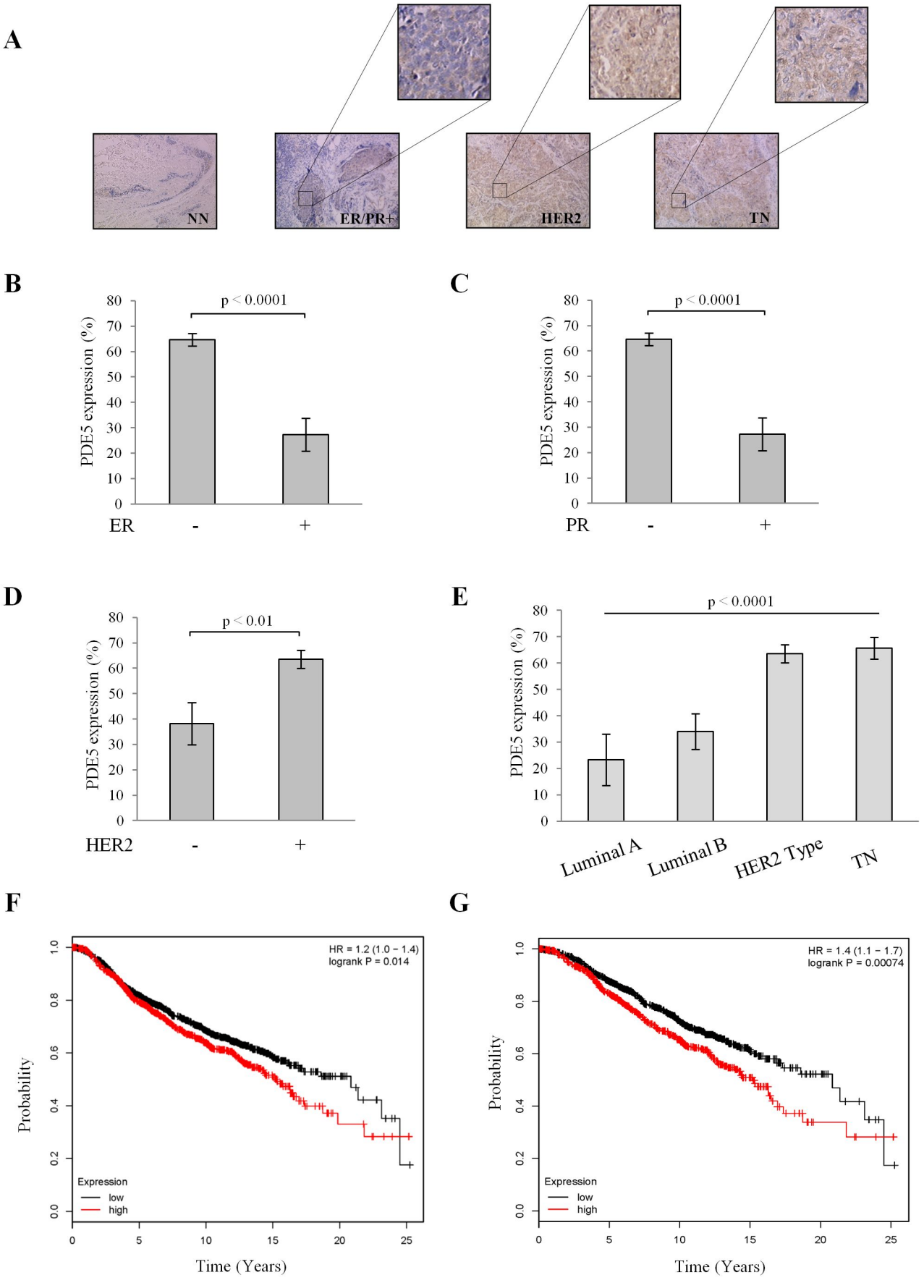
A
NN
ER/PR+
HER2
TN
B
p < 0.0001
PDE5 expression (%)
ER
-
+
C
p < 0.0001
PDE5 expression (%)
PR
-
+
D
p < 0.01
PDE5 expression (%)
HER2
-
+
E
p < 0.0001
PDE5 expression (%)
Luminal A
Luminal B
HER2 Type
TN
F
HR = 1.2 (1.0 − 1.4)
logrank P = 0.014
Probability
Expression
low
high
Time (Years)
G
HR = 1.4 (1.1 − 1.7)
logrank P = 0.00074
Probability
Expression
low
high
Time (Years)

Figure 6

Leptin as a mediator of tumor-stromal interactions promotes breast cancer stem cell activity

Cinzia Giordano[1,*], Francesca Chemi[2,*], Salvatore Panza[2,*], Ines Barone[2], Daniela Bonofiglio[2], Marilena Lanzino[2], Angela Cordella[3], Antonella Campana[2], Adnan Hashim[4,5], Pietro Rizza[2], Antonella Leggio[2], Balázs Győrffy[7,8,9], Bruno M. Simões[6], Robert B. Clarke[6], Alessandro Weisz[4], Stefania Catalano[2,], Sebastiano Andò[1,2,**]**

[1]Centro Sanitario, University of Calabria, Arcavacata di Rende, CS, Italy

[2]Department of Pharmacy, Health and Nutritional Sciences, University of Calabria, Arcavacata di Rende, CS, Italy

[3]IRCCS SDN (Istituto di Ricerca Diagnostica e Nucleare), Napoli, Italy

[4]Laboratory of Molecular Medicine and Genomics, Department of Medicine and Surgery, University of Salerno, Baronissi (SA), Italy

[5]Norwegian Centre for Molecular Medicine (NCMM), University of Oslo, Norway

[6]Breast Cancer Now Research Unit, Institute of Cancer Sciences, University Manchester, UK

[7]MTA TTK Lendület Cancer Biomarker Research Group, Budapest, Hungary

[8]2nd Dept. of Pediatrics, Semmelweis University, Budapest, Hungary

[9]MTA-SE Pediatrics and Nephrology Research Group, Budapest, Hungary

[*]These authors have equally contributed to this work

[**]Joint senior authors

Correspondence to:
Sebastiano Andò, **e-mail:** sebastiano.ando@unical.it
Stefania Catalano, **e-mail:** stefcatalano@libero.it

Keywords: *breast cancer, leptin, microenvironment, CAFs, breast cancer stem cells*

Received: *July 08, 2015* ***Accepted:*** *October 06, 2015* ***Published:*** *October 27, 2015*

ABSTRACT

Breast cancer stem cells (BCSCs) play crucial roles in tumor initiation, metastasis and therapeutic resistance. A strict dependency between BCSCs and stromal cell components of tumor microenvironment exists. Thus, novel therapeutic strategies aimed to target the crosstalk between activated microenvironment and BCSCs have the potential to improve clinical outcome. Here, we investigated how leptin, as a mediator of tumor-stromal interactions, may affect BCSC activity using patient-derived samples (n = 16) and breast cancer cell lines, and determined the potential benefit of targeting leptin signaling in these model systems. Conditioned media (CM) from cancer-associated fibroblasts and breast adipocytes significantly increased mammosphere formation in breast cancer cells and depletion of leptin from CM completely abrogated this effect. Mammosphere cultures exhibited increased leptin receptor (*OBR*) expression and leptin exposure enhanced mammosphere formation. Microarray analyses revealed a similar expression profile of genes involved in stem cell biology among mammospheres treated with CM and leptin. Interestingly, leptin increased mammosphere formation in metastatic breast cancers and expression of *OBR* as well as *HSP90*, a target of leptin signaling, were directly correlated with mammosphere formation in metastatic samples (r = 0.68/p = 0.05; r = 0.71/p = 0.036, respectively). Kaplan–Meier survival curves indicated that *OBR* and *HSP90* expression were associated with reduced overall survival in breast cancer patients (HR = 1.9/p = 0.022; HR = 2.2/p = 0.00017, respectively). Furthermore, blocking leptin signaling by using a full leptin receptor antagonist significantly reduced

mammosphere formation in breast cancer cell lines and patient-derived samples. Our results suggest that leptin/leptin receptor signaling may represent a potential therapeutic target that can block the stromal-tumor interactions driving BCSC-mediated disease progression.

INTRODUCTION

Carcinoma of the breast is the most common malignancy and the leading cause of cancer-related death in women worldwide [1]. Despite improvements in diagnosis and treatment, metastatic or recurrent disease and resistance to therapy remain the principal causes of death for breast cancer patients.

In the last years, multiple reports have shown that a subpopulation of cancer cells displaying stem cell properties and named as cancer stem cells (CSCs) plays a crucial role in sustaining tumor growth and progression. These cells are characterized by their ability to undergo self-renewal, a process that drives tumorigenesis, and to differentiate into the non-self-renewing cells forming the tumor bulk [2, 3]. From a clinical point of view, the main concern with CSCs is related to their resistance to conventional treatments (e.g. endocrine-, chemo- and radio-therapy), a feature that might be the underlying cause of tumor recurrence and metastases [4–6]. Similar to embryonic and somatic stem cells, the self-renewal and differentiation of CSCs are regulated by both intrinsic and extrinsic pathways whose dysregulation may be a key event initiating carcinogenesis. Among the intrinsic pathways, an important role is displayed by developmental signals such as Wnt, Hedgehog, Janus kinase 2-signal transducer and activator of transcription 3 (JAK2-STAT3) and Notch pathways that are frequently deranged in cancers [7]. Extrinsic signals that regulate stem cell behaviour originate in the surrounding stem cell microenvironment, termed as cancer stem niche. This niche contains a number of cell types, including mesenchymal stem cells (MSCs), cancer-associated fibroblasts (CAFs), adipocytes, endothelial and immune cells, all of which, through networks of cytokines and growth factors, have been shown to influence tumor growth and metastasis [8]. Thus, strategies aimed to specifically target the interaction between CSCs and their microenvironment may represent an important approach to improve patient outcome.

Adipocytes and CAFs are the major components in breast cancer microenvironment, and along with their secreted factors represent key players in stroma-epithelial cell interactions. As an important paracrine mediator, the adipocyte-derived cytokine leptin, that we have recently demonstrated to be also secreted by CAFs [9], has been correlated with breast cancer occurrence. Leptin exerts its biologic function through binding to its receptor (OBR) which activates multiple downstream signaling pathways such as those involving JAK2-STAT3, mitogen-activated protein kinase (MAPK), and phosphatidylinositol 3-kinase/protein kinase B (PI3K/AKT) [10]. Leptin and both short and long OBR isoforms are overexpressed in breast cancer, especially in higher grade tumors and are associated with distant metastases [11, 12]. It has been extensively demonstrated that this cytokine, acting in an autocrine, endocrine and paracrine manner, may modulate many aspects of breast tumorigenesis from initiation and primary tumor growth to metastatic progression [13–15]. Besides, crosstalk with other different signaling molecules such as estrogens, growth factors and inflammatory cytokines further increases leptin impact on breast tumor progression [16–21]. Moreover, leptin is able to shape the tumor microenvironment within the mammary gland by inducing multiple concurrent events such as migration of endothelial cells, angiogenesis and recruitment of macrophages and monocytes [13–15, 22]. Interestingly, recent studies have also reported that leptin signaling may be involved in the promotion of CSC phenotype [23–25] and that inhibition of STAT3 suppresses leptin-induced CSC activity and cancer progression in diet-induced obese rats [26].

The aim of the current study was to evaluate the role of leptin, as a mediator of the tumor-stroma interaction, in regulating breast CSC activity using breast cancer cell lines and patient-derived breast cancer cells isolated from metastatic ascites and pleural effusions. Particularly, we investigated: *i*) the impact of CAFs and adipocytes isolated from stromal breast tissues on mammosphere formation and self-renewal in breast cancer cells; *ii*) the specific role of leptin and its receptor in influencing breast CSC phenotype in the context of the tumor microenvironment; *iii*) the effect of inhibiting leptin signaling as potential therapeutic target to reduce breast CSC activity in *in vitro* and *ex vivo* models.

RESULTS

CAFs and adipocytes induce mammosphere formation in breast cancer cells through leptin secretion

To assess the ability of stromal cells to affect CSC activity in breast cancer cells we performed co-culture experiments. As experimental models for breast CSCs (BCSCs), we used estrogen receptor (ER)-α-positive MCF-7 cells grown as mammospheres. This culture system has been used to characterize, enrich and propagate breast cancer cells with stem-like phenotype, relying on the feature of stem cells to escape anoikis and grow as spheroids in anchorage-independent conditions [27]. MCF-7 mammosphere cells were characterized by flow

cytometric analysis that revealed an enrichment of $CD44^+/CD24^-$ subpopulation compared to MCF-7 monolayer cells (Supplementary Figure S1A). In addition, real-time PCR further revealed that genes associated with stem cell phenotype, including *OCT4, N-CAD, BMI1, SOX4*, were expressed in mammosphere cells at higher levels than in monolayer cells (Supplementary Figure S1B). Moreover, MCF-7 mammosphere cells were also analyzed for the expression of ERα (Supplementary Figure S1C and 1D). As stromal cells, we used either CAFs isolated from biopsies of primary breast tumors or human breast adipocytes obtained after preadipocyte differentiation. CAFs possessed the basic fibroblast characteristics with long and spindle-shaped morphology and highly expressed alpha-smooth muscle actin (α-SMA), vimentin, and fibroblast activation protein (*FAP*) (Supplementary Figure 2A and 2B). Adipocytes displayed a classical morphological phenotype characterized by accumulation of lipid droplets associated with the expression of specific markers as PPARγ and leptin (*OB*) (Supplementary Figure S2C). Using co-culture experiments, we examined mammosphere formation from MCF-7 cells in the presence or absence of conditioned media (CM) harvested from CAFs and adipocytes. Compared to the cells cultured alone, MCF-7 cells co-cultured with CAF- or adipocyte-derived CM showed a significant enhancement in mammosphere forming efficiency (MFE) (Figure 1A). Stem cells are maintained in the primary mammospheres through self-renewal, and are able to give rise to secondary mammospheres when cells from the primary spheres are dissociated and allowed to grow in anchorage-independent conditions. Therefore, we carried out secondary mammosphere cultures to examine the effects of CM on BCSC self-renewal. Our experiments demonstrated an increased self-renewal in MCF-7 cells treated with CAF- and adipocyte-derived CM in the first generation compared with the untreated spheres (Figure 1B and 1C). These data suggest that BCSC activity is influenced by

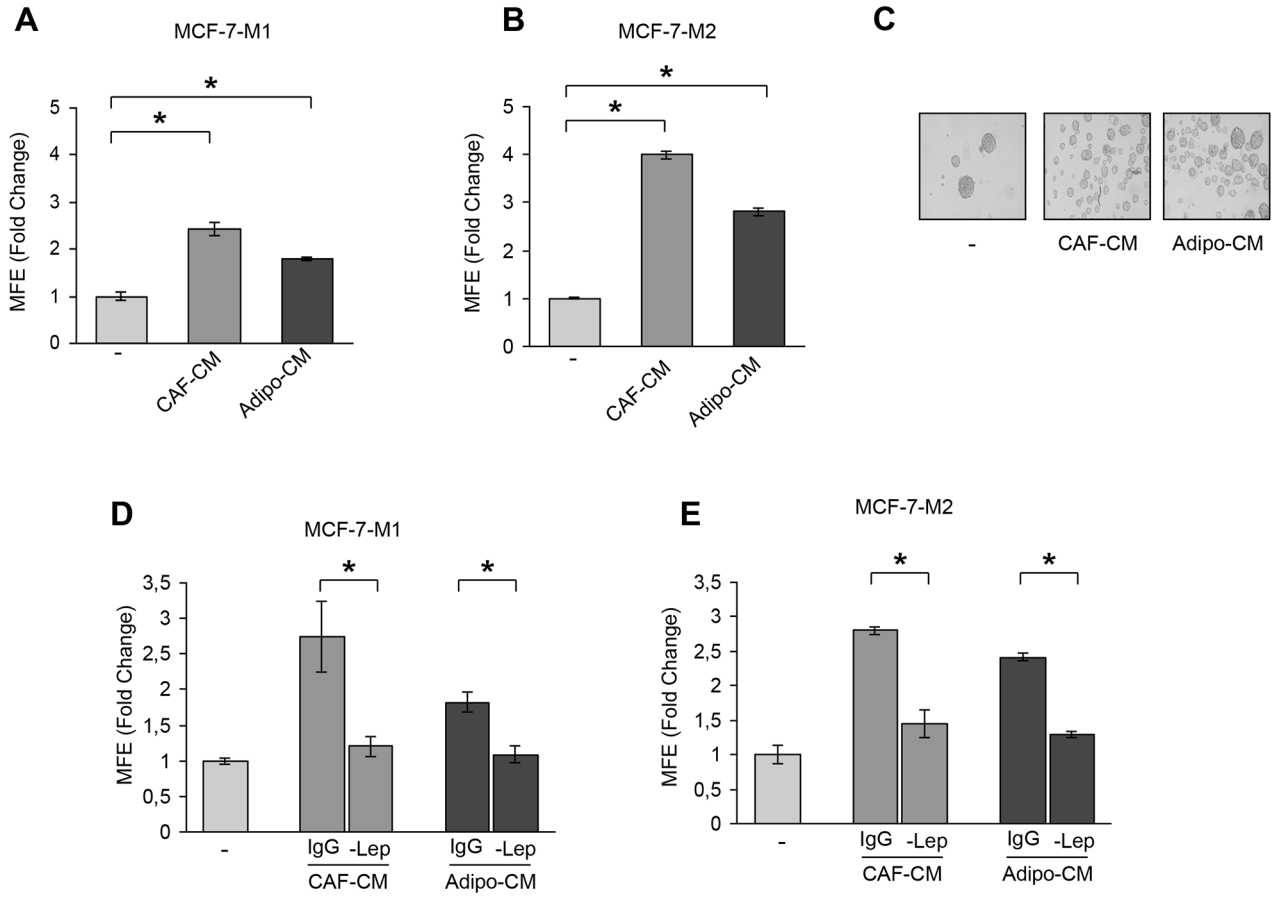

Figure 1: Leptin mediates the effects of stromal cell-CM on breast cancer cell mammosphere formation. Mammosphere Forming Efficiency (MFE) evaluated in MCF-7-M1 (**A**) and MCF-7-M2 (**B**) in the presence or absence (−) of CAF- and Adipocyte-derived Conditioned Media (CAF-CM and Adipo-CM, respectively). MFE was calculated by dividing the number of mammospheres (colonies > 50 μm) formed by the number of the cells plated and expressed as fold change compared to untreated cells (−). (**C**) Representative phase-contrast images of mammospheres treated as in panel (B) are shown. MFE evaluated in MCF-7-M1 (**D**) and MCF-7-M2 (**E**) in the presence or absence (−) of leptin-immunodepleted CAF-CM and Adipo-CM (-Lep). IgG: CM immunodepleted with nonspecific antibody. The values represent the means ± s.d. of three different experiments each performed in triplicate. $*p < 0.05$.

soluble factors secreted from stromal cells. Thus, given the role of leptin as an important cytokine secreted by both CAFs and adipocytes, we assessed the impact of leptin in the context of the heterotypic signaling working in BCSC–stromal interactions. First, ELISA measurement in CM from stromal cells showed that leptin levels were 2,4 ± 0,12 ng/mg protein and 20,32 ± 2 ng/mg protein in CAF- and adipocyte-derived CM, respectively. Leptin was then immunodepleted from CAF- and adipocyte-derived CM using a specific leptin antibody, and resulting media were tested for the ability to induce mammosphere formation in breast cancer cells. AS shown in Figure 1D and 1E, leptin depletion significantly decreased the MFE/self-renewal promoted by stromal cell-derived CM.

Targeting leptin signaling reduces stem cell activity mediated by stromal cells

Our previous experiments indicate that leptin may represent an important paracrine molecule that mediates the interaction between stromal cells and BCSCs. To support this observation, we tested the effect of a full leptin receptor antagonist, peptide LDFI, on BCSC activity. We have previously shown that this peptide inhibits leptin-induced breast cancer growth *in vitro* and exhibits anti-neoplastic activities *in vivo* [28]. Our data demonstrated that treatment with peptide LDFI significantly reduced MFE/self-renewal promoted by stromal cell-derived CM in MCF-7 cells (Figure 2A). To extend the results obtained, we have grown the ERα-negative MDA-MB-231 breast cancer cells as mammospheres and evaluated the effects of CAF- or adipocyte-CM in the presence or absence of peptide LDFI. Treatment of MDA-MB-231 mammosphere cultures with CAF- or adipocyte-derived CM significantly increased MFE/self-renewal and the addition of the OBR antagonist LDFI strongly reduced these effects (Figure 2B), confirming that leptin/leptin receptor may play a crucial role in maintaining the BCSC traits mediated by stromal cells in different cellular backgrounds.

Leptin signaling regulates mammosphere formation/self-renewal activity of breast cancer cells

Having shown that stromal cells regulate BCSC activity through secretion of leptin, we next investigated

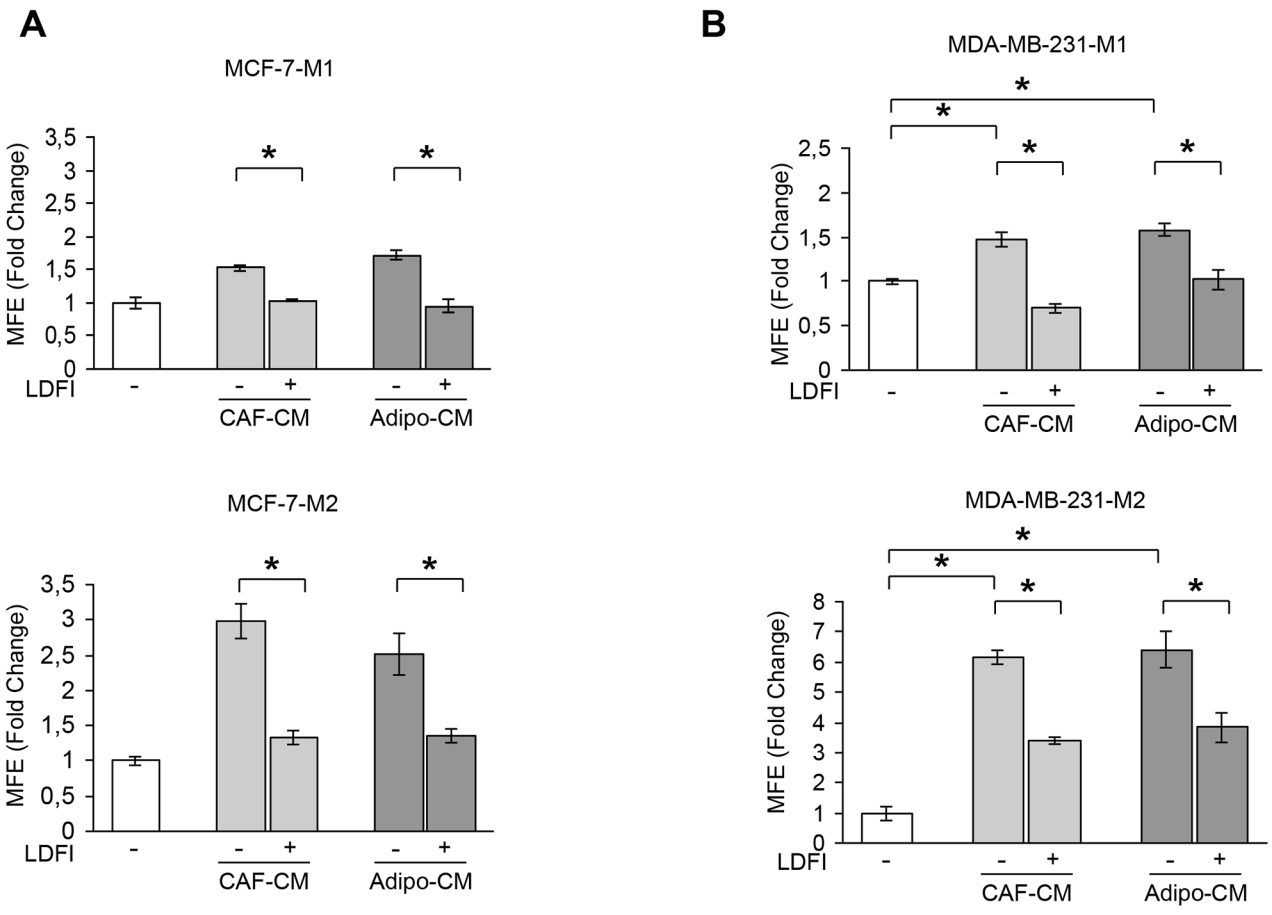

Figure 2: Effects of a selective leptin receptor antagonist on breast cancer stem cell activity. MFE evaluated in MCF-7-M1 and MCF-7-M2 (**A**) and in MDA-MB-231-M1 and MDA-MB-231-M2 (**B**) treated with CAF-CM and Adipo-CM with/without peptide LDFI (1 μg/ml). The values represent the means ± s.d. of three different experiments each performed in triplicate. *$p < 0.05$.

the direct involvement of this cytokine in the regulation of mammosphere formation/self-renewal in MCF-7 cells. In agreement with previous data demonstrating that leptin receptor plays a crucial role in maintaining cancers in a stem cell-like state [23–26], we found that MCF-7 mammosphere cultures exhibited increased *OBR* mRNA expression and in a greater extent the long isoform, compared to monolayer cells (Figure 3A). Accordingly, leptin treatment of mammosphere cultures resulted in a significant increase in MFE/self-renewal and in an enhanced percentage of $CD44^{+}/CD24^{-}$ population compared with untreated cells (Figure 3B, 3C and 3D). Accordingly, in MDA-MB-231 mammosphere cultures, we observed a significant increase in the long isoform of *OBR* mRNA expression compared to monolayer cells, and an enhanced MFE/self-renewal after leptin exposure (Supplementary Figure S3), demonstrating that this cytokine can directly regulate BCSC activity.

Since BCSCs display increased cell motility and invasion, we tested the effects of leptin on the migratory potential of MCF-7 mammospheres. Our data clearly showed that leptin exposure increased the number of migrated cells suggesting that this cytokine can facilitate the invasive behavior of BCSCs (Figure 3E). Next, *OBR* expression was stably knocked-down using lentiviral delivered short hairpin RNA (*OBR* sh) in MCF-7 cells (Figure 3F-*left panel*). Suppression of *OBR* expression led to a significant inhibition of MFE (Figure 3F-*right panel*), implying that this gene is necessary for maintaining cancer stem-like properties in breast cancer cells. In addition, we observed that leptin treatment induced the phosphorylation of specific OBR downstream signaling molecules such as STAT3, Akt and p42/44 MAPK (Figure 3G). As expected, the increase in MFE induced by leptin was reversed by the JAK2-STAT3 inhibitor AG490, the MEK1 inhibitor PD98059 and the PI3K/AKT inhibitor LY294002 (Figure 3H), suggesting

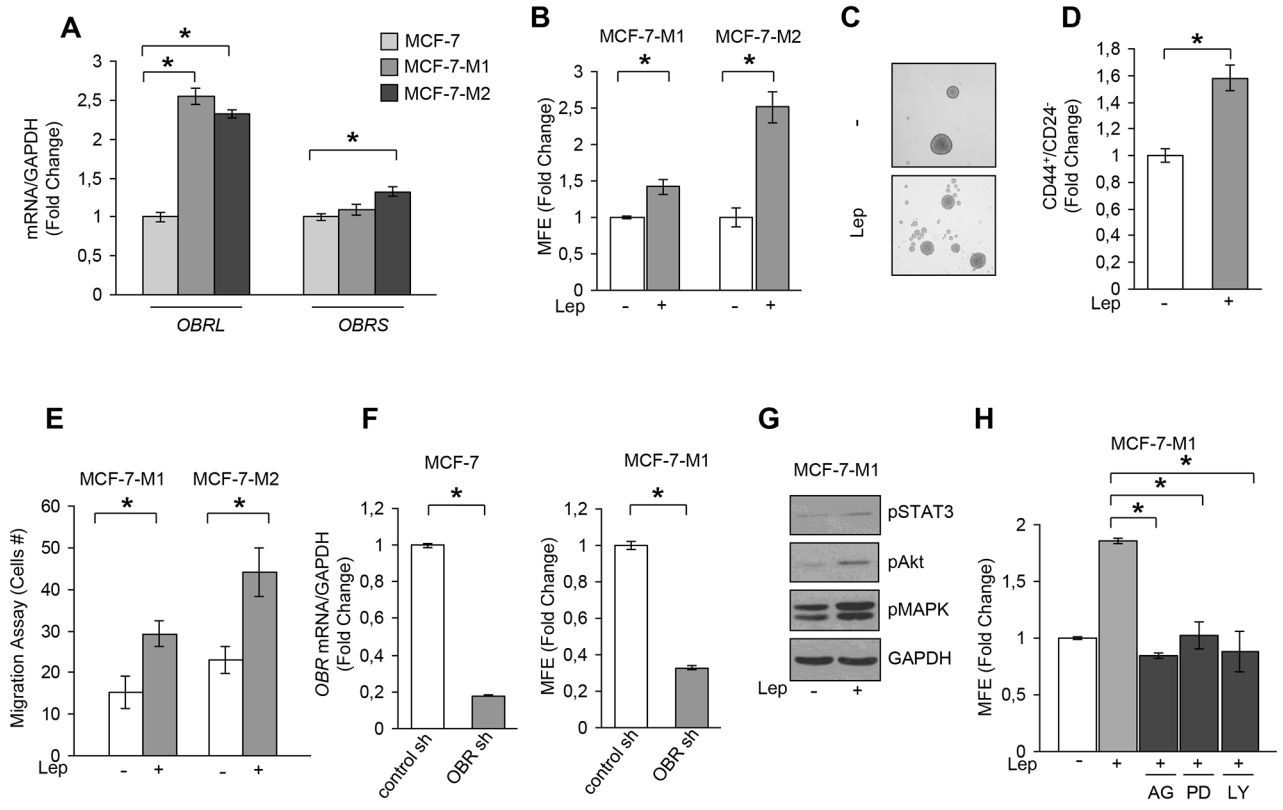

Figure 3: Leptin induces MFE in breast cancer cells. A. Leptin receptor long (*OBRL*) and short (*OBRS*) isoform mRNA levels, evaluated by real time RT-PCR, in MCF-7, MCF-7-M1 and MCF-7-M2 cells. Each sample was normalized to its *GAPDH* mRNA content. **B.** MFE in MCF-7-M1 and MCF-7-M2 in the presence or absence (−) of leptin 500 ng/ml (Lep). **C.** Representative phase-contrast images of mammospheres treated as in panel (B) are shown. **D.** $CD44^{+}/CD24^{-}$ population in MCF-7-M2 cells treated or not (−) with Lep. **E.** Transmigration assays in MCF-7-M1 and MCF-7-M2-derived cells treated or not (−) with Lep. **F.** MCF-7 cells were stably transfected with either a scrambled shRNA (control-sh) or OBR shRNA (OBR-sh). *OBRL* mRNA content was evaluated by real time RT-PCR (*left panel*). Each sample was normalized to its *GAPDH* mRNA content. MFE in MCF-7-M1 derived from either control-sh or OBR-sh clones (*right panel*). **G.** Immunoblotting of phosphorylated (p), STAT3 (Tyr^{705}), Akt (Ser^{473}), and MAPK (Thr^{202}/Tyr^{204}) at the indicated residues measured in cellular extracts from MCF-7-M1 cells treated or not (−) with Lep. GAPDH, loading control. **H.** MFE in MCF-7-M1 treated with Lep and AG490 (AG-20 μmol/L), PD98059 (PD-10 μmol/L) or LY294002 (LY-10 μmol/L). The values represent the means ± s.d. of three different experiments each performed in triplicate. *$p < 0.05$.

that leptin promotes stem cell properties *via* activation of classical leptin signaling pathways. In agreement with these observations, we also found an up-regulation of well-known leptin target genes as *OBR* and the heat shock protein 90 (HSP90) [20] in MCF-7 cells treated with leptin (Supplementary Figure S4A and 4B)

Gene expression profiling in leptin or stromal CM-treated mammosphere-derived cells

To determine whether leptin, CAF- and adipocyte-CM may similarly affect gene expression profile in mammosphere-derived cells, we performed gene expression profiling analysis on total RNA extracted from the second generation spheres. Microarray results highlighted several RNAs differentially expressed in treated *vs* untreated MCF-7 mammospheres. Venn diagram analysis was used to compare the gene lists and to identify those genes that are unique and in common among the three treatments (Figure 4A). A total of 2270 transcripts were commonly regulated in all treated samples (808 up- and 1462 down-regulated transcripts, respectively). It should be noted that the global overlap among genes expressed in treated samples includes a number of genes known to play a role in stem cell biology such as *BMI1*, *SUZ12*, *YES1*, *SOX4* (Figure 4B, *left panel*, Supplementary Table S2). Similar trends were also observed for the expression of other genes involved in cell cycle control (Figure 4B, *middle panel*, Supplementary Table S3). Moreover, treated samples displayed up-regulation of some transcripts related to the heat shock protein family, that recently have been suggested to be crucial in sustaining proliferation and self-renewal of stem cells [29] (Figure 4B, *right panel,* Supplementary Table S4). To validate our microarray study MCF-7 mammospheres treated with leptin were evaluated for the expression of a

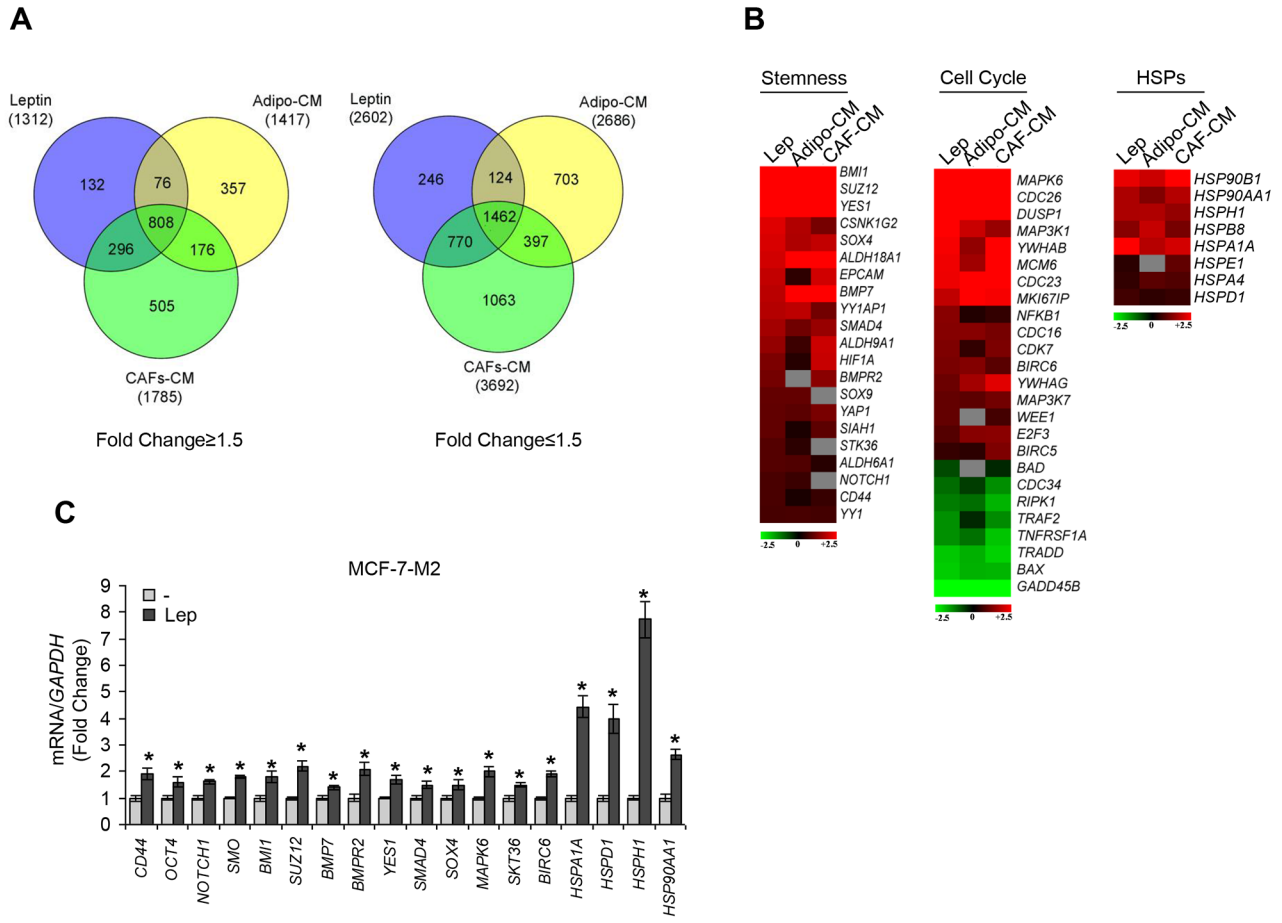

Figure 4: Gene expression profiling in mammosphere cultures treated with stromal cell-CM or leptin. A. Venn diagram of up-(*left panel*) and down-(*right panel*) regulated transcript identified by microarray analysis in MCF-7-M2 cells treated with CAF-CM, Adipo-CM or Lep compared to untreated samples. **B.** Heat-maps of stemness related-genes, cell cycle related-genes and HSP family genes from microarray data. Gene expression changes were calculated in treated cells with respect to the untreated controls. Transcript showing a DiffScore ≤ − 30 and ≥ 30, corresponding to a *p*-value of 0.001, and significant fold change in treated vs untreated ≥ 1.5 were considered. **C.** Real-time RT-PCR validation of a subset of genes in MCF-7-M2 cells treated or not (−) with Lep. Each sample was normalized to its *GAPDH* mRNA content. The values represent the means ± s.d. of three different experiments each performed in triplicate. **p* < 0.05 *vs* untreated (−) sample.

panel of genes by using real-time PCR (Figure 4C). Taken together, gene expression profile analyses strongly support the role of leptin as a crucial paracrine molecule able to mediate the microenvironment effects on BCSC activity.

Leptin increases patient-derived mammosphere formation/self-renewal activity

The role of leptin in the regulation of BCSC activity was then evaluated by using patient-derived breast cancer cells isolated from metastatic ascites or pleural effusions. Tumor histology, grade, hormone receptors and HER2 status of the primary tumors were reported in Table 1. Mammosphere cultures treated with leptin resulted in a significant increase in MFE compared to untreated samples (n = 10, Figure 5A). Secondary mammosphere formation was observed only in four samples and treatment with leptin significantly increased self-renewal in three of them (Figure 5B). Besides, four human metastatic samples taken from patients with breast cancer were also treated with peptide LDFI. MFE induced by leptin was significantly decreased with the addition of LDFI (Figure 5C). Interestingly, treatment with peptide LDFI alone reduced the mammosphere formation, underlying how this peptide negatively interferes with leptin autocrine loop (Figure 5C). Then, to investigate the direct involvement of OBR in the regulation of mammosphere formation, *OBR* gene expression was analyzed in cells from metastatic ascites and pleural effusion fluids using microarray data. There was a significant direct correlation between the expression of *OBR* mRNA in cells from the metastatic fluids and MFE (r = 0.68; p = 0.05, Figure 5D). In agreement with the microarray data obtained in MCF-7 mammospheres, a significant correlation between MFE and *HSP90* gene expression in the same metastatic patient-derived samples (r = 0.71; p = 0.036) was also observed (Figure 5E). These data suggest that patients with higher levels of *OBR* and *HSP90* mRNAs in cells of metastatic fluids have greater *ex vivo* CSC activity.

OBR expression correlates with reduced overall survival in breast carcinomas

To investigate the clinical significance of *OBR* gene expression in human breast cancers the relationship between *OBR* levels and overall survival (OS) of breast cancer patients (n = 781) was estimated by Kaplan–Meier analysis. Survival curves indicated that women with high *OBR* expression exhibited a lower rate of OS than those with low *OBR* expression (HR = 1.9, p = 0.022) (Figure 6A). Similarly, breast carcinoma patients with high *HSP90*

Table 1: Summary of metastatic patients-derived cancers

SAMPLE ID	AGE	SOURCE	Histology	GRADE	ER	PR	HER2
BB3RC29	70	ASC	UN	UN	POS	POS	NEG
BB3RC46	68	ASC	ILC	2	POS	POS	NEG
BB3RC50	46	ASC	IDC	2	POS	POS	NEG
BB3RC59[1]	69	ASC	ILC	2	POS	POS	NEG
BB3RC60	66	ASC	ILC	2	POS	POS	NEG
BB3RC65[2]	62	ASC	ILC	2	POS	POS	NEG
BB3RC66[1]	69	ASC	ILC	2	POS	POS	NEG
BB3RC70[2]	62	ASC	ILC	2	POS	POS	NEG
BB3RC71	48	PE	UN	3	POS	POS	POS
BB3RC79	UN	PE	IDC	3	NEG	NEG	NEG
BB3RC81	55	ASC	IDC	2	POS	POS	NEG
BB3RC84	UN	PE	UN	3	NEG	NEG	NEG
BB3RC90	66	PE	IDC/ILC	2	P0S	POS	NEG
BB3RC92	61	ASC	IDC	1	POS	POS	NEG
BB3RC93	UN	ASC	UN	UN	POS	POS	NEG
BB3RC94	41	ASC	UN	UN	POS	POS	NEG

[1, 2]These samples were obtained at different time points from the same patients
Sixteen patient-derived breast cancer samples were used in this study. Tumor histology and grade for metastatic samples (ASC and PE) relates to the primary cancer. Abbreviation: **UN** unknown, **PE** pleural effusion, **ASC** ascites sample, **ILC** invasive lobular carcinoma , **IDC** invasive ductal carcinoma, **POS** positive, **NEG** negative, **ER** Estrogen Receptor, **PR** Progesterone Receptor, **HER2**, epidermal growth factor receptor 2.

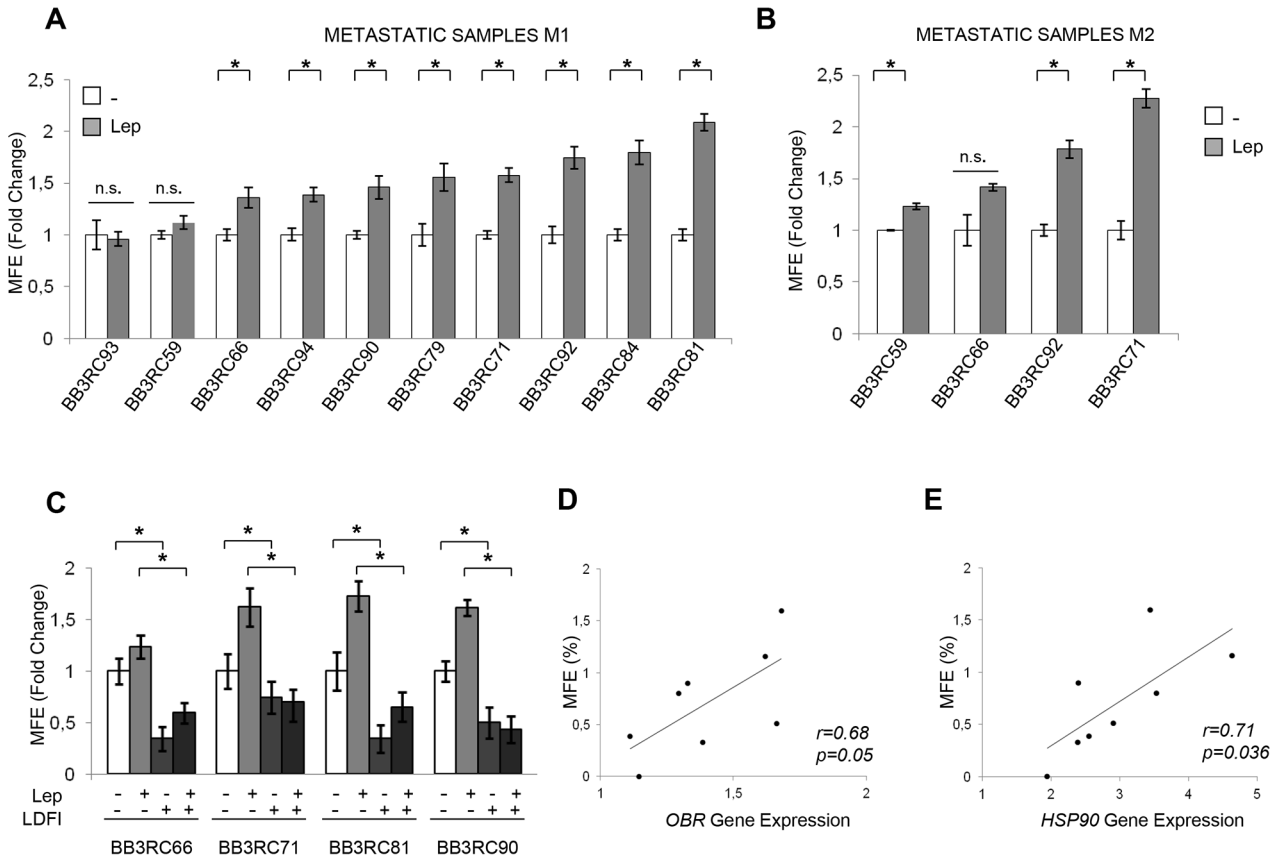

Figure 5: Leptin enhances mammospheres formation/self-renewal activity in patient-derived metastatic cells. 10 metastatic fluid samples obtained from breast cancer patients (BB3RC59/BB3RC66/BB3RC71–94) undergoing palliative drainage of symptomatic ascites or pleural effusions were used (Table 1). MFE in metastatic patient-derived cells grown as primary (Metastatic samples M1) (**A**) or secondary (Metastatic samples M2) (**B**) mammospheres in the presence or absence (−) of Lep. (**C**) MFE in 4 Metastatic sample M1 untreated (−) or treated with Lep, peptide LDFI (1 μg/ml), and Lep+LDFI. The values represent the means ± s.d. of three different experiments each performed in triplicate. *$p < 0.05$. n.s.:nonsignificant. Correlation between *OBR* (**D**) or *HSP90* mRNA expression (**E**) in cells of the metastatic fluids and MFE (8 patients/BB3RC29–70) (Pearson correlation coefficient, $r = 0.68$, $p = 0.05$; $r = 0.71$, $p = 0.036$, respectively).

expression had decreased OS compared with those with low *HSP90* expression (*HR = 2.2, p = 0.00017*) (Figure 6B).

Basal-like breast cancer is an aggressive tumor subtype, composed by primitive undifferentiated cells. Indeed, basal-like breast tumors, which are enriched for $CD44^{+}/CD24^{-}$ cells, exhibit epithelial–mesenchymal transition features and express high levels of stem cell-regulatory genes [30–34]. In agreement with these observations, the results of the Kaplan-Meier analysis indicated a more relevant discrimination in terms of overall survival between high and low expression of *OBR* and *HSP90* in basal breast cancer patients ($n = 143$) (*HR = 4.4, p = 0.011; HR = 5.2, p = 0.013* respectively) (Figure 6C and 6D).

DISCUSSION

The heterotypic signals arising in the tumor-associated stroma have been shown to be important in inducing and maintaining a stem-like state in the tumor cells through either the secretion of soluble molecules or cell–cell communication [35, 36]. Particularly, in the case of breast carcinoma, it has been reported that various types of stromal cells *via* growth factors and cytokines may enhance the proliferation and survival of BCSCs, induce angiogenesis, and recruit tumor-associated macrophages and other immune cells, which in turn secrete additional factors promoting tumor cell invasion and metastasis [8].

Here we demonstrated, for the first time, that leptin and its receptor play a crucial role in mediating the interaction between stromal cells (CAFs and adipocytes) and BCSCs. The initial conditioned media experiments indicated that the entire complement of secretory proteins released by CAFs and adipocytes significantly increase MFE/self-renewal in breast cancer cells. An important role is played by leptin as a fundamental environmental regulator of CSCs in the cancer stem niche. Indeed, either leptin immunodepletion from CAF- and adipocyte-derived CM or inhibition of leptin signaling by using peptide LDFI, a small-molecule that acts as a full leptin

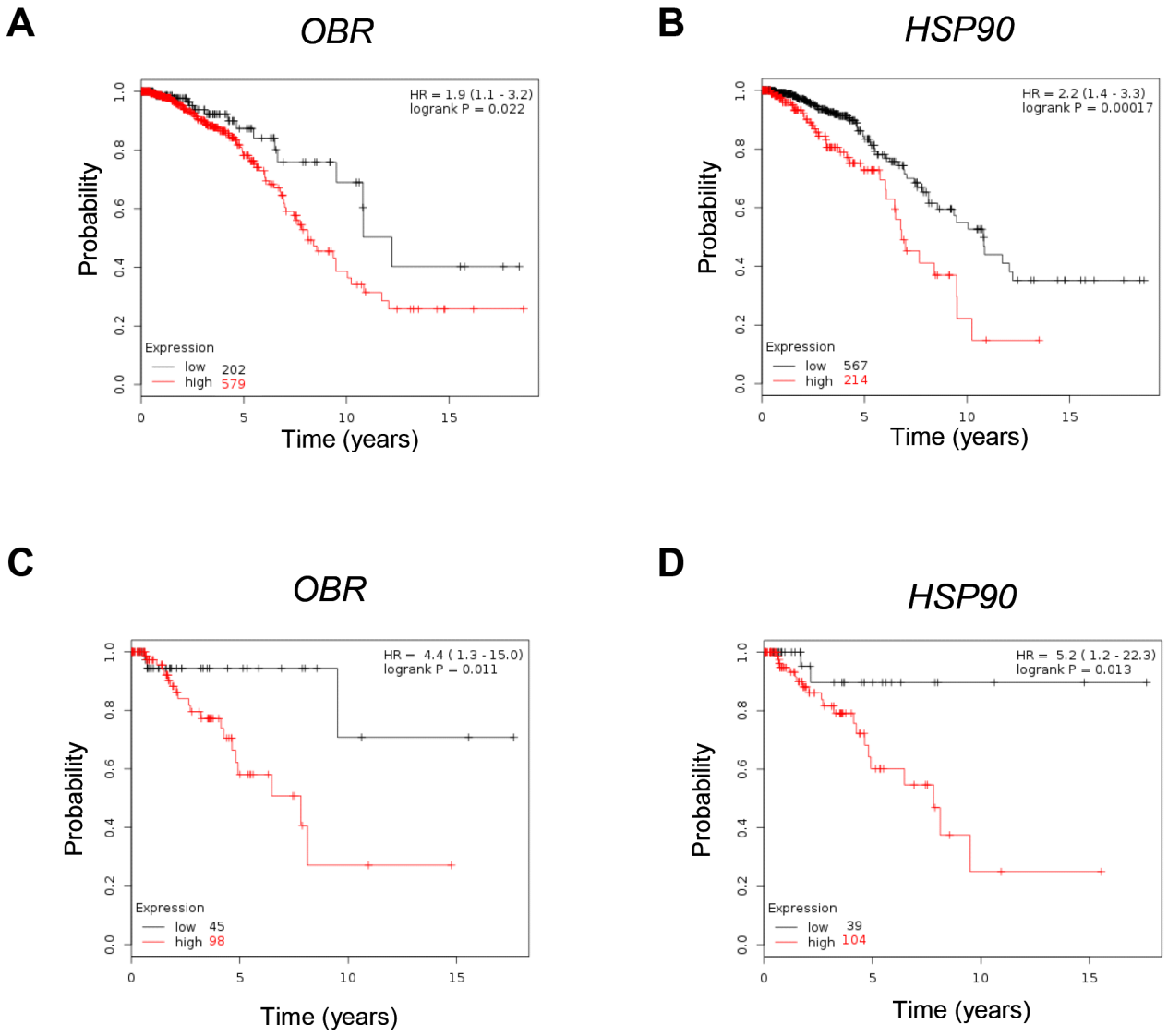

Figure 6: Correlation between *OBR* and *HSP90* mRNA levels and overall survival in breast cancer. Kaplan–Meier survival analysis in breast carcinoma patients (n = 781) with high and low *OBR* (**A**) or *HSP90* (**B**) expression analyzed as described in *Materials and Methods*. Kaplan–Meier survival analysis in basal breast cancer patients (n = 143) with high and low *OBR* (**C**) or *HSP90* (**D**) expression. Kaplan-Meier survival graph, and hazard ratio (HR) with 95% confidence intervals and logrank P value.

receptor antagonist [28], reduced the effects of CM on mammosphere formation. Gene expression profiling revealed a significant overlap of regulated genes in mammosphere cells following treatment with CAF-, adipocyte-derived CM or leptin. Of particular interest was the observation that genes commonly expressed in all treated-samples include several of those involved in stemness. Among these, the polycomb gene *BMI1*, which has been reported to play an important role in self-renewal of stem cells and has a positive correlation with clinical grade/stage and poor prognosis [37], was one of the most highly induced in all treated cells. One of the features of CSCs is the uncontrolled proliferation, perhaps due to a reduced responsiveness to negative growth regulators or to the loss of contact inhibition and gap junction intercellular communication [38]. Our results clearly evidenced that a number of genes involved in cell cycle control showed a similar expression profile upon treatment with stromal-CM and leptin. Another family of genes, crucial in sustaining self-renewal of stem cells [29], is the heat shock protein family. We have previously demonstrated that the HSP90, a main functional component of this chaperone complex, is a target of leptin in breast cancer cells [20]. Our microarray data showed that some transcripts of the HSP family were upregulated in stromal-CM and leptin-treated samples. Thus, since the expression pattern of genes regulated by leptin and involved in stem cell biology closely mirrors those modulated by stromal cells, it is reasonable to speculate that leptin may represent a critical paracrine

molecule in mediating the microenvironment effects on BCSC activity.

The expression of the leptin receptor is a characteristic feature of CSCs and of a broad array of embryonic and induced pluripotent stem cells, which exhibit an increased response to leptin including phosphorylation and activation of STAT3 and induction of stem cell markers, as *OCT4* and *SOX2* [23]. Leptin receptor has also been reported as a marker for identification and *in vivo* fate of bone marrow mesenchymal stem cells (MSCs) [39] and leptin signaling represents an essential step for the enhanced survival, chemotaxis and therapeutic properties of MSCs induced by hypoxia [40, 41]. Moreover, it has been reported that leptin is able to regulate and activate several signaling pathways and oncogenes which are critically implicated in BCSCs [42–46] and leptin deficiency in MMTV-Wnt-1 transgenic mice results in functional depletion of BCSCs leading to less tumor outgrowth [24]. More recently, it has also been demonstrated that OBR is necessary for maintaining a CSC-like state in TNBC cells [25] and high OBR expression induced by the adiposity-leptin enriched environment generates a population with enhanced CSC properties and tumorigenic capacity [26]. Our studies extended these previous findings by demonstrating a direct involvement of leptin in sustaining breast cancer stem cell behavior using both breast cancer cell lines and metastatic breast cancer patient-derived cells. We found that MCF-7 mammospheres exhibited increased *OBR* mRNA expression, while OBR silencing caused a significant reduction in the sphere-forming efficiency. Treatment with leptin induced an increase in MFE, self-renewal and an enhanced percentage of $CD44^{+}/CD24^{-}$ cell population, through the activation of the classical signaling pathways. Importantly, we also showed that leptin is able to increase the mammosphere formation and self-renewal activity in metastatic breast cancer cells isolated from patients. Moreover, *OBR* mRNA expression, analyzed in cells from metastatic fluids, was directly correlated with mammosphere formation activity *ex vivo*. In agreement with our data of gene expression profile, a significant positive correlation between MFE and *HSP90* mRNA expression in the same metastatic patient-derived samples was observed.

It has been previously reported that high-grade tumors associated with poor prognosis display an enrichment of BCSCs [47, 48]. Here, using Kaplan-Meier analysis we found that *OBR* expression, which is crucial in maintaining stem cell phenotype, was associated with reduced overall survival in breast carcinomas suggesting its potential role as a prognostic factor. Interestingly, in basal-like breast cancer patients, a more relevant discrimination in terms of overall survival between high and low *OBR* expression could be observed. Finally, we demonstrated that blocking leptin signaling by using the peptide LDFI significantly reduced mammosphere formation in metastatic breast cancer patient-derived cells, suggesting that strategies aimed at inhibiting leptin signaling represent a rationale therapeutic approach to target cancer stem cells.

In conclusion, our findings identify, for the first time, leptin as an important paracrine molecule that mediates the interaction between stromal cells and BCSCs, providing novel insights into understanding how BCSCs are influenced by the tumor microenvironment. As clinical implications, these data suggest that targeting leptin/leptin receptor signaling generated in the microenvironment may be useful for BCSC eradication and eventually to prevent recurrence and metastasis in patients with breast carcinoma.

MATERIALS AND METHODS

Cell culture

Human MCF-7 and MDA-MB-231 breast cancer epithelial cells were acquired in 2010 and 2015 respectively, from American Type Culture Collection where they were authenticated, stored according to supplier's instructions, and used within 4 months after frozen aliquots recovery. Breast subcutaneous human female preadipocytes (Lot.#:BR071812B; BR070810) were from Zen-Bio. Adipocytes, obtained following differentiation procedure, were routinely maintained in Adipocyte maintenance medium (Zen-Bio). Every 4 months, cells were authenticated by single tandem repeat analysis at our Sequencing Core; morphology, doubling times, estrogen sensitivity, and mycoplasma negativity were tested (MycoAlert, Lonza).

Cancer associated fibroblast (CAF) isolation

Human breast cancer specimens were collected in 2013 from primary tumors of patients who signed informed consent following the procedures previously described [9]. Briefly, small pieces of fresh tumor excision were digested (500 IU collagenase in Hank's balanced salt solution; Sigma; 37°C for 2 h). After differential centrifugation (90 g for 2 min), the supernatant containing CAFs was centrifuged (500 g for 8 min), resuspended, and cultured in RPMI-1640 medium supplemented with 15% FBS and antibiotics. The fibroblastic nature of the isolated cells was confirmed by microscopic determination of morphology, and characterization by αSMA, vimentin, pan-Cytokeratin and fibroblast activation protein (FAP) expression. CAFs between 4 and 10 passages were used.

Immunofluorescence

Immunofluorescence assay was performed as described [9] using anti-α-SMA or ERα antibodies and

fluorescein isothiocyanate-conjugated secondary antibody (Santa Cruz Biothecnology).

Conditioned medium (CM) and Leptin-immunodepleted CM

CM from CAFs and adipocytes and leptin-immunodepleted CM were obtained as described [9]. Leptin levels were measured by ELISA (LDN).

Metastatic breast cancer patient-derived cells

Pleural effusion and ascites samples were obtained from patients with metastatic breast cancer undergoing palliative drainage at The Christie Hospital NHS Foundation Trust Manchester (UK). Metastatic breast sample details in Table 1. Ascites and pleural effusions were centrifuged at 1000 g for 10 min at 4°C and suspended in PBS. Erythrocytes and leucocytes were removed by centrifugation through Lymphoprep solution (Axis Shield), followed by removal of CD45-positive cells using anti-CD45 magnetic beads (Miltenyi Biotec). Single cell suspension of breast cancer epithelial cells was then used to perform mammosphere assay.

Mammosphere culture

MCF-7 and MDA-MB-231 monolayer cells were enzymatically and manually disaggregated to obtain single-cell suspension. Single cells were plated in ultralow attachment plates (Corning) at a density of 500 cells/cm^2 in a serum-free Human mammary epithelial cell growth medium (HUMEC), supplemented with B27, 20 ng/mL human epidermal growth factor (EGF), 4 µg/mL heparin, 5 µg/ml insulin, 1 ng/ml hydrocortisone, 1 mg/ml penicillin-streptomycin and 0,25 µg/ml amphotericin B (Life Technologies). Growth factors and treatments (leptin, Life Technologies; AG490 Sigma; PD98059/LY294002 Calbiochem) were added to the mammosphere cultures every 3 days. After 7 days mammospheres > 50 µm (primary mammospheres-M1) were counted using a microscope (x40 magnification), collected, enzymatically dissociated, plated at the same seeding density used in the primary generation to obtain secondary mammospheres-M2. Mammosphere cultures from metastatic breast patient-derived cells was assessed as described [49]. Mammospheres forming efficiency (MFE) was calculated as number of mammospheres per well/number of cells seeded per well and reported as fold versus control.

Flow cytometry

Mammospheres were dispersed to obtain single-cell suspension. Cells were washed in PBS with 2,5% BSA and stained with FITC anti-human CD44 and PE anti-human CD24 (BD Biosciences), according to the supplier's protocol. Flow cytometric analysis was performed on a FACScan and acquisition was performed with WinDI software (Becton Dickinson).

Reverse transcription and real-time reverse transcriptase PCR assays

PPARγ/OB/FAP/36B4 mRNA expression was evaluated by the RT–PCR method as described [50]. Real-time RT-PCR was assessed using SYBR Green Universal PCR Master Mix (Biorad). Each sample was normalized on its *GAPDH* mRNA content. Relative gene expression levels were calculated as previously described [50]. Primers in Supplementary Table S1.

Immunoblot analysis

Protein extracts were subjected to SDS-PAGE as described [50]. Immunoblots show a single representative of 3 separate experiments.

Transmigration assays

Mammosphere derived MCF-7 cells were placed in the upper compartments of Boyden chamber (8-µm membranes/Corning Costar) and transmigration assay was performed as described [9].

Lentiviral transfection

We established stable OBR sh MCF-7 cell line using the lentiviral expression system (GeneCopoeia; lentiviral plasmid sh-clone #HSH010584). 48 h after transfection with packaging plasmids and pLentiviral plasmids of target gene in HEK293 cells, supernatants containing lentiviral particles were filtered (0.45 µm PES), mixed with polybrene (8 µg/ml) and used to infect MCF-7 cells. 24 h after infection, cells were selected with 2 µg/mL puromycin overtime to eliminate un-infected cells. *OBR* mRNA expression in stable MCF-7 clones was evaluated by real-time RT-PCR.

Microarray and data analysis

Microarray analyses were carried out on total RNA from MCF-7-M2 mammosphere-derived cells treated with CAF-CM, Adipocyte-CM or Leptin by pooling equal amounts of nucleic acids extracted from three independent cell cultures. Gene expression profiling was performed in triplicate using 500ng of each RNA pool as described [51], cRNAs were hybridized for 18 h at 55°C on Illumina HumanHT-12 v4.0 BeadChips (Illumina Inc.) and scanned with an Illumina iSCAN. Data analyses were performed with GenomeStudio software version 2011.1 (Illumina Inc.). Data were normalized with the quantile algorithm and genes were considered if the detection *p*-value was < 0.01. Statistical significance was calculated

with the Illumina DiffScore, a proprietary algorithm that uses the bead standard deviation to build an error model. Transcripts showing a DiffScore ≤ -30 and ≥ 30, corresponding to a *p*-value of 0.001 and significant fold change in treated *vs* untreated ≥ 1.5 were considered. Venn diagram was generated using Venny 2.0 software. Heat-maps were generated with the Multiexperiment Viewer 4.9 software after performing one way hierarchical clustering of transcripts with the average linkage method and Euclidian distance.

Raw microarray data have been deposited, in a format complying with the Minimum Information About a Microarray Gene Experiment (MIAME) guidelines of the Microarray Gene Expression Data Society (MGED), in the EBI ArrayExpress database (http://www.ebi.ac.uk/arrayexpress) with Accession Number: E-MTAB-3641.

Total RNA from 8 different metastatic breast cancer samples was extracted using the RNeasy Plus Mini Kit (QIAGEN). The Exon Gene Array ST1 platform (Affimetrix) was used to assess gene expression. Data obtained were analysed using Bioconductor R Software. The mean of log2 gene expression values was calculated across all 8 patient derived samples for each individual gene.

Construction of RNA-seq database

RNA-seq data was obtained from the TCGA depository. We transferred the pre-processed level 3 data generated by the Illumina HiSeq 2000 RNA Sequencing Version 2 platform. Expression levels for these samples were computed using a combination of MapSplice and RSEM. Individual patient files were merged into a single database using the plyr R package [52].

Statistical analyses

Each datum point represents the mean ± s.d. of three different experiments. Data were analyzed by Student's *t* test using the GraphPad Prism 4 software. $P < 0.05$ was considered as statistically significant. Pearson correlation coefficient (r) was used to measure the correlation between *OBR* or Heat Shock Protein 90 (*HSP90*) gene expression of 8 metastatic breast cancer samples and mean MFE; a 2-tailed $p \leq 0.05$ was considered statistically significant.

Kaplan-Meier analysis was performed as described [53]. Kaplan-Meier survival graph, and hazard ratio with 95% confidence intervals and logrank *P* value were calculated and plotted in R using Bioconductor packages.

CONFLICTS OF INTEREST

The authors declare they have no conflict of interest.

GRANT SUPPORT

This work was supported by PRIN-MIUR (Programmi di Ricerca Scientifica di Rilevante Interesse Nazionale-Ministero dell'Istruzione dell'Università della Ricerca) 2010–2011 and Associazione Italiana per la Ricerca sul Cancro (AIRC) grants: IG-11595 and IG-13176. European Commission/FSE/Regione Calabria to FC and SP and Lilli Funaro foundation to SP.

REFERENCES

1. Jemal A, Siegel R, Xu J, Ward E. Cancer statistics, 2010. CA Cancer J Clin. 2010; 60:277–300.
2. Visvader JE, Lindeman GJ. Cancer stem cells in solid tumours: accumulating evidence and unresolved questions. Nat Rev Cancer. 2008; 8:755–768.
3. Clarke MF, Dick JE, Dirks PB, Eaves CJ, Jamieson CH, Jones DL, Visvader J, Weissman IL, Wahl GM. Cancer stem cells—perspectives on current status and future directions: AACR Workshop on cancer stem cells. Cancer Res. 2006; 66:9339–9344.
4. Li X, Lewis MT, Huang J, Gutierrez C, Osborne CK, Wu MF, Hilsenbeck SG, Pavlick A, Zhang X, Chamness GC, Wong H, Rosen J, Chang JC. Intrinsic resistance of tumorigenic breast cancer cells to chemotherapy. J Natl Cancer Inst. 2008; 100:672–679.
5. Phillips TM, McBride WH, Pajonk F. The response of CD24(-/low)/CD44+ breast cancer-initiating cells to radiation. J Natl Cancer Inst. 2006; 98:1777–1785.
6. Kakarala M, Wicha MS. Implications of the cancer stem-cell hypothesis for breast cancer prevention and therapy. J Clin Oncol. 2008; 26:2813–2820.
7. Liu S, Dontu G, Wicha MS. Mammary stem cells, self-renewal pathways, and carcinogenesis. Breast Cancer Res. 2005; 7:86–95.
8. Korkaya H, Liu S, Wicha MS. Breast cancer stem cells, cytokine networks, and the tumor microenvironment. J Clin Invest. 2011; 121:3804–3809.
9. Barone I, Catalano S, Gelsomino L, Marsico S, Giordano C, Panza S, Bonofiglio D, Bossi G, Covington KR, Fuqua SA, Andò S. Leptin mediates tumor-stromal interactions that promote the invasive growth of breast cancer cells. Cancer Res. 2012; 72:1416–1427.
10. Cirillo D, Rachiglio AM, la Montagna R, Giordano A, Normanno N. Leptin signaling in breast cancer: an overview. J Cell Biochem. 2008; 105:956–964.
11. Ishikawa M, Kitayama J, Nagawa H. Enhanced expression of leptin and leptin receptor (OB-R) in human breast cancer. Clin Cancer Res. 2004; 10:4325–4331.
12. Miyoshi Y, Funahashi T, Tanaka S, Taguchi T, Tamaki Y, Shimomura I, Noguchi S. High expression of leptin receptor mRNA in breast cancer tissue predicts poor prognosis for

patients with high, but not low, serum leptin levels. Int J Cancer. 2006; 118:1414–1419.

13. Andò S, Barone I, Giordano C, Bonofiglio D, Catalano S. The Multifaceted Mechanism of Leptin Signaling within Tumor Microenvironment in Driving Breast Cancer Growth and Progression. Front Oncol. 2014; 4:340.
14. Andò S, Catalano S. The multifactorial role of leptin in driving the breast cancer microenvironment. Nat Rev Endocrinol. 2011; 8:263–275.
15. Saxena NK, Sharma D. Multifaceted leptin network: the molecular connection between obesity and breast cancer. J Mammary Gland Biol Neoplasia. 2013; 18:309–320.
16. Catalano S, Marsico S, Giordano C, Mauro L, Rizza P, Panno ML, Andò S. Leptin enhances, via AP-1, expression of aromatase in the MCF-7 cell line. J Biol Chem. 2003; 278:28668–28676.
17. Catalano S, Mauro L, Marsico S, Giordano C, Rizza P, Rago V, Montanaro D, Maggiolini M, Panno ML, Andò S. Leptin induces, via ERK1/ERK2 signal, functional activation of estrogen receptor alpha in MCF-7 cells. J Biol Chem. 2004; 279:19908–19915.
18. Fiorio E, Mercanti A, Terrasi M, Micciolo R, Remo A, Auriemma A, Molino A, Parolin V, Di Stefano B, Bonetti F, Giordano A, Cetto GL, Surmacz E. Leptin/HER2 cross-talk in breast cancer: *in vitro* study and preliminary *in vivo* analysis. BMC Cancer. 2008; 8:305.
19. Soma D, Kitayama J, Yamashita H, Miyato H, Ishikawa M, Nagawa H. Leptin augments proliferation of breast cancer cells via transactivation of HER2. J Surg Res. 2008; 149:9–14.
20. Giordano C, Vizza D, Panza S, Barone I, Bonofiglio D, Lanzino M, Sisci D, De Amicis F, Fuqua SA, Catalano S, Andò S. Leptin increases HER2 protein levels through a STAT3-mediated up-regulation of Hsp90 in breast cancer cells. Mol Oncol. 2013; 7:379–391.
21. Saxena NK, Taliaferro-Smith L, Knight BB, Merlin D, Anania FA, O'Regan RM, Sharma D. Bidirectional crosstalk between leptin and insulin-like growth factor-I signaling promotes invasion and migration of breast cancer cells via transactivation of epidermal growth factor receptor. Cancer Res. 2008; 68:9712–9722.
22. Newman G, Gonzalez-Perez RR. Leptin-cytokine crosstalk in breast cancer. Mol Cell Endocrinol. 2014; 382:570–582.
23. Feldman DE, Chen C, Punj V, Tsukamoto H, Machida K. Pluripotency factor-mediated expression of the leptin receptor (OB-R) links obesity to oncogenesis through tumor-initiating stem cells. Proc Natl Acad Sci U S A. 2012; 109:829–834.
24. Zheng Q, Dunlap SM, Zhu J, Downs-Kelly E, Rich J, Hursting SD, Berger NA, Reizes O. Leptin deficiency suppresses MMTV-Wnt-1 mammary tumor growth in obese mice and abrogates tumor initiating cell survival. Endocr Relat Cancer. 2011; 18:491–503.
25. Zheng Q, Banaszak L, Fracci S, Basali D, Dunlap SM, Hursting SD, Rich JN, Hjlemeland AB, Vasanji A, Berger NA, Lathia JD, Reizes O. Leptin receptor maintains cancer stem-like properties in triple negative breast cancer cells. Endocr Relat Cancer. 2013; 20:797–808.
26. Chang CC, Wu MJ, Yang JY, Camarillo IG, Chang CJ. Leptin-STAT3-G9a Signaling Promotes Obesity-Mediated Breast Cancer Progression. Cancer Res. 2015; .
27. Dontu G, Abdallah WM, Foley JM, Jackson KW, Clarke MF, Kawamura MJ, Wicha MS. *In vitro* propagation and transcriptional profiling of human mammary stem/progenitor cells. Genes Dev. 2003; 17:1253–1270.
28. Catalano S, Leggio A, Barone I, De Marco R, Gelsomino L, Campana A, Malivindi R, Panza S, Giordano C, Liguori A, Bonofiglio D, Liguori A, Andò S. A novel leptin antagonist peptide inhibits breast cancer growth *in vitro* and *in vivo*. J Cell Mol Med. 2015; 19:1122–1132.
29. Isolani ME, Conte M, Deri P, Batistoni R. Stem cell protection mechanisms in planarians: the role of some heat shock genes. Int J Dev Biol. 2012; 56:127–133.
30. May CD, Sphyris N, Evans KW, Werden SJ, Guo W, Mani SA. Epithelial-mesenchymal transition and cancer stem cells: a dangerously dynamic duo in breast cancer progression. Breast Cancer Res. 2011; 13:202.
31. Ben-Porath I, Thomson MW, Carey VJ, Ge R, Bell GW, Regev A, Weinberg RA. An embryonic stem cell-like gene expression signature in poorly differentiated aggressive human tumors. Nat Genet. 2008; 40:499–507.
32. Honeth G, Bendahl PO, Ringner M, Saal LH, Gruvberger-Saal SK, Lovgren K, Grabau D, Ferno M, Borg A, Hegardt C. The CD44+/CD24- phenotype is enriched in basal-like breast tumors. Breast Cancer Res. 2008; 10:R53.
33. Park SY, Lee HE, Li H, Shipitsin M, Gelman R, Polyak K. Heterogeneity for stem cell-related markers according to tumor subtype and histologic stage in breast cancer. Clin Cancer Res. 2010; 16:876–887.
34. Sarrio D, Rodriguez-Pinilla SM, Hardisson D, Cano A, Moreno-Bueno G, Palacios J. Epithelial-mesenchymal transition in breast cancer relates to the basal-like phenotype. Cancer Res. 2008; 68:989–997.
35. Pattabiraman DR, Weinberg RA. Tackling the cancer stem cells - what challenges do they pose?. Nat Rev Drug Discov. 2014; 13:497–512.
36. Beck B, Blanpain C. Unravelling cancer stem cell potential. Nat Rev Cancer. 2013; 13:727–738.
37. Siddique HR, Saleem M. Role of BMI1, a stem cell factor, in cancer recurrence and chemoresistance: preclinical and clinical evidences. Stem Cells. 2012; 30:372–378.
38. Trosko JE, Chang CC, Upham BL, Tai MH. Ignored hallmarks of carcinogenesis: stem cells and cell-cell communication. Ann N Y Acad Sci. 2004; 1028:192–201.

39. Zhou BO, Yue R, Murphy MM, 1 Peyer JG, Morrison S J. Leptin-Receptor-Expressing Mesenchymal Stromal Cells Represent the Main Source of Bone Formed by Adult Bone Marrow. Cell Stem Cell. 2014; 15:154–168.

40. Hu X, Wu R, Jiang Z, Wang L, Chen P, Zhang L, Yang L, Wu Y, Chen H, Chen H, Xu Y, Zhou Y, Huang X, Webster KA, Yu H, Wang J. Leptin signaling is required for augmented therapeutic properties of mesenchymal stem cells conferred by hypoxia preconditioning. Stem Cells. 2014; 10:2702–13.

41. Chen P, Wu R, Zhu W, Jiang Z, Xu Y, Chen H, Zhang Z, Chen H, Zhang L, Yu H, Wang J, Hu X. Hypoxia Preconditioned Mesenchymal Stem Cells Prevent Cardiac Fibroblast Activation and Collagen Production via Leptin. PloS ONE. 2014; 9:e103587.

42. Zhou J, Wulfkuhle J, Zhang H, Gu P, Yang Y, Deng J, Margolick JB, Liotta LA, Petricoin E 3rd, Zhang Y. Activation of the PTEN/mTOR/STAT3 pathway in breast cancer stem-like cells is required for viability and maintenance. Proc Natl Acad Sci U S A. 2007; 104:16158–16163.

43. Pratt MA, Tibbo E, Robertson SJ, Jansson D, Hurst K, Perez-Iratxeta C, Lau R, Niu MY. The canonical NF-kappaB pathway is required for formation of luminal mammary neoplasias and is activated in the mammary progenitor population. Oncogene. 2009; 28:2710–2722.

44. Guo S, Gonzalez-Perez RR. Notch, IL-1 and leptin crosstalk outcome (NILCO) is critical for leptin-induced proliferation, migration and VEGF/VEGFR-2 expression in breast cancer. PLoS One. 2011; 6:e21467.

45. Knight BB, Oprea-Ilies GM, Nagalingam A, Yang L, Cohen C, Saxena NK, Sharma D. Survivin upregulation, dependent on leptin-EGFR-Notch1 axis, is essential for leptin-induced migration of breast carcinoma cells. Endocr Relat Cancer. 2011; 18:413–428.

46. Guo S, Liu M, Wang G, Torroella-Kouri M, Gonzalez-Perez RR. Oncogenic role and therapeutic target of leptin signaling in breast cancer and cancer stem cells. Biochim Biophys Acta. 2012; 1825:207–222.

47. Farnie G, Clarke RB, Spence K, Pinnock N, Brennan K, Anderson NG, Bundred NJ. Novel cell culture technique for primary ductal carcinoma *in situ*: role of Notch and epidermal growth factor receptor signaling pathways. J Natl Cancer Inst. 2007; 99:616–627.

48. Pece S, Tosoni D, Confalonieri S, Mazzarol G, Vecchi M, Ronzoni S, Bernard L, Viale G, Pelicci PG, Di Fiore PP. Biological and molecular heterogeneity of breast cancers correlates with their cancer stem cell content. Cell. 2010; 140:62–73.

49. Shaw FL, Harrison H, Spence K, Ablett MP, Simoes BM, Farnie G, Clarke RB. A detailed mammosphere assay protocol for the quantification of breast stem cell activity. J Mammary Gland Biol Neoplasia. 2012; 17:111–117.

50. Catalano S, Malivindi R, Giordano C, Gu G, Panza S, Bonofiglio D, Lanzino M, Sisci D, Panno ML, Andò S. Farnesoid X receptor, through the binding with steroidogenic factor 1-responsive element, inhibits aromatase expression in tumor Leydig cells. J Biol Chem. 2010; 285:5581–5593.

51. Nassa G, Tarallo R, Giurato G, De Filippo MR, Ravo M, Rizzo F, Stellato C, Ambrosino C, Baumann M, Lietzen N, Nyman TA, Weisz A. Post-transcriptional regulation of human breast cancer cell proteome by unliganded estrogen receptor beta via microRNAs. Mol Cell Proteomics. 2014; 13:1076–1090.

52. Wickham . The Split-Apply-Combine Strategy for Data Analysis. J Stat Softw. 2011; 40:1–29.

53. Gyorffy B, Lanczky A, Eklund AC, Denkert C, Budczies J, Li Q, Szallasi Z. An online survival analysis tool to rapidly assess the effect of 22,277 genes on breast cancer prognosis using microarray data of 1,809 patients. Breast Cancer Res Treat. 2010; 123:725–731.

Androgens inhibit aromatase expression through DAX-1: insights into the molecular link between hormone balance and Leydig cancer development

Pamela Maris[1], Antonella Campana[1], Ines Barone[1], Cinzia Giordano[2], Catia Morelli[1], Rocco Malivindi[1], Diego Sisci[1,2], Saveria Aquila[1,2], Vittoria Rago[1], Daniela Bonofiglio[1,2], Stefania Catalano[1,2], Marilena Lanzino[1,2,*], and Sebastiano Andò[1,2,*]

[1]Department of Pharmacy and Health and Nutritional Sciences and [2]Centro Sanitario, University of Calabria, 87036 Arcavacata di Rende (CS), Italy. Key terms: Androgen Receptor, Aromatase, DAX-1, Leydig Cell Tumor

Leydig cell tumors (LCTs) of the testis are steroid-secreting tumors associated with various steroid biosynthetic abnormalities and endocrine dysfunctions. Despite their overall rarity, LCTs are still of substantial interest owing to the paucity of information regarding their exact nature and malignant potential. In the present study we disclose the ability of androgens to inhibit Leydig tumor cell proliferation by opposing to self-sufficient *in situ* estrogen production. In rat Leydig tumor cells, R2C, androgen treatment significantly decreases the expression and the enzymatic activity of P450 aromatase, responsible for the local conversion of androgens into estrogens. This inhibitory effect relies on androgen receptor activation and involves negative regulation of the *CYP19* gene transcriptional activity through the nuclear orphan receptor DAX-1. Ligand-activated androgen receptor up-regulates the expression of DAX-1 and promotes its increased recruitment within the SF-1-containing region of the PII-aromatase proximal promoter in association with the corepressor N-CoR. The biological relevance in LCTs of the newly highlighted functional interplay between androgen receptor, DAX-1 and aromatase is underlined by our *in vivo* observations revealing a marked down-regulation of AR and DAX-1 expression and a strong increase in aromatase levels in testes tissues from old Fisher rats with spontaneously developed Leydig cell neoplasia, compared to normal testes tissues from younger animals.

In elucidating a mechanism by which androgens modulate the growth of Leydig tumor cells, our finding support the hypothesis that maintaining the adequate balance between androgen and estrogens may represent the key for blocking estrogen-secreting Leydigioma development, opening new prospects for therapeutic intervention.

Testicular Leydig cell tumors (LCTs) are the most common neoplasms of male gonadal interstitium (1) and account for about 3% of all testicular cancers. Most frequently diagnosed in 5–10 years old prepubertal boys and 30–60 aged adult men (2, 3), LCTs are commonly benign, but about 10% of them reveal a malignant phenotype in adult patients (4). Metastatic Leydig cell tumors are resistant to irradiation and to most of the chemotherapic agents (5, 6), rendering it necessary to individuate as many new therapeutic target as possible, in the perspective of a multifaceted treatment.

As LCTs are steroid-secreting tumors, they are often associated with endocrine disturbance (7–10). It is now apparent that the adequate balance in the androgen/estrogen ratio is necessary for normal testicular development and function (11) and may potentially represent a clinical central factor in LCTs growth and progression. Androgens, which are mainly produced in testicular Ley-

ISSN Print 0013-7227 ISSN Online 1945-7170
Printed in U.S.A.

Received August 5, 2014. Accepted January 15, 2015.

Abbreviations:

dig cells, drive the expression of the male phenotype, including male sexual differentiation, development of secondary sex characteristics and manteinance of spermatogenesis (12). Androgen action is mediated by the androgen receptor (AR) that acts as a ligand-inducible transcription factor (13). In testicular cell-specific AR knockout mice, the lack of the receptor in Leydig cell compartment mainly affects steroidogenic functions (12). Mutations in the AR gene are responsible for the onset of varying levels of androgen insensitivity syndrome (AIS) (14, 15) that, as result of the hormonal imbalance, is associated to a higher risk of developing testicular tumors (16). Immuno-histochemical findings in the testes of AIS patients suggest the high expression of the cytochrome P450 aromatase as one of the molecular changes responsible for the increased risk of LTCs (17). The P450 aromatase enzyme is crucially involved in the maintenance of the androgen/estrogen essential balance since it governs estrogen biosynthesis within the testis by catalyzing the irreversible conversion of C_{19} androgenic substrates, testosterone (T) and androstenedione, into the C_{18} estrogens, estradiol (E_2) and estrone (18). Several observations suggest that estrogens can elicit proliferative effects in human and rodents tumor Leydig cells through an autocrine mechanism (19). Findings in transgenic mice show that increased estradiol/testosterone ratio, including excessive estrogen exposure, disturbs Leydig cell function and might cause hyperplasia, hypertrophy and development of Leydig cell adenomas (20–22). In humans, elevated P450 aromatase expression, with consequent high plasma estradiol levels has been described in patients with testicular LCTs, further substantiating the role played by P450 aromatase on the pathogenesis of leydigiomas (23–26). All these experimental and clinical observations strongly support that abnormalities of the male gonadal functions may be associated with the decreased ratio of androgen/estrogen levels. So far, it has been demonstrated that androgens are able to suppress the expression of a number of steroidogenic enzyme genes eventually resulting in decreased testicular steroidogenesis (27, 28). However, information regarding the precise function of AR in Leydig tumor cells is still lacking.

Here, we investigated the effect of androgens on the expression of the P450 aromatase in rat Leydig tumor cells R2C, a well-documented experimental model for leydigioma (19, 29–31). We demonstrated the existence of a novel mechanism through which androgens are able to down-regulate the in situ estrogen production and Leydig tumor cell proliferation by inhibiting the expression of the P450 aromatase gene. This occurs through a functional cross-talk between the AR, the orphan nuclear receptor DAX-1 and the P450 aromatase.

Materials and Methods

Reagents and antibodies

Mibolerone (Mb) from Perkin Elmer (Waltham, MA, USA); Bicalutammide (Casodex) from Astra-Zeneca; hydroxyflutamide (OH-Fl) and 4′,6-Diamidino-2-phenylindole (DAPI) from Sigma-Aldrich (Milano, Italy); bovine serum albumin (BSA) and AR (C-19), DAX-1 (K-17), N-CoR (H-303), β-Actin (AC-15), GAPDH (FL-335), cyclin D1(M-20), p21 (H-164), Ki-67 (M-19) antibodies from Santa Cruz Biotechnology (Dallas, TX, USA); cytochrome P450 aromatase antibody from Serotec (Oxford, UK).

Cell cultures

Authenticated Rat Leydig tumor cells R2C were acquired from American Type Culture Collection - ATCC (LGC Standards, Teddington, Middlesex UK), stored according to supplier's instructions and used within 4 months after frozen aliquots resuscitations. Cells were cultured in Ham/F-10 (Sigma) medium supplemented with 15% horse serum (HS), 2.5% fetal bovine serum (FBS), and antibiotics (Invitrogen, S.r.l., San Giuliano Milanese, Italy).

Before each experiment, cells were synchronized in phenol red-free serum free media (PRF-SFM) for 24h. All the experiments were performed in PRF-media containing 2.5% charcoal-treated Horse Serum (PRF–CT).

Animal studies

Male Fischer 344 rats (gift of σ-Tau), 6-month old Fisher rats (FRNT, $n = 3$) and 24-month old Fisher rats (FRTT, $n = 4$) were used for in vivo studies. Twenty-four-month-old animals presented spontaneously developed Leydig cell tumors, which were absent in younger animals. Testes of all animals were surgically removed by qualified, specialized animal care staff in accordance with the recommendation of the Guidelines for the Care and Use of Laboratory Animals (NIH) and with the Animal Care Committee of University of Calabria.

Cell viability and proliferation assays

Cell viability was evaluated by 3-[4,5-Dimethylthiaoly]-2,5-diphenyltetrazolium bromide (MTT) and cell counting assays, as previously described (32). Briefly, for MTT (MTT, Sigma, Milan, Italy) assay, a total of 5×10^4 cells were seeded onto 24-well plates and treated for 6 days with increasing concentrations of Mibolerone (Mb). The MTT assay was performed as the following: 100 ml MTT stock solution in PBS (2 mg/ml) was added into each well and incubated at 37°C for 2h followed by media removal and solubilization in 500 ml dimethyl sulfoxide (DMSO). After shaking the plates for 15 minutes, the absorbance in each well, including the blanks, was measured at 570 nm in Beckman Coulter.

For cell counting, R2C cells were seeded on six-well plates (2×10^5cells/well) in 2.5% PRF–CT. After 24h, cells were exposed for 6 days to 10^{-8}M Mb or vehicle treated. The effects of Mb on cell proliferation were measured 0, 3 and 6 days following initial exposure to treatments by counting R2C cells using a Burker's chamber, with cell viability determined by Trypan blue dye exclusion.

Anchorage-independent Soft Agar Growth Assays

R2C cells (10^4/well) were plated in 4 ml of Ham's F-10 with 0.5% agarose and 5% charcoal-stripped FBS, in 0.7% agarose base in six-well plates. After two days, media containing vehicle or treatments were added to the top layer and replaced every 2 days. Anchorage-independent growth was assessed as previously described (31).

Immunocytochemical staining

Immunocytochemical staining of R2C was performed as previously described (33). Cells were fixed for 30 minutes in freshly prepared para-formaldehyde (2%) and incubated for further 30 minutes with 10% normal rabbit serum to block the nonspecific binding sites. Immunocytochemical staining was performed using an affinity purified goat anti-KI67 antibody (Santa Cruz, CA). The cells were then incubated with the secondary antibody biotinylated rabbit-antigoat IgG (Vector Laboratories, Burlingame, CA) for 1 hour at room temperature followed by incubation with avidin/biotin/horseradish peroxidase complex (ABC Complex-HRP, Vector Laboratories). The peroxidase reaction was developed using Stable DAB (Sigma Chemical, Italy) for 3 minutes.

RNA extraction, reverse transcription (RT)-PCR and real time PCR

Cells were maintained overnight in serum-free medium and then treated for 24h or 48h in 2,5% PRF-CT medium. RNA extraction and reverse transcription were performed as previously described (33) with minor modifications. For RT-PCR, primers were: *DAX-1*; (forward), 5′-CAGGCCATGGCGTTCCTGTA-3′, (reverse), 5′-TCCTGCCGCCTGGTGGTGAG-3′; *CYP19*; (forward), 5′-CAGCTATACTGAAGGAAATCC-3′, (reverse), 5′-AATCGTTTCAAAAGTGTAACCA-3′.

Quantitative PCR was performed using SYBR Green universal PCR master mix (Bio-Rad Laboratories, Hercules, CA). Primers used were: *CYP19*: (forward), 5′-GAGAAACTGGAAGACTGTATGGATTTT-3′, (reverse), 5′-ACTGATTCACGTTCTCCTTTGTCA-3′; DAX-1: (forward), 5′-CTGGGTGGGGAGGGA CTGC-3′, (reverse), 5′-CCTGGCGCGGGTGGTTCTC-3′. PCR reactions were performed in the iCycler iQ Detection System (Bio-Rad), using 0.1 μM of each primer in a total volume of 30 μl of reaction mixture following the manufacturer's recommendations. Each sample was normalized on the basis of its 18S ribosomal RNA content. The 18S quantification was performed using a TaqMan Ribosomal RNA Reagent kit (Applied Biosystems, Applera Italia, Monza, Italy) following the method provided in the TaqMan Ribosomal RNA Control Reagent Kit. The relative gene expression levels were normalized to a calibrator that was chosen to be the basal, untreated sample. Final results were expressed as n-fold differences in gene expression relative to 18S ribosomal RNA and calibrator, calculated following the ΔΔCt method, as published previously (19).

Immunoblotting analysis

R2C cells or total tissue of FRNT and FRTT were lysed for protein extraction (31). Total and cytosolic/nuclear extracts were prepared and subjected to SDS-PAGE as described (34). The intensity of bands representing relevant proteins was measured by Scion Image laser densitometry scanning program.

Immunofluorescence

Immunofluorescence analysis was performed as previously described, with minor modifications (35). Briefly, cells were fixed with 4% paraformaldehyde, permeabilized with PBS+ 0.2% Triton X-100, followed by blocking with BSA (3%, 30min), and incubated with anti –P450 Aromatase or –DAX-1 antibodies (4°C, overnight) and with fluorescein-conjugated secondary antibody (30 minutes, room temperature). IgG primary antibody was used as negative control. 4′,6-Diamidino-2-phenylindole (DAPI, Sigma) staining was used for nuclei detection. Protein cellular localization was observed under a fluorescence microscope (Olympus BX51 fluorescence microscope, Olympus Italia srl). Cells were photographed at 100× magnification using ViewFinder™ Software, through an Olympus camera system dp50 and the optical densities of stained proteins were analyzed by ImageJ software (NIH).

P450 Aromatase activity assay

The P450 aromatase activity in subconfluent R2C cells culture medium was measured by the tritiated water release assay using 0.5 μM [$^{1\beta3}$H]androst-4-ene-3,17-dione as substrate (36). The incubations were performed at 37°C for 2h under an air/CO2 (5%) atmosphere. The results, obtained as picomoles per hours and normalized to milligrams of protein (pmol/h/mg of protein), were expressed as fold change over control.

Radio Immuno Assay

R2C cells were seeded on six-well plates (2×10^5cells/well) in 2.5% PRF–CT. After 24h, cells were exposed for 72 hours to vehicle or 10^{-8}M Mb and/or 10^{-6}M OH-Fl. The estradiol content of medium recovered from each well was determined against standards prepared in low-serum medium using a RIA kit (DSL 43 100; Diagnostic System Laboratories).

Plasmids, transfections and luciferase reporter assays

The plasmids containing different segments of the rat P450 aromatase PII sequence ligated to a luciferase reporter gene were kindly provided by Dr M.J. McPhaul and were –1037/+94 (p-1037), –688/+94 (p-688) and –688/+94 mut (5′CREm, 3′CREm, XCREm and SF-1m) containing mutations of 5′CRE, 3′CRE, XCRE and SF-1 respectively (29). Firefly luciferase reporter plasmid XETL is a construct containing an estrogen-responsive element from the Xenopus vitellogenin promoter (37). Cells were transfected using Fugene HD Transfection Reagent (Promega) according to manufacturer's instructions. Renilla reniformis luciferase expression vector pRL-Tk (Promega) was used for transfection efficiency. Empty pGL2-basic vector was used as a control to measure basal activity. Luciferase activity was measured using Dual Luciferase Assay System (Promega).

Chromatin Immunoprecipitation (ChIP)

ChIP assay was performed as described (38) using anti DAX-1 and N-CoR antibodies. Normal rabbit or mouse IgGs were used as negative controls. A 3μl volume of each sample and DNA input were used for PCR using the primers flanking SF-1 sequence in the rat P450 aromatase promoter region: (forward), 5′-ATGCACGTCACTCTACCCACTCAA-3′; (reverse),5′-TAGCACGCAAAGCAGTAGTTTGGC-3′. The amplification

products were analyzed in a 2% agarose gel and visualized by ethidium bromide staining.

Statistical analysis

All data were expressed as the mean ± standard deviation (S.D.) of three independent experiments. Statistical significances were analyzed using Student's *t* test or One way ANOVA, where appropriate. $*P < .05$ was considered as statistically significant.

Results

Androgens reduce cell proliferation rate in estrogen-dependent R2C Leydig tumor cells

To investigate whether androgens might play a role in the modulation of estrogen-dependent Leydig tumor cell growth we used the rat Leydig tumor cell line R2C, a well-documented experimental model for Leydigioma (19, 29–31). In the present study, experiments were carried out using the synthetic AR agonist Mibolerone (Mb) to minimize the metabolic conversion of androgen to estrogenic compounds by cultured cells. The effect of increasing concentrations of Mb on R2C Leydig tumor cell viability was evaluated by MTT assay. As shown in Figure 1A, Mb treatment significantly decreased R2C cell viability. The inhibitory effect of 10^{-8}M Mb was further confirmed by trypan blue exclusion test, showing that it began 2 days after androgen administration and persisted thereafter. The inhibitory effect exerted by 10^{-8}M Mb was abrogated by the addition of the androgen receptor antagonist Hydroxiflutamide (OH-Fl) (Figure 1B). In addition, Mb treatment was also able to decrease the number of colonies present in soft agar (Figure 1C). Reduction of cell proliferation following Mb administration was further proved by evaluating the expression levels of the proliferation marker Ki-67 (Figure 1D), the cyclin-dependent kinase inhibitor p21 which is also a well-known androgen-dependent gene (39) and cyclin D1 (Figure 1E), which represents a key factor in the estradiol-induced proliferative effects in estrogen-responsive tissues (40). According to the reduced cell number, Mb-treated R2C cells exhibited a decreased expression of Ki-67 and cyclin D1 but increased levels of p21.

Similar results on cell proliferation (eg, R2C cell number and Ki-67 expression) were obtained by treating R2C cell with the androgen receptor natural ligand dihydrotestosterone (DHT) (Supplemental Figure 1A and B).

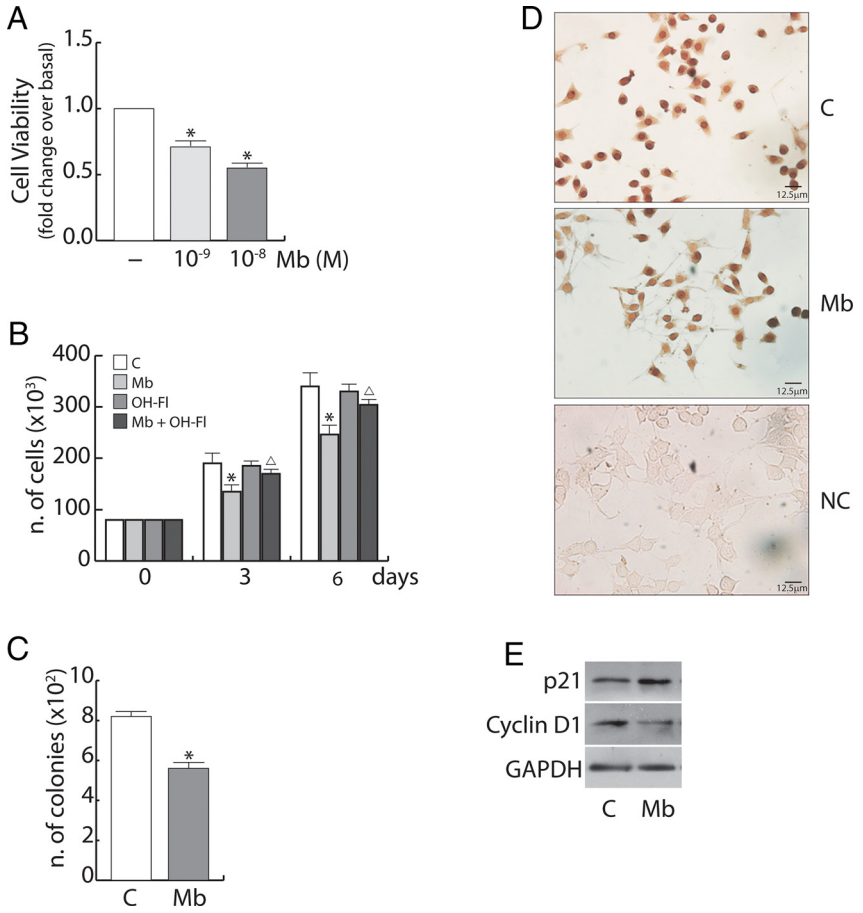

Figure 1. Mibolerone treatment reduces proliferation in R2C cells. A, MTT assays in R2C cells treated with vehicle (-) or different Mibolerone (Mb) concentrations (M) as indicated for 6 days. **(B)** Cells were treated with vehicle (C) or 10^{-8}M Mb and/or 10^{-6}M hydroxyflutamide (OH-Fl). Drug effects on cell proliferation were measured at day 0, 3 and 6 following initial exposure to treatments by cell counting using a Burker's Chamber, with cell viability determined by trypan blue dye exclusion. **(C)** R2C cells were seeded (1×10^4/well) in 0.5% agarose and treated as described above. Cells were allowed to grow for 14 days and then the number of colonies > 50 μm were quantified and the results graphed. The results represent the mean ± S.D. of three different experiments each performed with triplicate samples. Data from **(A), (B)** and **(C)** represent the mean ± S.D. of three separate experiments, each performed in triplicate. $*P < .05$ vs vehicle; $^{\Delta}P < .05$ vs Mb- treated. **(D)** Immunocytochemical staining of proliferation marker Ki-67 in R2C cells treated with vehicle (C) or 10^{-8}M Mibolerone (Mb) for 72h. No immunoreactivity was detected when R2C cells were incubated without the primary antibody (negative control, NC) Scale bar = 12,5 μm. **(E)** Immunoblotting of p21 and cyclin D1 in R2C cells treated with vehicle (C) or 10^{-8}M Mibolerone (Mb) for 72h. GAPDH, loading control. Data from from **(D)** and **(E)** are representative of three separate experiments.

Androgen administration decreases P450 aromatase expression and activity in R2C cells

Local estrogen production by highly expressed P450 aromatase represents a major feature involved in the positive control of R2C cell proliferation (19, 23). Thus, we explored the possibility that androgen treatment might impact on P450 aromatase gene expression in R2C cells. Mb administration was able to reduce the cellular content of the enzyme at both mRNA and protein levels, as detected by Real Time-PCR, (Figure 2A) and immunoblotting (Figure 2B) assays, respectively. Similar findings were obtained following DHT administration (Supplemental Figure 1C and D). These results were further confirmed by immunofluorescence analysis detecting a reduced P450 aromatase immunoreactivity in the cytoplasm of R2C cells as well as in the perinuclear region, when cells were treated with Mb. No reaction was noticed in the nuclei and in the cells processed without primary antibody (NC) (Figure 2C). Notably, the reduction of P450 aromatase protein levels upon Mb treatment was also reflected by a change in its enzymatic activity, as measured by the tritiated water release assay (Figure 2D) and a reduction in estradiol (E_2) production (E_2 production in vehicle-treated samples was 3138 ± 140 pg/ml) (Figure 2E). The inhibitory effect exerted by androgen treatment on P450 aromatase expression and activity was abrogated by the contemporary addition of AR antagonists, Hydroxyflutamide (OH-Fl) or Bicalutammide (Bic), indicating that it was mediated by AR activation (Figure 2). Having demonstrated the ability of Mb to downregulate aromatase expression and activity in R2C cells, we investigated whether it was able to affect estradiol/estrogen receptor signaling in R2C cells. To this aim we performed a transient transfection experiment using the XETL plasmid, which carries firefly luciferase sequences under control of an estrogen response element upstream of the thymidine kinase promoter. As shown in Figure 2 F we observed that R2C cell exposure to Mb significantly reduced

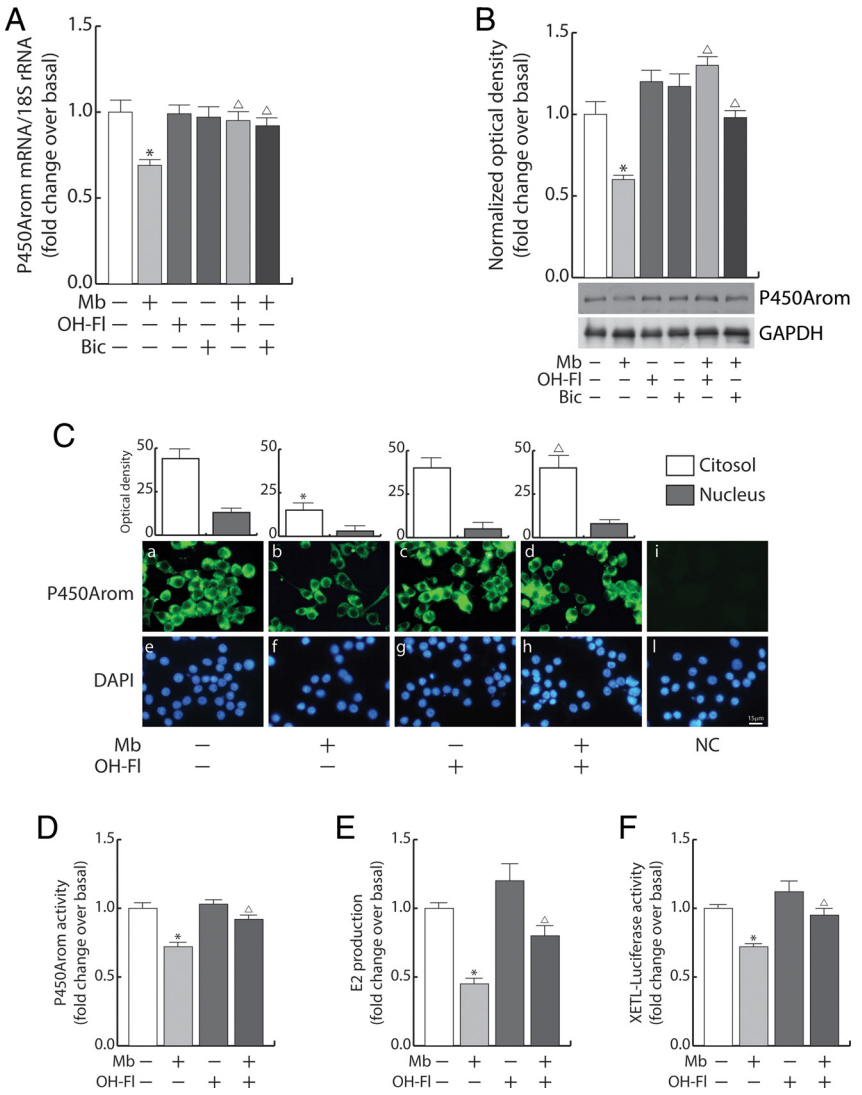

Figure 2. Effects of Mibolerone on P450 aromatase expression and activity in R2C cells. A, P450 aromatase mRNA content evaluated by real-time RT-PCR in cells treated for 24h with vehicle (-), or 10^{-8}M Mb and/or 10^{-6}M hydroxyflutamide (OH-Fl) or 10^{-6}M Bicalutamide (Bic) as indicated. Each sample was normalized to its 18S rRNA content. The values represent the means ± S.D. of three different experiments each performed in triplicate. **(B)** Total protein extracts from R2C cells treated with vehicle (-), 10^{-8}M Mb and/or 10^{-6}M OH-Fl or 10^{-6}M Bic as indicated for 48h were used for immunoblotting analysis of P450 aromatase expression. GAPDH, loading control. Histograms represent the mean±S.D. of three separate experiments in which band intensities were evaluated in terms of optical density arbitrary units and expressed as fold change over basal which was assumed to be 1. **(C)** Immunofluorescence of P450 aromatase (*a-d*) in cells treated for 48h with vehicle (-), 10^{-8}M Mb and/or 10^{-6}M OH-Fl. 4′,6-Diamidino-2-phenylindole (DAPI) staining was used to visualize the cell nucleus (*e-h*). Scale bar = 15 μm. NC, negative control (*i,l*). Histograms represent the mean±S.D. of four separate experiments in which stained P450 aromatase protein was evaluated in terms of optical density arbitrary units by ImageJ software (NIH). **(D)** P450 Aromatase activity and **(E)** estradiol production in cells treated for 72 hours with vehicle (-), 10^{-8}M Mb and/or 10^{-6}M OH-Fl. **(F)** R2C cells were transiently cotransfected with XETL (0.5 μg/well) and treated for 48 hours with vehicle (-), 10^{-8}M Mb and/or 10^{-6}M OH-Fl. Activation of reporter gene expression XETL in vehicle-treated cells is arbitrarily set at 100%. Data represent the mean ± S.D. of three different experiments each performed in triplicate. $^{*}P < .05$ vs vehicle; $^{\Delta}P < .05$ vs Mb-treated.

XETL activation. As expected, addition of Hydroxyflutamide completely reversed this effect.

Ligand-activated AR down-regulates the transcriptional activity of P450 aromatase PII-proximal promoter

Next, we investigated if the down-regulatory effect of Mb on P450 aromatase expression could be due to a negative influence on P450 aromatase gene transcriptional activity. In human fetal and adult testes, R2C and H540 rat Leydig tumor cells and in purified preparation of rat Leydig, Sertoli and germ cells, P450 aromatase expression is regulated by a promoter proximal to the translational starting site named promoter II (PII) (41–43).

Thus, R2C cells were transiently transfected with a luciferase reporter plasmid containing the PII P450 aromatase promoter (PII-Arom) sequence (-1037/+94). As shown in Figure 3A, a significant reduction in PII-Arom activity could be observed upon Mb administration. This effect was no longer detectable following the addition of the AR antagonist OH-Fl, further confirming the involvement of AR activation. In addition no inhibitory effects were observed in Mb-treated cells transfected with the empty-luciferase reporter plasmid (data not shown). PII-regulated P450 aromatase expression is driven by specific response elements: a nuclear receptor half site binding SF-1/LRH-1 (44) and CRE-like sequences binding CREB/ATF protein family members (29). Therefore, to characterize PII-Arom regions that are functionally important for transcriptional regulation by androgens, transient transfection experiments were performed by using different sized or mutated PII P450 aromatase promoter fragments fused to the luciferase reporter gene (29), as schematically exemplified in Figure 3B, left panel.

Similarly to what observed for the PII-Arom (-1037/+94), the transcriptional activity of the PII-Arom construct (-688/+94) which still includes the 5′CRE, 3′CRE, XCRE and SF-1 binding sites, was decreased in response to Mb stimulation, thus confirming the importance of these sites for PII-driven regulation of P450 aromatase expression (Figure 3B, *right panel*). Mutations of the 5′CRE (5′CRE m), the 3′CRE (3′CRE m) or the XCRE (XCREm) did not influence the response to androgens, since PII-Arom transcriptional activity was still reduced following Mb administration, mirroring wild type PII-Arom activity. On the contrary, we evidenced the loss of the inhibitory effect exerted by Mb in the presence of the construct bearing a SF-1/LRH-1 mutated binding site (SF-1m), demonstrating that P450 aromatase regulation by androgens requires the integrity of the SF-1 motif.

Mibolerone induces DAX-1 expression and its recruitment within the P450 aromatase gene promoter in R2C cells

One of the major repressors of SF-1-mediated transactivation of target genes in steroidogenic tissues is the nuclear orphan receptor DAX-1 (28, 45–47). Moreover, previous findings demonstrated that P450 aromatase is a physiologic target gene of the nuclear orphan receptor DAX-1 that, acting as an adaptor molecule, represses

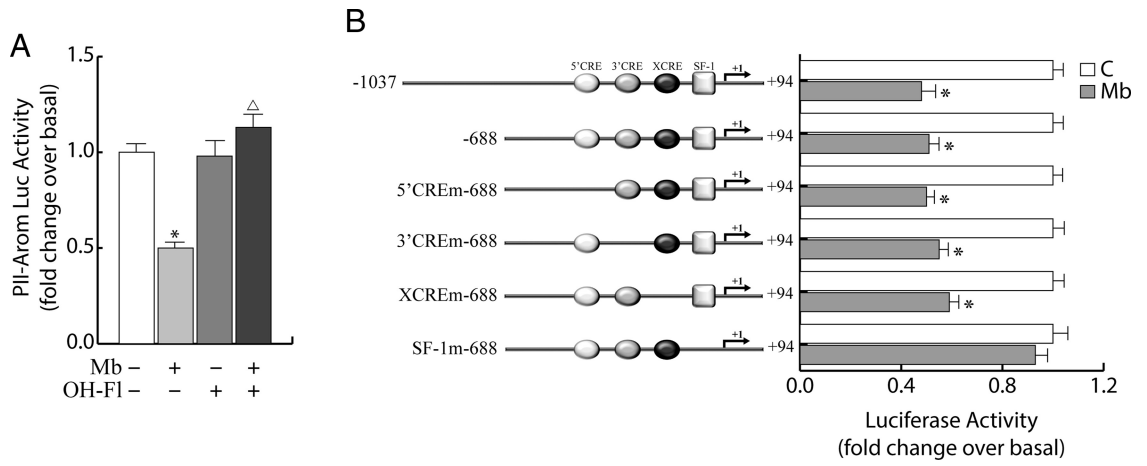

Figure 3. Effects of Mibolerone on P450 aromatase promoter activity in R2C cells. A, R2C cells were transiently transfected with a luciferase reporter plasmid containing the PII P450 aromatase promoter (PII-Arom; –1037/+94) and treated for 24h with vehicle (-), 10^{-8}M Mb and/or 10^{-6}M OH-Fl. Activation of reporter plasmids in vehicle treated samples is arbitrarily set at 1. **(B)** Schematic representation of the PII P450 aromatase proximal promoter constructs used in this study (*left panel).* All of the promoter constructs contain the same 3′ boundary (+94). The 5′ boundaries of the promoter fragments varied from –1037 to –688. Three putative CRE motifs (5′-CRE at –335; 3′-CRE at –231; XCRE at –169) are indicated as *circles*. The SF-1 motif at –90 is indicated as a *square.* A mutated 5′CRE, 3′CRE, XCRE and SF-1-binding site is present respectively in 5′CREm, 3′CREm, XCREm and SF-1m constructs. PII P450 aromatase transcriptional activity in R2C cells, transfected with the above described promoter constructs and treated with vehicle (C) or 10^{-8}M Mb for 24h, is shown (*right panel).* Activation of reporter plasmids in vehicle treated samples is arbitrarily set at 1. Results represent the mean ± S.D. of three different experiments each performed in triplicate. $^{*}P < .05$ vs vehicle; $^{\Delta}P < .05$ vs Mb-treated.

P450 aromatase transactivation through a variety of mechanisms (48–50). Thus, we investigated, in our experimental system, whether DAX-1 may represent a molecular link between androgens and P450 aromatase. First, we evaluated, in R2C cells, the effects of Mb administration on DAX-1 levels.

By using quantitative Real Time PCR we performed a time-course study to evaluate DAX1 mRNA levels in R2C cells. As shown in Figure 4A, a Mibolerone-dependent induction of DAX-1 mRNA levels could be already observed following a 12 hrs treatment and persisted thereafter. The enhanced DAX-1 mRNA levels was concomitant with a decreased P450aromatase mRNA content (Figure 4B). Induction of DAX-1 expression by Mb (Figure 4C) or DHT (Supplemental Figure 1E and F) was confirmed by western blotting analysis also revealing that DAX-1 protein localizes prevalently into the nucleus wherein it was further enhanced upon Mb administration. Immunofluorescence analysis confirmed these observations (Figure 4D). DAX-1 regulation involves AR activation since addition of the androgen receptor antagonists OH-Fl reduced the Mb-dependent up-regulation of DAX-1 (Figure 4C).

To provide evidence of the participation of DAX-1 in the androgen-dependent modulation of P450 aromatase expression we assessed, by ChIP assay, the ability of DAX-1 to associate to the SF-1/LRH-1 containing region of the PII P450 aromatase proximal promoter upon androgen treatment. According with previous findings, both DAX-1 and N-CoR were recruited at the SF-1/LRH-1 motif containing region of the PII P450 aromatase gene promoter (Figure 4E). Interestingly, DAX-1 occupancy of the SF-1/LRH-1 site containing sequence of the PII promoter was induced in a ligand-dependent manner, since DAX-1 recruitment was enhanced by Mb administration. Concomitantly, recruitment of the steroid receptor corepressor N-CoR within the same promoter region was also

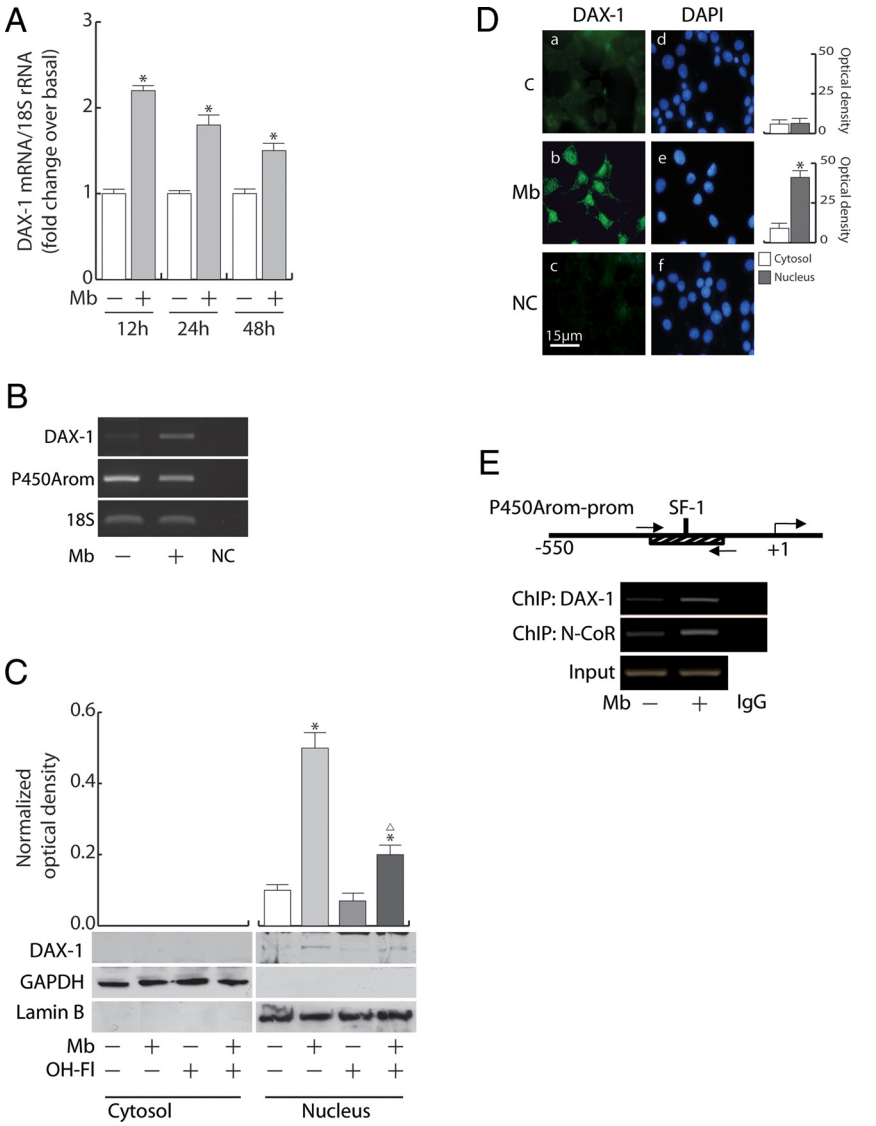

Figure 4. Mibolerone up-regulates DAX-1 expression in R2C cells. A, Time-course analysis of DAX-1 mRNA content evaluated by real-time RT-PCR in cells treated with vehicle (-), or 10^{-8}M Mb, as indicated. Each sample was normalized to its 18S rRNA content. Values represent the means ± S.D. of three different experiments each performed in triplicate. **(B)** RT-PCR for DAX-1 and P450 aromatase mRNA expression in R2C cells treated with vehicle (-) or 10^{-8}M Mb for 48h. 18S, internal standard; NC, negative control. **(C)** Immunoblotting for DAX-1 expression in cytosolic or nuclear extracts from cells treated for 48h with vehicle (-), 10^{-8}M Mb and/or 10^{-6}M OH-Fl. GAPDH and Lamin B were assessed as control of protein loading and purity of lysate fractions. Histograms represent the mean±SD of three separate experiments in which band intensities were evaluated in terms of optical density arbitrary units. **(D)** Immunofluorescence of DAX-1 (*a,b*) in cells treated for 48h with vehicle (C) or 10^{-8}M Mb. 4′,6-Diamidino-2-phenylindole (DAPI) staining was used to visualize the cell nucleus (*d,e*). Scale bar = 15 μm. NC, negative control (*c,f*). Histograms represent the mean±S.D. of four separate experiments in which stained proteins were evaluated in terms of optical density arbitrary units by ImageJ software (NIH). **(E)** Sheared chromatin from R2C cells treated with vehicle (-) or 10^{-8}M Mb for 2h was precipitated using anti-DAX-1 or anti-N-CoR antibodies. The 5′-flanking sequence of the PII P450 aromatase proximal promoter containing the SF-1 site was detected by PCR with specific primers listed in the 'Materials and Methods' section. Inputs DNA were amplified as loading controls. IgG, control samples. $^{*}P < .05$ vs vehicle; $^{\Delta}P < .05$ vs Mb-treated.

significantly increased by Mb treatment (Figure 4E).

These results demonstrate, for the first time, how DAX-1 enhancement by androgens may negatively affect the modulation of the P450 aromatase gene in Leydig tumor cells.

AR/DAX-1/ P450 Aromatase expression pattern in male Fisher rats

As a final step of the current study, we evaluated the expression pattern of DAX-1, P450 aromatase and AR in testis tissues from younger (Fisher Rats Normal Testes: FRNT) and older (Fisher Rats Tumor Testes: FRTT) Fisher rats. Aged animals presented spontaneous Leydig cell tumors, a phenomenon not observed in younger animals (51, 52), allowing us to use them as a good in vivo model useful to corroborate our in vitro observations. As shown in Figure 5, DAX-1 protein was expressed in FRNT but scarcely detectable in FRTT. A similar expression pattern was displayed by AR. On the contrary, a strongly increased P450 aromatase immunoreactivity could be observed in FRTT compared to FRNT. The AR/DAX-1/P450 Aromatase protein expression pattern in normal (FRTT) and tumoral (FRNT) testis tissues, was mirrored by the corresponding mRNA content, as detected by RT-PCR analysis (data not shown). Thus, our in vivo results indicate that the occurrence of Leydigioma is associated to a significant decrease in AR and DAX-1 levels and to a remarkable enhancement of P450 aromatase expression, confirming results obtained in R2C cell line.

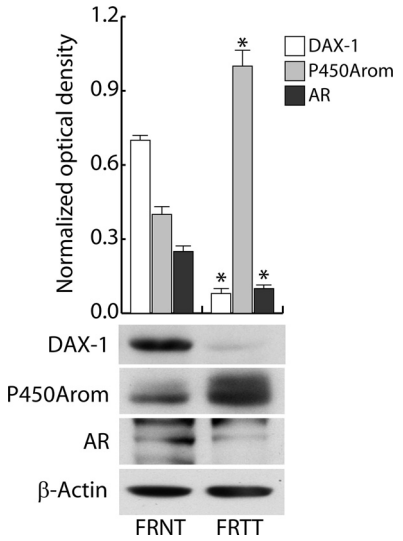

Figure 5. DAX-1, P450 aromatase and androgen receptor expression in Fisher rat testes. Immunoblotting of DAX-1, P450 aromatase and androgen receptor (AR) in tissues from normal (FRNT) and tumor (FRTT) Fisher rat testes. β-actin, loading control. Immunoblots show a single representative result. Histograms represent the mean±S.D. of three separate experiments in which band intensities were evaluated in terms of optical density arbitrary units. $^*P < .05$ vs FRNT.

Discussion

In the present study we highlighted, in Leydig tumor cells, the existence of a novel functional interplay between the androgen receptor (AR), the orphan nuclear receptor DAX-1 and the P450 aromatase enzyme, that could play a role in leydigiomas' development and progression.

Testicular sex steroid synthesis is an elaborated dynamic process that, in addition to the negative feedback throughout the hypothalamic-pituitary-gonadal axis, is also finely regulated by various autocrine/paracrine factors (53, 54). In this scenario the maintenance of a delicate balance between androgens and estrogens appears to have a fundamental role for male gonadal integrity and function (55). This balance is governed by cytochrome P450 aromatase, encoded by the *CYP19* gene, that catalyzes the local conversion of androgens to estrogens and whose expression has been detected in Leydig cells and some population of germ cells (56). Interestingly, the expression of AR at the same site of P450 aromatase and estrogen receptor (ER) in the testis (23, 57–59), suggests a possible cross-regulation between the two steroid-induced signaling pathways.

It is now generally accepted that locally secreted estrogens may act as autocrine factors exerting proliferative effects on human and rodents Leydig cells (10, 19). Increased estradiol/testosterone ratio disrupts Leydig cell function and might cause hyperplasia, hypertrophy and Leydig cell adenomas (20, 21). Indeed, in mice, chronic estrogen treatment induces Leydig cell tumors (LCTs) (60) eventually regressing following estrogen withdrawal with cellular alterations suggestive of apoptosis (61). On the other hand, in male occult LCTs patients, gynecomastia, the more frequent clinical sign observed, is accompanied by increased estradiol and decreased testosterone levels, strongly suggesting the presence of an estrogen-secreting tumor (7, 8, 10, 62). However less is known regarding the role of AR in the modulation of the complex testis paracrine/autocrine signaling especially concerning the molecular mechanism for androgen/AR regulation of Sertoli cell, Leydig cell and peritubular myoid cell proliferation and/or differentiation (12). Here we demonstrate that prolonged administration of the synthetic androgen receptor agonist Mibolerone is able to reduce proliferation rate in a well-documented in vitro model for Leydig cell neoplasms, such as rat Leydig tumor cells R2C (63). Our study indicates that androgen-dependent reduction of cell growth is consequent to the decrease of the self-sufficient in situ estrogen production which represents a major feature of R2C cells (19, 23). Indeed, in this cell type, androgen treatment negatively impacts on P450 aromatase by down-regulating its expression at both mRNA and protein

levels and determining a decrease of its enzymatic activity. It has been shown that androgens are able to affect the expression of steroidogenic enzymes via an AR-mediated (64) or a local feed-back mechanism (65, 66). Our results indicate that the inhibitory effects induced by androgen administration on P450 aromatase expression involve androgen receptor activation since they disappear in the presence of the AR antagonist hydroxyflutamide or bicalutamide. These data confirm previous in vitro and in vivo findings that AR signaling in Leydig cells displays autocrine regulation and that lacking functional AR in Leydig cells has a major influence on Leydig cell steroidogenic function (12, 27). The observed AR-mediated inhibition of P450 aromatase cellular levels involves regulation of *CYP19* gene transcriptional activity. Distinctive tissue-specific *CYP19* promoters are employed to direct the expression of P450 aromatase mRNA (67). The main regulator of normal testicular cell aromatization is the *CYP19* proximal promoter II (PII), located immediately upstream of the transcriptional initiation site. PII is also been reported as the main active promoter in LCTs and in R2C cells (24, 25, 31, 42, 43). Different response elements have been identified in PII: three motifs resembling CRE and an SF-1 binding site (29, 68), but no androgen response element have been defined. By functional studies, using constructs containing wild-type or different 5′-deleted regions of rat PII P450 aromatase promoter, we demonstrated the ability of androgens to decrease PII transcriptional activity. This inhibitory effect was abrogated when a promoter fusion containing a mutated SF-1 element was employed, suggesting that the integrity of the SF-1 sequence is a prerequisite for the down-regulatory effects of the AR ligands on P450 aromatase promoter activity. The above described observations are consistent with recent studies showing that AR inhibits the transactivation of SF-1 in Leydig cells (27) as in gonadotrope-derived cells (69). The importance of the androgen-induced inhibition of SF-1-dependent P450 aromatase gene transactivation in Leydig tumor cells is highlighted by a recent case-report of a 29-year-old male diagnosed with an estrogen-producing LCT, severe gynecomastia and elevated plasma estradiol levels. In fact, in this report, authors demonstrate elevated estrogen synthesis in LCT to be consequent to enhanced PII-driven *CYP19* transcription, most likely caused by elevated levels of the transcription factor SF-1 (26). Thus, our findings are suggestive of the possibility that androgen action on testicular estrogen production might be accomplished by cross-talk between androgen signaling and major transcription factors responsible for P450 aromatase gene expression.

In the aim of getting insights into this issue we investigated the involvement of the nuclear orphan receptor DAX-1 that has key roles in the development and the maintenance of reproductive function as it is a crucial regulator of steroidogenesis in mammals. Indeed, DAX-1 has a restricted expression pattern to tissues directly involved in steroid hormone production (70). Within these tissues, DAX-1 colocalize with SF-1 (45) and acts as a global antisteroidogenic factor likely by suppressing SF-1-mediated transcription through a variety of mechanisms (28, 46, 47, 49, 50, 71). For instance, DAX-1 is a repressor of several steroidogenic enzymes (28, 70, 72), blocking steroid production at multiple levels and decreasing the formation of steroids that are precursors of estrogens. In Y-1 adrenocortical cells, DAX-1 blocks the rate-limiting step in steroid biosynthesis by repressing StAR protein expression (46) as well as by inhibiting both P450scc (*CYP11A*) and 3-β-hydroxysteroid dehydrogenase cellular levels (50). Moreover, it has also been shown that in insulin-treated MA-10 Leydig cells, triggering of the insulin receptor signaling pathway decreases cAMP-induced StAR, P450scc and 3-β-hydroxysteroid dehydrogenase via induction of DAX-1, without any change in serum LH or FSH levels (73). Worthily the aromatase coding gene, *CYP19* represents a physiological target for DAX-1 in Leydig cells. A very elegant study examining the consequences of DAX-1 deficiency on Leydig steroidogenesis in vivo, demonstrated that there was no alteration in the expression of the five steroidogenic genes required for testosterone biosynthesis, while P450 aromatase mRNA, protein and enzymatic activity was increased significantly in DAX-1-deficient Leydig cells. Enhanced P450 aromatase expression was accompanied by a 40-fold increase in intra-testicular estradiol (48). Consistently, in a patient with adrenal insufficiency and hypogonadotropic hypogonadisms, deletion of the exon 2 of *DAX-1* gene, dramatically affecting its function (74), has been associated with disturbed biological function of testis, especially hyperplasia of Leydig cells (75). Our findings indicate that, in rat Leydig tumor cells R2C, DAX-1 expression is regulated by androgens. In our experimental system, androgen-dependent up-regulation of nuclear DAX-1 is associated to a significant increase of its recruitment within the SF-1 site containing region of the PII P450 aromatase proximal promoter. According to previous observations (49), DAX-1 occupancy of the PII promoter is concomitant with the enhanced recruitment of the steroid receptor corepressor N-CoR. Therefore, the mechanism we described might contribute to explain the negative influence of androgens on rat Leydig tumor cell proliferation, and well correlates with observations in endometrial carcinoma, where loss or decreased DAX-1 expression results in increased intratumoral steroid production and enhanced estrogen-dependent proliferation of cancer cells (76).

Thus, in Leydig tumor cells, the induction of DAX-1 expression and the consequent modulation of P450 aromatase expression and activity exerted by androgens, may represent an in situ defensive mechanism for modulating unopposed estrogenic effects. Thus, the maintenance of a proper ratio between androgen and estrogen testicular levels appears to be fundamental. As shown in the present study, long term administration (3 and 6 days) of low doses of androgens (in the nanomolar range) decrease R2C cell number by binding the AR and reducing the effect of locally produced estradiol. On the contrary, high doses (in the micromolar range) of aromatisable and nonaromatisable anabolic androgenic steroids induce, following a 24 hours treatment, proliferation of R2C cells as a consequence of the binding to the estrogen receptor (32). While reinforcing the concept that the finely tuned balance between androgens and estrogens is critical in the development of proliferative diseases, these observations make it appealing to speculate whether such a mechanism can also exist in other endocrine-related cancers. In fact, the aberrant expression of P450 aromatase is believed to contribute to the development and progression of breast cancer (18, 36, 77–79). To this regard, we recently demonstrated that ligand-activated AR negatively regulates in situ estrogen production by activating *DAX-1* gene transcription in estrogen-related MCF-7 breast cancer cells, providing new clues for the inhibitory role exerted by androgens on estrogen-dependent cancer cell proliferation (79). More surprisingly, emerging evidences indicate the prostate as a target for locally produced estrogens (80, 81). Specifically, P450 aromatase is expressed in nonmalignant prostatic stroma but not in normal epithelial cells. In contrast, the onset and/or progression of malignancy is accompanied by the appearance and increase of P450 aromatase expression and activity within the prostate epithelium together with potential alteration of P450 aromatase promoter usage, similarly to that occurred in breast cancer (82, 83). Besides, prostate epithelium phenotypic changes are also associated to dysregulation of DAX-1 whose expression is considerably reduced in benign prostate hyperplasia compared to normal prostate tissue (84, 85), thus leaving the issue opened for future challenges. Direct confirmation of the biological relevance of our findings comes from results obtained in normal (FRNT) and tumoral (FRTT) testes tissues from younger and older, respectively, Fisher rats which are characterized by exceptionally high incidence of spontaneous Leydig cell neoplasm associated with aging (51, 52). It appears extremely interesting to observe that tumor development is concomitant with a marked down-regulation of AR and DAX-1 expression and a strong increase in P450 aromatase levels, as it emerges comparing young normal rat testes with the older ones showing the presence of the neoplasia. Specifically, FRNT are characterized by high expression levels of DAX-1 and very low levels of P450 aromatase enzyme. On the contrary, Leydig tumor development in FRTT is associated with an opposite expression pattern showing a barely detectable DAX-1 content and a strongly increased P450 aromatase expression. Importantly, DAX-1 expression pattern is mirrored by AR expression.

Collectively, our study, for the first time, identifies the existence of a functional AR/DAX-1/ P450 aromatase interplay involved in the inhibition of the estrogen-dependent testicular cancer cell proliferation. In elucidating a mechanism by which androgens modulate the growth of Leydig tumor cells, these findings reinforce the hypothesis that restoring the correct balance between androgen and estrogen levels, may open new opportunities for therapeutic intervention in this type of endocrine-related cancer.

Acknowledgments

The authors thank Dr. E.R. Simpson, Dr. C.D. Clyne and Dr. M.J. McPhaul for generously providing P450 aromatase promoter plasmids.

Address all correspondence and requests for reprints to: Prof. Sebastiano Andò, Department of Pharmacy and Health and Nutritional Sciences, University of Calabria, Via P. Bucci, 87 036, Arcavacata di Rende (CS), Italy, Phone. +39 0984 496 201, Fax. +39 0984 496 203, e-mail: sebastiano.ando@unical.it.

This work was supported by Progetti di Ricerca di Interesse Nazionale (PRIN)-Ministero Istruzione Università e Ricerca (MIUR) [grant number 20085Y7XT5]; and Associazione Italiana Ricerca sul Cancro (AIRC) [grant number 11 595].

* Marilena Lanzino and Sebastiano Andò are joint senior authors

Disclosure Summary: The authors have nothing to disclose.

References

1. **Hawkins C, Miaskowski C. Testicular cancer: a review. Oncol Nurs Forum 1996 23:1203–1211; quiz 1212–1203.**
2. **Kim I, Young RH, Scully RE. Leydig cell tumors of the testis. A clinicopathological analysis of 40 cases and review of the literature. Am J Surg Pathol 1985 9:177–192.**
3. **Mostofi FK. Proceedings: Testicular tumors. Epidemiologic, etiologic, and pathologic features.** *Cancer* 1973 32:1186–1201.
4. **McCluggage WG, Shanks JH, Arthur K, Banerjee SS. Cellular proliferation and nuclear ploidy assessments augment established prognostic factors in predicting malignancy in testicular Leydig cell tumours. Histopathology 1998 33:361–368.**
5. **Woolveridge I, Taylor MF, Rommerts FF, Morris ID. Apoptosis related gene products in differentiated and tumorigenic rat Leydig cells and following regression induced by the cytotoxin ethane dimethanesulphonate. Int J Androl 2001 24:56–64.**

6. Azer PC, Braunstein GD. Malignant Leydig cell tumor: objective tumor response to o,p'-DDD. *Cancer* 1981 47:1251–1255.
7. Anderson MS, Brogi E, Biller BM. Occult Leydig cell tumor in a patient with gynecomastia. Endocr Pract 2001 7:267–271.
8. Wasniewska M, Raiola G, Teresa A, Galati MC, Zirilli G, Catena MA, Ascenti G, Arasi S, De Luca F. Gynecomastia disclosing diagnosis of Leydig cell tumour in a man with thalassemia, secondary hypogonadism and testis microlithiasis. Acta Biomed 2009 80:286–288.
9. Al-Agha OM, Axiotis CA. An in-depth look at Leydig cell tumor of the testis. *Arch Pathol Lab Med* 2007 131:311–317.
10. Zarrilli S, Lombardi G, Paesano L, Di Somma C, Colao A, Mirone V, De Rosa M. Hormonal and seminal evaluation of Leydig cell tumour patients before and after orchiectomy. Andrologia 2000 32:147–154.
11. Carreau S, Wolczynski S, Galeraud-Denis I. Aromatase, oestrogens and human male reproduction. Philos Trans R Soc Lond B Biol Sci 2010 365:1571–1579.
12. Wang RS, Yeh S, Tzeng CR, Chang C. Androgen receptor roles in spermatogenesis and fertility: lessons from testicular cell-specific androgen receptor knockout mice. Endocr Rev 2009 30:119–132.
13. McPhaul MJ. Androgen receptor mutations and androgen insensitivity. Mol Cell Endocrinol 2002 198:61–67.
14. Avila DM, Zoppi S, McPhaul MJ. The androgen receptor (AR) in syndromes of androgen insensitivity and in prostate cancer. J Steroid Biochem Mol Biol 2001 76:135–142.
15. Quigley CA, De Bellis A, Marschke KB, el-Awady MK, Wilson EM, French FS. Androgen receptor defects: historical, clinical, and molecular perspectives. Endocr Rev 1995 16:271–321.
16. Rutgers JL, Scully RE. The androgen insensitivity syndrome (testicular feminization): a clinicopathologic study of 43 cases. Int J Gynecol Pathol 1991 10:126–144.
17. Jarzabek K, Philibert P, Koda M, Sulkowski S, Kotula-Balak M, Bilinska B, Kottler ML, Wolczynski S, Sultan C. Primary amenorrhea in a young Polish woman with complete androgen insensitivity syndrome and Sertoli-Leydig cell tumor: identification of a new androgen receptor gene mutation and evidence of aromatase hyperactivity and apoptosis dysregulation within the tumor. Gynecol Endocrinol 2007 23:499–504.
18. Simpson ER, Clyne C, Rubin G, Boon WC, Robertson K, Britt K, Speed C, Jones M. Aromatase–a brief overview. Annu Rev Physiol 2002 64:93–127.
19. Sirianni R, Chimento A, Malivindi R, Mazzitelli I, Ando S, Pezzi V. Insulin-like growth factor-I, regulating aromatase expression through steroidogenic factor 1, supports estrogen-dependent tumor Leydig cell proliferation. Cancer Res 2007 67:8368–8377.
20. Fowler KA, Gill K, Kirma N, Dillehay DL, Tekmal RR. Overexpression of aromatase leads to development of testicular leydig cell tumors : an in vivo model for hormone-mediated TesticularCancer. *Am J Pathol* 2000 156:347–353.
21. Li X, Strauss L, Kaatrasalo A, Mayerhofer A, Huhtaniemi I, Santti R, Makela S, Poutanen M. Transgenic mice expressing p450 aromatase as a model for male infertility associated with chronic inflammation in the testis. *Endocrinology* 2006 147:1271–1277.
22. Li X, Rahman N. Impact of androgen/estrogen ratio: lessons learned from the aromatase over-expression mice. Gen Comp Endocrinol 2008 159:1–9.
23. Carpino A, Rago V, Pezzi V, Carani C, Ando S. Detection of aromatase and estrogen receptors (ERalpha, ERbeta1, ERbeta2) in human Leydig cell tumor. Eur J Endocrinol 2007 157:239–244.
24. Brodie A, Inkster S, Yue W. Aromatase expression in the human male. Mol Cell Endocrinol 2001 178:23–28.
25. Bulun SE, Rosenthal IM, Brodie AM, Inkster SE, Zeller WP, DiGeorge AM, Frasier SD, Kilgore MW, Simpson ER. Use of tissue-specific promoters in the regulation of aromatase cytochrome P450 gene expression in human testicular and ovarian sex cord tumors, as well as in normal fetal and adult gonads. *J Clin Endocrinol Metab* 1993 77:1616–1621.
26. Straume AH, Lovas K, Miletic H, Gravdal K, Lonning PE, Knappskog S. Elevated levels of the steroidogenic factor 1 are associated with over-expression of CYP19 in an oestrogen-producing testicular Leydig cell tumour. Eur J Endocrinol 2012 166:941–949.
27. Song CH, Gong EY, Park J, Lee K. Testicular steroidogenesis is locally regulated by androgen via suppression of Nur77. Biochem Biophys Res Commun 2012 422:327–332.
28. Hanley NA, Rainey WE, Wilson DI, Ball SG, Parker KL. Expression profiles of SF-1, DAX1, and CYP17 in the human fetal adrenal gland: potential interactions in gene regulation. Mol Endocrinol 2001 15:57–68.
29. Young M, McPhaul MJ. A steroidogenic factor-1-binding site and cyclic adenosine 3′,5′-monophosphate response element-like elements are required for the activity of the rat aromatase promoter in rat Leydig tumor cell lines. *Endocrinology* 1998 139:5082–5093.
30. Catalano S, Panza S, Malivindi R, Giordano C, Barone I, Bossi G, Lanzino M, Sirianni R, Mauro L, Sisci D, Bonofiglio D, Ando S. Inhibition of Leydig tumor growth by farnesoid X receptor activation: the in vitro and in vivo basis for a novel therapeutic strategy. Int J Cancer 2013 132:2237–2247.
31. Catalano S, Malivindi R, Giordano C, Gu G, Panza S, Bonofiglio D, Lanzino M, Sisci D, Panno ML, Ando S. Farnesoid X receptor, through the binding with steroidogenic factor 1-responsive element, inhibits aromatase expression in tumor Leydig cells. J Biol Chem 2010 285:5581–5593.
32. Chimento A, Sirianni R, Zolea F, De Luca A, Lanzino M, Catalano S, Ando S, Pezzi V. Nandrolone and stanozolol induce Leydig cell tumor proliferation through an estrogen-dependent mechanism involving IGF-I system. J Cell Physiol 2012 227:2079–2088.
33. Lanzino M, Garofalo C, Morelli C, Le Pera M, Casaburi I, McPhaul MJ, Surmacz E, Ando S, Sisci D. Insulin receptor substrate 1 modulates the transcriptional activity and the stability of androgen receptor in breast cancer cells. Breast Cancer Res Treat 2009 115:297–306.
34. Morelli C, Lanzino M, Garofalo C, Maris P, Brunelli E, Casaburi I, Catalano S, Bruno R, Sisci D, Ando S. Akt2 inhibition enables the forkhead transcription factor FoxO3a to have a repressive role in estrogen receptor alpha transcriptional activity in breast cancer cells. Mol Cell Biol 2010 30:857–870.
35. de Amicis F, Lanzino M, Kisslinger A, Cali G, Chieffi P, Ando S, Mancini FP, Tramontano D. Loss of proline-rich tyrosine kinase 2 function induces spreading and motility of epithelial prostate cells. J Cell Physiol 2006 209:74–80.
36. Barone I, Giordano C, Malivindi R, Lanzino M, Rizza P, Casaburi I, Bonofiglio D, Catalano S, Ando S. Estrogens and PTP1B function in a novel pathway to regulate aromatase enzymatic activity in breast cancer cells. *Endocrinology* 2012 153:5157–5166.
37. Bunone G, Briand PA, Miksicek RJ, Picard D. Activation of the unliganded estrogen receptor by EGF involves the MAP kinase pathway and direct phosphorylation. EMBO J 1996 15:2174–2183.
38. Giordano C, Vizza D, Panza S, Barone I, Bonofiglio D, Lanzino M, Sisci D, De Amicis F, Fuqua SA, Catalano S, Ando S. Leptin increases HER2 protein levels through a STAT3-mediated up-regulation of Hsp90 in breast cancer cells. Mol Oncol 2012.
39. Lu S, Liu M, Epner DE, Tsai SY, Tsai MJ. Androgen regulation of the cyclin-dependent kinase inhibitor p21 gene through an androgen response element in the proximal promoter. Mol Endocrinol 1999 13:376–384.
40. Altucci L, Addeo R, Cicatiello L, Dauvois S, Parker MG, Truss M, Beato M, Sica V, Bresciani F, Weisz A. 17beta-Estradiol induces cyclin D1 gene transcription, p36D1–p34cdk4 complex activation and p105Rb phosphorylation during mitogenic stimulation of G(1)-arrested human breast cancer cells. Oncogene 1996 12:2315–2324.
41. Young M, Lephart ED, McPhaul MJ. Expression of aromatase cy-

tochrome P450 in rat H540 Leydig tumor cells. J Steroid Biochem Mol Biol 1997 63:37–44.
42. Young M, McPhaul MJ. Definition of the elements required for the activity of the rat aromatase promoter in steroidogenic cell lines. J Steroid Biochem Mol Biol 1997 61:341–348.
43. Lanzino M, Catalano S, Genissel C, Ando S, Carreau S, Hamra K, McPhaul MJ. Aromatase messenger RNA is derived from the proximal promoter of the aromatase gene in Leydig, Sertoli, and germ cells of the rat testis. Biol Reprod 2001 64:1439–1443.
44. Pezzi V, Sirianni R, Chimento A, Maggiolini M, Bourguiba S, Delalande C, Carreau S, Ando S, Simpson ER, Clyne CD. Differential expression of steroidogenic factor-1/adrenal 4 binding protein and liver receptor homolog-1 (LRH-1)/fetoprotein transcription factor in the rat testis: LRH-1 as a potential regulator of testicular aromatase expression. *Endocrinology* 2004 145:2186–2196.
45. Ikeda Y, Swain A, Weber TJ, Hentges KE, Zanaria E, Lalli E, Tamai KT, Sassone-Corsi P, Lovell-Badge R, Camerino G, Parker KL. Steroidogenic factor 1 and Dax-1 colocalize in multiple cell lineages: potential links in endocrine development. Mol Endocrinol 1996 10: 1261–1272.
46. Zazopoulos E, Lalli E, Stocco DM, Sassone-Corsi P. DNA binding and transcriptional repression by DAX-1 blocks steroidogenesis. Nature 1997 390:311–315.
47. Tremblay JJ, Viger RS. Nuclear receptor Dax-1 represses the transcriptional cooperation between GATA-4 and SF-1 in Sertoli cells. Biol Reprod 2001 64:1191–1199.
48. Wang ZJ, Jeffs B, Ito M, Achermann JC, Yu RN, Hales DB, Jameson JL. Aromatase (Cyp19) expression is up-regulated by targeted disruption of Dax1. Proc Natl Acad Sci U S A 2001 98:7988–7993.
49. Crawford PA, Dorn C, Sadovsky Y, Milbrandt J. Nuclear receptor DAX-1 recruits nuclear receptor corepressor N-CoR to steroidogenic factor 1. Mol Cell Biol 1998 18:2949–2956.
50. Lalli E, Melner MH, Stocco DM, Sassone-Corsi P. DAX-1 blocks steroid production at multiple levels. *Endocrinology* 1998 139: 4237–4243.
51. Jacobs BB, Huseby RA. Neoplasms occurring in aged Fischer rats, with special reference to testicular, uterine, and thyroid tumors. J Natl Cancer Inst 1967 39:303–309.
52. Coleman GL, Barthold W, Osbaldiston GW, Foster SJ, Jonas AM. Pathological changes during aging in barrier-reared Fischer 344 male rats. J Gerontol 1977 32:258–278.
53. Hong CY, Park JH, Ahn RS, Im SY, Choi HS, Soh J, Mellon SH, Lee K. Molecular mechanism of suppression of testicular steroidogenesis by proinflammatory cytokine tumor necrosis factor alpha. Mol Cell Biol 2004 24:2593–2604.
54. Lee SY, Gong EY, Hong CY, Kim KH, Han JS, Ryu JC, Chae HZ, Yun CH, Lee K. ROS inhibit the expression of testicular steroidogenic enzyme genes via the suppression of Nur77 transactivation. Free Radic Biol Med 2009 47:1591–1600.
55. Haverfield JT, Ham S, Brown KA, Simpson ER, Meachem SJ. Teasing out the role of aromatase in the healthy and diseased testis. Spermatogenesis 2011 1:240–249.
56. Turner KJ, Macpherson S, Millar MR, McNeilly AS, Williams K, Cranfield M, Groome NP, Sharpe RM, Fraser HM, Saunders PT. Development and validation of a new monoclonal antibody to mammalian aromatase. J Endocrinol 2002 172:21–30.
57. Bremner WJ, Millar MR, Sharpe RM, Saunders PT. Immunohistochemical localization of androgen receptors in the rat testis: evidence for stage-dependent expression and regulation by androgens. *Endocrinology* 1994 135:1227–1234.
58. Aquila S, Middea E, Catalano S, Marsico S, Lanzino M, Casaburi I, Barone I, Bruno R, Zupo S, Ando S. Human sperm express a functional androgen receptor: effects on PI3K/AKT pathway. Hum Reprod 2007 22:2594–2605.
59. Guido C, Perrotta I, Panza S, Middea E, Avena P, Santoro M, Marsico S, Imbrogno P, Ando S, Aquila S. Human sperm physiology: estrogen receptor alpha (ERalpha) and estrogen receptor beta (ERbeta) influence sperm metabolism and may be involved in the pathophysiology of varicocele-associated male infertility. J Cell Physiol 2011 226:3403–3412.
60. Nishizawa Y, Sato B, Miyashita Y, Tsukada S, Hirose T, Kishimoto S, Matsumoto K. Autocrine regulation of cell proliferation by estradiol and hydroxytamoxifen of transformed mouse Leydig cells in serum-free culture. *Endocrinology* 1988 122:227–235.
61. Huseby RA. Dormancy versus extinction of mouse Leydig cell tumors following endocrine-induced regression. Cancer Res 1983 43: 5365–5378.
62. Kayemba-Kays S, Fromont-Hankard G, Lettelier G, Gabriel S, Levard G. Leydig cell tumour revealed by bilateral gynecomastia in a 15-year-old adolescent: a patient report. J Pediatr Endocrinol Metab 2010 23:1195–1199.
63. Catalano S, Panza S, Malivindi R, Giordano C, Barone I, Bossi G, Lanzino M, Sirianni R, Mauro L, Sisci D, Bonofiglio D, Ando S. Inhibition of leydig tumor growth by farnesoid X receptor activation: The in vitro and in vivo basis for a novel therapeutic strategy. Int J Cancer 2012.
64. Burgos-Trinidad M, Youngblood GL, Maroto MR, Scheller A, Robins DM, Payne AH. Repression of cAMP-induced expression of the mouse P450 17 alpha-hydroxylase/C17–20 lyase gene (Cyp17) by androgens. Mol Endocrinol 1997 11:87–96.
65. Houk CP, Pearson EJ, Martinelle N, Donahoe PK, Teixeira J. Feedback inhibition of steroidogenic acute regulatory protein expression in vitro and in vivo by androgens. *Endocrinology* 2004 145:1269–1275.
66. Eacker SM, Agrawal N, Qian K, Dichek HL, Gong EY, Lee K, Braun RE. Hormonal regulation of testicular steroid and cholesterol homeostasis. Mol Endocrinol 2008 22:623–635.
67. Simpson ER, Mahendroo MS, Means GD, Kilgore MW, Hinshelwood MM, Graham-Lorence S, Amarneh B, Ito Y, Fisher CR, Michael MD, et al. Aromatase cytochrome P450, the enzyme responsible for estrogen biosynthesis. Endocr Rev 1994 15:342–355.
68. Parker KL, Schimmer BP. Steroidogenic factor 1: a key determinant of endocrine development and function. Endocr Rev 1997 18:361–377.
69. Jorgensen JS, Nilson JH. AR suppresses transcription of the LHbeta subunit by interacting with steroidogenic factor-1. Mol Endocrinol 2001 15:1505–1516.
70. Lalli E, Sassone-Corsi P. DAX-1, an unusual orphan receptor at the crossroads of steroidogenic function and sexual differentiation. Mol Endocrinol 2003 17:1445–1453.
71. Ehrlund A, Anthonisen EH, Gustafsson N, Venteclef N, Robertson Remen K, Damdimopoulos AE, Galeeva A, Pelto-Huikko M, Lalli E, Steffensen KR, Gustafsson JA, Treuter E. E3 ubiquitin ligase RNF31 cooperates with DAX-1 in transcriptional repression of steroidogenesis. Mol Cell Biol 2009 29:2230–2242.
72. Jo Y, Stocco DM. Regulation of steroidogenesis and steroidogenic acute regulatory protein in R2C cells by DAX-1 (dosage-sensitive sex reversal, adrenal hypoplasia congenita, critical region on the X chromosome, gene-1). *Endocrinology* 2004 145:5629–5637.
73. Ahn SW, Gang GT, Kim YD, Ahn RS, Harris RA, Lee CH, Choi HS. Insulin directly regulates steroidogenesis via induction of the orphan nuclear receptor DAX-1 in testicular Leydig cells. J Biol Chem 2013 288:15937–15946.
74. Salvi R, Gomez F, Fiaux M, Schorderet D, Jameson JL, Achermann JC, Gaillard RC, Pralong FP. Progressive onset of adrenal insufficiency and hypogonadism of pituitary origin caused by a complex genetic rearrangement within DAX-1. *J Clin Endocrinol Metab* 2002 87:4094–4100.
75. Ponikwicka-Tyszko D, Kotula-Balak M, Jarzabek K, Bilinska B, Wolczynski S. The DAX1 mutation in a patient with hypogonadotropic hypogonadism and adrenal hypoplasia congenita causes functional disruption of induction of spermatogenesis. J Assist Reprod Genet 2012 29:811–816.
76. Saito S, Ito K, Suzuki T, Utsunomiya H, Akahira J, Sugihashi Y,

Niikura H, Okamura K, Yaegashi N, Sasano H. Orphan nuclear receptor DAX-1 in human endometrium and its disorders. Cancer Sci 2005 96:645–652.
77. Sasano H, Miki Y, Nagasaki S, Suzuki T. In situ estrogen production and its regulation in human breast carcinoma: from endocrinology to intracrinology. Pathol Int 2009 59:777–789.
78. Catalano S, Barone I, Giordano C, Rizza P, Qi H, Gu G, Malivindi R, Bonofiglio D, Ando S. Rapid estradiol/ERalpha signaling enhances aromatase enzymatic activity in breast cancer cells. Mol Endocrinol 2009 23:1634–1645.
79. Lanzino M, Maris P, Sirianni R, Barone I, Casaburi I, Chimento A, Giordano C, Morelli C, Sisci D, Rizza P, Bonofiglio D, Catalano S, Ando S. DAX-1, as an androgen-target gene, inhibits aromatase expression: a novel mechanism blocking estrogen-dependent breast cancer cell proliferation. Cell Death Dis 2013 4:e724.
80. Prins GS, Birch L, Couse JF, Choi I, Katzenellenbogen B, Korach KS. Estrogen imprinting of the developing prostate gland is mediated through stromal estrogen receptor alpha: studies with alphaERKO and betaERKO mice. Cancer Res 2001 61:6089–6097.
81. Jarred RA, Cancilla B, Prins GS, Thayer KA, Cunha GR, Risbridger GP. Evidence that estrogens directly alter androgen-regulated prostate development. *Endocrinology* 2000 141:3471–3477.
82. Ellem SJ, Schmitt JF, Pedersen JS, Frydenberg M, Risbridger GP. Local aromatase expression in human prostate is altered in malignancy. *J Clin Endocrinol Metab* 2004 89:2434–2441.
83. Ellem SJ, Risbridger GP. Aromatase and regulating the estrogen: androgen ratio in the prostate gland. J Steroid Biochem Mol Biol 2010 118:246–251.
84. Holter E, Kotaja N, Makela S, Strauss L, Kietz S, Janne OA, Gustafsson JA, Palvimo JJ, Treuter E. Inhibition of androgen receptor (AR) function by the reproductive orphan nuclear receptor DAX-1. Mol Endocrinol 2002 16:515–528.
85. Agoulnik IU, Krause WC, Bingman WE, 3rd, Rahman HT, Amrikachi M, Ayala GE, Weigel NL. Repressors of androgen and progesterone receptor action. J Biol Chem 2003 278:31136–31148.

J. Cell. Mol. Med. Vol XX, No X, 2015 pp. 1-11

A novel leptin antagonist peptide inhibits breast cancer growth *in vitro* and *in vivo*

Stefania Catalano [a,#], Antonella Leggio [a,#], Ines Barone [a], Rosaria De Marco [a], Luca Gelsomino [b], Antonella Campana [a], Rocco Malivindi [a], Salvatore Panza [a], Cinzia Giordano [c], Alessia Liguori [d], Daniela Bonofiglio [a], Angelo Liguori [a,†,*], Sebastiano Andò [a,c,†,*]

[a] *Department of Pharmacy, Health and Nutritional Sciences, University of Calabria, Arcavacata di Rende, CS, Italy*
[b] *Breast Center, Baylor College of Medicine, Houston, TX, USA*
[c] *Centro Sanitario, University of Calabria, Arcavacata di Rende CS, Italy*
[d] *Department of Medical Oncology, University of Messina, Messina, Italy*

Received: June 16, 2014; Accepted: November 7, 2014

Abstract

The role of the obesity cytokine leptin in breast cancer progression has raised interest in interfering with leptin's actions as a valuable therapeutic strategy. Leptin interacts with its receptor through three different binding sites: I–III. Site I is crucial for the formation of an active leptin–leptin receptor complex and in its subsequent activation. Amino acids 39-42 (Leu-Asp-Phe-Ile- LDFI) were shown to contribute to leptin binding site I and their mutations in alanine resulted in muteins acting as typical antagonists. We synthesized a small peptide based on the wild-type sequence of leptin binding site I (LDFI) and evaluated its efficacy in antagonizing leptin actions in breast cancer using *in vitro* and *in vivo* experimental models. The peptide LDFI abolished the leptin-induced anchorage-dependent and -independent growth as well as the migration of ERα-positive (MCF-7) and -negative (SKBR3) breast cancer cells. These results were well correlated with a reduction in the phosphorylation levels of leptin downstream effectors, as JAK2/STAT3/AKT/MAPK. Importantly, the peptide LDFI reversed the leptin-mediated up-regulation of its gene expression, as an additional mechanism able to enhance the peptide antagonistic activity. The described effects were specific for leptin signalling, since the developed peptide was not able to antagonize the other growth factors' actions on signalling activation, proliferation and migration. Finally, we showed that the LDFI pegylated peptide markedly reduced breast tumour growth in xenograft models. The unmodified peptide LDFI acting as a full leptin antagonist could become an attractive option for breast cancer treatment, especially in obese women.

Keywords: leptin • leptin receptor • leptin receptor modulators • breast cancer • peptides

Introduction

Carcinoma of the breast is the most common cancer among women in industrialized countries, and results in substantial morbidity and mortality. Breast carcinogenesis is thought to involve genetic predisposition, but modifiable factors such as overweight (body mass index, BMI 25–30 kg/m^2) or obesity (BMI >30 kg/m^2) conditions have also been reported to play an important role [1, 2]. Indeed, a number of epidemiological studies have suggested that obesity and high adipose tissue mass are associated with an increased risk of breast cancer development, as well as with an aggressive tumour phenotype and a poor survival [3–5]. Among obesity-related factors that are known to impact breast cancer development and progression, the adipose-derived adipokine leptin, whose synthesis and plasma levels increase proportionally to total adipose tissue mass [6, 7] has been extensively examined in this regard.

Leptin, a 16 kD polypeptide hormone encoded by the obese (*Ob*) gene, is a pleiotropic molecule that regulates food intake, hematopoiesis, inflammation, cell differentiation and proliferation, but it is also required for mammary gland development and tumourigenesis [8]. Both leptin and its receptor (ObR) are overexpressed in breast cancer, especially in higher grade tumours and are associated with distant metastasis [9, 10]. Genetically obese leptin-deficient Lep$^{ob/ob}$ and leptin receptor-deficient Lepr$^{db/db}$ mice do not develop mammary tumours which provide evidence that leptin and its receptor are

[†]Joint senior authors.
[#]These authors contributed equally to this work.
*Correspondence to: Sebastiano ANDÒ, and Angelo LIGUORI,
Department of Pharmacy, Health and Nutritional Sciences, University of Calabria, 87036 Arcavacata di Rende (CS), Italy.
Tel.: + 39 0984 496201/0984 493205
Fax: +39 0984 496203/ 0984 493107
E-mails: sebastiano.ando@unical.it; a.liguori@unical.it

doi: 10.1111/jcmm.12517

involved in breast tumourigenesis [11, 12]. In line with these observations, a growing body of evidence have shown that leptin is able to induce a variety of responses, such as mitogenesis, survival, transformation, migration and invasion in breast cancer cells [13–20] through the activation of several signalling pathways, such as those involving Janus kinase 2–signal transducer and activator of transcription 3 (JAK2-STAT3), mitogen-activated protein kinase (MAPK), and phosphatidylinositol 3-kinase-protein kinase B (PI3K-AKT) [21]. In addition to its direct action, we and other authors have demonstrated that leptin can exert its tumourigenic activities also interacting with different signalling molecules. Indeed, leptin signalling in human breast cancer cells enhances aromatase gene expression promoting *in situ* oestrogen production [22] and directly transactivates oestrogen receptor alpha (ERα) [17, 23]. It has also been reported an interplay between leptin signalling and the transmembrane tyrosine kinase receptor HER2, a member of epidermal growth factor receptor (EGFR) family [24–26]. Saxena *et al.* have demonstrated the existence of a bidirectional crosstalk between leptin and insulin-like growth factor I (IGF-I) signalling, mediated by synergistic transactivation of EGFR, which influences breast cancer cell invasion and migration [27]. Of note, we have demonstrated that leptin acting as a mediator of tumour /stroma interaction within tumour microenvironment may promote mammary carcinogenesis [8, 17].

Several potential therapeutic approaches able to inhibit leptin activity, especially in obese cancer patients, have been proposed. Antagonists to the leptin receptor are being developed both as mutants of the full protein and peptide fragments representing single receptor-binding site [20, 28–30]. In this regard, it has been previously demonstrated that inhibition of leptin signalling by a pegylated leptin peptide receptor antagonist (PEG-LPrA2), a short peptide corresponding to amino acids 70-95 of human leptin, resulted in decreased growth of mammary tumours derived from mice and humans [31–33]. Similar data were reported by another group using a different leptin antagonist, a 9 residue peptidomimetic named as Allo-aca. This peptide inhibits leptin-mediated proliferation and signalling *in vitro* and exhibits anti-neoplastic activities *in vivo* [34, 35].

In this study, we have generated a novel peptide, LDFI, corresponding to amino acid residues 39-42 from one of the putative sites of interaction of leptin with its receptor. Our results have shown that LDFI inhibits leptin-induced proliferation and motility as well as leptin signalling activation in both ERα-positive and ERα-negative human breast cancer cells. Furthermore, the peptide markedly reduces breast tumour growth in xenograft models.

Materials and methods

Reagents and antibodies

DMEM, McCoy's 5A Medium, L-Glutamine, penicillin, streptomycin, bovine serum albumin (BSA), phosphate-buffered saline, TRIzol, 100 bp DNA ladder were purchased from Invitrogen (Carlsbad, CA, USA). TaqDNA polymerase was provided by Promega (Madison, WI, USA). The RETROscript kit and DNase I were purchased from Ambion (Austin, TX, USA). Aprotinin, leupeptin, phenylmethylsulfonyl fluoride, sodium orthovanadate, formaldehyde, NP-40, MTT, dimethyl sulphoxide, proteinase K, leptin and epidermal growth factor (EGF) by Sigma-Aldrich (Milan, Italy).

Cyclin D1, GAPDH, total Akt and phosphorylated pAkt (Ser^{437}), Ki-67 antibodies were from Santa Cruz Biotechnology (Santa Cruz, CA, USA). Total ERK1,2/MAPK, JAK2, STAT3 and phosphorylated p42/44 ERK1,2/MAPK (Thr^{202}/Tyr^{204}), JAK2 ($Tyr^{1007/1008}$), STAT3 (Tyr^{705}) were from Cell Signaling Technology (Beverly, MA, USA).

Peptide synthesis

The peptides were synthesized by solid phase methods using reagent systems and methodologies of standard Fmoc-chemistry [36, 37]. Fmoc-L-Asp-(OtBu)-OH, Wang resin, diisopropylethylamine (DIPEA), trifluoroacetic acid (TFA) and triisopropylsilane (TIS) were purchased from Sigma-Aldrich. All other Fmoc-protected amino acids (Fmoc-L-AA-OH) were prepared from the corresponding α-amino acids and 9-fluorenylmethyloxycarbonyl chloride [38]. O-Benzotriazole-*N,N,N′,N′*-tetramethyluronium-hexafluoro-phosphate (HBTU) was purchased from Matrix Innovation.

For the synthesis of polyethylene glycol (PEG)-attached peptide was used TentaGel® PAP Resin (Rapp Polymere GmbH, Tuebingen, Germany), a polystyrene/DVB matrix with amine terminated polyethylene oxide attached *via* a cleavable linkage with TFA. Dichloromethane (DCM), *N,N*-dimethylformamide (DMF), *N*-methylpyrrolidone (NMP), diethyl ether, formic acid (FA), HPLC grade water and acetonitrile were obtained by VWR.

The peptides were characterized by NMR spectroscopy and LC/MS analysis. Electrospray ionization source-quadrupole time of flight (ESI-QTOF) mass spectra and ^{1}H NMR and ^{13}C NMR spectra identified correct and pure samples (more details in Data S1).

ESI-QTOF mass spectra were recorded on a Agilent 6540 Q-TOF mass spectrometer

^{1}H NMR and ^{13}C NMR spectra were recorded on a Bruker Avance 300 spectrometer using DMSO-d_6 as solvent. Chemical shifts (δ) are reported in units of parts per million (ppm) and all coupling constants (J) are reported in hertz (Hz). LC-MS analysis was carried out using a UHPLC instrument coupled to a QTOF mass spectrometer fitted with a ESI operating in positive ion mode. Chromatographic separation was achieved using a C18 RP analytical column (Eclipse Plus C18, 50 × 2.1 mm, 1.8 μm) at 50°C with a elution gradient from 5% to 50% of B over 15 min., A being H_2O (0.1% FA) and B CH_3CN (0.1% FA). Flow rate was 0.5 ml/min.

Standard microwave synthesis protocol: the peptide chain assembly was made on a CEM-Liberty microwave-assisted automated synthesizer. The resin was swollen in DMF for 30 min. before use. Coupling reactions were performed in DMF with fivefold excess of Fmoc-AA-OH in the presence of HBTU (5.0 equivalents) and DIPEA (10 equivalents) for 5 min. at 75°C. The Fmoc protecting group was removed by treatment of the resin with a 20% solution of piperidine in DMF (v/v) (7 ml). Deprotection was performed in two stages with an initial deprotection of 30 sec. followed by 3 min. at 75°C. Between each step the resin was washed thoroughly with DMF. The completed peptide was washed with DMF and DCM. The peptide was cleaved from the resin using a mixture of TFA, water, and TIS (9.5/0.25/0.25 by volume) for 30 min. at 38 °C. Following cleavage the peptide was precipitated and washed with diethyl ether.

LDFI peptide

ESI-QTOF-MS: 507.2814 $(M+H)^+$, 529.2636 $(M+Na)^+$, 545.2367 $(M+K)^+$.
ESI-QTOF-MS: calcd for $C_{25}H_{39}N_4O_7^+$ 507.2813, found 507.2814.

Scramble peptide LLLA

ESI-QTOF-MS: 429.3078 $(M+H)^+$, 451.2899 $(M+Na)^+$, 467.2576 $(M+K)^+$.
ESI-QTOF-MS: calcd for $C_{21}H_{41}N_4O_5^+$ 429.3071, found 429.3078.

LDFI-PEG peptide

LDFI-PEG peptide was characterized by LC-ESI-QTOF-MS analysis which shows that the peptide LDFI is linked to PEG. The chromatogram shows a peak eluting at 3.21 min. that comprises a mass of 626.3514 with $z = 2$. The MS/MS spectrum of the peak at 3.21 min. (m/z 626.3514, $z = 2$) confirmed the structure of an adduct between LDFI and PEG.

ESI-QTOF MS/MS: (626.3514; z = 2): 376.1824 (b_3- H_2O), 229.1173 (b_2), 86.0963 (L,I).

Cell cultures

The human breast cancer cell lines MCF-7 and SKBR3 were acquired from American Type Culture Collection (Manassas, VA, USA) where they were authenticated, stored according to supplier's instructions, and used within a month after frozen aliquots resuscitations. MCF-7 cells were cultured in DMEM medium supplemented with 10% foetal bovine serum (FBS; Invitrogen), 2 mmol/l L-glutamine, and 50 units/ml penicillin/streptomycin. SKBR3 cells were cultured in McCoy's 5A Medium modified containing 10% FBS, 1% L-glutamine, 1% Eagle's nonessential amino acids, and 1 mg/ml penicillin-streptomycin. Before each experiment, cells were grown in phenol red-free medium, containing 5% charcoal-stripped FBS for 2 days and treated as described.

Cell proliferation assays

MTT anchorage-dependent growth assays

Cell viability was determined using the 3-(4,5-dimethylthiazol-2-yl)-2,5-diphenyltetrazolium (MTT) assay as described previously [39]. Results are representative of at least three independent experiments and expressed as the absorbance readings at 570 nm.

Soft agar anchorage-independent growth assays

Cells (10^4/well) were plated in 4 ml of 0.35% agarose with 5% charcoal stripped-FBS in phenol red-free media, with a 0.7% agarose base in six well plates. Two days after plating, media containing vehicle or treatments, as indicated, were added to the top layer and replaced every 2 days. After 14 days, colonies were counted as described [40]. Data shown are the mean colony numbers of three independent experiments each performed in triplicate.

Wound-healing migration assays

Motility was assessed as described previously [17]. Briefly, cell monolayers were scraped and cells were treated as indicated. Closure of the wound was monitored over 24 hrs, cells were then fixed and stained with Comassie Brillant Blue. Pictures were taken at 10× magnifications using phase-contrast microscopy and are representative of three independent experiments.

Transmigration assays

Cells treated as indicated were placed in the upper compartments of Boyden chamber (8-μm membranes; Corning Costar, NY, USA). Bottom well contained regular full media. After 24 hrs, migrated cells were fixed and stained with Coomassie brilliant blue. Migration was quantified by viewing 5 separate fields per membrane at 20× magnification and expressed as the mean number of migrated cells. Data represent 3 independent experiments assayed in triplicate.

Reverse transcription-PCR and real-time RT-PCR assays

The gene expression of Ob (leptin) and 36B4 was evaluated by reverse transcription PCR (RT-PCR) method as previously described [41], using the following primers: 5′-GAGACCTCCTCCATGTGCTG-3′ (Ob forward) and 5′-TGAGCTCAGATATCGGGCTGAAC-3′ (Ob reverse), 5′-CTCAACATCTCCCCCTTCTC-3′ (36B4 forward) and 5′-CAAATCCCATATCCTCGT-3′ (36B4 reverse). Negative control contained water instead of first strand cDNA was used.

The gene expression of the long and short leptin receptor isoforms (ObRL/ObRsh), VEGF receptor (VEGFR) was assessed by real-time RT-PCR, using SYBR Green Universal PCR Master Mix (Bio-Rad, Hercules, CA, USA). Each sample was normalized on GAPDH mRNA content. Primers used for the amplification were: forward 5′-ATTGTGCCAGTAATTATT TCCTCTTCC-3′ and reverse 5′-CCACCATATGTTAAC TCTCAGAAGTTCAA-3′ (ObRl), forward 5′-GATAGA GGCCCAGGCATTTTTTA-3′ and reverse 5′-ACACCACTCTCTCTCTTTTTGATTGA-3′ (ObRs), forward 5′-CTTCGAAGCATCAGCATAAGAAACT-3′ and reverse 5′-TGGTCAGCC CACTGGAT-3′ (VEGFR), forward 5′-CCCACTCCTCCACCTTTGAC-3′ and reverse 5′-TGTTGCTGTAGCCAA ATTCGT T-3′ (GADPDH). The relative gene expression levels were normalized to a calibrator that was chosen to be the basal, vehicle-treated sample. Final results were expressed as n-fold differences in gene expression relative to GAPDH rRNA and calibrator, calculated using the ΔΔCt method as follows: n-fold $= 2^{-(\Delta Ctsample - \Delta Ctcalibrator)}$, where ΔCt values of the sample and calibrator were determined by subtracting the average Ct value of the GAPDH rRNA reference gene from the average Ct value of the different genes analyzed.

Immunoblotting analysis

Whole-cell lysates were prepared as previously described [42]. Protein extracts from tumour tissues were prepared as previously described [43]. Equal amounts of total protein were resolved on 11% SDS-PAGE as indicated [44]. Blots shown are representative of at least three independent experiments.

Tumour xenografts

In vivo studies were conducted in 45-day-old female nude mice (nu/nu Swiss). Mice were inoculated with exponentially growing SKBR3 cells (5.0×10^6 per mouse) in 0.1 ml of matrigel (BD Biosciences, Bedford, MA, USA) into the intrascapular region. Once tumours reached an approximate volume of 100 mm^3 5 mice/group were randomly allocated

Journal of Cellular and Molecular Medicine published by John Wiley & Sons Ltd and Foundation for Cellular and Molecular Medicine.

into three groups. The mice were then treated with LDFI-PEG (1 and 10 mg/kg/day) diluted in saline 0.3% BSA or saline 0.3% BSA only (control) by i.p. injection. The treatment was done for 5 days a week until the 4th week. All animals were maintained and handled in accordance with the recommendation of the Guidelines for the Care and Use of Laboratory Animals and were approved by the Animal Care Committee of University of Calabria. Tumour development was followed twice a week by caliper measurements along two orthogonal axes: length (L) and width (W). The volume (V) of tumours was estimated by the following formula: $V = L (W_2)/2$. Relative tumour volume (RTV) was calculated from the following formula: RTV = (Vx/V1), where Vx is the tumour volume on day X and V1 is the tumour volume at initiation of the treatment. Growth curve was obtained by plotting the mean volume of RTV on Y axis against time (X axis expressed as days after starting of treatment). Antitumour activity was evaluated according to tumour growth inhibition, calculated from the following formulae: percent $GI = 100 - (RTVt/RTVc) \times 100$, where RTVt is the medium RTV of treated mice and RTVc is the median RTV of controls, both at a given time-point when the antitumour effect was optimal. At the time of killing, tumours were dissected out from the neighboring connective tissue, frozen and stored in nitrogen for further analysis.

Histopathological analysis

Tumours, livers, lungs, spleens, and kidneys were fixed in 4% formalin, sectioned at 5 μm, and stained with hematoxylin and eosin Y, as suggested by the manufacturer (Bio-Optica, Milan, Italy).

Immunohistochemical analysis

Paraffin embedded sections, 5 μm thick, were mounted on slides precoated with poly-lysine, and then they were deparaffinised and dehydrated (7–8 serial sections). Immunohistochemical experiments were performed with rabbit polyclonal Ki-67 primary antibody at 4°C overnight. Then, a biotinylated goat-anti-rabbit IgG was applied for 1 hr at room temperature, followed by the avidin biotin-horseradish peroxidase complex (ABC/HRP; Vector Laboratories, CA, USA). Immunoreactivity was visualized using the diaminobenzidine chromogen (DAB) (Sigma-Aldrich). Counterstaining was carried out with methylene-blue (Sigma-Aldrich). The primary antibody was replaced by normal rabbit serum in negative control sections.

Statistical analysis

Data were analyzed for statistical significance ($P < 0.05$) using a two-tailed student's Test, performed by Graph Pad Prism 4. Standard deviations (SD) are shown.

Results

Design and synthesis of Peptide LDFI

Leptin, whose structure consists of 4 α helices (A-D helices), binds its receptor through three binding sites (I, II and III) [45]. The amino acid sequence 39-42, located in the loop that connects helices A and B, is essential for activation of the leptin receptor and represents the main target region that can be modified for obtaining ObR antagonists. Mutations of some or all of these amino acids to Ala in human and ovine leptin do not change their binding properties, but they abolish their biological activity and converts the muteins into potent antagonists [46, 47]. In this context and considering that the subsequence 39-42 represents a key residue in the activation of leptin-receptor complex, we designed and synthesized the small peptide derived from the wild-type sequence 39-42 of leptin Leu-Asp-Phe-Ile (LDFI). The tetrapeptide designed mimics the sequence of leptin binding site I, involved in the interaction with CRH2 (cytokine receptor homology domain) from the ObR and therefore in its activation. The tetrapeptide was synthesized by solid phase peptide synthesis, using Fmoc-chemistry. A 'scramble' tetrapeptide consisting of a random sequence of amino acids was also synthesized. Specifically the tetrapeptide Leu-Leu-Leu-Ala was prepared and its biological activity was tested by performing the same biological tests carried out for the tetrapeptide LDFI. The tetrapeptide was also synthesized in the pegylated form (LDFI-PEG). For this purpose the PEG was introduced through an amidic bond on the C-terminal amino acid, using a PEG with an amine linker.

Peptide LDFI inhibits leptin-induced cell growth and motility in breast cancer cells

First, we tested the biological activity of the peptide LDFI on anchorage-dependent cell proliferation using as experimental models ObR-positive and leptin-sensitive MCF-7 (ERα-positive) and SKBR3 (ERα-negative) breast cancer cells. Both MCF-7 and SKBR3 cells were treated with the peptide at increasing concentrations (10 nM, 100 nM, 1 μM and 10 μM) for 96 hrs. The peptide did not interfere with cell proliferation in the absence of leptin and did not produce any significant cytotoxic effects at all the doses tested (Fig. 1A).

Next, we explored the ability of peptide LDFI to interfere with leptin-induced cell proliferation (Fig. 1B). As expected, in both cell lines treatment with leptin (500 ng/ml) increased cell proliferation. The peptide LDFI at 10 nM–1 μM concentrations significantly reversed the leptin-induced cell growth in a dose-dependent manner. The ability of peptide LDFI to inhibit leptin-mediated cell growth was also evaluated using anchorage-independent growth assays, which better reflect *in vivo* three-dimensional tumour growth (Fig. 1C). The peptide significantly reduced the increase in colony numbers induced by leptin in MCF-7 and SKBR3 cell lines. In contrast, a scramble peptide (S), consisting of a random sequence of amino acids, used as a negative control, showed no leptin antagonistic properties. Data from growth assays were well correlated with a reduction in leptin-induced expression of Cyclin D1, a well known marker for cell proliferation, in cells treated with the peptide (Fig. 1D).

Moreover, we assessed, in MCF-7 and SKBR3 cells, the ability of the peptide to inhibit cell motility induced by leptin in wound-healing scratch assays. As shown in Figure 2A, both cell lines moved the farthest in eitheir directions to close the 'gap' following

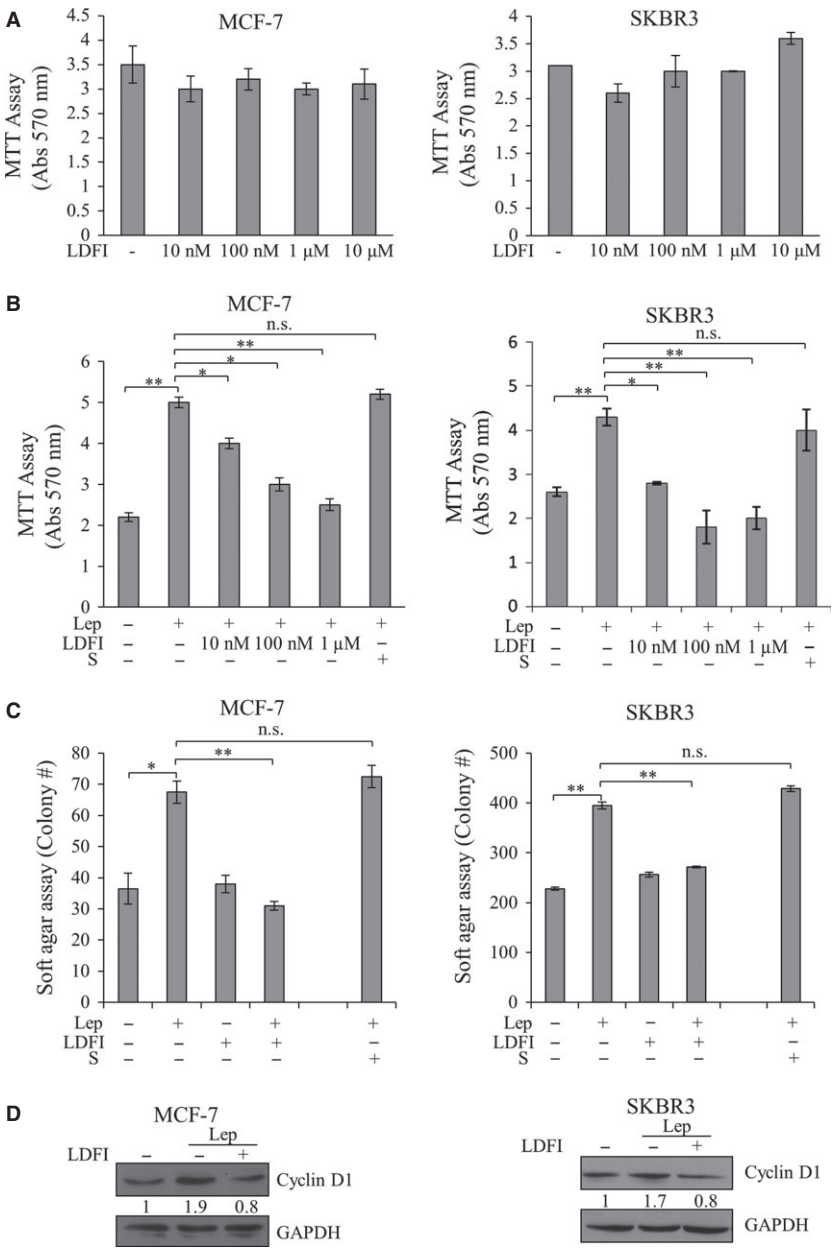

Fig. 1 Effects of peptide LDFI on leptin-induced breast cancer cell proliferation. (**A**) MTT growth assays in MCF-7 and SKBR3 breast cancer cells treated with vehicle (-) or increasing doses of peptide LDFI (10 nM, 100 nM, 1 μM, 10 μM) for 96 hrs. (**B**) MTT growth assays in MCF-7 and SKBR3 cells treated with vehicle (-), leptin (Lep, 500 ng/ml), with or without peptide LDFI (10 nM, 100 nM, 1 μM) for 96 hrs. A scramble peptide (S, 1 μM) was used as negative control. (**C**) Soft agar anchorage-independent growth assays in MCF-7 and SKBR3 cells treated with vehicle (-), leptin (Lep, 500 ng/ml), alone or in combination with peptide LDFI (1 μM) or a scramble peptide (S, 1 μM). n.s. non-significant; $*P < 0.05$, $**P < 0.01$. (**D**) Immunoblotting for Cyclin D1 expression in MCF-7 and SKBR3 cells treated for 24 hrs with vehicle (-), leptin (500 ng/ml) with or without peptide LDFI (1 μM). GAPDH was used as control of equal loading and transfer. Numbers below the blots represent the average fold change in Cyclin D1/GAPDH ratio relative to vehicle-treated cells.

leptin treatment compared to vehicle control conditions. Pretreatment with peptide LDFI counteracted leptin effects on cell motility. Then, the capacity of cells to migrate across uncoated membrane in transmigration assays was tested in the presence of leptin and peptide LDFI (Fig. 2B). Leptin increased the number of migrated cells in both cell lines and again pretreatment with peptide LDFI resulted in a clear reduction in leptin-induced cell motility. In both wound-healing scratch and transmigration assays the exposure to the scramble peptide (S) did not influence leptin-induced effects on MCF-7 and SKBR3 cells (Fig. 2A and B).

Peptide LDFI blocks leptin signalling pathways

Leptin exerts its biologic function through binding to its receptor which mediates a downstream signal by activating multiple signalling pathways. Thus, we conducted time-course studies to examine the effects of peptide LDFI on phosphorylation of the major leptin signalling molecules, that are known to mediate proliferation and motility in breast cancer cells, using immunoblot analysis (Fig. 3A). As expected, in MCF-7 and SKBR3 cells, leptin treatment induced phosphorylation of JAK2/STAT3, AKT and MAPK, whereas pretreatment

Journal of Cellular and Molecular Medicine published by John Wiley & Sons Ltd and Foundation for Cellular and Molecular Medicine.

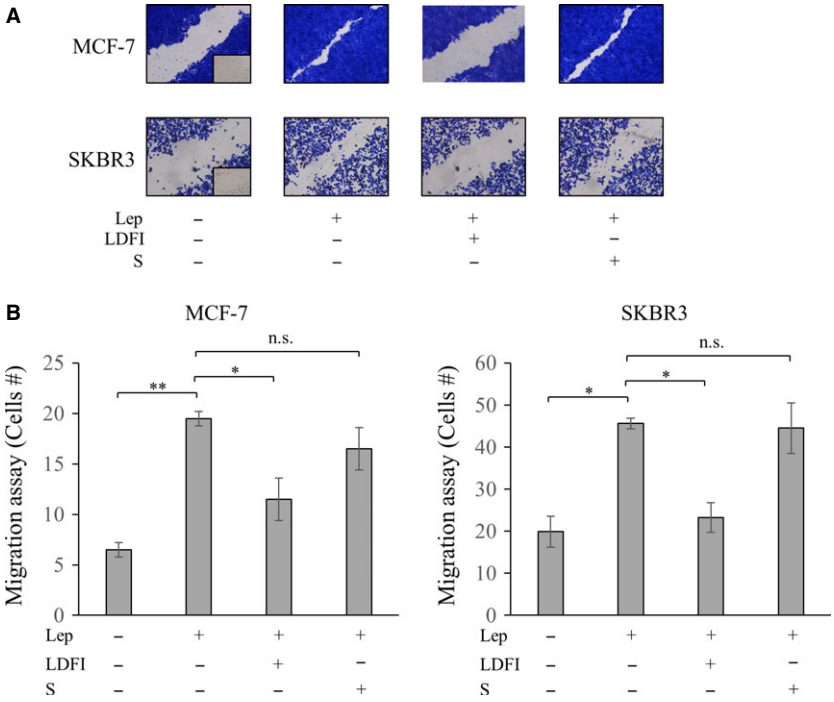

Fig. 2 Peptide LDFI inhibits leptin-induced cell motility. (**A**) MCF-7 and SKBR3 breast cancer cells were subjected to wound-healing migration assays with images captured at 0 and 24 hrs after incubation with vehicle (-), leptin (Lep, 500 ng/ml) alone or in combination with peptide LDFI (1 μM) or a scramble peptide (S, 1 μM) using phase-contrast microscopy. Small squares, time 0. (**B**) Transmigration assays in MCF-7 and SKBR3 cells treated as in A. n.s. non-significant; $*P < 0.05$, $**P < 0.005$.

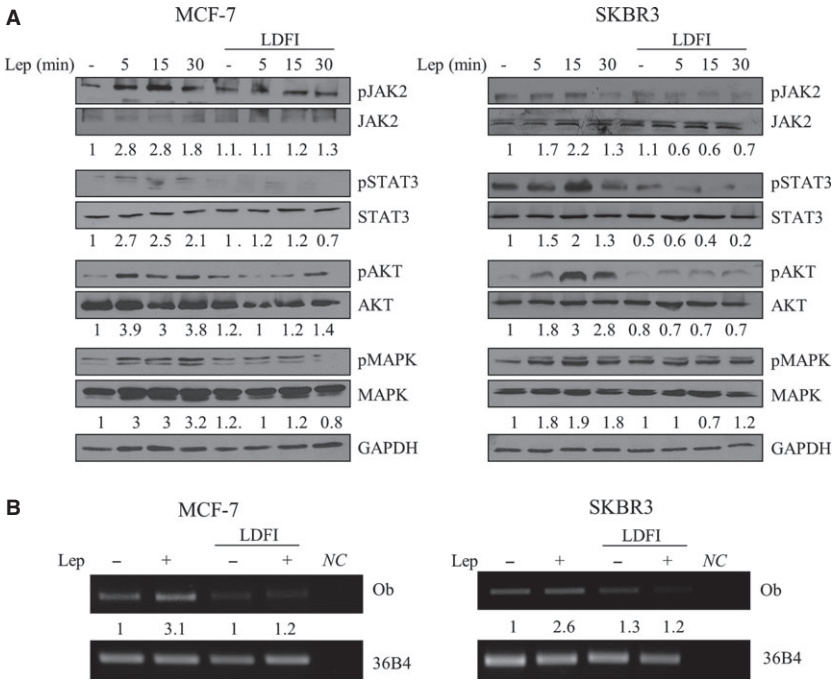

Fig. 3 Peptide LDFI antagonizes leptin signalling activation. (**A**) Immunoblotting of phosphorylated (p) JAK2, STAT3, AKT, MAPK and total proteins from cells treated with vehicle (-), leptin (Lep, 500 ng/ml for 5, 15 and 30 min.) with or without peptide LDFI (1 μM). GAPDH was used as control of equal loading and transfer. Numbers below the blots represent the average fold change in phospho-proteins/total proteins/GAPDH ratio relative to vehicle-treated cells. (**B**) RT-PCR for leptin (Ob) and 36B4 (internal standard) mRNA expression in cells treated for 24 hrs with vehicle (-), leptin (Lep, 500 ng/ml) with or without peptide LDFI (1 μM). Numbers represent the average fold change in Ob/36B4 levels relative to vehicle-treated cells. NC, negative control.

with peptide LDFI completely abrogated the leptin activation of these signalling pathways.

Since we have previously demonstrated that leptin was able to up-regulate its own gene expression [48], we investigated whether LDFI could also counteract this effect. RT-PCR analysis showed that the levels of the Ob gene increased by leptin were strongly reduced in the presence of the peptide in both breast cancer cells (Fig. 3B). Moreover, we examined by real time PCR the expression of OBRL, OBRsh

and VEGFR that are well-known leptin-induced genes. As expected, treatment with peptide LDFI was able to reverse the stimulatory effects induced by leptin on these genes (Fig. S1).

Specifity of peptide LDFI in antagonizing leptin effects

To test if LDFI action was specific for leptin effects, cell biological assays were performed in cells treated with a molecule able to elicit cellular responses through a different mechanism from leptin, such as EGF. Thus, we investigated, in MCF-7 and SKBR3 cell lines pre-treated with LDFI, the effect of short-term stimulation with EGF (100 ng/ml) on phosphorylation levels of AKT and MAPK, the main downstream effectors of the growth factor signalling. The enhanced AKT and MAPK phoshorylation observed after treatment with EGF was not affected by the peptide (Fig. 4A). In addition, data obtained from MTT growth assays (Fig. 4B) and wound-healing scratch assays (Fig. 4C) revealed that LDFI treatment did not reverse EGF-induced cell growth and motility.

Efficacy of LDFI-PEG treatment in breast cancer xenograft models

As a final step of this study, we assessed the therapeutic potential of the novel ObR antagonist LDFI by evaluating the efficacy of the peptide in mouse xenograft models. To this aim, we developed a pegylated leptin receptor antagonist (LDFI-PEG) to increase the peptide bioavailability. Pegylation may result in improved *in vivo* potency related to a better stability, greater protection against proteolytic degradation and lower clearance. After verifying the structure and the purity of LDFI-PEG, we tested its effects on cell growth and motility in MCF-7 and SKBR3 cells (Fig. S2A and B). The LDFI-PEG peptide showed comparable biological activity with native LDFI in inhibiting leptin-induced cell proliferation and migration in both cell lines.

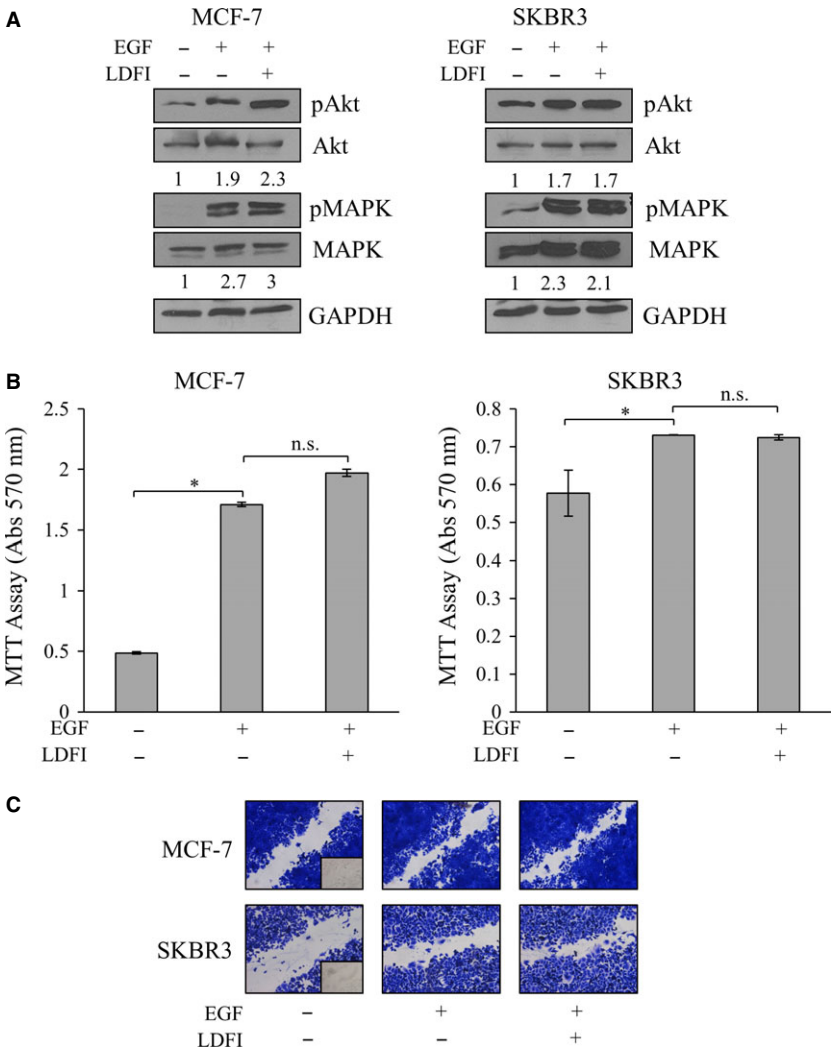

Fig. 4 LDFI effects are specific for leptin signalling. (**A**) Immunoblotting of phosphorylated (p) AKT, MAPK and total proteins from cells treated with vehicle (-), EGF (100 ng/ml, for 5 min.) with or without peptide LDFI (1 μM). GAPDH was used as control of equal loading and transfer. Numbers below the blots represent the average fold change in phosphoproteins/total proteins/GAPDH ratio relative to vehicle-treated cells. (**B**) MTT growth assays in MCF-7 and SKBR3 cells treated with vehicle (-), EGF (100 ng/ml) alone or in combination with peptide LDFI (1 μM) for 96 hrs. ns, non-significant, $*P < 0.05$. (**C**) Cells were subjected to wound-healing migration assays with images captured at 0 and 24 hrs after incubation with vehicle (-), EGF (100 ng/ml) with or without peptide (LDFI, 1 μM) using phase-contrast microscopy. Small squares, time 0.

Journal of Cellular and Molecular Medicine published by John Wiley & Sons Ltd and Foundation for Cellular and Molecular Medicine.

Therefore, we then used the SKBR3 orthotopic xenograft model to examine the effects of peptide LDFI-PEG on tumour growth *in vivo*. We injected SKBR3 breast cancer cells into the intrascapular region of female nude mice and followed tumour growth after administration of LDFI-PEG at 1 and 10 mg/kg/day. As SKBR3 cells can produce endogenous leptin, exogenous leptin was not inoculated into the mice. LDFI-PEG was not toxic and did not affect the energy balance since no change in body weight or in food and water consumption was observed. In addition, no significant differences in the mean weights or histological features of the major organs (liver, lung, spleen and kidney) after sacrifice were observed between vehicle-treated mice and those that received treatment.

Tumour volume was measured from the first day of treatment and the RTV was calculated as described in details in Materials and Methods. As shown in Figure 5A, after LDFI-PEG treatment tumour volumes continued to reduce over control for the duration of experiment. Particularly, at the end of treatment (28 days) we observed that both dosages of PEG-LDFI induced a significant tumour growth inhibition (44% and 74.7% respectively) compared to vehicle-treated mice, although to a higher extent after treatment with 10 mg/kg/day. To determine whether the reduction in breast tumour growth induced by treatment with PEG-LDFI was associated with any changes in the mitotic index, we evaluated in tumours the expression of Ki-67 as a marker of proliferation. Sections of tumours from PEG-LDFI-treated mice exhibited a dose-dependent reduction in the expression of Ki-67 compared with that in tumours from vehicle-treated mice (Fig. 5B). In addition, immunoblot analysis revealed that the phosphorylation levels of STAT3, MAPK and AKT were significantly lower in SKBR3 xenograft tumours from mice treated with LDFI-PEG than in tumours from vehicle-treated controls (Fig. 5C).

Discussion

The critical role played by leptin in mammary tumourigenesis has generated a great interest in the design and development of several leptin signalling modulators that could interfere with the action of leptin and thereby prevent or delay breast cancer development and progression. The most important issue in modulating leptin pathways is to achieve target specificity since this adipokine does not only influence cancer tissues, but it is implicated in a wide spectrum of physiological processes in peripheral organs as well as in the central nervous system.

Biological actions of leptin are mediated through binding to the extracellular domain of specific leptin receptor (ObR) present in a variety of tissues and localized to the cell membranes. It has been reported that the structure of leptin resembles four alpha-helix bundle cytokines and ObR is a member of the class I cytokine receptor family. The ObR, encoded by *db* gene, includes six isoform (ObR_{a-f}), resulting from alternative splicing: the long isoform with full intracellular signalling capabilities and shorter isoforms with less biological activities. The large extracellular domain of ObR (816 amino

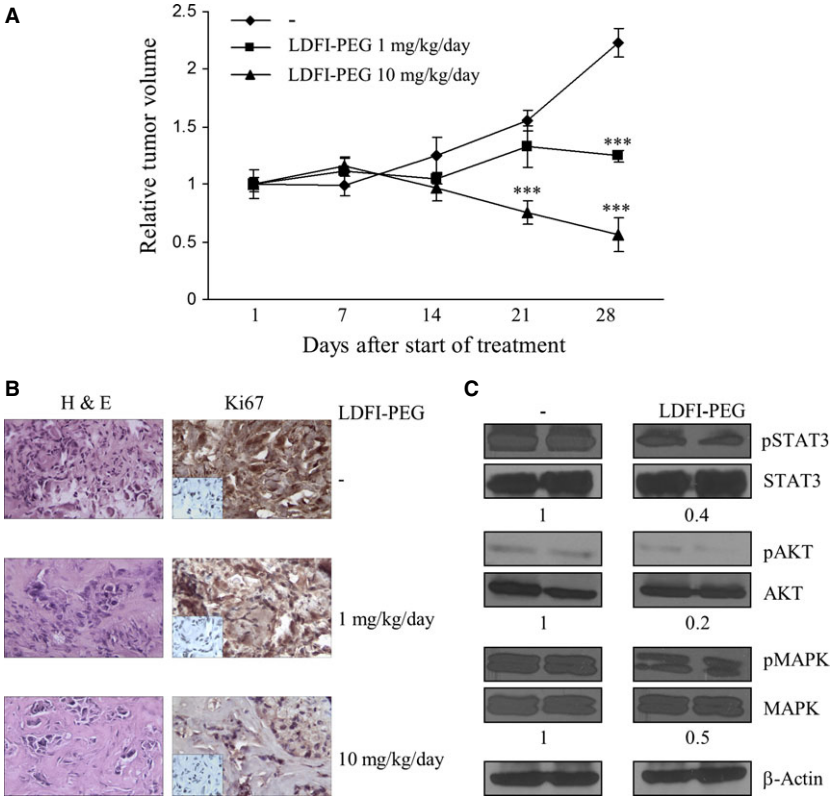

Fig. 5 Impact of LDFI-PEG treatment on tumour growth of SKBR3 xenografts. (**A**) SKBR3 cells were inoculated into the intrascapular region of female nude mice (15 mice) and then treated 5 days a week with vehicle (-) or peptide PEG-LDFI (1 and 10 mg/kg/day) by intraperitoneal injection for 28 days (5 mice each group). Relative tumour volume (RTV) was calculated from the following formula: RTV= (Vx/V1), where Vx is the tumour volume on day X and V1 is the tumour volume at initation of the treatment (day 1). ***$P < 0.0001$. (**B**) Haematoxylin and eosin, Ki-67 staining of tumour sections from vehicle (-) and LDFI-PEG treated mice. Small squares, negative control. (**C**) Immunoblotting of phosphorylated (p) STAT3, AKT, MAPK and total proteins from tumours excised from vehicle (-) and LDFI-PEG treated mice (10 mg/kg/day). β-actin was used as control of equal loading and transfer. Numbers below the blots represent the average fold change in phospho-proteins/total proteins/β-actin ratio relative to vehicle-treated mice.

acids) is common to all ObR isoforms, and the variable length cytoplasmic tail (300 amino acids residues) distinguished the several isoforms [21, 49]. Leptin interacts with its receptor through three potential binding sites. Binding site I is located around leptin residue 40, the bivalent site II consists of a leptin domain around the N-terminus (aa 3–21) and another in the middle (aa 70–93), and site III is positioned at the leptin's C terminus (aa 110–142) [45]. Even though the three-dimensional structure of leptin was elucidated a few years after its discovery [50], the crystallographic structure of leptin-leptin receptor complex has not been reported yet. Until today, all data available are based on theoretical models [45, 51] from which it is clear that the amino acid sequence 39-42, located in the loop that connects helices A and B, constitutes a key sequence in the leptin-receptor-binding site. Several groups have developed short leptin fragments containing specific ObR interacting domains that demonstrated antineoplastic activity both *in vitro* and *in vivo* cancer models [31–35].

Here, we generated a four amino acids peptide corresponding to leptin wild-type sequence 39-42 that plays a crucial role in the activation of ObR. Our results showed that the novel ObR antagonist peptide LDFI inhibits the leptin-induced anchorage-dependent and -independent growth as well as migration in both ERα-positive and -negative breast cancer cells without exhibiting any partial agonistic activity in the absence of leptin. The anti-tumour action of LDFI was associated with the inhibition of several leptin-induced pathways such as JAK2, STAT3, AKT and MAPK and a reduction in Cyclin D1 expression. Interestingly, we demonstrated the ability of the peptide LDFI to reverse the leptin-mediated up-regulation of its own gene expression underlying how this peptide negatively interferes in the short autocrine loop maintained by leptin on Ob gene in breast cancer cells. The described effects were specific for leptin signalling since the developed peptide was not able to antagonize the other growth factor's actions on signalling activation, proliferation and migration.

To assess the clinical utility of our leptin antagonist against human breast cancer progression, we tested LDFI effects in SKBR3 xenografts implanted in female nude mice. Because the peptide normally would have a relatively short biological half-life, we pegylated it to increase its bioavailability and potentiate its effects. Indeed, covalent modification with high molecular weight PEG chains is a very efficient method for improving the pharmacokinetics of biomolecules [52] and has been shown to increase the half-life of wild-type leptin [53–55]. Several PEG-conjugated medications have proven to be superior to their unmodified parent molecules and they are now widely used in clinical practice [56, 57]. A significant growth reduction in SKBR3 xenografts was found after LDFI-PEG treatment. Moreover, we observed in tumour sections from LDFI-treated mice a marked decrease in the expression of the nuclear proliferation antigen Ki-67 as well as in the phosphorylation levels of leptin downstream effectors. Importantly, in mice, LDFI produced no signs of systemic toxicity and did not affect the energy balance. Indeed, no significant effects on body weight were found between vehicle-treated and LDFI-PEG-treated mice.

Overall, our data demonstrate that LDFI may represent a novel leptin receptor antagonist able to reduce breast cancer progression both *in vitro* and *in vivo*, suggesting its potential use in the treatment of breast cancer, especially in obese women.

Acknowledgements

This work was supported by Associazione Italiana Ricerca sul Cancro (AIRC) grant IG 11595 and by QUASIORA project funded by Calabria Region. Reintegration AIRC/Marie Curie International Fellowship in Cancer Research to IB.

Conflicts of interest

The authors declare no conflicts of interest.

Supporting information

Additional Supporting Information may be found in the online version of this article:

Figure S1 LDFI effects on leptin-induced genes.

Figure S2 LDFI-PEG effects on breast cancer cell growth and motility.

Data S1 Table of content of NMR (S2-S5) and RP U-HPLC/MS (S6-S8) analyses of the peptides used in the present study.

References

1. **Calle EE, Kaaks R.** Overweight, obesity and cancer: epidemiological evidence and proposed mechanisms. *Nat Rev Cancer*. 2004; 4: 579–91.
2. **Calle EE, Rodriguez C, Walker-Thurmond K, *et al.*** Overweight, obesity, and mortality from cancer in a prospectively studied cohort of U.S. adults. *N Engl J Med*. 2003; 348: 1625–38.
3. **Harvie M, Hooper L, Howell AH.** Central obesity and breast cancer risk: a systematic review. *Obes Rev*. 2003; 4: 157–73.
4. **Lahmann PH, Hoffmann K, Allen N, *et al.*** Body size and breast cancer risk: findings from the European Prospective Investigation into Cancer And Nutrition (EPIC). *Int J Cancer*. 2004; 111: 762–71.
5. **Michels KB, Terry KL, Willett WC.** Longitudinal study on the role of body size in premenopausal breast cancer. *Arch Intern Med*. 2006; 166: 2395–402.
6. **Considine RV, Sinha MK, Heiman ML, *et al.*** Serum immunoreactive-leptin concentrations in normal-weight and obese humans. *N Engl J Med*. 1996; 334: 292–5.
7. **Maffei M, Halaas J, Ravussin E, *et al.*** Leptin levels in human and rodent: measurement of plasma leptin and ob RNA in obese and weight-reduced subjects. *Nat Med*. 1995; 1: 1155–61.
8. **Ando S, Catalano S.** The multifactorial role of leptin in driving the breast cancer microenvironment. *Nat Rev Endocrinol*. 2011; 8: 263–75.

Journal of Cellular and Molecular Medicine published by John Wiley & Sons Ltd and Foundation for Cellular and Molecular Medicine.

9. **Ishikawa M, Kitayama J, Nagawa H.** Enhanced expression of leptin and leptin receptor (OB-R) in human breast cancer. *Clin Cancer Res*. 2004; 10: 4325–31.
10. **Garofalo C, Koda M, Cascio S, *et al.*** Increased expression of leptin and the leptin receptor as a marker of breast cancer progression: possible role of obesity-related stimuli. *Clin Cancer Res*. 2006; 12: 1447–53.
11. **Cleary MP, Phillips FC, Getzin SC, *et al.*** Genetically obese MMTV-TGF-alpha/Lep(ob) Lep(ob) female mice do not develop mammary tumors. *Breast Cancer Res Treat*. 2003; 77: 205–15.
12. **Cleary MP, Juneja SC, Phillips FC, *et al.*** Leptin receptor-deficient MMTV-TGF-alpha/Lepr(db)Lepr(db) female mice do not develop oncogene-induced mammary tumors. *Exp Biol Med*. 2004; 229: 182–93.
13. **Dieudonne MN, Machinal-Quelin F, Serazin-Leroy V, *et al.*** Leptin mediates a proliferative response in human MCF7 breast cancer cells. *Biochem Biophys Res Commun*. 2002; 293: 622–8.
14. **Hu X, Juneja SC, Maihle NJ, *et al.*** Leptin–a growth factor in normal and malignant breast cells and for normal mammary gland development. *J Natl Cancer Inst*. 2002; 94: 1704–11.
15. **Mauro L, Catalano S, Bossi G, *et al.*** Evidences that leptin up-regulates E-cadherin expression in breast cancer: effects on tumor growth and progression. *Cancer Res*. 2007; 67: 3412–21.
16. **Yin N, Wang D, Zhang H, *et al.*** Molecular mechanisms involved in the growth stimulation of breast cancer cells by leptin. *Cancer Res*. 2004; 64: 5870–5.
17. **Barone I, Catalano S, Gelsomino L, *et al.*** Leptin mediates tumor-stromal interactions that promote the invasive growth of breast cancer cells. *Cancer Res*. 2012; 72: 1416–27.
18. **Garofalo C, Surmacz E.** Leptin and cancer. *J Cell Physiol*. 2006; 207: 12–22.
19. **Vona-Davis L, Rose DP.** Adipokines as endocrine, paracrine, and autocrine factors in breast cancer risk and progression. *Endocr Relat Cancer*. 2007; 14: 189–206.
20. **Surmacz E.** Leptin and adiponectin: emerging therapeutic targets in breast cancer. *J Mammary Gland Biol Neoplasia*. 2013; 18: 321–32.
21. **Cirillo D, Ranchiglio AM, La Montagna R, *et al.*** Leptin signaling in breast cancer: an overview. *J Cell Biochem*. 2008; 105: 956–64.
22. **Catalano S, Marsico S, Giordano C, *et al.*** Leptin enhances, *via* AP-1, expression of aromatase in the MCF-7 cell line. *J Biol Chem*. 2003; 278: 28668–76.
23. **Catalano S, Mauro L, Marsico S, *et al.*** Leptin induces, *via* ERK1/ERK2 signal, functional activation of estrogen receptor alpha in MCF-7 cells. *J Biol Chem*. 2004; 279: 19908–15.
24. **Fiorio E, Mercanti A, Terrasi M, *et al.*** Leptin/HER2 crosstalk in breast cancer: *in vitro* study and preliminary *in vivo* analysis. *BMC Cancer*. 2008; 8: 305.
25. **Soma D, Kitayama J, Yamashita H, *et al.*** Leptin augments proliferation of breast cancer cells *via* transactivation of HER2. *J Surg Res*. 2008; 149: 9–14.
26. **Giordano C, Vizza D, Panza S, *et al.*** Leptin increases HER2 protein levels through a STAT3-mediated up-regulation of Hsp90 in breast cancer cells. *Mol Oncol*. 2013; 7: 379–91.
27. **Saxena NK, Taliaferro-Smith L, Knight BB, *et al.*** Bidirectional crosstalk between leptin and insulin-like growth factor-I signaling promotes invasion and migration of breast cancer cells *via* transactivation of epidermal growth factor receptor. *Cancer Res*. 2008; 68: 9712–22.
28. **Gertler A.** Development of leptin antagonists and their potential use in experimental biology and medicine. *Trends Endocrinol Metab*. 2006; 17: 372–8.
29. **Peelman F, Couturier C, Dam J, *et al.*** Techniques: new pharmacological perspectives for the leptin receptor. *Trends Pharmacol Sci*. 2006; 27: 218–25.
30. **Leggio A, Catalano S, De Marco R, *et al.*** Therapeutic potential of leptin receptor modulators. *Eur J Med Chem*. 2014; 78: 97–105.
31. **Gonzalez RR, Cherfils S, Escobar M, *et al.*** Leptin signaling promotes the growth of mammary tumors and increases the expression of vascular endothelial growth factor (VEGF) and its receptor type two (VEGF-R2). *J Biol Chem*. 2006; 281: 26320–8.
32. **Rene Gonzalez R, Watters A, Xu Y, *et al.*** Leptin-signaling inhibition results in efficient anti-tumor activity in estrogen receptor positive or negative breast cancer. *Breast Cancer Res*. 2009; 11: R36.
33. **Battle M, Gillespie C, Quarshie A, *et al.*** Obesity induced a leptin-Notch signaling axis in breast cancer. *Int J Cancer*. 2014; 1: 1605–16.
34. **Otvos L, Kovalszky I, Riolfi M, *et al.*** Efficacy of a leptin receptor antagonist peptide in a mouse model of triple-negative breast cancer. *Eur J Cancer*. 2011; 47: 1578–84.
35. **Beccari S, Kovalszky I, Wade JD, *et al.*** Designer peptide antagonist of the leptin receptor with peripheral antineoplastic activity. *Peptides*. 2013; 44: 127–34.
36. **Fields GB, Noble RL.** Solid phase peptide synthesis utilizing 9fluorenylmethoxycarbonyl amino acids. *Int J Pept Protein Res*. 1990; 35: 161–214.
37. **Di Gioia ML, Leggio A, Liguori A, *et al.*** Solid-phase synthesis of N-nosyl- and N-Fmoc-N-methyl-alpha-amino acids. *J Org Chem*. 2007; 72: 3723–8.
38. **Leggio A, Belsito EL, De Marco R, *et al.*** An efficient preparation of N-methyl-alpha-amino acids from N-nosyl-alpha-amino acid phenacyl esters. *J Org Chem*. 2010; 75: 1386–92.
39. **Gu G, Barone I, Gelsomino L, *et al.*** Oldenlandia diffusa extracts exert antiproliferative and apoptotic effects on human breast cancer cells through ERα/Sp1-mediated p53 activation. *J Cell Physiol*. 2012; 227: 3363–72.
40. **Selever J, Gu G, Lewis MT, *et al.*** Dicer-mediated upregulation of BCRP confers tamoxifen resistance in human breast cancer cells. *Clin Cancer Res*. 2011; 17: 6510–21.
41. **Bonofiglio D, Santoro A, Martello E, *et al.*** Mechanisms of divergent effects of activated peroxisome proliferator-activated receptor-γ on mitochondrial citrate carrier expression in 3T3-L1 fibroblasts and mature adipocytes. *Biochim Biophys Acta*. 2013; 1831: 1027–36.
42. **Barone I, Giordano C, Malivindi R, *et al.*** Estrogens and PTP1B function in a novel pathway to regulate aromatase enzymatic activity in breast cancer cells. *Endocrinology*. 2012; 153: 5157–66.
43. **Catalano S, Panza S, Malivindi R, *et al.*** Inhibition of Leydig tumor growth by farnesoid X receptor activation: the *in vitro* and *in vivo* basis for a novel therapeutic strategy. *Int J Cancer*. 2013; 132: 2237–47.
44. **Giagulli C, Marsico S, Magiera AK, *et al.*** Opposite effects of HIV-1 p17 variants on PTEN activation and cell growth in B cells. *PLoS ONE*. 2011; 6: e17831.
45. **Peelman F, Van Beneden K, Zabeau L, *et al.*** Mapping of the leptin binding sites and design of a leptin antagonist. *J Biol Chem*. 2004; 279: 41038–46.
46. **Niv-Spector L, Gonen-Berger D, Gourdou I, *et al.*** Identification of the hydrophobic strand in the A-B loop of leptin as major binding site III: implications for large-scale preparation of potent recombinant human and ovine leptin antagonists. *Biochem J*. 2005; 391: 221–30.
47. **Salomon G, Niv-Spector L, Gussakovsky EE, *et al.*** Large-scale preparation of

biologically active mouse and rat leptins and their L39A/D40A/F41A muteins which act as potent antagonists. *Protein Expr Purif*. 2006; 47: 128–36.

48. **Catalano S, Mauro L, Bonofiglio D, *et al.*** *In vivo* and *in vitro* evidence that PPARγ ligands are antagonists of leptin signaling in breast cancer. *Am J Pathol*. 2011; 179: 1030–40.
49. **Tartaglia LA, Dembski M, Weng X, *et al.*** Identification and expression cloning of a leptin receptor, OB-R. *Cell*. 1995; 83: 1263–7.
50. **Zhang F, Basinsk MB, Beals JM, *et al.*** Crystal structure of the obese protein leptin-E100. *Nature*. 1997; 387: 206–9.
51. **Peelman F, Iserentant H, De Smet AS, *et al.*** Mapping of binding site III in the leptin receptor and modeling of a hexameric leptin.leptin receptor complex. *J Biol Chem*. 2006; 281: 15496–504.
52. **Hamidi M, Azadi A, Rafiei P.** Pharmacokinetic consequences of pegylation. *Drug Deliv*. 2006; 13: 399–409.
53. **Hukshorn CJ, Saris WH, Westerterp-Plantenga MS, *et al.*** Weekly subcutaneous pegylated recombinant native human leptin (PEG-OB) administration in obese men. *J Clin Endocrinol Metab*. 2000; 85: 4003–9.
54. **Hukshorn CJ, Menheere PP, Westerterp-Plantenga MS, *et al.*** The effect of pegylated human recombinant leptin (PEG-OB) on neuroendocrine adaptations to semi-starvation in overweight men. *Eur J Endocrinol*. 2003; 148: 649–55.
55. **Elinav E, Niv-Spector L, Katz M, *et al.*** Pegylated leptin antagonist is a potent orexigenic agent: preparation and mechanism of activity. *Endocrinology*. 2009; 150: 3083–91.
56. **Fuertges F, Abuchowski A.** The clinical efficacy of poly(ethylene glycol)-modified proteins. *J Controlled Release*. 1990; 11: 139–48.
57. **Bailon P, Berthold W.** Polyethylene glycol-conjugated pharmaceutical proteins. *Pharm Sci Technol Today*. 1998; 1: 352–6.